

Cardiac magnetic resonance in left ventricular dyssynchrony: implications for cardiac resynchronization therapy

Camilla Kjellstad Larsen, MD

Thesis for the degree of Philosophia Doctor (Ph.D)

Institute of Clinical Medicine,

Faculty of Medicine, University of Oslo

and

Institute for Surgical Research and Department of Cardiology,

Oslo University Hospital, Rikshospitalet,

Oslo, Norway

© Camilla Kjellstad Larsen, 2024

*Series of dissertations submitted to the
Faculty of Medicine, University of Oslo*

ISBN 978-82-348-0409-0

All rights reserved. No part of this publication may be reproduced or transmitted, in any form or by any means, without permission.

Cover: UiO.

Print production: Graphic center, University of Oslo.

Table of contents

Acknowledgments	5
Thesis summary.....	7
Norsk sammendrag.....	9
List of papers	11
Abbreviations	12
Introduction	15
Dyssynchrony	15
Left bundle branch block.....	16
Cardiac imaging.....	19
Myocardial work.....	20
Septal flash	22
Myocardial fibrosis.....	22
Heart failure.....	24
Cardiac resynchronization therapy	25
Aims	29
General aims	29
Specific aims.....	29
Materials and methods	30
Study population.....	30
Cardiac Magnetic Resonance	33
Left ventricular volumes and ejection fraction	33
Myocardial strain	33
Regional non-invasive myocardial work index	33
Septal flash.....	34
Late gadolinium enhancement	35
Echocardiography	36
Positron Emission Tomography	36
Endpoints	37
CRT implantation	37
Statistics.....	38
Summary of results.....	39
Paper 1	39
Paper 2	42

Paper 3	45
Discussion	49
Clinical value of myocardial work	49
Identification of LV lateral wall scar in CRT candidates	50
Identification of septal scar in CRT candidates	52
Septal scar as determinant of CRT response	53
Lateral wall scar and CRT response	54
Septal flash: the optimal marker of electromechanical dyssynchrony?.....	54
Septal markers predict CRT response	56
Restrictions on clinical use of CMR.....	57
The predicament of defining CRT response.....	59
Methodological considerations	62
Patient inclusion	62
Myocardial work.....	62
Myocardial strain.....	64
Quantification of scar (LGE).....	65
Septal flash	66
Glucose metabolism	67
Statistics.....	68
Specific limitations	70
Ethical considerations	71
Clinical implications and future perspectives	72
Conclusions	74
General conclusions.....	74
Specific conclusions	74
Paper 1	74
Paper 2	74
Paper 3	74
References	75

Acknowledgments

The present work was carried out at the Institute for Surgical Research and Department of Cardiology, Oslo University Hospital, Rikshospitalet, from 2015 to 2023.

First, I would like to thank my main supervisor, Dr Einar Hopp. Through his leading expertise in cardiac magnetic resonance (CMR), Einar has been essential to all parts of this project, from hypothesis generation to data collection and critical appraisal. I am thankful for his comprehensive knowledge, positive attitude and endurance. Despite a very busy schedule, Einar has patiently, and with a friendly smile, taken the time to discuss findings, and repeatedly explained the puzzles of CMR to me. Working with Einar these years has been a privilege.

Second, I would like to thank my co-supervisors. Professor Otto Smiseth initiated the CRID-CRT study and developed many of the ideas behind it. His extraordinary insights in cardiac physiology, enthusiasm, constructive feedback and hard work has been essential for this PhD. Professor Jan Gunnar Fjeld has provided invaluable input to the nuclear imaging part of this project, both in the practical implementation of the study, as well as in thorough methodological discussions and constructive review of the papers.

I would like to express my gratitude towards my research group at the Institute for Surgical Research. Associate Professor Helge Skulstad provided important input and encouragement, and was always available to discuss unexpected echocardiographic findings with me. My office-roommate and senior researcher, Espen Remme, has provided constructive comments and inputs along the way. Co-PhD fellow John Moene Aalen has been my companion throughout this project, and we have shared both frustrations and laughter over the years. I have greatly appreciated our fruitful discussions, as well as his (and his father's) impressive knowledge in statistics. Study Nurse Kari Melberg led patient recruitment with a steady hand and friendly nature, and has become a good friend. I would also thank the rest of my research fellows, Espen Bøe, Petter Storsten, Øyvind Senstad Andersen, Ole Jakob Sletten and Faraz Kahn for their contributions, support and friendship throughout the years.

In parallel to the research work, I have had the privilege of working as a resident in the inspirational environment at the Department of Cardiology at Rikshospitalet. For this, I am forever thankful to Professor and Head of the department, Thor Edvardsen, and to Dr Cecilie Risøe, who has facilitated this combined position. I greatly appreciate the positive attitude and flexibility Cecilie has shown me during this project. I would also like to thank all my colleagues at the Department of Cardiology, in particular the arrhythmia section, led by Dr Erik Kongsgård. Erik's expertise in cardiac resynchronization therapy has been essential for the implementation of the study. Thank you Drs Erik Lyseggen and Torbjørn Holm, for your flexibility and support in comprehensive study logistics, your positive attitude, and your help in ensuring technically well-functioning devices.

Our international collaborators, in particular Professor Jens-Uwe Voigt, Professor Erwan Donal, Jürgen Duchenne and Dr Elena Galli, have been essential in preparing and conducting the CRID-CRT study. I am thankful for the opportunity to work with such leading experts in the field. Furthermore, I would like to express my gratitude to physicist Caroline Stokke, PET radiographer Alexander Gul Sherwani and Drs Per Anton Sirnes and Jørg Saberniak for their important contributions to different parts of the project. I am thankful for the radiographers at the CMR unit, with Bac Nguyen in front, for excellent patient care and cardiac imaging, and for their positive attitude towards research studies. Not least, I am grateful to all the patients

who participated in the study to promote scientific progress. Without you, there would not have been a project at all.

I have greatly valued the office facilities and the good environment at the Institute for Surgical Research led by Professor Håvard Attramadal. Moreover, I am grateful to the South-Eastern Norway Regional Health Authority for funding and to the University of Oslo for research fellowship and support from the Inger and John Fredriksen fund.

Thankyou Arild Dimmen and Olve Skjetne and the Departments of Internal Medicine, Kristiansund and Gjøvik Hospitals, for the opportunity to obtain broad cardiology experience during the first part of my training, and for introducing me to echocardiography.

Finally, I would like to thank my family. My parents, Åse and Eirik, and my sister Christina, for their love, support, and encouragement. Thank you Tove and Geir, for your kindness and loyal up backing through these years. Most importantly, my deepest appreciation goes to my hero at home – my husband Andreas – and to our dear children, Julian and Filippa – both born during my time as a PhD fellow. You are a constant reminder of what is most important in life. Thank you for all the love, joy and purpose you give me. I dedicate this work to you.

Camilla 2023

Thesis summary

Left bundle branch block (LBBB) causes delayed electrical activation of the left ventricle. This causes the left ventricular (LV) lateral wall to contract later than the interventricular septum, because it is activated through fibres from the right ventricle. The result is asynchronous contractions (dyssynchrony), which negatively affects LV function. Typically, there is an early septal contraction, prior to opening of the aortic valve. Septum is then mostly stretched during the rest of systole, as a result of the delayed and forceful LV lateral wall contraction. The uncoordinated contractions result in an asymmetric distribution of myocardial workload within the ventricle, where septum performs little work, while the LV lateral wall performs compensatory increased work compared to normal. The pathological septum movement, with an initial shortening and then lengthening, can also be visualized directly by cardiac imaging and is named septal flash.

Cardiac resynchronization therapy (CRT) restores synchronous activation of the left ventricle through pacing leads both in the right and left ventricle (biventricular pacemaker). Current guidelines recommend CRT in patients with LBBB, LV ejection fraction $\leq 35\%$ and heart failure symptoms. CRT improves symptoms and reduces mortality in many patients, but the large amount of non-responders remains a persistent problem. Myocardial scar is associated with poor response to CRT, while septal flash indicates increased likelihood of response to the treatment. Cardiac magnetic resonance (CMR) is gold standard for identifying scar, but not always available. Accuracy of alternative imaging techniques is not well studied. The poor septal function in LBBB (septal flash and uneven LV work distribution) has traditionally been assessed by echocardiography, while feasibility and clinical relevance of these parameters assessed by CMR is largely unknown.

In the present thesis, we have studied regional LV function in LBBB to improve understanding of LV dyssynchrony on myocardial function and CRT response. We tested the feasibility of a new method to calculate regional myocardial work in LBBB using CMR. We also explored how glucose metabolism and strain/work, correlate with regional LV scar in dyssynchronous ventricles. Finally, we hypothesized that a viable but dysfunctional septum is a substrate for CRT, which can be identified by CMR. In a prospective, multicentre study, we studied patients referred for CRT based on current guidelines. Included patients performed comprehensive CMR and echocardiography, as well as PET if possible. CMR with late gadolinium enhancement (LGE) was used to determine scar. In the first paper, we also included healthy controls without LBBB, these were examined with CMR and echocardiography.

The thesis is based on three papers. In the first paper, we examined if we could identify the uneven work distribution typical for LBBB using strain from CMR (derived from a semiautomatic software) and a non-invasive estimate of LV pressure. In patients with heart failure and LBBB, we found, as expected, significantly lower amount of myocardial work in septum compared to the LV lateral wall. In contrast, in the healthy controls without LBBB, there was a homogenous work distribution and no regional differences. Despite some variations in the absolute numbers of myocardial work, we found good reproducibility between readers. We also demonstrated good correlation between work by CMR and the more established equivalent method by echocardiography. Moreover, we showed that the inhomogeneous work distribution correlated well with regional glucose metabolism by PET, which we used a marker of myocardial energy demand. The study was relatively small, and the findings should be validated in larger cohorts and with different strain software. Nevertheless, our results show that the method is useful to evaluate regional LV function in

patients with heart failure and LBBB, which may be particularly useful in patients with poor echocardiographic image quality.

In paper two, we aimed to determine if glucose metabolism by PET and strain by echocardiography could be used to identify LV scar in patients with heart failure and LBBB. LGE-CMR was used as reference standard for scar. The main finding in this paper is that glucose metabolism by PET is a good alternative to CMR to identify transmural LV lateral wall scar (area under the curve (AUC) 0.96). Strain by echocardiography was only moderately accurate (AUC 0.77) and must be interpreted with caution. Relatively preserved peak strain in the LV lateral wall suggests that transmural scar in this region is unlikely, while reduced strain is inconclusive in terms of scar. Neither PET nor echocardiography could distinguish reduced septal metabolism/strain due to LBBB itself from reduced values due to septal scar. Hence, PET and echocardiography cannot identify septal scar in dyssynchrony. The findings should have implications for cardiac imaging prior to CRT implantation, strengthening the role of CMR in the pre-operative setting.

In the third paper, we tested if septal scar and septal flash, both derived from CMR, could predict CRT response. We included all patients from the prospective, multicentre study with available CMR and follow-up data (n=136). Patients with preserved renal function were examined with gadolinium contrast (n=128). Primary endpoint was CRT response defined as LV reverse remodelling at six months follow-up. Septal scar and septal flash were significant predictors of CRT response. Septal scar reduced the likelihood of response, while septal flash increased the probability. The parameters combined predicted CRT response with AUC 0.86. In patients without septal scar, response rate was excellent (96%), irrespective of other parameters. In comparison, response rate was only 58% in patients with septal scar. Importantly, septal flash accurately separated responders from non-responders in this latter group. If patients with septal scar also had septal flash, there was still a high likelihood of response (78%). In contrast, in patients with septal scar and no septal flash, response rate was low (23%). A novel algorithm based on a simple, dichotomous determination of septal scar and septal flash identified CRT responders with 86% accuracy. Of special promise, was the finding that the algorithm was equally accurate in the subgroup of patients with intermediate QRS-duration, where the indication for CRT is more uncertain according to current guidelines. Septal scar and septal flash, both alone and together, predicted long-term survival without heart transplantation. The study was observational, and our findings should be validated in randomized trials before clinical practice can be changed.

In total, the results from the present thesis demonstrate that CMR may characterize both structural (scar) and functional (low work/septal flash) changes in septum in patients with heart failure and LBBB. Moreover, through such characterization, CMR may identify a septal substrate for CRT response. Our results show that a combined assessment of septal scar and septal flash by CMR as single image modality accurately identifies CRT responders. Echocardiography and PET, on the other hand, cannot identify septal scar, and rely on CMR for this relevant information. Based on these findings, we advocate increased priority for CMR in patients referred for CRT.

Norsk sammendrag

Venstre grenblokk innebærer en forsinkelse i den elektriske aktiveringen av venstre ventrikkel. Dette gjør at lateralveggen av venstre ventrikkel kontraherer på et senere tidspunkt i systolen enn det interventrikulære septum. Resultatet blir asynkrone kontraksjoner (dyssynkroni) med negative effekter på venstre ventrikkels funksjon. Typisk sees tidlig kontraksjon i septum, før aortaklaffen åpner seg. Deretter vil septum for det meste strekkes gjennom resten av systolen, som et resultat av den sene og kraftfulle kontraksjonen i venstre ventrikkels laterale vegg. De ukoordinerte kontraksjonene medfører en asymmetrisk fordeling av arbeid innad i venstre ventrikkel hvor septum gjør lite arbeid, mens lateralveggen kompenserer og gjør mer arbeid enn normalt. Den patologiske septumbevegelsen, med initial forkortning og deretter strekking, kan visualiseres direkte ved hjelp av kardiale bildemodaliteter, og har fått navnet septal flash.

Kardial resynkroniseringsterapi (CRT) gjenoppretter synkron aktivering av venstre ventrikkel ved å aktivere både høyre og venstre ventrikkel samtidig (biventrikulær pacemaker). Dagens retningslinjer sier at pasienter med venstre grenblokk, ejsjonsfraksjon $\leq 35\%$ og symptomer forenlig med hjertesvikt er kandidater for CRT. På gruppenivå er CRT vist å bedre symptomer og overlevelse, men det er et vedvarende problem at en stor andel av pasienten som får CRT i dag ikke responderer på behandlingen. Arr i venstre ventrikkel er assosiert med non-respons til CRT, mens septal flash indikerer økt sannsynlighet for gunstig respons. Magnetisk resonans (MR) er gullstandard for påvisning av arr, men er ikke alltid tilgjengelig. Det er ikke kjent hvorvidt ekkokardiografi og positronemisjonstomografi (PET) kan erstatte MR for å identifisere arr hos pasienter med dyssynkroni. Redusert septum funksjon hos pasienter med venstre grenblokk (bedømt som septal flash og ujevn arbeidsfordeling innad i venstre ventrikkel) har til nå stort sett vært gjort ved ekkokardiografi, mens egnethet og klinisk relevans av slike parametere bedømt ved MR har vært lite studert.

I denne avhandlingen har vi studert regional venstre ventrikkel funksjon ved venstre grenblokk. Målet var å bedre forståelsen av hvordan dyssynkroni påvirker ventrikkelfunksjonen og CRT respons. Vi har validert en ny metode for å kvantifisere arbeidsfordelingen innad i venstre ventrikkel ved hjelp av MR. Vi har også undersøkt hvordan glukosemetabolismen og strain/arbeid korrelerer med arr i ulike deler av ventrikkelen ved dyssynkroni. Videre postulerte vi at en viabel, men dysfunksjonell septum, utgjør et substrat for CRT, som kan identifiseres ved hjelp av MR uten bruk av andre bildemodaliteter. I en prospektiv multisenterstudie studerte vi pasienter henvist til CRT på bakgrunn av nåværende retningslinjer. Pasienten gjennomførte omfattende MR undersøkelse og ekkokardiografi, en del også PET. MR med kontrastmiddel ble brukt til å påvise arr. I den første artikkelen undersøkte vi også friske kontrollpersoner uten grenblokk med MR og ekkokardiografi.

Avhandlingen er basert på tre artikler. I den første undersøkte vi hvorvidt vi kunne påvise den ujevne arbeidsfordelingen typisk for venstre grenblokk ved å bruke en halvautomatisk programvare til å beregne strain fra MR, og kombinere det med et ikke-invasivt mål for venstre ventrikketrykk. Hos pasientene med hjertesvikt og venstre grenblokk fant vi, som forventet, signifikant lavere arbeid i septum enn i venstre ventrikkels laterale vegg. Hos de friske kontrollpersoner uten grenblokk derimot, fant vi en homogen arbeidsfordeling og ingen forskjell mellom de samme regionene. Selv om de absolutte tallene for arbeid avvek litt ved gjentatt undersøkelse, fant vi at funnene overordnet hadde god reproduserbarhet. Det var også god korrelasjon med tilsvarende arbeidsberegning ved ekkokardiografi, som er en etablert metode for arbeidsberegning. I tillegg fant vi at den ujevne arbeidsbelastningen korrelerte godt med regional glukose metabolisme bedømt ved PET, som vi brukte som markør på metabolsk behov og oksygenforbruk, og som forventes å samsvare med arbeidsfordelingen.

Studien var relativt liten, og funnene bør valideres i større grupper og med ulike programvarer. Likevel viser resultatene at metoden kan være nyttig til å vurdere regional funksjon hos pasienter med venstre grenblokk, og vil kunne spesielt være nyttig hos de med redusert ekkokardiografisk bildekvalitet.

I artikkel nummer 2 ønsket vi å avgjøre om glukose metabolisme ved PET og strain ved ekkokardiografi kan brukes til å identifisere arr i venstre ventrikel hos pasienter med hjertesvikt og venstre grenblokk. Vi brukte MR med kontrastmiddel som referanse for arr. Hovedfunnet i denne artikkelen var at glukose metabolisme ved PET er et godt alternativ til MR for å påvise transmural arr i lateralveggen (areal under kurven (AUC) 0.96). Strain ved ekkokardiografi var bare moderat treffsikker (AUC 0.77) og må tolkes med forsiktighet. En relativt bevart strainverdi i lateralveggen tyder på at transmural arr i denne regionen er lite sannsynlig, mens en redusert strainverdi er uegnet til å si om det foreligger arr eller ikke. Verken PET eller ekkokardiografi kunne skille redusert metabolisme/strain i septum på grunn av grenblokket i seg selv fra reduserte verdier på grunn av septale arr. Det betyr at PET og ekkokardiografi ikke bør brukes til å identifisere arr i septum ved dyssynkroni. Funnene er klinisk relevant, og bør få direkte kliniske implikasjoner for valg av bildemodalitet før CRT.

I den tredje artikkelen testet vi ut om septale arr og septal flash, begge fra MR, kunne forutsi respons på CRT. Til denne studien inkluderte vi alle pasientene fra den prospektive multisenter studien som hadde gjennomført MR og hadde tilgjengelig oppfølgingsdata (n=136). Pasienter med adekvat nyrefunksjon fikk gadolinium kontrast (n=128). Primært endepunkt var CRT respons definert som revers remodellering av venstre ventrikel ved seks måneders oppfølging. Arr i septum og septal flash var signifikante prediktorer for CRT respons. Septale arr reduserte sannsynligheten for respons, mens septal flash predikerte økt sannsynlighet for effekt av CRT. AUC for kombinasjonen av parameterne var 0.86. Av pasientene uten arr i septum, responderte hele 96%. Til sammenligning, responderte bare 58% i gruppen med arr i septum. Et viktig funn var at septal flash skilte godt mellom respondere og non-respondere i denne siste gruppen. Dersom septal flash var tilstede, var sannsynligheten for respons fortsatt god (78%), mens responsraten var lav (23%) hos pasientene med arr i septum som ikke hadde septal flash. Et flytskjema basert på enkel dikotom bestemmelse av septale arr og septal flash identifiserte CRT respondere med 86% treffsikkerhet. Flytskjemaet var like nøyaktig i undergruppen av pasienter med intermediær QRS-varighet, hvor indikasjonen for CRT er mer usikker i henhold til dagens retningslinjer. Parameterne predikerte langtidsoverlevelse uten hjertetransplantasjon.

Total sett viser funnene i denne avhandlingen at MR kan kartlegge både strukturelle (arr) og funksjonelle (lavt arbeid/septal flash) endringer i septum hos pasienter med hjertesvikt og venstre grenblokk. Vi har også vist at MR på denne måten kan identifisere et septalt substrat for CRT respons. Kombinert vurdering av septale arr og septal flash fra MR identifiserte CRT respondere med høy grad av treffsikkerhet. Ekkokardiografi og PET, på den andre siden, kunne ikke identifiserer septale arr i denne pasientgruppen. Utkomme-studien (artikkel tre) var observasjonell og av begrenset størrelse, slik at funnene må valideres i randomiserte studier før det er indikasjon for endrede kliniske retningslinjer. Likevel mener vi funnene i avhandlingen betyr at hjerte-MR fortjener en større rolle enn i dag i utredning av pasienter henvist til CRT.

List of papers

- 1. Regional myocardial work by cardiac magnetic resonance and non-invasive left ventricular pressure: a feasibility study in left bundle branch block**
Larsen CK, Aalen JM, Stokke C, Fjeld JG, Kongagaard E, Duchenne J, Degtiarova G, Gheysens O, Voigt JU, Smiseth OA, Hopp E.
Eur Heart J Cardiovasc Imaging. 2020;21:143-153.
- 2. Scar imaging in the dyssynchronous left ventricle: Accuracy of myocardial metabolism by positron emission tomography and function by echocardiographic strain**
Larsen CK, Galli E, Duchenne J, Aalen JM, Stokke C, Fjeld JG, Degtiarova G, Claus P, Gheysens O, Saberniak J, Sirnes PA, Lyseggen E, Bogaert J, Kongsgaard E, Penicka M, Voigt JU, Donal E, Hopp E, Smiseth OA.
Int J Cardiol. 2023;372:122-9.
- 3. Cardiac magnetic resonance identifies responders to cardiac resynchronization therapy by assessment of septal scar and left ventricular dyssynchrony**
Larsen CK, Smiseth OA, Duchenne J, Galli E, Aalen JM, Lederlin M, Bogaert J, Kongsgaard E, Linde C, Penicka M, Donal E, Voigt JU, Hopp E.
Submitted October 2023.

Abbreviations

2D = two-dimensional

ACE = angiotensin-converting enzyme

ARB = angiotensin receptor blocker

ARNI = angiotensin receptor-neprilysin inhibitor

AUC = area under the curve

AV = atrioventricular

AVC = aortic valve closure

AVO = aortic valve opening

CI = confidence interval

CMR = cardiac magnetic resonance

CRT = cardiac resynchronization therapy

CRT-D = cardiac resynchronization therapy defibrillator

CRT-P = cardiac resynchronization therapy pacemaker

ECG = electrocardiogram

ECV = extracellular volume

EDV = end diastolic volume

EF = ejection fraction

ESC = European Society of Cardiology

ESV = end systolic volume

FDG = ¹⁸F-fluorodeoxyglucose

FT = feature tracking

GLP-1 = glucagon-like peptide-1

GLS = global longitudinal strain

HF = heart failure

HFmEF = heart failure with mildly reduced ejection fraction

HFpEF = heart failure with preserved ejection fraction

HFrfEF = heart failure with reduced ejection fraction

ICC = intra-class correlation coefficient

ICD = implantable cardioverter-defibrillator

ICR = isovolumic contraction
IVCD = intraventricular conduction delay
IVR = isovolumic relaxation
LBBB = left bundle branch block
LGE = late gadolinium enhancement
LV = left ventricular
LVP = left ventricular pressure
MVC = mitral valve closure
MVO = mitral valve opening
NYHA = New York Heart Association
PET = positron emission tomography
RBBB = right bundle branch block
ROC = receiver operating characteristic
RV = right ventricular
SGLT2 = sodium-glucose cotransporter 2
SPECT = single photon emission computed tomography
STE = speckle tracking echocardiography

Introduction

Dyssynchrony

Dyssynchrony can be defined in different ways. In the present thesis, left ventricular (LV) intraventricular dyssynchrony is defined as uncoordinated regional contractions within the ventricle. These out-of-sync contractions are in contrast to the synchronous ventricular contractions in normal hearts. Synchronous LV contractions ensures effective pumping of blood from the ventricle into the ascending aorta, while uncoordinated wall motions alter LV performance and result in less effective pumping of blood. This thesis focuses on LV intraventricular dyssynchrony, which is considered the main substrate for cardiac resynchronization therapy (CRT) (1, 2). However, cardiac dyssynchrony can also be atrioventricular (AV) or interventricular. AV dyssynchrony results from a block in the AV-node and may have negative effects on LV filling due to premature atrial contractions. Interventricular dyssynchrony is a consequence of divergent timing of contractions in the right and left ventricle (3).

Simultaneous contractions of all LV regions depends on both rapid electrical conduction through a specialized conduction system and normal contractile forces within the myocardium. There are two main causes of LV dyssynchrony: electromechanical or primary mechanical (4). Electromechanical dyssynchrony results from blocks in the conduction system of the heart. Normally, the electrical impulses, originating from the sinus node and slowed in the AV-node, enter the base of the ventricle at the Bundle of His and then follow the left and right bundle branches along the interventricular septum. The bundle branches then divide into an extensive system of Purkinje fibres that conduct the impulses at high velocity and provides a rapid and synchronous activation of the ventricles. A block in the electrical conduction system means that the myocardial tissue distal to the block is activated late, because the impulses have to go through the slower conducting myocardial cells instead of the specialized conduction tissue. The late activated region contracts later in systole than the normally activated regions, and the time needed for the electric impulse to reach all LV segments is prolonged. Slowed conduction through the left bundle branch is called left bundle branch block (LBBB), and results in delayed activation of the LV lateral wall compared to septum and the right ventricular (RV) free wall because the LV is activated via the right bundle branch (Figure 1). If conduction through the right bundle branch is slowed, the conduction delay is called right bundle branch block (RBBB). Compared to LBBB, RBBB is less frequently of clinical relevance. This thesis focuses on LBBB, which is most relevant in LV dyssynchrony and CRT.

Primary mechanical dyssynchrony is regional disparities in contractility despite an intact electrical conduction system. Causes may be regional myocardial ischemia, regional loading abnormalities or abnormalities in excitation-contraction coupling. As opposed to electromechanical dyssynchrony, primary mechanical dyssynchrony is not likely to be correctable by CRT (4, 5).

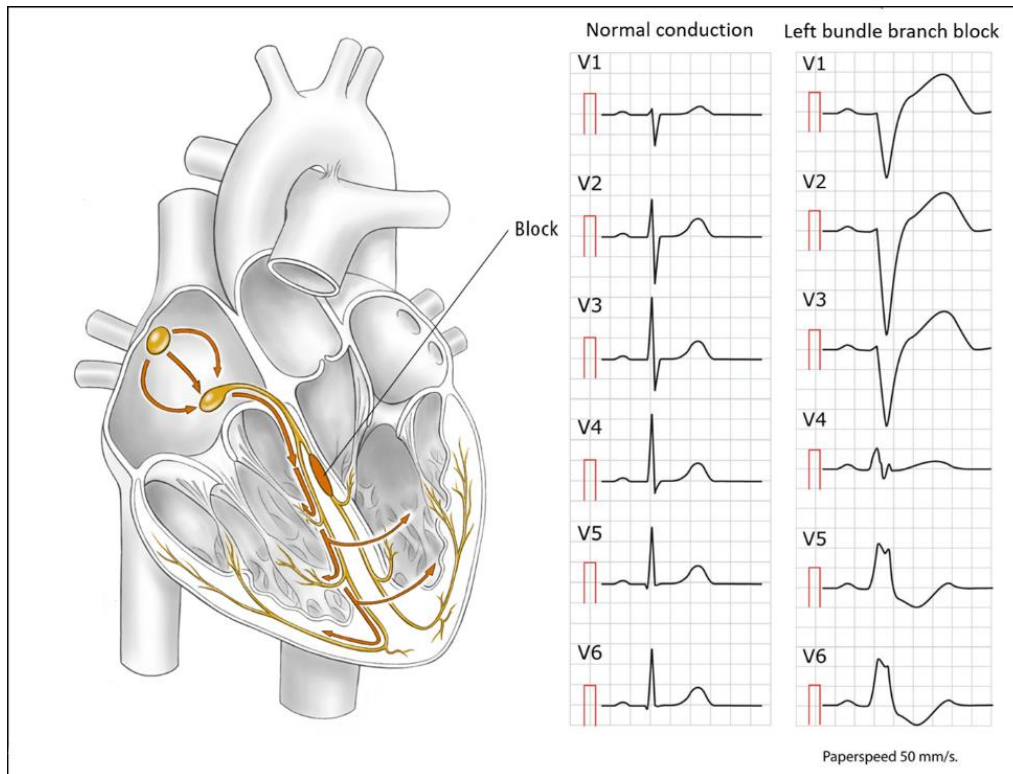


Figure 1. Illustration of left bundle branch block (LBBB).

Slowed conduction through the left bundle branch (LBBB) results in delayed activation of the left ventricle (LV) compared to septum and the right ventricle (RV), because the LV is activated through the RV as indicated by the arrows (left part of the figure). This leads to longer QRS-duration and characteristic QRS-morphology on surface electrocardiogram (ECG) (right part of the figure).

Reproduced and modified with permission from McMaster Textbook of Internal Medicine (6) with credit to artwork artist Dr Shannon Zhang (left part of figure) and ecgwaves.com (7) (right part of figure), respectively.

Left bundle branch block

LBBB results in characteristic features on the electrocardiogram (ECG) (Figure 1), but the exact definition of LBBB varies. The European Society of Cardiology (ESC) guidelines defines LBBB as 1) QRS-width ≥ 120 ms and 2) characteristic morphology of the QRS-complex with QS or rS in lead V1, broad R waves in leads I, aVL, V5 or V6, and absent Q waves in leads V5 and V6 (8). These are widely recognized criteria applied in large clinical trials. However, it is worth noting that endocardial mapping studies have demonstrated that $>30\%$ of patients fulfilling the conventional ECG criteria do not have significant delays between activation start of the right and left endocardium (9, 10), and therefore do not actually have complete LBBB. In light of this, Strauss and co-workers advocate for stricter ECG criteria for complete LBBB, demanding a wider QRS (130 ms in women and 140 ms in men), as well as mid-QRS notching in at least two lateral leads (11). The value of “true LBBB” using Strauss’ criteria in improving selection of patients to CRT is not yet determined. RV pacing at the conventional pacing site (the RV apex) induces an LBBB-like electrical activation pattern of the LV, and may lead to myocardial derangements similar to LBBB (12, 13). Like LBBB, RBBB causes specific features on the ECG. Patients with broad

QRS complexes without typical features of LBBB or RBBB are classified as non-specific intraventricular conduction delay (IVCD) (8).

The prevalence of LBBB increases with age, suggesting it is likely an acquired phenomenon (14). Reported prevalence in general population studies is 0.5-1% in middle-aged men (15, 16). In patients with chronic heart failure (HF), however, prevalence of LBBB is much higher, approximately 20-30% (17-19). LBBB in this patient group is also associated with increased disease severity and mortality (18). The cause-and-effect relationship between LBBB and mortality in HF has been vigorously debated, but several studies have reported LBBB to be a strong independent predictor of mortality in HF (18, 20).

There are gaps in knowledge about the aetiology of LBBB, because it usually has a silent onset. Furthermore, LBBB often coexists with other cardiovascular diseases such as arterial hypertension, coronary artery disease, valvular heart disease and cardiomyopathies. In some individuals, however, LBBB may be an incidental finding in subjects with no symptoms and apparently normal hearts (14, 21, 22). Tolerance of LBBB on cardiac function varies between individuals. Possible explanations may be coexisting diseases that directly affect myocardial function independent of LBBB, and different anatomical location and extent of LBBB (despite similar surface ECG) (9, 22, 23).

In a normal heart, all LV segments contract almost simultaneously, against similar LV pressure (LVP). This is, however, not the case in many patients with LBBB. Typically, in LBBB, the early activated septum contracts before aortic valve opening (AVO), when LVP is low (pre-ejection shortening) (Figure 2). This early septal contraction does not contribute to LV stroke volume, but causes stretch of the LV lateral wall, which results in a higher preload than normal. When the late activated pre-stretched LV lateral wall contracts later in systole, the contraction is extra forceful (according to the Starling mechanism). Contraction of the LV lateral wall causes blood to be displaced towards septum. As a result, septum is stretched and displaced towards the right ventricle (rebound stretch). Contraction of the lateral wall leads to LV ejection, but systolic function is impaired because of markedly reduced septal contribution. Furthermore, the added workload on the lateral wall due to septal dysfunction stimulates adverse LV remodelling with septal thinning and lateral wall hypertrophy (24). Because of uncoordinated regional contractions, LBBB is often characterized by markedly reduced septal work compared to LV lateral wall work (24-26). Correspondingly, there is generally reduced septal glucose metabolism and myocardial perfusion relative to the lateral wall, which is a direct consequence of impaired septal systolic thickening and reduced septal workload (24, 27, 28). However, because the ECG criteria are not optimal markers of delayed LV activation and dyssynchrony, these regional heterogeneities in function are not present in all patients who fulfil the ECG-criteria for LBBB. This may explain some of the shortcomings of ECG in identifying patients likely to respond to CRT (29).

The dyssynchronous LV contraction may both cause and aggravate mitral regurgitation in LBBB, further reducing effective stroke volume (30). Present knowledge of the consequences of dyssynchrony on LV diastolic function is more limited, but experimental studies have demonstrated that LBBB markedly reduces LV filling time (31), indicating that LBBB also negatively affects LV diastolic function. Furthermore, a dysfunctional left ventricle may indirectly lead to RV failure by increasing LV filling pressure, causing pulmonary hypertension and increased RV afterload.

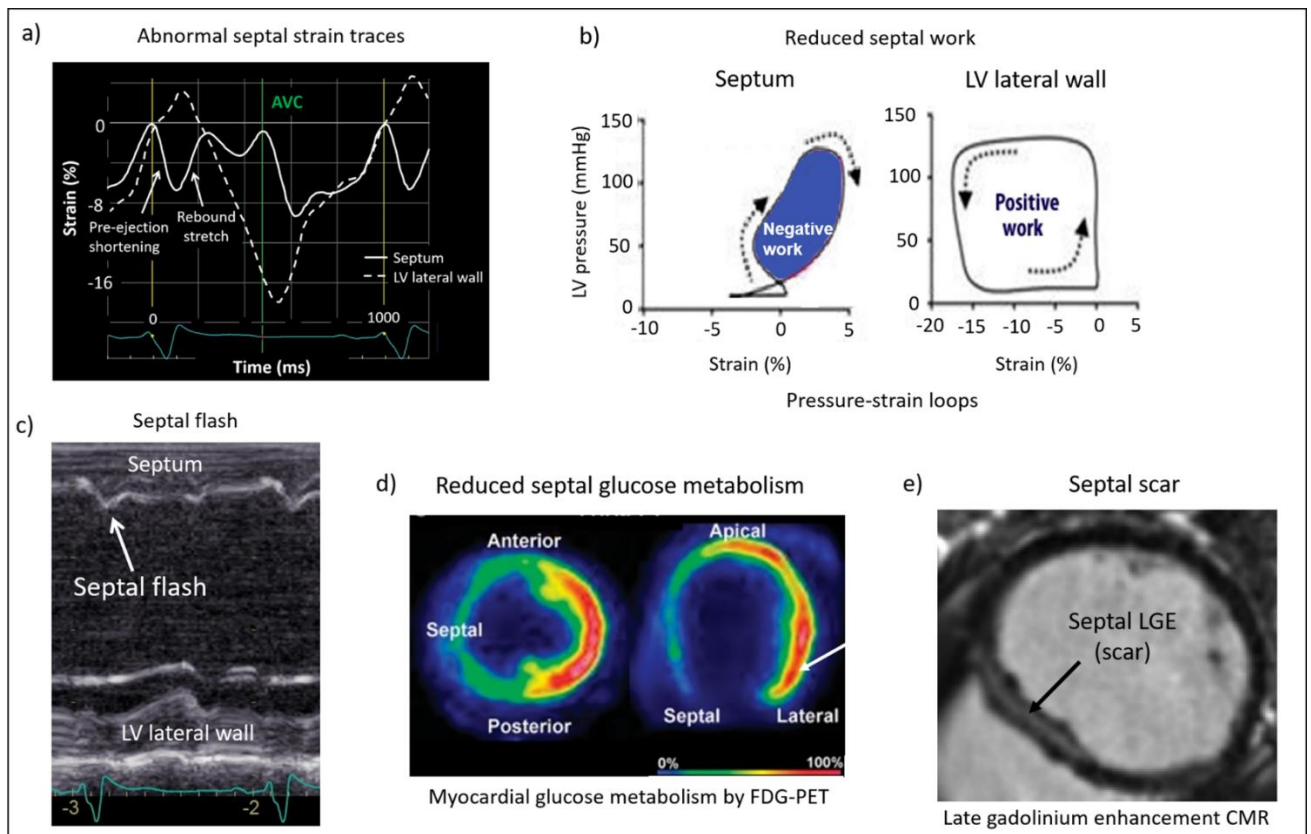


Figure 2. Different features of left bundle branch block (LBBB).

- In LBBB, the early activated septum contracts in the pre-ejection phase before aortic valve opening (AVO), when left ventricular (LV) pressure is low (pre-ejection shortening). The early septal contraction causes pre-stretch of the LV lateral wall, which then later in systole contracts more forcefully due to higher preload. Contraction of the LV lateral wall stretches septum (rebound stretch). Reproduced with permission (32).
- The septal stretching described in a) represents negative myocardial work, resulting in a septal pressure-strain loop that rotates both clockwise and counter-clockwise. The coloured area illustrates negative work. In contrast, the loop from the LV lateral wall rotates counter-clockwise as a result of normal systolic shortening. Hence, the LV lateral wall performs positive work. Reproduced with permission (25).
- Septal flash (septal beaking) as seen by M-mode echocardiograph. Septum initially moves leftward in early systole prior to opening of the aortic valve. Then, when the LV lateral wall contracts, septum is pushed rightward. Reproduced with permission (32).
- Septal hypo-metabolism in LBBB, by ^{18}F -fluorodeoxyglucose (FDG) Positron Emission Tomography (PET). Segments are reported as percentage of the segment with the highest glucose uptake. Metabolic activity corresponds to myocardial work. Reproduced with permission (25)
- Illustration of non-ischemic septal scar (midwall fibrosis) by late gadolinium enhancement (LGE) cardiac magnetic resonance (CMR).

Cardiac imaging

Echocardiography uses ultrasound waves to create images of the heart chambers, valves and surrounding structures. It is the first line imaging modality in diagnosing and follow-up of patients with heart failure, and assesses both ventricular contractile function, valvular function and parameters of LV diastolic function, in addition to for example pericardial effusion. Echocardiography is readily available, poses no exposure to radiation and has no contraindications. On the other hand, the technique is operator-dependent and hampered with poor image quality in some patients.

Cardiac magnetic resonance (CMR) uses a magnetic field and computer-generated radio waves to create images of the heart. The unique strength of CMR is the ability to characterize myocardial tissue non-invasively independent of wall motion in any 3-dimensional acquisition plane, either without or enhanced by a gadolinium based contrast agent. CMR image quality is independent of acoustic window, allowing depiction of the heart in patients where echocardiography is inconclusive. However, CMR is less available and more expensive than echocardiography, and temporal resolution (frame rate) is lower. The CMR situation brings risk for unsatisfactory medical surveillance. In this respect, it may make patients with serious arrhythmia and heart failure prone to fatalities. Additionally, it is essential that patients cooperate while in the magnet to avoid motion artefacts.

In nuclear imaging, external detectors (gamma cameras) detect radiation emitted by radioactive tracers, most often administered intravenously. Procedures based on oral, subcutaneous, intramuscular, intracutaneous or intrathecal administration also exist. Single photon emission computed tomography (SPECT) and positron emission tomography (PET) scans are today the two most common nuclear imaging modalities. The acquired tracer uptake can further be fused with images from for example computerized tomography (CT) to provide accurate anatomical location of the radioactive tracer. The tissue density map registered with the CT is also used for radiation attenuation correction of the nuclear images. Depending on tracer, PET can assess both regional glucose metabolism and myocardial perfusion. Compared to SPECT, PET offers higher spatial resolution, but is more expensive and less accessible. Nuclear imaging is prone to moderate image quality due to low photon flux, attenuation artefacts and partial volume effect.

LV systolic function has traditionally been characterized by EF, defined as the fraction of stroke volume and end-diastolic volume (EDV). EF is often used in clinical guidelines to guide patient treatment, but contractile function may be impaired despite normal EF (33). Strain imaging is a newer technique that measures myocardial deformation. It is a dimensionless index describing the percentage change in a myocardial segment length relative to baseline in the longitudinal, circumferential or radial direction. Negative strain values are by convention assigned to shortening and thinning, while strain values for lengthening and thickening are positive. Strain allows for more accurate assessment of systolic function than EF, and is more sensitive to subtle regional impairments.

The most established strain technique is strain by speckle-tracking echocardiography (STE). STE is based on tracking of “speckles”, which are natural acoustic markers of grey scale ultrasound images. These speckles are distributed throughout the myocardium. Deformation curves are produced by tracking the relative positions of speckles in different anatomical areas or standardized segments, and reported as myocardial strain (34). However, STE requires high image quality with a specific frame rate (50-70 frames/s). Poor acoustic windows hinders strain by STE in a substantial amount of patients (35, 36).

CMR also assesses myocardial strain. The most validated CMR technique to measure myocardial deformation is myocardial tagging. The tagging technique measures regional deformation by applying non-invasive demagnetization lines throughout the myocardium, and track their movements through cardiac cycle. Strain by CMR tagging has high intrer- and intraobserver reproducibility. On the other hand, tagging is hampered with suboptimal spatial and temporal resolution, as well as tag fading throughout cardiac cycle. Furthermore, clinical usefulness of the technique is limited due to the need for specialized scanning sequences and complex post-processing analyses. The recently introduced technique of CMR feature tracking (FT) allows strain measurement from ordinary cine sequences, measuring deformation along the endocardial or epicardial border. The features tracked are anatomic elements, which are found by methods of maximum likelihood in two regions of interest between two frames. The endocardial/epicardial borders (excluding papillary muscles and trabeculae) are first defined manually. Then, the automatic algorithm identifies a relatively small window on one image and searches for the most comparable image pattern in a window of the same size in successive images of the sequence. The displacement found between the two patterns is interpreted as local displacement of the tissue (strain). The main limitation of the method is artefacts due to through-plane motion, as features moving out of plane cannot be tracked. CMR-FT is also limited by pixel size (displacement of less than pixel size may not be detected). Furthermore, blood motion can affect the tracking close to the endocardial regions, which may result in unreal strain values, and good tracking requires high image quality with adequate spatial and temporal resolution. The main advantages of CMR-FT is that the method does not require additional image acquisition time in the scanner as it can be acquired on routine CMR cine acquisitions, and is rapid and semi-automated (37, 38). This makes it more accessible than tagging and a relevant alternative to STE, for example in patients with poor echocardiographic image quality.

Indices of LV electromechanical dyssynchrony by echocardiography and CMR, such as asymmetric work distribution and visual dyssynchronous contraction pattern (septal flash) will be discussed in the following. LV dyssynchrony by nuclear imaging, beyond the regional disparities in glucose metabolism and perfusion, is considered outside the scope of this thesis.

Myocardial work

Indices of myocardial shortening, such as EF or strain, suffer from load-dependency (39). Afterload (wall stress) represents the load on the ventricle during contraction, and is determined by (transmural) ventricular pressure, wall thickness and radius of curvature (Law of Laplace) (40). Preload is the load prior to contraction. The uncoordinated contractions of walls in LBBB results in heterogeneous wall stress due to different LV geometry between regions. This reduces the usefulness of strain and EF in patients with LBBB, where septal shortening (strain) may be preserved, but loading conditions abnormal. Myocardial work, on the other hand, incorporates load, and may therefore provide a more comprehensive assessment of myocardial function than shortening indices alone (25, 26). Myocardial work reflects both regional oxygen consumption (41) and glucose metabolism (25). Global LV work coincides with the area of the LV pressure-volume loop, while the area of the local myocardial force-segmental length loop corresponds to regional myocardial work (42). Calculations of force (which is similar to wall stress), however, is cumbersome as it requires continuous recordings of both pressure, wall thickness and radius of curvature. A more relevant clinical measure is achieved by substituting myocardial force with LVP and segment

length with strain (Figure 3). This index of myocardial work has been shown to be a reasonable estimate of myocardial work in various clinical scenarios (43).

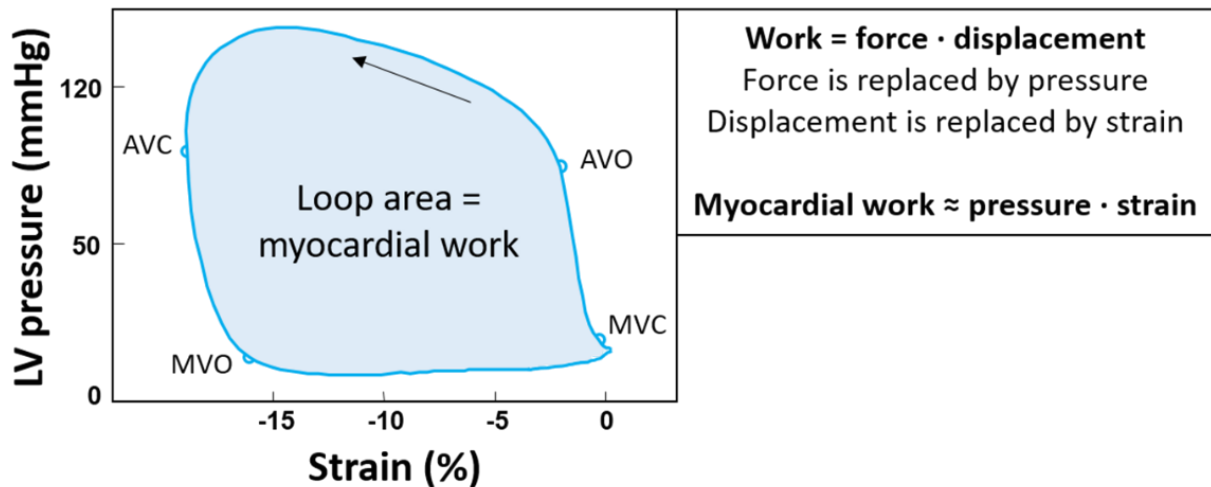


Figure 3. Schematic illustration of a pressure strain loop.

Arrow indicates counter-clockwise rotation during systole, which means systolic shortening and positive work.

LV=left ventricular; MVC=mitral valve closure; AVO=aortic valve opening; AVC=aortic valve closure; MVO=mitral valve opening

A non-invasive LVP curve, personalized to fit the individual patient by timing of valvular opening/closing and scaled by the patient’s systolic brachial cuff pressure, has been extensively tested and validated (25). Of note, this curve is only validated for pressure-strain loop analysis, and cannot be used to calculate diastolic pressure. Moreover, systolic brachial cuff pressure is only validated for this purpose in the absence of significant LV outflow obstruction, and not in patients with severe aortic stenosis (25).

Normally, ventricular segments shorten in systole, when LVP increases, and by definition perform positive work. Contrary, segments that lengthens in systole perform negative work. Net work is positive work minus negative work. The early systolic septal shortening in LBBB represents little work because it occurs at a time point when LVP is low. The late-activated (and pre-stretched) LV lateral wall, on the other hand, performs a high amount of work. By incorporating the effects of variable loading, myocardial work captures these differences between regions, while peak strain may be essential the same (44). Furthermore, in contrast to peak strain, which only captures a single point of time, the myocardial work index provides a quantitative measure of regional myocardial function throughout systole.

The non-uniform distribution of myocardial work in LBBB is reflected in divergent pressure-strain loops from the two opposing regions. As illustrated in Figure 2, in the LV lateral wall, the loop rotates counter-clockwise as a result of normal systolic shortening, and hence performs positive work. The septal pressure-strain loop, on the other hand, rotates both clockwise and counter-clockwise, as septum is stretched throughout most of systole, resulting in a large amount of negative work (25).

Strain by STE combined with non-invasive LVP has been shown to be a valuable measure of regional myocardial function in LBBB, and correlates well with both invasive pressure-segment length in experimental studies and with regional glucose metabolism by FDG-PET in patients with LBBB (25). Still, inadequate echocardiographic image quality precludes strain assessment in some patients. Myocardial work can also be assessed by strain by CMR myocardial tagging in combination with invasive LVP (26). However, clinical utility is limited, as previously mentioned. There is a need for an alternative clinically relevant method to measure regional myocardial work in patients with poor echocardiographic image quality. The present thesis explored the feasibility of calculating septal and lateral wall work in LBBB using strain by FT-CMR and non-invasive LVP.

Septal flash

Septal flash is a hallmark of LV electromechanical dyssynchrony, which was first introduced in the field of CRT by Parsai and co-workers in 2008 (45). However, a dyssynchronous LV contraction pattern was first described in the 1970s using M-mode echocardiography, and named septal beaking (Figure 2) (46, 47). Later, the same phenomenon was identified as a rapid early-systolic colour shift on colour M-mode and named septal flash.

Septal flash is characterized by a rapid leftward-rightward movement of the interventricular septum that mainly takes place during the isovolumic contraction phase, prior to AVO. The pathological septal movement can be seen by simple eye-balling of images or using m-mode echocardiography. Pre-ejection shortening and rebound stretch can also be identified by characteristic strain patterns. The first part of the movement is characterized by an early septal leftward motion during LV pre-ejection phase. The second part consists of rightward motion of septum at the time of LV lateral wall contraction (Figure 2) (45, 46). Although considered a feature of LBBB, the prevalence of septal flash among patients with LBBB varies substantially (45–63%) (48, 49). Coexisting cardiac disease that affects regional contractility in the LV lateral wall and septum may affect the appearance of septal flash (50).

This thesis focuses on septal flash. However, other features of electromechanical dyssynchrony, such as apical rocking, is strongly interrelated with septal flash (49). Apical rocking refers to the “rocking motion” of the apex seen in many patients with LBBB. The early septal shortening first pulls the apex rightward, before the vigorous LV lateral wall contraction moves the apex leftward. This right-left motion causes a characteristic transverse motion of the apex, hence the name apical rocking (51).

The introduction of CRT in modern heart failure treatment has led to a renewed interest in the abnormal septal motion in LBBB. Septal flash and apical rocking assessed by echocardiography has repeatedly been shown to be associated with CRT response in observational and retrospective studies (45, 49, 52, 53). CMR also assesses septal flash, but may be inferior to echocardiography in detecting rapid short-lived septal deformation due to lower temporal resolution (frame rate) (54). Clinical relevance of septal flash assessed by CMR has been scarcely investigated (55).

Myocardial fibrosis

Myocardial fibrosis may be focal or diffuse. Focal fibrosis (scar) is called replacement fibrosis since fibrotic tissue replaces necrotic cardiomyocytes, and is considered irreversible.

In contrast, diffuse fibrosis occurs without cardiomyocyte necrosis, is in principle localized between cardiomyocytes and affects the myocardium in a rather uniform and global distribution. Diffuse fibrosis is potentially reversible (56).

CMR precisely defines the extent and location of focal fibrosis (scar) by the technique of late gadolinium enhancement (LGE), and LGE extent correlates excellently to localized myocyte necrosis on histological examination (57). For distinction between fibrosis and viable myocardium, LGE-CMR relies on administration of a contrast agent, usually gadolinium based. The gadolinium chelate is a tracer that freely distributes in extracellular space, but does not cross the intact cell membrane. Due to a combination of increased extracellular volume and slower washout kinetics, there is a relative accumulation of gadolinium in areas of necrosis, fibrosis, infiltration, and inflammation in the late washout phase. Since gadolinium shortens T1 relaxation time in nearby water protons, it produces brighter signal intensity in T1 weighted sequences. The inversion recovery LGE sequences are designed to increase intensity difference caused by even quite small T1 time differences. Hence, local areas with fibrotic myocardium appears bright white, in contrast to the normal nulled black myocardium.

LGE-CMR is considered reference standard to identify myocardial scar, of both ischemic and non-ischemic aetiology (58). Furthermore, LGE allows differentiation of ischemic cardiomyopathy (ICM) from dilated cardiomyopathy (DCM), and directly informs on the underlying pathogenesis in DCM in some cases. In ICM, LGE is usually located subendocardially or transmurally, in line with the perfusion territories of epicardial coronary arteries. In DCM, the distribution of LGE tends to be patchy, subepicardial or midmyocardial (59). LGE is associated with worsened LV function, abnormal cardiac remodelling and increased ventricular stiffness (60). Furthermore, in DCM, as well as ICM, patients with visible LGE have worse prognosis and outcome, including all-cause mortality, HF hospitalizations and sudden cardiac death (61, 62), supporting independent risk stratification of LGE beyond the contribution of EF. Approximately one-fourth of DCM patients have midwall LGE, illustrated in Figure 2 (61, 62).

Despite high accuracy, LGE-CMR is limited by accessibility and contraindications in some patients. Hence, there is a need for alternative methods to image myocardial scars. Alternative techniques include FDG-PET and echocardiography. The principle behind FDG-PET as method to identify scar, is that myocardial uptake of the radioactive glucose analogue reflects metabolic activity and, hence, viability of the myocardium. Echocardiography may assess myocardial shortening by strain imaging, which would be directly related to viability since non-viable myocardium does not contract. When only part of the wall is viable, there is reduced contraction as reflected in reduced systolic strain. Metabolism and strain correlate with infarct mass in hearts with otherwise preserved contractility and normal electrical conduction (63, 64). In CRT candidates, however, scar imaging by FDG-PET and strain may be challenging, because these patients have variable degree of myocardial dysfunction independent of scar. Furthermore, LBBB itself markedly affects regional myocardial function and metabolism within the ventricle irrespective of scar.

No previous study has validated scar imaging by FDG-PET against the reference standard LGE-CMR in CRT candidates. Former studies have investigated the agreement between strain and LGE in pre-specified patient groups with ischemic cardiomyopathy only (65-67). However, strain has not previously been validated against LGE-CMR in an unselected population of CRT candidates, as encountered in clinical practice, including both ICM and DCM. There is a need to determine if assessment of myocardial metabolism by FDG-PET and LV systolic function by strain echocardiography can identify LV scar in patients referred for CRT, defined by LGE-CMR.

In contrast to focal fibrosis (scar), LGE imaging does not visualize diffuse fibrosis. The more recently introduced technique of CMR T1-mapping, on the other hand, allows these diffuse conditions to be diagnosed by measurement of T1 values and calculation of extracellular volume (ECV). Currently, with a few exceptions, T1 mapping is not implemented in clinical practice and is mainly a research tool. Diffuse (interstitial) fibrosis is considered outside the scope of this thesis.

Heart failure

Heart failure (HF) is a clinical syndrome of symptoms and signs caused by a structural and/or functional cardiac abnormality, resulting in an inadequate cardiac output and/or elevated intracardiac pressures at rest or during stress (68). Patients typically present with shortness of breath, fatigue and/or peripheral oedema. The signs and symptoms of HF result partly from compensatory mechanisms by which the body attempts to adjust for a primary deficit in cardiac output. Although these compensatory neurohormonal mechanisms provide valuable support for the heart in normal physiological circumstances, they also have a fundamental role in the development and subsequent progression of chronic HF. The principal neurohormonal systems involved in the response to HF are the sympathetic nervous system and the renin-angiotensin-aldosterone system (RAAS). The effect is progressive cardiac dilation and/or alterations in cardiac structure (remodelling) where myocardial fibrosis replaces normal cardiomyocytes (69, 70).

HF is common and its prevalence increases with age. In the developed world approximately 1-2% of the adult population is affected, and prevalence is >10% in the age group over 70 years (71-74). The prognosis of HF is generally poor, with 1-year mortality of 20% in all patients hospitalized for HF, even higher among the oldest (75, 76). The diagnosis of HF is based on patient history, physical examination, ECG, cardiac imaging and laboratory testing of natriuretic peptides (usually BNP or NT-proBNP). For further information on diagnostic criteria, the reader is encouraged to consult current guidelines (68, 77).

Depending on the time course and the primary affected ventricle, HF may be classified as acute or chronic, and right-sided or left-sided. Symptomatic burden is commonly graded according to the New York Heart Association (NYHA) functional classification, from class I (no symptoms) to IV (symptoms at rest) (68). The syndrome of chronic LV HF is further subdivided in categories based on LV EF, as measured by echocardiography. If EF is considered preserved (typically $\geq 50\%$), the patient is described as having HF with preserved EF (HFpEF), while a clearly reduced EF ($< 40\%$) is denoted as HF with reduced EF (HFrEF). HF with EF in between (40-49%) is termed HF with mildly reduced EF (HFmrEF) (68). HFrEF and HFpEF typically have different underlying aetiologies, demographics, co-morbidities and response to treatment, although the entities overlap (78). HFmrEF is recognized as a “grey area” with characteristics of both the other groups. This thesis focuses on HFrEF, where CRT is most relevant.

The general goals of treatment are to reduce symptoms and mortality of HF, increase physical capacity and quality of life, and prevent recurrent hospital admissions due to worsening HF. Acute HF can represent a life-threatening condition where specific treatment options consisting of cardio-pulmonary support may be necessary. The further discussion focuses on treatment of chronic LV HFrEF. Underlying aetiology (coronary artery disease, hypertension, arrhythmias, valvular pathology, myocarditis etc.) should be treated according to current guidelines, customized to the individual patient (68).

Pharmacotherapy is the cornerstone of treatment for HFrEF, and should be implemented before considering device therapy, and alongside non-pharmacological interventions. The 2021 ESC guidelines recommend a tetrad of 1) an angiotensin-converting enzyme inhibitor (ACE-I)/angiotensin receptor-neprilysin inhibitor (ARNI), 2) a beta-blocker, 3) a mineralocorticoid receptor antagonists (MRA), and 4) a sodium-glucose co-transporter 2 (SGLT2) inhibitor as cornerstone therapies for patients with HFrEF (68). Angiotensin receptor blockers (ARBs) are alternatives to ACE-I, for example in patients intolerant for ACE-I (79). Guidelines recommend up titrating the medications to maximum tolerated evidence-based doses. Diuretics should be used in addition to the above medications in patients with symptoms and/or signs of congestion. Other drugs may be used for selected patients with HFrEF (68).

In contrast to HFrEF, clinical trials have until recently failed to demonstrate effect on clinical endpoints in patients with HFpEF. In the last years, however, SGLT2-inhibitors have demonstrated reduced cardiovascular mortality and HF hospitalisations in patients with HFpEF, regardless of coexisting diabetes (80). Additionally, ARNI and MRA have gained a place in the guideline directed therapy of HFpEF, primarily in patients with EF in the lower spectrum (81). Latest results show that the glucagon-like peptide-1 (GLP-1) receptor agonist semaglutide reduces symptoms and increases functional capacity in patients with HFpEF and obesity (82). Similar to HFrEF, diuretics should be used to reduce congestion and improve symptoms. Identification and treatment of specific causes such as amyloidosis, and management of contributing comorbidities such as hypertension, coronary artery disease and atrial fibrillation are essential parts of the care of HFpEF patients.

In addition to medical therapies, implantable cardioverter-defibrillator (ICD) and CRT are device therapies for selected groups of patients with heart disease. Implantation of an ICD is recommended in patients who have recovered from a ventricular arrhythmia causing hemodynamic instability (secondary prevention), and for patients with symptomatic HF (ischemic heart disease or dilated cardiomyopathy) with EF \leq 35% (primary prevention) (68). An ICD does not affect the progression of the HF, but prevents sudden cardiac death from arrhythmias. Eligible patients should have a life expectancy substantially longer than 1 year and with good functional status (68). CRT will be discussed separately. Additionally, selected patients with end-stage LV HF who fulfil specific criteria may be candidates for heart transplantation or left ventricular assist device, which is a mechanical pump that pumps blood from the LV and transfers it to the ascending aorta. These are highly specialized treatment options beyond the scope of this thesis.

Cardiac resynchronization therapy

CRT, also known as biventricular pacing, involves simultaneous pacing of the right and left ventricle. In addition to a conventional RV endocardial lead (with or without a right atrial lead), CRT involves an additional coronary sinus lead placed for LV pacing. The LV lead should preferably be placed in a posterolateral vein to pace the otherwise usually last activated myocardial region. The aim is to reverse the pathological consequences of uncoordinated activation, restoring AV-, intra- and interventricular synchrony. CRT decreases morbidity and mortality, improves functional status and reverses pathological LV remodelling in selected patients with chronic HFrEF, compared to optimal medical treatment alone (83, 84) (Figure 4).

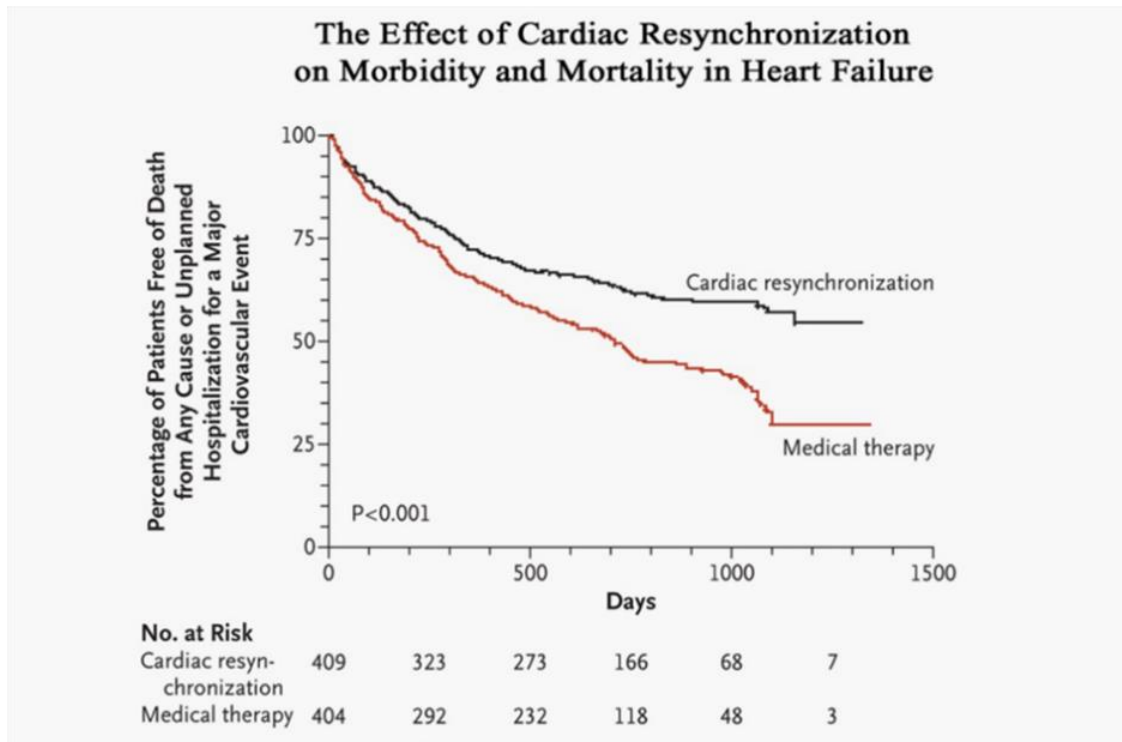


Figure 4. Cardiac resynchronization therapy (CRT) reduces morbidity and mortality in heart failure compared to optimal medical treatment alone.

Reproduced with permission (83), Copyright Massachusetts Medical Society.

Based on current guidelines, CRT is recommended treatment of chronic HF in patients with prolonged QRS (≥ 130 ms and LBBB, or ≥ 150 ms and non-LBBB morphology), with reduced LV function ($EF \leq 35\%$) in NYHA functional class II-IV, despite optimal medical therapy (8, 68). Benefit is less clear for patients in atrial fibrillation, hence criteria are somewhat stricter and recommendations weaker. Patients in NYHA class I may also profit from CRT according to a meta-analysis, suggesting that CRT may also be beneficial in earlier stages of HF (85). For CRT to be successful, biventricular pacing close to 100% of the time is essential (86, 87). In patients with atrial fibrillation, AV node ablation should be considered if inadequate amount of biventricular pacing (8).

Patients with indication for a conventional pacemaker where a high proportion of RV pacing is expected, should be considered for CRT as first line option (88). Guidelines recommend upgrading from a traditional pacemaker to CRT in patients with $EF \leq 35\%$ on optimal medical therapy with significant amount of RV pacing (8). CRT is contraindicated in patients with narrow QRS (89).

The CRT device comes as two options: a sole biventricular pacemaker with pacing only (CRT-P) or combined with a defibrillator (CRT-D). The decision on what device to implant is based on patient comorbidity, age, functional stage and whether the main purpose of the treatment is symptom relief or life prolongation. The defibrillator comes with increased costs and complications, and the mortality benefit is uncertain in non-ischemic HF (90).

Despite convincing effect of CRT in many patients, approximately one-third of the patients who fulfil current selection criteria do not show clinical improvement, and some even

deteriorates. Furthermore, the therapy is costly, and afflicted by risk of serious device related complications (91). Factors known to increase the likelihood of favourable response to the treatment include female gender, longer QRS duration, LBBB morphology, non-ischemic aetiology and absence of myocardial scar (8). The relative importance of QRS duration and QRS morphology (LBBB vs. non-LBBB) is an ongoing debate (92-95). Recent studies also suggest that there might be a “point of no return” where severely depressed LV systolic function implies little chance of CRT response (96, 97).

Current guidelines rely on ECG criteria to identify electrical dyssynchrony and thereby probable CRT response (8). However, baseline QRS-duration is only a moderate predictor of CRT response (29). Furthermore, there are discrepancies between electrical activation by ECG and mechanical contraction by echocardiography in a considerable amount of patients with LBBB (98). Hence, there is a need for better predictive tools to reduce the number of non-responders, especially in the subgroup of patients with intermediate QRS-duration (130-150 ms), where response is particularly variable and guidelines recommendations weaker (8). In light of this, extensive research has been conducted to identify suitable indices of LV dyssynchrony, predominately from echocardiography (99-101), but also from CMR (102-104) and nuclear imaging (105, 106). The majority of the indices are timing indices, based on regional heterogeneity in timing of contractions, either within the left ventricle or between the ventricles. Although initially useful in single-centre studies, none was advantageous over current guidelines in a multicentre setting (107). One reason for the shortcoming of time-to-peak indices may be that they are sensitive to non-electrical causes of LV dyssynchrony (for example scar or fibrosis) (4, 5, 108). If the cause of dyssynchrony is non-electrical, correction by CRT is not likely. Hence, timing indices may be suboptimal markers of a CRT substrate (109, 110). As a result, recent focus has shifted from timing indices towards identifying specific contraction patterns associated with electromechanical dyssynchrony, primarily the abnormal septal contraction pattern in LBBB (111-113).

Former observational studies have indicated that a poorly functioning septum, whether identified visually as abnormal wall motion (septal flash/apical rocking) (45, 49), reduced septal myocardial work (114, 115) or low septal glucose metabolism (116), may reflect septal dysfunction correctable by CRT. Findings that CRT normalizes these changes (25, 49, 117, 118) favour the idea of reduced septal function as a target for CRT. Nevertheless, not all patients respond to CRT despite an apparent septal substrate. We hypothesize that septal recovery to CRT may depend on irreversible septal structural changes (scar).

Transmural posterolateral wall scar is an established risk factor for reduced response to CRT (119-125). In comparison, the significance of septal scar is less clear (121, 122). Still, there is accumulating evidence that also septal scar negatively affects CRT response (126, 127). This is a plausible finding when considering recovery of septal function a main mechanism for CRT response.

Beyond assessing LVEF (most commonly by echocardiography), cardiac imaging has no explicit role in selecting patients for CRT. Guidelines recommend to avoid placing the LV lead in non-viable tissue, but routine scar assessment is not included in current selection criteria, neither is imaging assessment of LV dyssynchrony (8).

The persistently high proportion of non-response to CRT are probably caused by multiple factors, ranging from suboptimal patient selection criteria, technological failure to maximize the potential of the therapy, as well as post-implant monitoring. Targeting implantation of the LV lead at the site of latest mechanical activation as measured by strain improves response rate (128). Optimizing AV-delay in non-responders using echocardiography is suggested to

improve response, but the clinical value is uncertain (8). The adaptive CRT algorithm allows fusing of LV pacing with the intrinsic electrical activation (provided PR-interval is normal), to achieve a more physiological LV activation (129). The present thesis focuses on improving patient selection to CRT by cardiac imaging.

Aims

General aims

The overall aim of this thesis was to study regional LV function in LBBB to improve understanding of LV dyssynchrony on myocardial function and CRT response. We sought to explore if CMR-FT in combination with non-invasive LVP is a relevant measure of regional myocardial function in LBBB. Furthermore, we investigated how regional LV function, in terms of glucose metabolism and strain/work, correlate with regional LV scar in dyssynchronous ventricles. Finally, we hypothesized that a viable, but dysfunctional septum is a substrate for CRT. We postulated that this substrate is identifiable by CMR as single image modality, and that CMR therefore can improve patient selection to CRT beyond current guidelines criteria.

Specific aims

Paper 1

We aimed to test the feasibility of calculating regional myocardial work from strain by CMR-FT and non-invasive LVP in patients with HFrEF and LBBB.

Paper 2

We aimed to determine if myocardial metabolism by FDG-PET and LV systolic function by strain echocardiography could identify LV scar in patients referred for CRT, compared to LGE-CMR as reference standard.

Paper 3

We aimed to test the hypothesis that combined assessment of septal scar and LV dyssynchrony (septal flash) by CMR as single image modality predicts response to CRT in a prospective, multicentre study.

Materials and methods

Study population

Two hundred and thirty-six patients referred for CRT implantation were prospectively included at Oslo University Hospital, Rikshospitalet (Norway) (n=101), University Hospitals Leuven (Belgium) (n=50), Rennes University Hospital (France) (n=71), OLV Clinic, Aalst (Belgium) (n=11) and Karolinska University Hospital (Sweden) (n=3). Patient inclusion lasted from September 2015 to November 2017. Potential CRT candidates were referred from local hospitals to their respective tertiary centre, where suitability was assessed and, if deemed appropriate, CRT implanted. During study inclusion, approximately 200 CRTs were implanted in Oslo, 300 in Rennes and 120 in Leuven. This means that roughly 35% of patients that received CRT in the main contributing centres were included. Inclusion criteria was indication for CRT according to 2013 ESC guidelines (130). Study exclusion criteria were recent myocardial infarction or coronary artery bypass surgery, previous heart transplantation, implanted intraventricular assist device, severe aortic stenosis, uncorrected congenital heart disease or failure to obtain adequate LV volumes by echocardiography.

The name of the study was “Contractile Reserve in Dyssynchrony: A Novel Principle to Identify Candidates for Cardiac Resynchronization Therapy (CRID–CRT)”. The study was registered at clinicaltrials.gov (identifier NCT02525185).

Of the total 236 patients, 153 performed a CMR scan and were subsequently considered for inclusion in one or more of the present studies. Main reason for not performing CMR was previous CMR unsafe intracardiac devices (n=53). For the remaining patients (n=30) reasons included patient refusal, intracranial metal implants and logistical causes/no available CMR slot. Three CMR examinations were excluded from further analysis because of technical failure/reduced image quality. The remaining 150 patients were considered for inclusion in one or more of the studies according to study inclusion criteria (described later). Of these, eight patients were examined without contrast agent because of reduced renal function ($eGFR \leq 45 \text{ ml/min/1.73m}^2$). A flowchart illustrating patient inclusion for the different studies is presented in Figure 5. Naturally, there was a great overlap between patients included. Of the 37 patients in paper 1, all were also included in paper 2, while 35 were included in paper 3. The remaining two were excluded from the outcome-paper because criteria for CRT was not fulfilled ($LVEF > 35\%$) or because the leads had to be extracted shortly after implantation (due to endocarditis). The ten patients that did not fulfil the inclusion criteria for paper 2, did not receive CRT, and were consequently also excluded from paper 3. One patient did not fulfil the criteria for CRT because LVEF had improved substantially since the time of referral, but was still eligible for inclusion in paper 2. Correspondingly, so were the three patients without appropriate follow-data (Figure 5). The eight patients that were examined without administration of a contrast agent were all excluded from paper 2, but included in paper 3 (except for scar analyses).

FDG-PET was performed at two centres (Oslo and Leuven). Of the 151 patients potentially eligible, 93 patients successfully underwent a FDG-PET scan. The main reason for not undergoing PET was patient refusal/no available time slot (n=51). Others were discarded from analysis due to inadequate image quality (n=6) or failure to carry out preparation protocol because of insufficiently controlled diabetes mellitus (n=1).

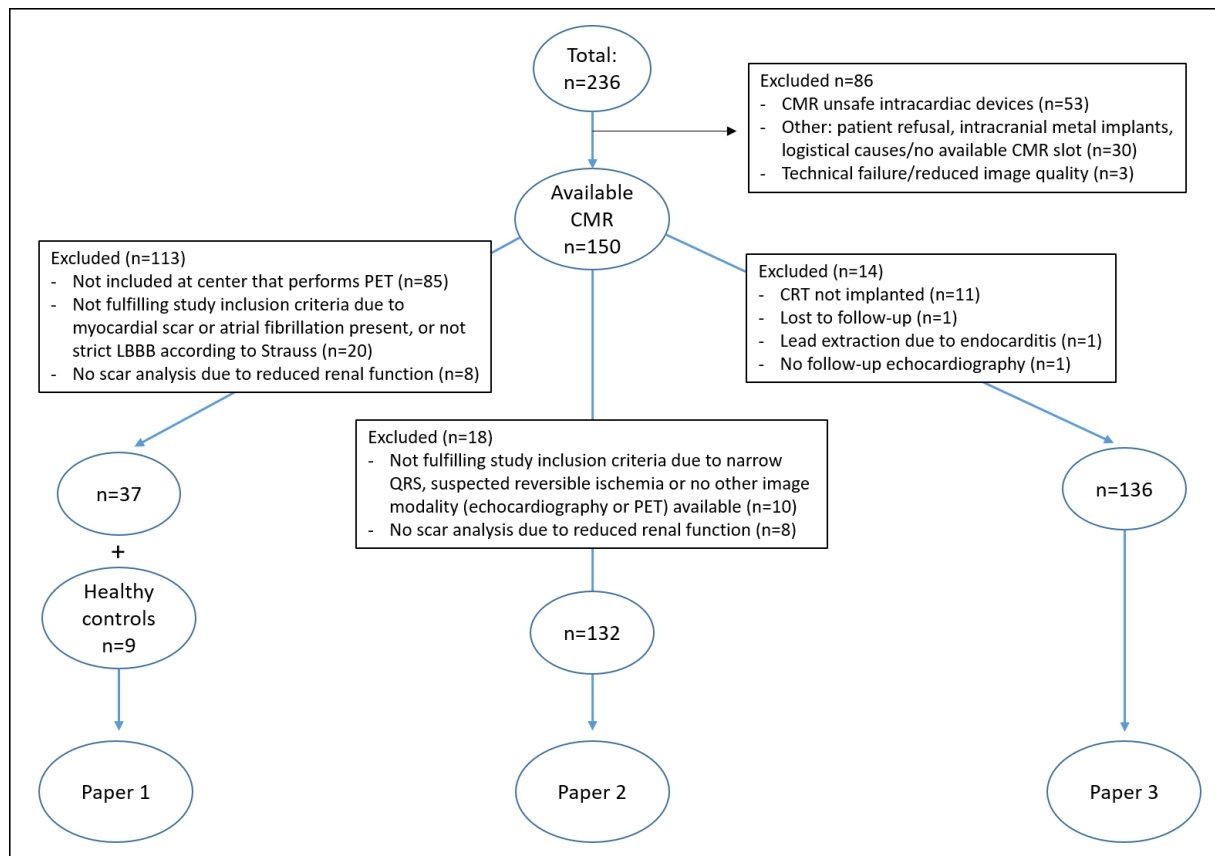


Figure 5. Flowchart illustrating patient inclusion in all three studies.

CMR=cardiac magnetic resonance; PET=positron emission tomography, LBBB=left bundle branch block; CRT=cardiac resynchronization therapy

Medical history, including cardiac symptoms (NYHA class) and medications, as well as a 12-lead electrocardiogram (ECG) were obtained at study enrolment, usually the day before CRT was implanted. The author of this thesis, together with PhD fellow John Moene Aalen and study nurse Kari Melberg, included all study patients in Oslo.

Paper 1 also included nine control subjects without LBBB or other known cardiac disease. These subjects were recruited through voluntary enrolment in the community. Normal QRS duration was defined as ≤ 120 ms.

The Regional Committee for Medical Research Ethics at all participating centres approved the studies, which complied with the Declaration of Helsinki. Written informed consent was obtained from all study participants.

Paper 1

Paper 1 was a feasibility study to investigate if regional myocardial work could be assessed from strain by FT-CMR and non-invasive LVP in patients with HF and LBBB. The estimated regional myocardial work distribution was compared to work distribution assessed by speckle tracking echocardiography and non-invasive LVP, and to the distribution of glucose metabolism by FDG-PET. Glucose metabolism was used as a marker of myocardial energy

demand and hence as a useful correlate for regional myocardial work. The distribution of LV workload in patients with LBBB was compared to the results of healthy controls with normal ECGs.

For this study, we aimed for a homogenous patient population, minimizing confounding factors that could influence the results. We therefore studied patients with strict LBBB as defined by Strauss and co-workers (11) selectively, and excluded patients with myocardial scar by LGE-CMR or renal failure not permitting administration of a contrast agent ($eGFR \leq 45\text{ml/min/1.73m}^2$). We also excluded patients with atrial fibrillation at the time of examination given the difficulty in obtaining strain traces and myocardial work in the case of significant R-R variability. Furthermore, to achieve the highest possible number of patients with FDG-PET, we included patients from the two centres that performed FDG-PET only (Oslo and Leuven) (Figure 5).

In total, 37 patients with HF and LBBB (QRS-duration $165 \pm 15\text{ms}$), as well as nine healthy controls (QRS-duration $90 \pm 9\text{ms}$), were studied.

Paper 2

In paper 2, we investigated if assessment of myocardial metabolism by FDG-PET and LV systolic function by strain echocardiography can identify LV scar in patients referred for CRT. In addition to strain, we measured myocardial work from strain combined with non-invasive LVP. As reference method for scar, we used LGE-CMR. Focus was on the LV lateral wall and septum. For this study, we included all patients from the multicentre study with QRS width $>120\text{ms}$, no signs of reversible ischemia and available echocardiographic images who completed a successful LGE-CMR scan ($n=132$) (Figure 5). Reversible ischemia was excluded based on clinical history, supplemented with coronary angiography if considered necessary by the physician in charge. All patients underwent echocardiography and 53 completed FDG-PET to assess regional glucose metabolism.

Paper 3

Paper 3 was a prospective observational study where we investigated if combined assessment of septal scar and LV dyssynchrony by CMR as single image modality could identify CRT responders beyond current guidelines criteria. We performed CMR with LGE to define myocardial scar. LV dyssynchrony was assessed visually as septal flash on cine sequences, and as asymmetric LV work distribution (by FT-strain and non-invasive LVP). The 136 patients with available CMR and follow-up data from the total study population were included. Reasons for lack of follow-up data were CRT not implanted ($n=11$), study withdrawal ($n=1$), no available follow-up echocardiography ($n=1$) and lead extraction due to endocarditis ($n=1$) (Figure 5). Study inclusion criteria was indication for CRT according to European Society of Cardiology (ESC) 2013 guidelines (130). To assess volumetric response, echocardiography was repeated at 6 ± 1 months follow-up. Survival was assessed at 39 ± 13 months follow-up.

LBBB in paper 2 and 3 was defined according to the guidelines of the European Society of Cardiology (68).

Cardiac Magnetic Resonance

Patients were scanned with a 1.5 or 3.0 Tesla unit (in Oslo, Rennes and Stockholm: Aera, Skyra or Verio, Siemens, Erlangen, Germany, in Leuven: Ingenia, Philips Healthcare, Best, the Netherlands, in Aalst: Signa HDXT, GE, Boston, US). Frame rate was 31 ± 3 frames per heart cycle.

Left ventricular volumes and ejection fraction

Long- and short axis cine sequences were acquired using a steady-state free precession sequence. Acquisition was performed with ECG gating and during breath-holds as routinely performed in clinical practice. Short axis slices to cover the entire left ventricle were obtained. From these images, endo- and epicardial borders were delineated, and subsequently LV volumes and EF measured with *Segment software v2.0 R5270* (Medviso AB, Lund, Sweden) (131).

Myocardial strain

Circumferential strain from cine images was analysed for paper 1 and 3. Analyses were performed semi-automatically with FT software (2D CPA MR; TomTec Imaging Systems, Unterschleissheim, Germany) in mid-ventricular short-axis view. The endocardial border was delineated manually and adjusted to achieve optimal tracking throughout heart cycle. Tracking quality was evaluated visually by the operator, and if a case had inadequate tracking despite repeated adjustments, it was excluded. In paper 1, no patient was excluded due to inadequate tracking, but in paper 3, six patients were excluded for this reason.

Regional non-invasive myocardial work index

We used the previously mentioned non-invasive estimate of LVP curve to calculate an index of segmental myocardial work based on pressure-strain analysis. In 2012, the method was innovated in our lab and validated against invasive LVP (25). First, a large number of invasively measured LVP traces were sampled. Then, peak LVP, and the isovolumic and ejection phases, were normalized to create an average reference curve. The reference curve is subsequently adjusted to the individual patient by adding timing of valvular events (provides information on cardiac phases) and scaled by peak LVP (usually approximated as brachial systolic cuff pressure). The work index (mmHg·%) is calculated by multiplying the rate of segmental shortening (strain rate) with instantaneous LVP from the individually adjusted reference curve. This is integrated over time from mitral valve closure to mitral valve opening, and the result is net work performed during systole, which largely corresponds to the area of the pressure-strain loop.

For all work analyses in the present studies, the estimated LVP curve was derived from a semi-automated analysis tool (Echopac, version 202, GE Vingmed Ultrasound, Horten, Norway), and adjusted to the duration of the cardiac phases by visual assessment of valvular events by CMR and echocardiography, respectively. Strain was assessed as described in the respective sections. Polar maps were constructed using a 17-segment model (AHA) (132). “Septum” was defined as the anteroseptal and septal segments and the “LV lateral wall” as the

lateral and posterolateral segments. Blood pressure was measured by the brachial cuff method at the beginning of the echocardiographic examination. Septal and LV lateral wall work were calculated as the average of the two associated segments. LV segments that shorten in systole, when LVP increases, by definition do positive work. Contrary, elongation in systole when LVP increases by definition implies negative work. We calculated net work as the sum of positive and negative work. Lateral-to-septal work difference, which was used as a measure of LV dyssynchrony in paper 3, was calculated as the difference in net work between the LV lateral wall and septum. In paper 1, we used pressure-strain curves to illustrate the deformation pattern in LBBB.

The author of this thesis performed the strain and work analyses by FT-CMR, without knowledge of echocardiographic volume data. For the reproducibility testing in paper 1, a colleague in Oslo performed repeated analyses.

Septal flash

In paper 3, septal flash was used as parameters of abnormal septal function and LV dyssynchrony. Septal flash (45) was defined as an early and fast left-right motion (thickening/thinning) of the interventricular septum that starts and mostly ends during the isovolumic contraction phase prior to aortic valve opening, illustrated in Figure 6.

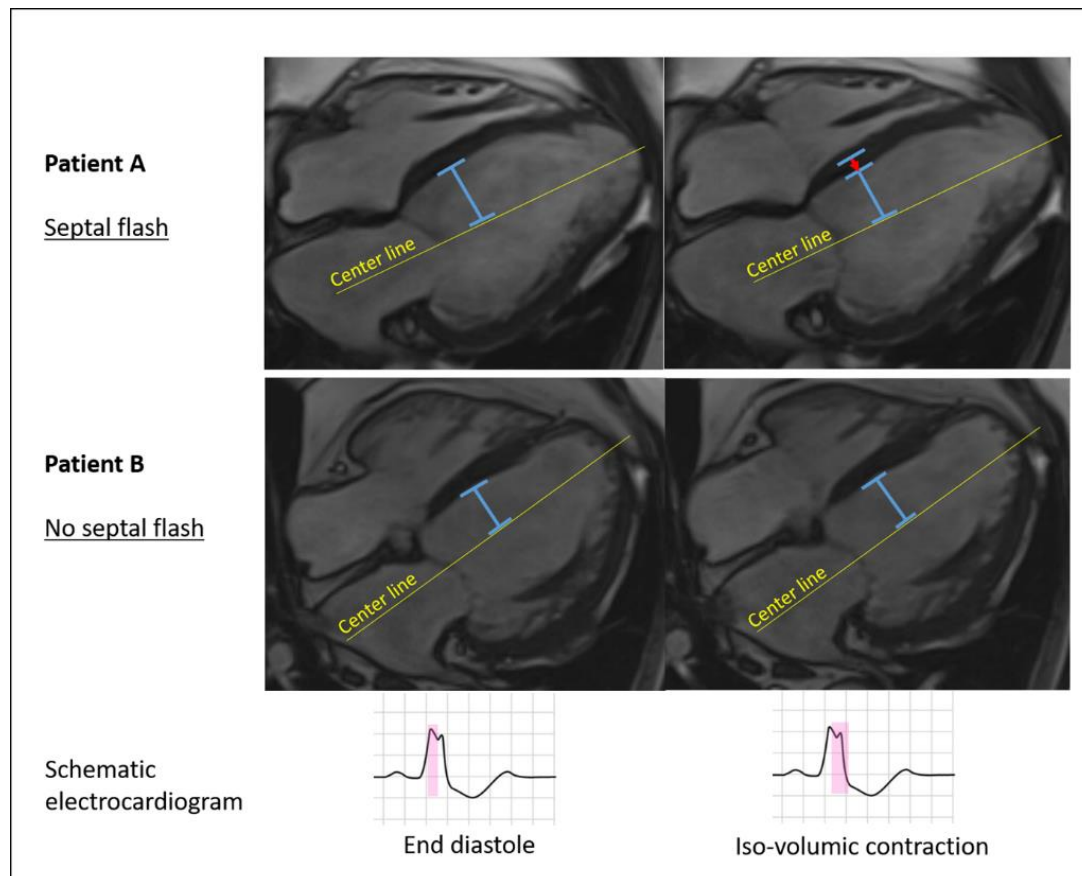


Figure 6. Schematic illustration of septal flash by CMR cine images.

Patient A displays an early contractile motion of the interventricular septum (septal flash) with no apparent motion of the lateral wall during iso-volumic contraction phase. Patient B demonstrates no pre-ejection septal movement (no septal flash).

We determined septal flash visually as a binary phenomenon (yes or no) on cine sequences from the apical 4-chamber long axis view or any of the short axis views. To test reproducibility of septal flash, we performed inter-centre variability testing in 25 randomly selected patients. The author of this thesis performed the analyses of septal flash in all patients, without knowledge of echocardiographic volume data. A colleague in Leuven performed repeated analyses to test inter-centre reproducibility.

Late gadolinium enhancement

LGE was assessed in 142 of the 150 patients with successful CMR scan, while eight patients were examined without administration of a contrast agent because of reduced renal function ($eGFR \leq 45\text{ml/min/1.73m}^2$). LGE images were obtained after intravenous injection of either 0.15 (n=86) or 0.20 (n=51) mmol/kg gadoterate meglumine (Doteram™, Guerbet, Villepinte, France), or 0.15 mmol/kg gadobutrol (Gadovist™, Bayer AB, Stockholm, Sweden) (n=3), or 0.15 mmol/kg gadobenate dimeglumine (MultiHance®, Bracco, Milan, Italy) (n=2).

Presence of LGE was determined visually by an experienced radiologist, and classified as ischemic or non-ischemic. Thereafter, if present, fibrotic foci were quantified semi automatically with the freely available Segment software v2.0 R5270 (Medviso AB, Lund, Sweden) (133) from a stack of short axis slices using the automatic algorithm EWA (expectation maximization, weighted intensity, a priori information) (Figure 7).

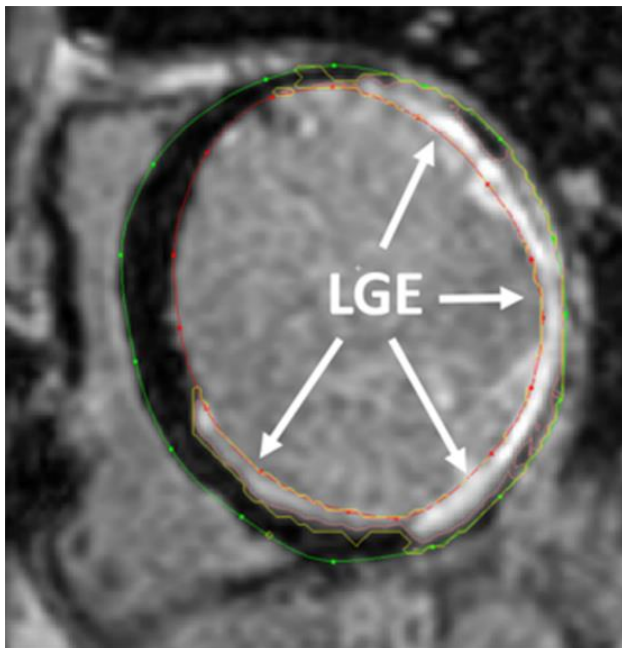


Figure 7. Illustration of transmural LV lateral wall scar identified by LGE-CMR.

The image is a short-axis view, with the contours of the left ventricle manually drawn. The scarred regions (LGE) appear bright white and are delineated by the semi-automatic software. The transmural lateral wall scar extends to the anterior and inferior walls.

LV=left ventricular, LGE-CMR=late gadolinium enhancement cardiac magnetic resonance.

The automatic quantification of scar size was corrected manually if appropriate. Papillary muscles were regarded as part of the ventricular cavity. Polar maps were constructed using a 17-segment model (AHA) (132), and the apical segment (segment number 17) were excluded from analysis. Myocardial scar was reported as percentage LGE of total tissue volume per segment (paper 2) or per wall (average of associated segments) (paper 3). LGE was analysed and reported the same way independent of underlying aetiology (ischemic or non-ischemic). Any LV myocardial LGE was reported, including RV insertion fibrosis and midmural LGE.

All patients with previous infarctions were excluded from paper 1. In paper 2, we defined non-transmural scar as LGE <50% of segmental tissue volume, and transmural scar as LGE ≥50% of segmental tissue volume. In paper 3, we used LGE as a continuous variable in regression and ROC curve analysis. However, in the same paper, we also categorized patients by using septal LGE as a binary parameter (present or not present) in the suggested flowchart.

Echocardiography

Transthoracic two-dimensional echocardiography was performed in all patients. A Vivid E9 or E95 ultrasound scanner (GE Vingmed Ultrasound, Horten, Norway) was used to acquire grey-scale echocardiographic images from the parasternal and apical views. Average frame rate was 65±10 frames/s. Together with John Moene Aalen, the author of this thesis performed the echocardiograms in patients from Oslo.

Ventricular volumes and LV ejection fraction were calculated by the biplane Simpson's method at baseline and at 6 months follow-up. Longitudinal strain was measured by speckle tracking echocardiography from the three apical views using an 18-segment model (Echopac, GE Vingmed Ultrasound, Horten, Norway) in paper 1 and 2. A colleague from Oslo blinded to the scar analyses, performed the strain analyses. The same investigator also calculated segmental myocardial work by pressure-strain analysis as described in previous sections. In paper 1, "septum" and "the LV lateral wall" was defined similarly to CMR analysis (anteroseptal/septal segments and lateral/posterolateral segments, respectively). In paper 2, we averaged the two apical septal and the two apical lateral wall segments from echocardiography (18 segments) to achieve comparable results with CMR (16 segments used).

Radial strain, originally intended included in paper 2, was excluded from analysis because measurements were often unsuccessful due to thin LV wall in many patients.

Positron Emission Tomography

Segmental glucose metabolism was assessed by ¹⁸F-fluorodeoxyglucose (FDG) Positron Emission Tomography (PET) at two centers (Oslo and Leuven). Scanners used were Biograph 64 or 16 HiRez PET/CT (Siemens, Erlangen, Germany) and Discovery MI PET/CT (GE Healthcare, Chicago, Illinois, US). Patient preparation consisted of a hyperinsulinemic euglycemic clamping method (134) or an oral glucose loading protocol. After stabilization of the glucose levels, 370 MBq FDG was administered and a 40 minutes acquisition was performed 45 minutes after injection. PET-images were reconstructed using ordered-subsets expectation maximization algorithms (4 iterations and 8 subsets), matrix size 256x256, and a 5.0 mm Gaussian filter. Attenuation correction with CT was performed. Polar maps using a 17 segment model (AHA) (132) were constructed, and segmental values expressed in percentage

of the segment with maximum mean glucose uptake. The investigation was performed during resting conditions and the patients were instructed to avoid exercise the days before.

In paper 1, where glucose metabolism was used as a correlate to regional myocardial work, septal and lateral glucose uptake was calculated as average of the respective segments (corresponding to the segments from which regional work was derived). In paper 2, where agreement to LGE-CMR was tested, all segments except the apex (segment 17) were reported separately. A trained colleague in Leuven performed all the PET analyses.

Endpoints

In paper 1, we used work calculations from STE-strain and non-invasive LVP as a comparison to work by FT-strain and non-invasive LVP. We chose this reference method because of its previous extensive testing and validation in different scenarios (25). To strengthen our findings further, we also used glucose metabolism by FDG-PET as a marker of myocardial energy demand and as a correlate for regional myocardial work (in patients with available FDG-PET results). To test reproducibility of the work estimates, we performed inter- and intraobserver analysis.

In paper 2, we used segmental LGE to define myocardial scar, to which agreement of strain by echocardiography and FDG-uptake by PET were tested. As stated previously, transmural scar was defined as LGE $\geq 50\%$ of segmental volume, and non-transmural scar as LGE $< 50\%$ of segmental volume.

Primary endpoint in paper 3 was reverse remodelling at six (6 ± 1) months follow-up defined as $\geq 15\%$ reduction in LV end systolic volume indexed to body surface area (ESV_i). Volumes were measured by echocardiography using the biplane Simpson method from the apical 2- and 4-chamber view. Due to significant inter- and intraobserver variability of such measurements (135), all volumes were measured at three different locations (Oslo, Leuven and Rennes) by different observers blinded to other parameters. In case of disagreement on response, a majority decision was made. We used the average of agreeing volumes to determine CRT response, and change in $LVESV_i$ was used as a continuous variable in regression analysis to identify predictors of reverse remodelling.

Secondary endpoint in paper 3 was death of any cause or heart transplantation, and was assessed at 39 ± 13 months follow-up.

CRT implantation

The decision to implant CRT was based on current ESC guidelines, and the responsible electrophysiologist made the final decision. Implantation procedure and device manufacturer were according to clinical routine at the respective centres. Coronary venography was used to guide implantation, and the LV lead was placed in a lateral or posterolateral vein if possible, preferably away from scar. The device was programmed in a conventional biventricular pacing mode and retested prior to hospital discharge.

Statistics

Continuous variables are expressed as mean \pm standard deviation (SD) if normally distributed, or as median (interquartile range) if distribution is skewed. Categorical variables are presented as percentages. Comparisons between groups were performed with two-sampled t-tests, Mann–Whitney U test or chi-square test as appropriate.

To measure the linear relationship between continuous variables in paper 1, we used scatter plots and Pearson's correlation coefficient. Intra- and inter-observer variability was assessed by intraclass correlation coefficient (ICC) (paper 1 and 3) and Bland–Altman plots with calculation of the 95% limits of agreement (paper 1). In paper 3, we used linear regression analysis with left ventricular end systolic volume change as dependent continuous variable to identify significant predictors for reverse remodeling (primary endpoint). Receiver operating characteristic (ROC) curves with area under the curve (AUC) and 95% confidence interval (CI) were used to evaluate agreement of different parameter to scar (paper 2) and to determine properties of suggested approaches to select CRT responders (paper 3). To test combined assessment of two parameters, we first performed logistic regression analysis to calculate probability of response, which was subsequently used to construct ROC curves. ROC curves were compared by the Hanley and McNeil method (MedCalc Software version 19.8) (136). To assess long-term survival (secondary endpoint in paper 3), we used hazard ratio with 95% CI from Cox regression and log-rank test from Kaplan-Meier curves. Censoring was administrative due to individuals entering the study on different time points and, hence, different observation times.

All tests were two-tailed, and a P-value <0.05 was considered statistically significant. SPSS version 25.0 (IBM Corporation, Armonk, NY) was used for analyses.

Summary of results

Paper 1

All patients had ECG features of LBBB according to Strauss, while controls had normal ECGs. QRS-duration in the two groups was 165 ± 15 and 90 ± 9 ms, respectively ($p<0.001$). Systolic blood pressure was similar between groups (133 ± 23 vs 129 ± 19 mmHg, $p=0.62$). All studied subjects were in sinus rhythm.

In the LBBB patients, circumferential strain by FT-CMR demonstrated a classical LBBB deformation pattern and associated pressure-strain loops (Figure 8). Contrarily, in the control subjects, the septal and LV lateral wall strain traces were more synchronous and the pressure-strain loops more homogenous. Patients with LBBB displayed higher amount of myocardial work in the LV lateral wall compared to septum (1978 ± 1084 vs 51 ± 537 mmHg·%, $p<0.001$). In contrast, there was no difference in workload between the two walls in the controls (2182 ± 747 vs 2131 ± 563 mmHg·%, $p=0.73$). Both net septal work and septal/LV lateral wall work ratio were significantly lower in LBBB patients compared to controls ($p<0.001$ for both). LV lateral wall work was not different between the groups ($p=0.37$).

Reproducibility of the measurements was good. Repeated analysis by two independent observers showed a mean difference in regional work of 11 mmHg·%, with an average work of 870 mmHg·%. Repeated work analyses by the same observer revealed a mean difference of 41 mmHg·%, with an average work of 897 mmHg·% (Figure 9). Inter- and intra-observer ICC was 0.96 (95% CI 0.91-0.98) and 0.98 (95% CI 0.96-0.99).

To further support our hypothesis that regional myocardial work by FT-CMR and non-invasive LVP is a relevant measure of function in LBBB, we used analogous work estimates from STE and glucose metabolism by FDG-PET for comparison. Strain traces, pressure-strain loops and regional work distribution derived from echocardiography were very similar to the ones from CMR, and correlation between segmental values was good (average $r=0.71$ within the same patient). Corresponding to the asymmetric work distribution there was an imbalance in regional glucose metabolism within the ventricle, where septal glucose uptake was reduced compared to lateral wall uptake ($51.1\pm 17.6\%$ vs $94.5\pm 4.2\%$, $p<0.001$) (Figure 10). The correlation between segmental values of regional work by CMR and glucose metabolism by FDG-PET was strong, with average $r=0.80$ and individual values ranging from 0.54 to 0.96.

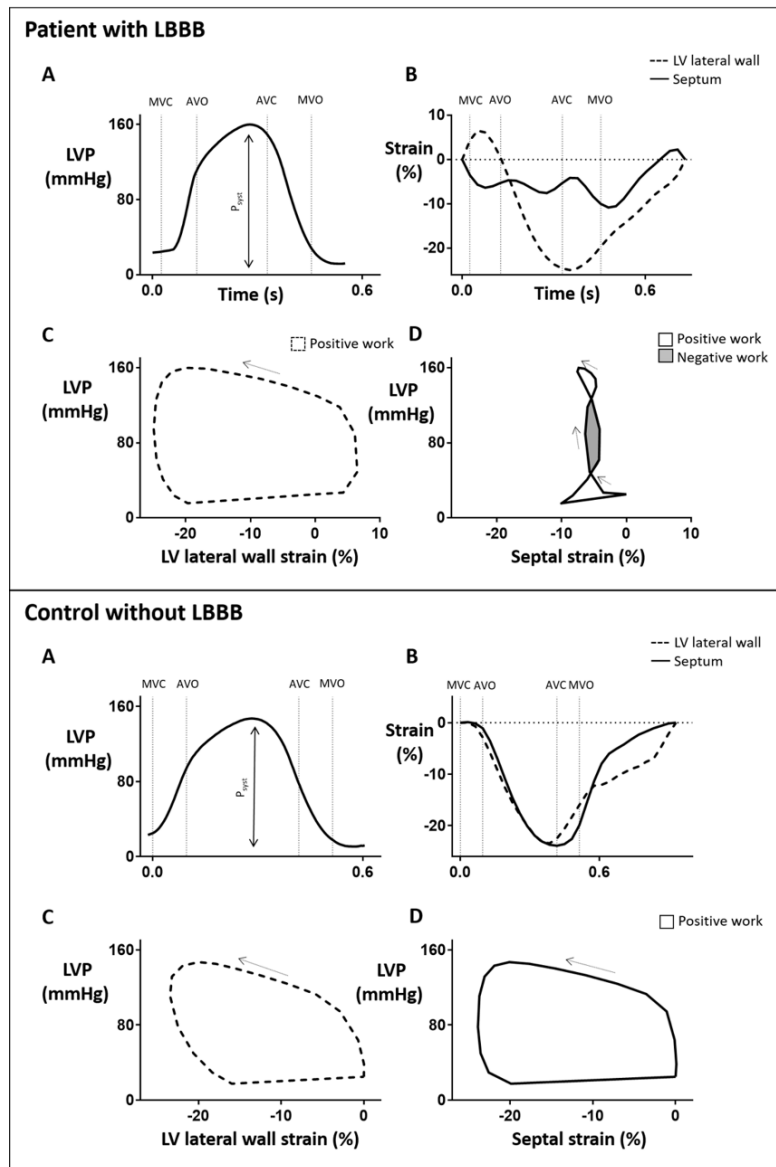


Figure 8. Calculation of pressure-strain loops from non-invasive LVP and circumferential strain from FT-CMR.

Data from one representative LBBB-patient (upper panel) and one control with normal electrical conduction (lower panel).

Estimated LVP curves (A) and strain traces (B). In the healthy control, the strain traces from septum and the LV lateral wall are synchronous. In contrast, the strain traces from the LBBB patient shows classical LBBB deformation pattern, where the septal segment, after an early short contraction, is mainly stretched through most systole. The lateral wall is slightly stretched during early systole, followed by a forceful contraction.

Pressure-strain loops (C and D). In the LBBB patient, the pressure-strain loop from the lateral wall rotates counter clockwise, indicating positive work throughout the entire heart cycle. In septum, on the other hand, the pressure-strain loop rotates clockwise during part of systole (negative work), reducing net work. The pressure-strain loops from the LV lateral wall and septum in the healthy control both perform positive work (counter clockwise rotation).

AVC=aortic valve closure; AVO= aortic valve opening; FT-CMR=feature tracking cardiovascular magnetic resonance; LV=left ventricular; LVP=left ventricular pressure; MVC=mitral valve closure; MVO=mitral valve opening; P_{syst} =systolic arterial cuff pressure

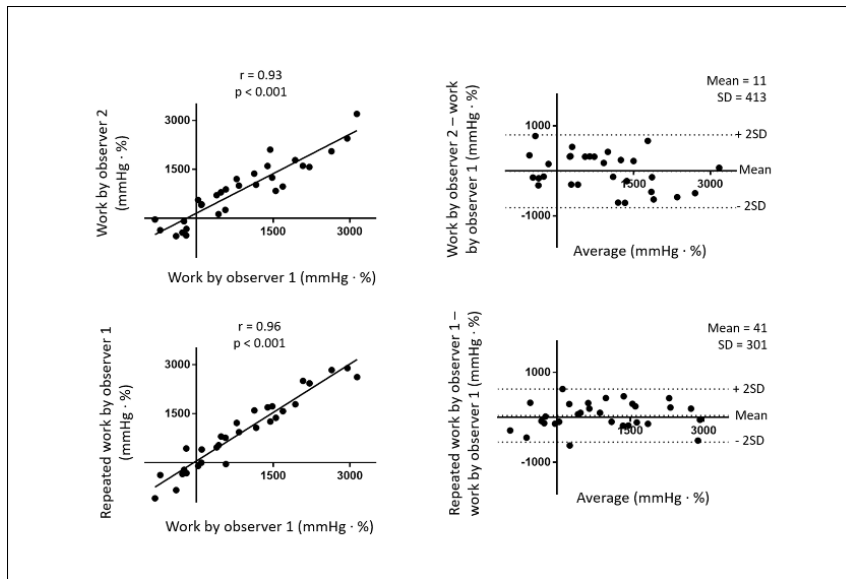


Figure 9. Correlation and agreement between reproducibility analysis of myocardial work by FT-CMR and non-invasive LVP.

Scatterplots with linear regression lines (left) and Bland-Altman plots (right) for inter- and intraobserver variability of regional myocardial work in 15 randomly selected patients.

FT-CMR=feature tracking cardiovascular magnetic resonance; LVP=left ventricular pressure; LV=left ventricular

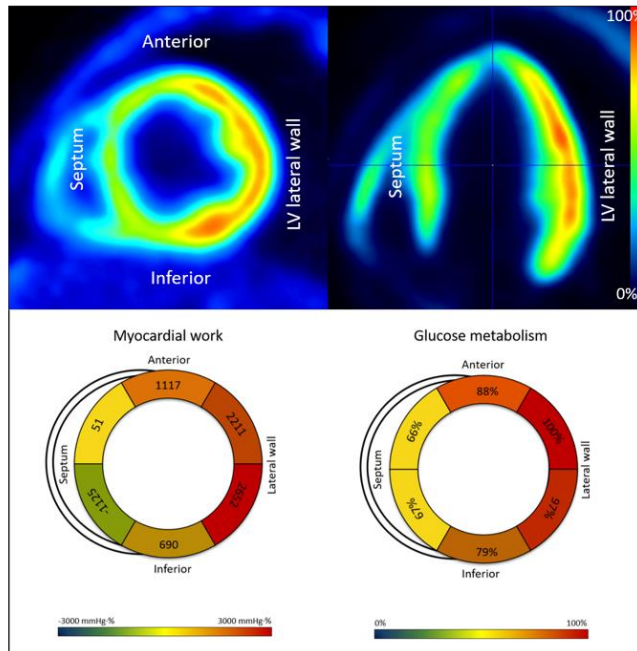


Figure 10. Regional distribution of glucose metabolism and myocardial work in LBBB.

Low septal metabolism by FDG-PET (upper panel) and myocardial work by FT-CMR and non-invasive LVP (lower panel) compared to the LV lateral wall in one representative patient with LBBB. Segments with reduced metabolism correspond to segments with reduced work.

FDG-PET=fluorodeoxyglucose positron emission tomography; FT-CMR=feature tracking cardiovascular magnetic resonance, LBBB=left bundle branch block; LVP=left ventricular pressure

Paper 2

In total, 2106 segments were available for scar analysis. Mean QRS-width was 164 ± 17 ms, and 91% of the patients had LBBB.

Patients with no myocardial scar and patients with septal scar had markedly reduced myocardial glucose metabolism in septum compared to the LV lateral wall. Maximum glucose uptake was generally located in the LV lateral wall, except in patients with transmural lateral wall scar, who had clearly reduced glucose metabolism in this region (Figure 11).

FDG-PET identified transmural scars ($LGE \geq 50\%$) in the LV lateral wall with high accuracy (AUC=0.96, 95% CI 0.90-1.00) (Figure 12). Optimal cut off was glucose uptake $< 70\%$ relative to the segment with highest uptake. Using this cut off, sensitivity and specificity for identifying transmural lateral wall scar was 94% and 91%, respectively.

In contrast to the LV lateral wall, there was substantial overlap in glucose metabolism in septal segments with no myocardial scar (52%, 95% CI: 25-86%) and septal segments with transmural scar (42%, 95% CI: 21-74%). In both cases, septal metabolism was clearly reduced compared to the LV lateral wall (Figure 11). The weak association between glucose metabolism by FDG-PET and scar by LGE-CMR in septal segments means that FDG-PET did not identify septal scar in this patient population.

Corresponding to regional asymmetry in glucose metabolism, the LV lateral wall had higher absolute values of peak systolic strain compared to septum in ventricles with no scar (-12.6% , 95% CI: -1.3 to -24.7 versus -8.9% , 95% CI: -0.4 to -20.1 , $p < 0.001$). The asymmetry in FDG metabolism correlated with asymmetry in workload ($r = 0.44$, $p = 0.001$).

The accuracy of peak systolic strain to identify lateral wall transmural scar was only moderate, with AUC of 0.77 (95% CI: 0.71-0.84) (Figures 11 and 12). However, absolute peak systolic strain $> 10\%$ identified lateral wall segments without transmural scar with high sensitivity (80%) and high negative predictive value (96%). In contrast to rather preserved strain, peak strain $< 10\%$ was inconclusive with regard to transmural scar.

The accuracy of peak systolic strain to identify transmural septal scar was low (AUC 0.69, 95% CI: 0.60-0.78) (Figures 11 and 12). Myocardial work provided no added value to identify transmural scar in neither the LV lateral wall nor septum, compared to peak systolic strain.

Neither FDG-PET nor echocardiography identified non-transmural scar ($LGE < 50\%$) in either wall.

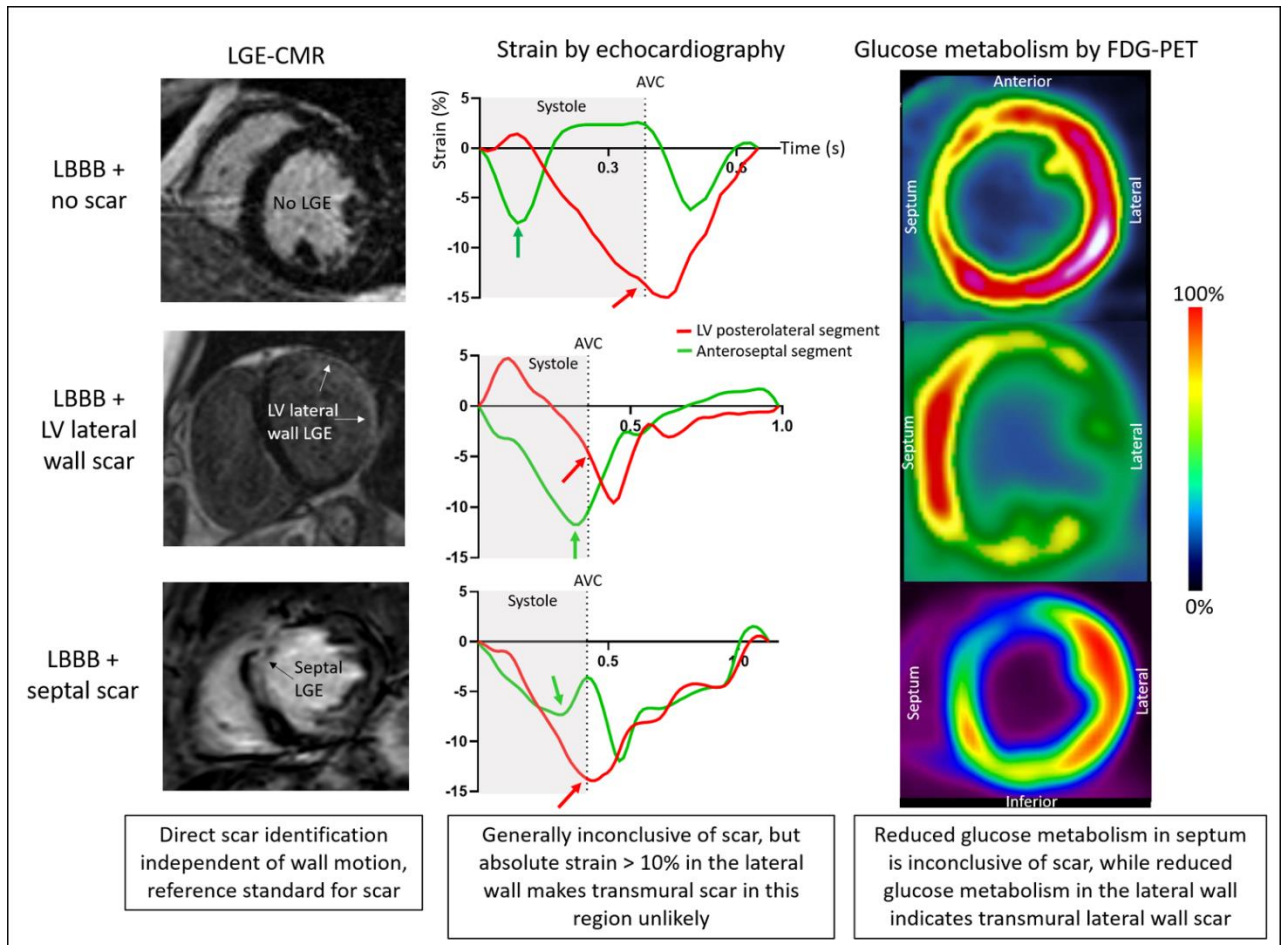


Figure 11. The ability of peak systolic strain by echocardiography and glucose metabolism by FDG-PET to identify transmural LV lateral and septal scar in CRT candidates compared to LGE-CMR, illustrated in three representative patients.

The images are from patients where LGE-CMR shows no myocardial scar (upper panels), transmural scar in the LV lateral wall (middle panels) and transmural scar in the septum (lower panels). Green and red arrows indicate peak septal systolic strain for septum and LV lateral wall, respectively.

The figure illustrates the heterogeneous distribution of myocardial workload and glucose metabolism in LBBB. The patient with no scar has markedly reduced septal strain and metabolism relative to the LV lateral wall. In the patient with lateral wall scar there is reduction in both metabolism and strain in the lateral wall relative to septum. In the patient with septal scar, there are reductions in both septal metabolism and strain. Please note that the patient with no septal scar has approximately similar reduction in peak systolic strain as the patient with septal scar, and both patients have reductions in septal metabolism relative to the lateral wall.

LV=left ventricular, LBBB=left bundle branch block, LGE-CMR=late gadolinium enhancement cardiac magnetic resonance, FDG-PET=¹⁸F-fluorodeoxyglucose Positron Emission Tomography, AVC=aortic valve closure.

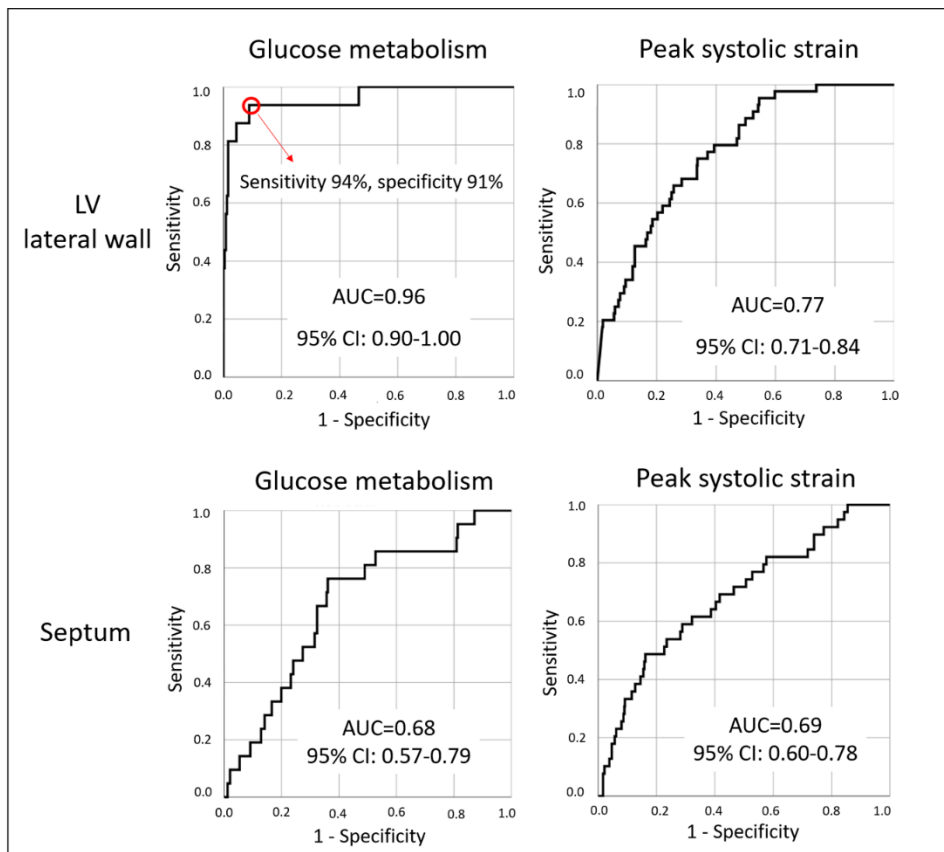


Figure 12. ROC curves of the ability of peak systolic strain and glucose metabolism to identify transmural scars (LGE $\geq 50\%$) in the LV lateral wall and septum

Glucose metabolism by FDG-PET predicted transmural scars in the LV lateral wall with high accuracy, with glucose uptake of 70% as optimal cut off. Myocardial strain and work by echocardiography were less precise. Neither FDG-PET (glucose metabolism) nor echocardiographic parameters identified transmural septal scars.

ROC=receiver operating characteristic; AUC=area under the curve; CI=confidence interval; LV=left ventricular; LGE=late gadolinium enhancement; FDG-PET= ^{18}F -fluorodeoxyglucose Positron Emission Tomography

Paper 3

Baseline patient characteristics are presented in Table 1. In the total population (n=136), 103 patients (76%) responded to CRT in terms of reverse remodelling. In the subgroup with intermediate QRS-duration of 130-150ms (n=29), response rate was 62%. As expected, responders had broader QRS complexes and were more likely to have LBBB morphology compared to non-responders. Eighteen patients (13%) died or underwent heart transplantation during follow-up.

Multivariable regression analysis, including septal LGE, septal flash, QRS-duration and QRS-morphology (LBBB/no LBBB), identified septal LGE and septal flash as the only significant independent predictors of reverse remodelling (Table 2). Septal LGE reduced the likelihood of positive CRT response, while septal flash was associated with increased likelihood of response. Furthermore, percentage septal LGE and septal flash showed significant incremental value to a multivariable model for CRT response including QRS-duration, QRS-morphology, heart failure aetiology and indexed LV ESV (both $p < 0.01$, $R^2 = 0.44$). The combined approach of percentage septal LGE and septal flash predicted CRT response with AUC=0.86 (95% CI: 0.78-0.94) in the complete population and AUC=0.99 (95% CI 0.97-1.00) in the subgroup with intermediate QRS-duration (Figure 13).

There was a declining response rate with increasing amount of septal LGE. However, the mere presence of septal LGE significantly reduced the likelihood of CRT response. If there was no septal LG, response rate was excellent (93%). In comparison, response rate was only 58% if septal LGE of any amount was present ($p < 0.001$, compared to no septal LGE). However, if patients with septal LGE also had septal flash, there was still a high likelihood of response (78%). In contrast, in patients with septal LGE and no septal flash, CRT response rate was low (23%). An algorithm based on dichotomously categorising these two parameters (Figure 14) correctly classified 86% of all patients as responders or non-responders. Importantly, the accuracy of the method was similar in the subgroup of patients with intermediate QRS-duration, where 93% of patients were correctly classified.

Patients that were classified as likely responders by the algorithm were also had significantly better long-term survival without heart transplantation compared to patients that were classified as likely non-responders (hazard ratio 0.27 (95% CI: 0.10-0.79)) (Figure 15).

Reproducibility testing of septal flash revealed agreement in 24 of the 25 randomly selected patients. Intercentre ICC was 0.96 (95% CI 0.90-0.98), indicating excellent reproducibility.

Table 1. Baseline clinical and CMR characteristics

	All patients (n=136)	Responders (n=103)	Non-responders (n=33)	P-value
Age (years)	66±10	67±9	64±11	0.071
Male sex (%)	68	63	82	0.046
NYHA functional class	2.3±0.6	2.3±0.6	2.4±0.6	0.125
Medications (%)				
<i>ACE-inhibitor/ARB</i>	96	97	94	0.403
<i>Beta blocker</i>	91	89	97	0.178
<i>Aldosterone antagonist</i>	41	41	44	0.797
Sinus rhythm (%)	95	96	91	0.239
Heart failure etiology (%)				
<i>Ischemic</i>	31	22	56	<0.001
<i>Non-ischemic</i>	69	78	42	<0.001
QRS duration (milliseconds)	164±17	166±16	158±18	0.021
Left bundle branch block (%)	91	95	79	0.004
LV EDV indexed (ml/m²)	145±46	139±46	164±41	0.008
LV ESV indexed (ml/m²)	76±32	73±31	88±32	0.580
LV ejection fraction (%)	27±8	28±8	23±6	0.003
Anterior LGE (%)	0 (0-6.5)	0 (0-0.1)	12.2 (0.8-36.2)	<0.001
Septal LGE (%)	0 (0-12.2)	0 (0-3.2)	16.3 (1.7-39.6)	<0.001
Inferior LGE (%)	0 (0-9.8)	0 (0-3.9)	10.5 (0.4-30.1)	<0.001
Lateral LGE (%)	0 (0-5.5)	0 (0-0)	5.6 (0-23.1)	<0.001
Septal flash (%)	76	89	36	<0.001
Lateral-to-septal work difference (mmHg·%)	1551±1080	1710±1085	1061±917	0.003

Continuous variables are given as mean±standard deviation or median (interquartile range), as appropriate. P-value reports comparison of responders vs. non-responders.

CMR=cardiac magnetic resonance; LBBB = left bundle branch block; NYHA = New York Heart Association; LV = left ventricular; LGE=late gadolinium enhancement

Table 2. Multivariable linear regression analysis with left ventricular end systolic volume change as dependent continuous variable

Regression variable	Multivariable analysis			
	B	95% CI	VIF	P-value
QRS duration (ms)	-0.036	-0.249 to 0.177	1.158	0.738
Left bundle branch block (yes/no)	-9.18	-21.31 to 2.94	1.110	0.136
Septal LGE (%)	0.521	0.311 to 0.731	1.153	<0.001
Septal flash (yes/no)	-18.39	-27.16 to -9.61	1.325	<0.001
Constant term	-8.513			

N=125. R²=0.40. Septal LGE is given as a continuous variable (%).

CI=confidence interval; VIF=variance inflation factor; LGE=late gadolinium enhancement

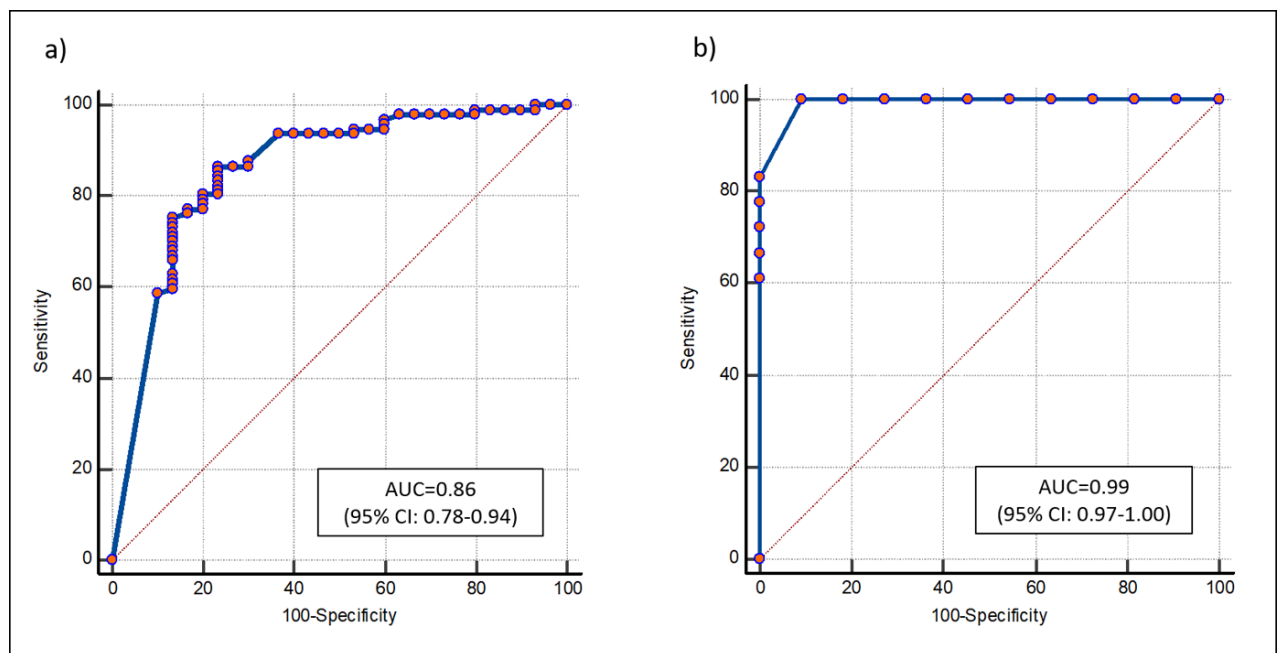


Figure 13. Receiver operator characteristic curve for predicting CRT response by the combined approach of percentage septal LGE and septal flash.

- a) In all available patients (n=127).
- b) In the subgroup of patients with intermediate QRS-duration (n=29).

CRT=cardiac resynchronization therapy; LGE=late gadolinium enhancement; AUC=area under the curve; CI=confidence interval

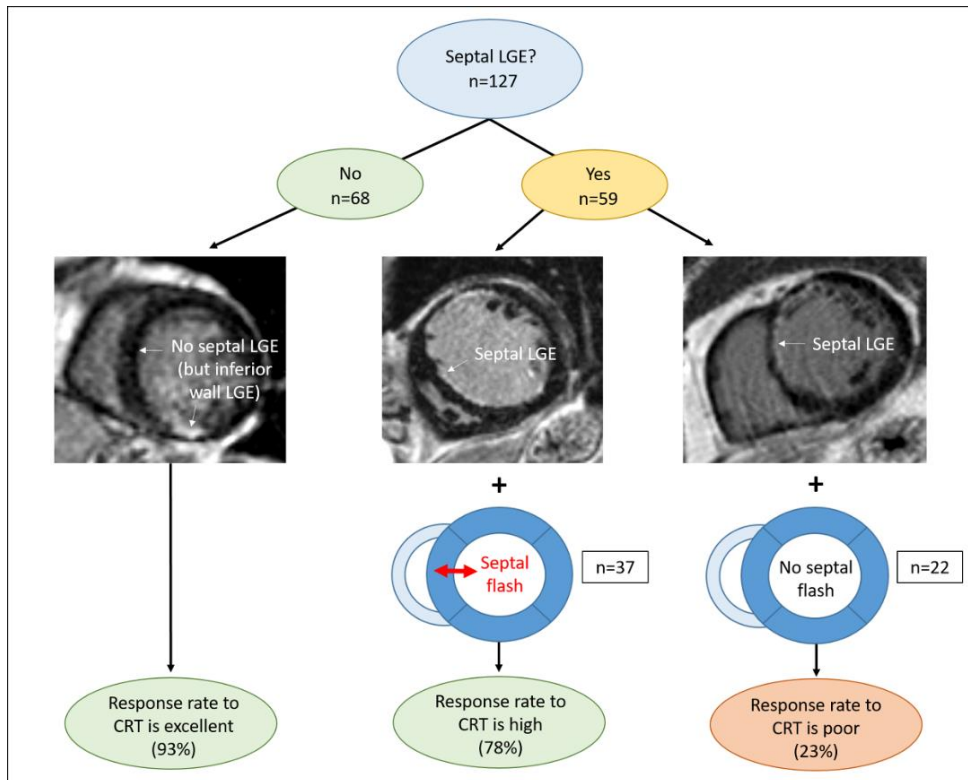


Figure 14. Novel algorithm to improve patient selection for CRT.

Without septal scar (LGE), response rate to CRT is excellent (93%), irrespective of other parameters. If septal scar is present, and the patient displays septal flash, response rate is also high (78%). However, if septal scar is present and there is no septal flash, response rate to CRT is low (23%). The algorithm correctly separated CRT responders from non-responders with 86% accuracy.

CRT=cardiac resynchronization therapy; LGE=late gadolinium enhancement

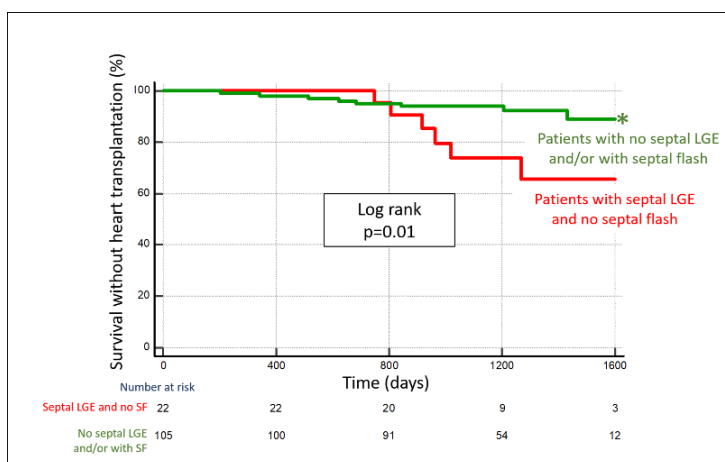


Figure 15. Patients without septal LGE and/or with septal flash have significantly better long-term survival as compared to patients with septal scar and no septal flash.

Kaplan-Meier curve stratified according to whether patients had 1) no septal LGE and/or with septal flash – and classified as likely responders (green) or 2) septal LGE and no septal flash – and classified as likely non-responders (red).

LGE=late gadolinium enhancement; SF=septal flash

Discussion

The present thesis explores the potential of CMR to identify different aspects of regional myocardial function and structure in LV dyssynchrony, and their relevance in identifying CRT responders. In paper 1, we demonstrated that calculation of regional myocardial work in LBBB is feasible by strain by FT-CMR and non-invasive LVP. In paper 2, we showed that while FDG-PET is a relevant alternative to CMR to identify transmural lateral wall scar in CRT candidates, only CMR identifies septal scar in the same patient group. We also demonstrated that strain by echocardiography is less reliable to identify scar in both regions and should be interpreted with caution. In paper 3, we explored the potential of CMR as single image modality to improve patient selection to CRT. In short, we found that a combined approach based on septal scar (LGE) and septal flash, by CMR only, accurately identifies CRT responders. In total, our findings support more extensive use of pre-implant CMR in CRT candidates, given that CMR is the only image modality to simultaneously provide relevant information on both septal structure and function, and hence may be a powerful tool to improve responder rates to CRT.

Clinical value of myocardial work

The main advantage of myocardial work in describing LV systolic function, compared to strain alone, is the incorporation of afterload. As previously described, this may be especially important in patients with LBBB, where loading conditions are abnormal, and a substantial amount of septal shortening is performed during low LVP (26). Additionally, the work index takes into account both positive and negative work, the latter a result of systolic stretching. The resulting net work represents function throughout systole, either globally or regionally, and not just shortening at a specific time point.

In paper 1, we demonstrated that regional myocardial work by strain from FT-CMR and non-invasive LVP is a relevant measure of regional myocardial function in LBBB. We showed that the workload was markedly different in the early activated septal region compared to the late activated lateral region in LBBB, which is consistent with previous findings by established methods for work calculations (25, 26). Moreover, CMR-derived work correlated with STE-derived work and glucose metabolism by FDG-PET (a marker of myocardial energy demand). In contrast to the LBBB patients, the healthy controls displayed a homogenous LV work distribution. The low amount of work performed in septum adequately distinguished the LBBB patients from the control subjects, while there was no difference in lateral wall work between the two groups, in line with previous findings of septal dysfunction as hallmark of LBBB (25, 26).

Other studies have also demonstrated that in the early stages of LBBB-induced HF, septal work is reduced, while lateral wall work is preserved or increased. When the LV lateral wall function starts to deteriorate, the progression of HF in LBBB accelerates (137). The reduction in septal performance in early phases of electromechanical dyssynchrony may not be identified using strain alone, as the absolute value of peak systolic negative strain may be maintained. However, because the timing of peak strain is in early systole when LVP is low, this shortening is contributing little to effective pumping of blood, hence septal work is low.

In the main echocardiographic paper from the CRID-study, we showed that a high difference in net work between the LV lateral wall and septum, assessed by echocardiography and non-

invasive LVP, indicates positive CRT response (138). The findings in paper 3 demonstrate that the corresponding parameter derived from CMR also is a marker of good CRT response. Low septal compared to LV lateral wall work implies a potential for improving septal function (work) by resynchronizing the LV with CRT. In line with this, the acute redistribution of regional myocardial work between the septal and LV lateral wall is an important determinant of reverse remodelling after CRT implantation (139). The acute redistribution of work load may more precisely identify CRT responders than the pre-CRT work difference, because it takes into account the capacity of the myocardium to successfully recruit and homogenize the work heterogeneity (which may be limited for example in case of septal scar). An obvious disadvantage of the method is that work needs to be calculated after CRT has already been implanted. This makes the parameter less clinical useful to improve patient selection.

Additionally, recent studies indicate that the myocardial work index may a valuable supplement in identifying CRT patients at increased risk of ventricular arrhythmias, where low global constructive work is associated with increased arrhythmic risk (140).

The myocardial work index is also relevant as a measure of RV function, potentially superior to other standard echocardiographic parameters (141). In an experimental model, pre-implant RV free wall work appeared to be an independent determinant of CRT response. LBBB reduces the workload on the RV free wall due to abnormal rightward septal motion. Hence, restoring septal function by CRT increases RV free wall work (142). A failing RV probably does not tolerate the extra workload, which may explain why patients with RV failure respond poorly to CRT. RV function as an independent predictor of CRT response is in accordance with previous studies (143, 144).

Other areas of use for the work index may include patients with non-ST-elevation acute coronary syndrome, where it more accurately than strain alone identifies acute coronary occlusion (145). Furthermore, myocardial work may potentially be clinically useful to distinguish chemotherapy-induced cardiotoxicity from normal afterload-dependent reduction in strain. Recent literature suggest a 10-15% relative reduction in global longitudinal strain (GLS) to identify cardiotoxicity in patients undergoing oncologic treatment (146). However, in healthy controls, GLS may be reduced below this threshold as a result of increased blood pressure solely (while global myocardial work is preserved or increased) (147). Hence, diagnosing cardiotoxicity based on reduction in GLS may result in many false positives, with potentially large implications for the patient in question, who may be encouraged to discontinue essential treatment. The role of myocardial work in the follow-up of these patients requires further investigation, and is explored in an ongoing study from our group. Application of the work method should also be explored in patients with HFpEF to demonstrate LV systolic dysfunction.

Identification of LV lateral wall scar in CRT candidates

In paper 2, we validated FDG-PET as method to identify myocardial scar in CRT candidates, compared to LGE-CMR as reference standard. Our finding that glucose uptake <70% relative to maximum uptake accurately identifies transmural lateral wall scar is clinically relevant, and may have implications for the decision to implant CRT and for positioning of the LV lead. Accordingly, FDG-PET is a good alternative to CMR to identify these important scars in patients potentially eligible for CRT. The threshold of 70% glucose uptake is relatively high, and restricted to the LV lateral wall in patients with LBBB. In comparison, 50% relative

glucose uptake is considered threshold for viability in other patient groups (148). This apparent inconsistency is probably related to the abnormal distribution of myocardial metabolism in LBBB, with relative hypo-metabolism in septum compared to the LV lateral wall. Previous CRT studies have adopted the 50% threshold (149). The results of paper 2 may have implications for what threshold value should be used to define scar by FDG-PET in patients referred for CRT. However, because our study group was relatively small, and with a limited number of transmurally scarred lateral wall segments, optimal cut off value to define transmural lateral wall scar, should ideally be validated in a larger cohort. It has previously been shown that high glucose metabolism in the LV lateral wall (relative to septum) is a marker of positive CRT response (116, 150).

In contrast to glucose metabolism by FDG-PET, echocardiographic strain was only moderately accurate in identifying clinically relevant lateral wall scar. However, relatively *preserved* lateral wall peak strain could rule out transmural scar in this region with high sensitivity and high negative predictive value. Hence, strain may have a role in excluding clinically relevant transmural lateral wall scar, and may have implications for LV lead placement. Consistent with our findings, Kydd et.al found that a cut off value of 10% radial strain identified segments with >50% segmental scar area with a high negative, but low positive predictive value (67). The same group has previously shown that peak segmental radial strain >10% at the site of the LV lead can be used to predict LV remodelling response following CRT (151). This finding further supports the assumption that relatively preserved lateral wall strain is clinically meaningful because it indicates that transmural lateral wall scar is unlikely.

Reduced lateral wall strain, on the other hand, was inconclusive of scar according to our results, and should not be used to discriminate scar from viable, but dysfunctional tissue in this patient group. This finding is in apparent conflict with findings of previous studies that have found a strong association between LV lateral wall strain and scar (65, 66, 152). However, study populations are different as the former studies included pre-specified groups of patients with ischemic cardiomyopathy only, while we included all-comers of patients referred for CRT, irrespective of HF aetiology. In DCM patients, there is typically reduced shortening in the majority of LV segments regardless of tissue viability. This is a plausible explanation why low values of lateral wall strain had no diagnostic value as marker of myocardial scar in our patient group. Additionally, different gold standard for scar may also have affected the results, as some of the previously referred studies used absent tracer uptake by SPECT to define significant lateral wall scar, and not LGE-CMR (152). It is likely that absent tracer uptake in the LV lateral wall in patients with LBBB represents extensive scarring, probably exceeding the 50% LGE threshold. Moreover, the previously referred studies suggest different cut offs for strain to define scar. This may reflect the small patient population in each study, and supports the notion that peak strain should be used with caution to identify lateral wall scar in CRT candidates.

Although the myocardial work index better reflects regional myocardial function in dyssynchrony compared to peak strain, the work indices were not superior to peak systolic strain in identifying myocardial scar in our study, and therefore provided no added value. This is probably related to the heterogeneity in the present patient population, where myocardial contractility is reduced of variable degree with or without scar. Hence, myocardial work index, like strain, has limited value in identifying myocardial scar prior to CRT.

Identification of septal scar in CRT candidates

The results from paper 2 demonstrated that neither glucose metabolism nor strain could identify septal scar in CRT candidates, not even those with transmural involvement. This is probably related to the pathological septal function (low septal work) in LV dyssynchrony. As previously demonstrated in an experimental study by Prinzen and co-workers, reduced septal work in dyssynchronous ventricles reduces septal metabolic demand (26). This probably explains the reduced septal glucose metabolism observed in clinical studies (28). In paper 2, we tested this concept by calculating a ratio between local glucose metabolism and local myocardial work. Our results confirmed a significant association between asymmetry in work and metabolism between septum and LV lateral wall. The impaired septal function (work) in this population leads to reduced septal oxygen demand, and hence reduced metabolism to levels that overlapped with those in patients with septal scar. This likely explains why FDG-PET did not identify septal scar in this patient group.

In LBBB, septum is affected different from the other LV regions: Septal strain (function) is dependent on multiple factors beyond septal viability and contractility. Previous studies have demonstrated that moderately increased afterload markedly decreases septal shortening in LBBB (more than the normal afterload dependency of strain observed in healthy controls). On the other hand, with reduced LV lateral wall contractility, septal strain seems to improve (147, 153). Other factors may also affect the degree of septal shortening, such as the degree of electrical delay of the lateral wall, local radius of curvature and the amount of remodelling (septal thinning). In total, the complex interactions of factors that influence septal shortening (strain) in dyssynchronous ventricles probably makes strain an unreliable marker of septal viability in this patient group.

Of the tested parameters in paper 2, we found that negative myocardial work correlated more closely with percentage septal scar than strain and positive work. The correlation as inverse, as increasing amount of septal scar resulted in less negative work. This probably reflects that scarred (fibrotic) septal tissue is less likely to be stretched by remote segments. However, negative work was not a reliable measure of septal scar, and our results suggest that myocardial strain, work and glucose metabolism should not be used to identify septal scar in patients with HFrEF and LBBB. Such parameters of septal performance do not distinguish reasons for reduced septal function (LV dyssynchrony or septal scar). Consequently, assessment of septal structure by CMR, which is independent of dyssynchrony, is preferable.

As previously mentioned, our material did not permit investigating agreement between LGE and perfusion imaging by SPECT. However, in principle, a similar limitation as for FDG-PET may apply to perfusion imaging since myocardial microvascular flow is autoregulated and determined by metabolism. In accordance with this, a previous study in patients with LBBB indicates that resting SPECT images may show fixed perfusion defects which may be misinterpreted as septal scar (154). Combined assessment of myocardial perfusion and metabolism may improve scar identification by nuclear imaging. Matched perfusion and metabolism defects indicates scar, whereas reduced perfusion and preserved metabolism (perfusion-metabolism mismatch) signals hibernation and viable myocardium (155). In LBBB, however, septal perfusion is relatively better preserved than septal metabolism (reversed mismatch) (27, 28). The diagnostic accuracy of a dual approach to identify septal scar in LBBB requires further investigation.

Nuclear imaging studies have identified LV lateral wall scar as a predictor of poor response to CRT (123, 156), but failed to identify the significance of septal scar evident in CMR studies (122). This is in accordance with our findings that nuclear imaging does not recognize septal

scar in CRT candidates. Furthermore, because even minor septal LGE significantly reduces the likelihood of positive CRT response (paper 3), also non-transmural septal scars are important to identify in these patients. The smaller scars are even more difficult to identify by echocardiography and nuclear imaging. Therefore, LGE-CMR is necessary to characterize septal scar in CRT candidates. Accordingly, several echocardiographic and nuclear medicine studies on the improved CRT responder rate identification depend on LGE-CMR to identify septal scar (138, 150, 157).

Septal scar as determinant of CRT response

The results of paper 3 add to the growing evidence that septal scar (LGE) markedly affects CRT response rate. Previously, White et.al demonstrated that septal scar $\leq 40\%$ provided a 100% sensitivity and specificity for CRT response in a small cohort of 23 CRT recipients (126). Duckett and co-workers also found that septal scar was associated with poor acute and long-term response in their study of 50 patients (127). The authors of the latter study suggest that the underlying mechanism for non-response may be trouble with placing the RV lead in septum. This explanation, however, is questionable as LV only pacing augments systolic function in LBBB similarly to biventricular pacing (158, 159). More recently, Zweerink et al. identified septal LGE as a predictor of long-term survival after CRT in a larger cohort of 218 patients (160).

We found septal LGE to be a strong independent predictor for CRT response (reverse remodelling), as well as for long-term survival without heart transplantation. The unfavourable effects were not different whether LGE was ischemic or non-ischemic. Unlike the former study of White, the results of our larger study indicate that the mere presence of septal LGE, rather than the absolute amount, is the factor to affect response to CRT. In fact, our results showed that if there was no septal LGE, response rate was excellent (93%) irrespective of other parameters (in patients pre-selected based on current guidelines criteria). In contrast, if septal LGE was present, response rate was markedly lower (58%). Although we found successively declining CRT response rates with increasing amount of septal LGE, the most significant distinction, was between patients with no septal LGE and patients with small amounts of septal LGE.

LGE is a marker of adverse structural remodelling that develops in response to myocardial injury and increased wall stress, and the degree of LGE varies in patients despite similar degrees of myocardial dysfunction (161). LGE is a substrate for re-entry circuits and associated with ventricular arrhythmias in both ICM and DCM (162, 163). Furthermore, LGE may lead to ventricular dilatation and remodelling, further increasing morbidity and mortality. LGE in DCM relates to increasing age, as well as the cumulative duration and severity of the underlying pathophysiological process (61, 62). Midwall (non-ischemic) LGE, apparent in approximately 25% of patients with DCM, is commonly located in septum, especially if the patient has concomitant LBBB. Midwall LGE is an independent predictor for mortality in DCM, even after correction for LV size and systolic function (62, 164-166). The cause-and-effect relationship between midwall LGE and LBBB is not clear. On one hand, septal fibrosis could potentially interfere directly with the electrical activation of the ventricles because of its anatomical location. On the other hand, increased fibrotic remodelling may be a result of long-standing LBBB and unfavourable cardiac mechanics, or represent other underlying myocardial disease less responsive to CRT. Because both ischemic and non-ischemic LGE is clinically relevant in CRT candidates, we analysed and reported LGE the same way independent of aetiology in both paper 2 and 3.

Lateral wall scar and CRT response

Although an established risk factor for reduced response to CRT, lateral wall LGE per se appeared less relevant in our material (paper 3). A plausible explanation for this apparent inconsistency could be the relatively low number of transmural lateral wall scar in our study. Suggested explanations for poor response in patients with transmural posterolateral wall scar include inefficient LV pacing in non-viable tissue (119-121) and modulated (improved) septal movement because of reduced lateral wall function (50, 153). An impaired/scared LV lateral wall is not able to stretch septum in systole (rebound stretch), and septal systolic shortening is therefore markedly improved compared to septal function in dyssynchronous ventricles without lateral wall scar (153). Consequently, there is little potential for improving septal function by CRT in these patients, as septal performance under the given condition is already maximized.

Smaller, non-transmural lateral wall scars probably alter electrical conduction properties and lateral wall function/contractility less than transmural scars do. Therefore, it seems reasonable that their effect on CRT response is less pronounced. Moreover, large transmural lateral wall scar often extends into the inferior/anterior wall and septum. Hence, the effects of these scars may have been incorporated in septal LGE to some extent. Furthermore, as discussed in more detail later, lateral wall scar directly modulates the appearance of septal flash (167), which was a significant predictor for CRT response. In total, transmural scars in the posterolateral wall probably exerted its effect indirectly through other mechanisms, even though the significance of lateral LGE appeared minor compared to septal LGE in our study.

Septal flash: the optimal marker of electromechanical dyssynchrony?

Septal flash (and apical rocking) assessed by echocardiography has been shown to be a robust marker of positive response to CRT in observational studies (45, 49, 52). Clinical relevance of septal flash assessed by CMR, on the other hand, has been scarcely investigated in the past. Previously, Sohal and co-workers assessed septal flash by analysing time-volume curves in a study of 52 CRT recipients. They found that septal flash by CMR was an independent predictor of CRT response (55). Analysing time-volume curves is more cumbersome and time-consuming compared to the rapid visual interpretation we performed in paper 3. Visually assessed septal flash as a binary parameter (present/not present) proved to be a good parameter of CRT response in our material, with excellent inter-centre reproducibility, which makes it an appealing clinical parameter. However, it did not allow us to quantify the degree of pathological septal motion. Additionally, identification of septal flash requires training. Hence, reproducibility might have been lower if performed by less experienced readers. In a purely descriptive study, Revah et.al also demonstrated good reproducibility of CMR assessed septal flash (54). Compared to our study, which included all available CRT recipients, the patients in the study of Revah consisted of selected patients without myocardial scar (LGE). Apical rocking probably reflects more or less the same pathological septal movement as septal flash. However, we chose to leave apical rocking out of paper 3, due to slightly lower accuracy and reproducibility compared to septal flash.

There is no consistent definition of septal flash throughout existing literature. The first component of abnormal septal motion in LBBB consists of the pre-ejection shortening (in the longitudinal and circumferential directions), septal thickening (in the radial direction) and leftward septal motion (transverse motion). The second component, which follows immediately after, is opposite, with septal rebound stretch, septal thinning and paradoxical

rightward septal motion. The original definition of septal flash by Parsai et al. (45) included both the leftward and the rightward septal motion, while others have included only the leftward motion (168). Moreover, there are divergent opinions as to whether or not pre-ejection shortening assessed by strain should be counted as septal flash or not. A universal definition is essential for septal flash to be a reproducible marker of good CRT response.

The mechanism of septal flash has been vigorously debated. Initial experimental studies concluded that the leftward septal motion was a result of passive septal displacement from altered transseptal pressure gradient. By this logic, septum is forced leftward when RV pressure (RVP) transiently increases relative to LVP, because the RV is activated prior to the LV (169, 170). Gjesdal et.al, however, demonstrated in more recent experiments that the pre-ejection septal shortening in LBBB occurred against rising LVP, consistent with active contraction (171). Mathematical simulation models indicate that the early contraction of the RV free wall, pulling on and straightening the interventricular septum when unopposed by the LV lateral wall, is the main mechanism of the leftward septal motion during septal flash. Simulation studies have also demonstrated that while generation of the leftward motion of septal flash relies on early contraction of the RV, the early septal shortening followed by septal rebound stretch depends primarily on early onset of septal active stress generation relative to the LV lateral wall. Both septal flash and septal rebound stretch require the LV lateral wall to be late activated (50, 172). These results indicate that septal flash and septal rebound stretch have somewhat different underlying mechanisms, even though both can occur in LBBB. Along the same line, previous results indicate that that septal flash appears to be independent of EF, while septal rebound stretch is markedly associated with reduced EF and reduced septal shortening (32).

In total, the precise mechanism of septal flash is incompletely understood and inevitably complex. Both passive and active components are likely to be involved. Additionally, non-electrical factors may modulate the presence and magnitude of septal flash, which may explain why a substantial amount of patients with LBBB does not demonstrate septal flash (48, 49). As mentioned previously, loss of LV lateral wall contractility abolishes the paradoxical rightward septal motion, causing a pseudo-normalized septal motion pattern (50, 153). Similarly, it has been documented that septal flash often is absent in patients with large LV lateral wall scar due to lack of rebound stretch. Most patients with anteroseptal scar, on the other hand, still display septal flash (153). Consequently, the hemodynamic effect of large LV lateral wall scar, an established risk factor for poor response to CRT, is incorporated in septal flash.

Depending on the chosen definition, septal flash may or may not include assessment of LV lateral wall function. We defined septal flash according to the definition of Parsai (45). The reason for our choice is that it seems preferable to include the rightward septal motion assuming that LV lateral wall contractility is a key determinant of LBBB-induced septal dysfunction and CRT recovery potential.

Septal flash is also influenced by the effect of RV function. Impaired RV contractility and RV volume overload may reduce or abolish the leftward septal motion of septal flash (172, 173), and poor RV function is associated with reduced CRT response (144, 174, 175). By integrating the effects of complex regional interactions, and contractile forces within the heart, septal flash may be an excellent marker of myocardial substrate amenable to correction by CRT.

Septal markers predict CRT response

In paper 3, we demonstrated that combined assessment of septal scar (LGE) and septal flash by CMR as single image modality identifies CRT responders with high accuracy. The abnormal septal contraction pattern (impaired septal function) constitutes a substrate for CRT. In responders, CRT normalizes septal contraction pattern and improves septal function (45, 49). However, the likelihood of correction depends on potential for septal reverse remodelling (LGE).

Previous echocardiographic studies have explored different measures of impaired septal function as suitable substrates for CRT. Examples include the systolic stretch index, the baseline lateral-to-septal work difference, as well as the acute redistribution of workload from the lateral wall to septum after CRT (97, 138, 139). Along the same line, a former CMR study has shown that a low septal-to-lateral myocardial work ratio, assessed by CMR tagging and invasive LVP, is a marker of acute response to CRT (115). In paper 3, we demonstrated that also LV work asymmetry assessed by FT-CMR and non-invasive LVP is a relevant determinant of CRT response. However, our results showed that the work difference was less suited to separate responders from non-responders in the patients with septal LGE, where response was more heterogeneous. This poses a critical methodological limitation of the work method in identifying CRT responders as the LV work difference may be high both in cases of pure LV electromechanical dyssynchrony (with excellent response rate to CRT) and in cases with large septal scar and a viable LV lateral wall – and no electrical substrate for CRT response.

Similar to myocardial work, septal hypo-metabolism relative to the LV lateral wall (by FDG-PET) suggests good response to CRT (116, 150). Like work, though, metabolism is limited as parameter to identify CRT responders by the inability to identify the reason for low septal activity (pure LV dyssynchrony or septal scar). Accordingly, previous work has demonstrated that septal-to-lateral glucose uptake ratio identifies CRT responders with high accuracy in non-ischemic cardiomyopathy, but appears to be less precise in patients with ischemic cardiomyopathy (150). The poor agreement of both work and metabolism to septal scar (LGE) demonstrated in paper 2, is consistent with these methodological limitations.

Septal flash, on the other hand, quite accurately identified CRT responders among patients with septal scar in our material. Hence, septal flash appears to reflect better the dyssynchrony pattern correctable by CRT in these patients. Furthermore, septal flash is also suited in patients with permanent atrial fibrillation (53), where strain/work may be less applicable due to irregular PR-intervals. Nevertheless, it is likely that abnormal septal motion, as well as asymmetric distribution of LV workload and metabolism, all reflect the same phenomenon; the inefficient septal contraction pattern in LBBB.

Accuracy of both work and metabolism in predicting CRT response improves significantly when combined with information on septal scar (138, 150). Because neither echocardiography nor PET identifies septal scar in LBBB (paper 2), these former studies relied on supplemental information from CMR, in addition to either echocardiography or FDG-PET. By bypassing the need for multimodality imaging, the approach from paper 3 represents a simplification, as CMR singlehandedly may characterize the myocardial substrate responsive to CRT.

In line with our findings, Zweerink and co-workers have recently demonstrated that systolic septal stretching, measured on CMR cine sequences, is a prognostic measure for good clinical outcome after CRT (160). Consistent with our results, that study also identified septal LGE as an independent predictor of long-term mortality. In the previous mentioned study of Sohal and co-workers (55), the authors did not identify (global) LGE as an independent predictor of

CRT response, in contrast to the great significance of LGE in our material. Different study groups, with a lower number of patients with LGE in Sohal et al.'s manuscript, might explain the discrepancies. Indeed, our results demonstrated that septal recovery to CRT depends on whether septal LGE is present or not. In total, the results of paper 3 adds to the growing evidence that septum plays an essential role in transferring the detrimental effects of LBBB on cardiac mechanics, and that septal dysfunction constitutes a substrate for CRT response.

The sequential approach outlined in paper 3, where quantification of parameters is redundant, is relatively easy and quick to perform, compared to the more complex analyses of Zweerink and Sohal. Hence, it is probably more clinically appealing. On the other hand, it did not allow us to quantify the degree of septal dysfunction and its relation to CRT response. Importantly, the accuracy of the algorithm was similar in patients with intermediate QRS-duration. In these patients, indication for CRT is less clear compared to patients with QRS-duration >150 ms. Therefore, there is a greater need for parameters to discriminate patients likely to respond to CRT from those who probably will not benefit in this subgroup. It is, however, important to emphasize that our study was observational only with a limited amount of patients included. Previous echocardiographic studies on septal flash are also all observational or retrospective in design. There is a need for randomized clinical trials before considering implementing septal markers of CRT response in clinical practice.

Restrictions on clinical use of CMR

Patients with pacemakers and ICDs have commonly been withheld from magnetic resonance imaging (MRI) because of safety concerns. Concerns have involved life-threatening arrhythmias due to magnet-induced heating of the device, disturbances of the programming and memory of the generator caused by the MRI-unit, loss of arrhythmic protection due to lack of pacing, and inappropriate shocks from the ICD. However, fear of device or lead failure may have been excessive. In response to the increasing amount of patients with implanted pacemaker devices, MRI-conditional devices have been developed to allow these patients access to MRI. "Conditional" means that they are approved for MRI scans given certain conditions. Some general rules include minimum timespan of 6 weeks after device implantation, good battery voltage in the generator, re-programming to MRI-modus prior to examination (and programming back afterwards) and proper surveillance of patient in the magnet. The device will not be able to sense the patient's intrinsic rhythm, therefore pacing should either be turned-off (for patients who are not pacing-dependent) or programmed asynchronously, for example in VVI (pacing-dependent patients). The shock function in ICDs must be turned off and a defibrillator must be stand-by. Therefore, individual risk assessment should be performed to define the proper level of surveillance during MRI examination. The device should always be re-checked after the MRI, including any changes in pacing capture threshold, and original settings reinstated. Several studies support the safety profile for MRI-conditional devices, also when repeated MRI scans are performed (176-178). More recently, studies have shown that patients with non-MRI-conditional pacemakers/ICDs also can safely perform MRI scans when following recommended protocols (179, 180). Even though the procedure gets slightly more complicated, it seems reasonable that fear of complications from intracardiac electrical devices should not lead to underuse of clinically indicated MRI.

During the course of patient inclusion for our study, local guidelines for handling of patients with pacemakers or ICDs were upgraded, allowing more patients MRI, provided indication is good (181). In our study, all study participants with non-MRI conditional devices were omitted from CMR to avoid any harm inflicted upon study participants. Hence, implanted

non-MRI conditional pacemaker/ICD was a main reason for not performing CMR. The weighting of the individual patient safety against more robust research results is a common situation in medical research, and individual safety of volunteers usually weighs heaviest. Nevertheless, it would have increased the strength of our research results if we had included patients with already implanted cardiac devices (“upgrades”), as they constitute a substantial amount of patients referred for CRT.

Another factor that traditionally have restricted the use of CMR is the fear of nephrogenic systemic fibrosis (NSF). NSF is an idiopathic, progressive, and potentially fatal, multi-organ fibrotic disease with no known cure. The association between NSF and gadolinium based contrast agents (GBCA) in patients with advanced renal failure is well-established (182). However, the risk of NSF after GBCA exposure depends on which agent is used. The vast majority of the studied patients in our material received gadoterate meglumine (Dotarem®), which is classified as a group 2 GBCA agent. According to a recent meta-analysis, the risk of NSF from any group 2 GBCA administration in advanced renal failure (stage 4 or 5) is less than 0.007%. Hence, the potential diagnostic harms of withholding these agents for indicated examinations may outweigh the risk of NSF in this population (183). In light of this, recent guidelines open for administration of low-risk GBCAs even in patients with $\text{GFR} < 30 \text{ ml/min/1.73m}^2$, provided indication for examination is good and proper precaution is taken (184). In our study, we used a strict threshold of eGFR to allow contrast agent ($\geq 45 \text{ ml/min/1.73m}^2$), again to be on the safe side. However, given the demonstrated importance of diagnosing septal LGE in CRT candidates, less stringent requirements for renal function may be advisable for further studies, as well as clinical practice. If patients with reduced renal function had been included, it would have increased the clinical relevance of our findings as renal failure often coexists with HF.

Some patients may also develop acute adverse reaction to GBCAs. We did not experience any such reactions in our study. Moreover, pacing systems containing ferromagnetic material may hamper the diagnostic quality of CMR images. In our study, we performed CMR in one patient with a MRI-conditional ICD. In this patient, the generator caused artefacts in the anterior and anteroseptal segments, which were therefore excluded from LGE analysis. Furthermore, we abandoned strain/work analysis in all segments because of disturbances of the ECG signal. Despite the challenges we experienced in this patient, there are methods for reducing artefacts in CMR examinations of pacemaker patients, markedly improving image quality (185). Diagnostic image quality is probably dependent on experience and mass training. Hence, increased numbers of MRI-conditional devices in the coming years will probably result in better image quality in these patients.

Finally, CMR is inevitably limited by cost and accessibility, and claustrophobia or inability to hold one’s breath throughout the sequences preclude CMR in some subjects. Many centres do not perform CMR at all. Even in centres that perform CMR, there often is a fierce battle for CMR spots. Limited accessibility means that the suggested approach to select patients for CRT based on CMR only (paper 3) may not be available to all CRT implanting physicians. Still, our results indicate that LGE-CMR offers essential information in CRT candidates, which probably should lead to higher priority for CMR than today. Further research is essential.

The predicament of defining CRT response

Non-response to therapy has been a limitation of CRT since the introduction of the treatment over 20 years ago, but the proportion of non-responders vary depending on the definition and criteria applied in each study (91, 186). Lack of consensus regarding the definition of response complicates the evaluation and comparison between CRT trials. Markers of response include event-based measures (death, HF hospitalizations), indices of reverse LV remodelling, measures of functional capacity and quality of life, and composite endpoints. The main aim of the therapy may differ between patients. For patients with less advanced disease, preventing disease progression is essential. For patients with more progressive disease, on the other hand, alleviation of symptoms and lower morbidity are usually the main objectives (187). Hence, optimal marker of CRT response varies between patients.

The most unbiased definition of CRT response is all-cause mortality, although it inevitably includes events unrelated to CRT. Furthermore, hard outcome measures like mortality and HF decompensations may be less suitable in patients with mild disease. In these patients, event rate during study follow-up is low irrespective of CRT, and any difference between groups will be more difficult to identify. Accordingly, CRT has failed to demonstrate decreased mortality and HF events in NYHA functional class I (188, 189), but the low number of patients and low event rate limit the knowledge we can draw from these studies. In contrast, CRT has convincingly demonstrated superior long-term survival compared to conventional HF therapy among patients in NYHA class III-IV (83) where adverse event rate is much higher.

Other markers of CRT response, commonly applied in clinical trials, include surrogate markers, such as echocardiographic measures of reverse remodelling (reduced LV ESV, with or without concomitant improved EF, at follow-up compared to baseline). Change in LV ESV is a strong predictor of long-term mortality and HF hospitalizations in CRT recipients (190-193). Additionally, it is a relevant parameter in all patients independent of pre-implant HF severity and symptoms. Consequently, ESV reduction is commonly employed in clinical trials as marker of CRT response. However, LV volume estimate by two-dimensional echocardiography is dependent on image quality and geometric assumptions, and is only moderately reproducible (194). Furthermore, there is no agreement on optimal threshold values for LV ESV reduction, which ranges from 10% to 25% among studies (107, 195, 196). A minimum of 15% reduction in LV ESV at 6 months follow-up compared to baseline was pre-defined primary endpoint in our study (paper 3), which is probably the most widely used threshold. We tried to minimize the effect of measurement inaccuracies by measuring LV volumes three times, by independent readers at different centres, and use majority decision in cases of disagreement on response. Reversed remodelling was measured 6 months after CRT implantation, when the reversal process is likely to have stabilized (195).

On a general level, a binary classification of outcome is probably too simplistic to evaluate response to treatment. Furthermore, there is a wide spectrum of response to CRT, and no measurable improvement is not necessarily equal to non-response, as it is unknown if CRT has prevented further deterioration of HF in these patients. An advantage of using LV ESV as marker of response is that the variable can be applied both binary (response or non-response) and continuously (delta change in LV ESV). By using change in LV ESV as a continuous variable in regressions analysis, we demonstrated direct correlation between studied parameters and the degree of reverse remodelling (paper 3).

Symptomatic improvement is often regarded as positive CRT response from a patient's point of view, particularly for patients in NYHA functional class III-IV. However, as parameter of

CRT response, symptomatic relief alone has obvious limitations. Studies have demonstrated poor correlation between symptomatic response and prognosis in CRT recipients (190). A plausible explanation may be that less symptomatic patients experience little reduction in symptoms, but generally have longer life expectancy than patients with more advanced symptoms have. Consequently, patients may benefit from the treatment despite lack of symptomatic improvement, especially patients in NYHA class I-II, where symptomatic relief is less likely. Functional measures are also limited by the natural fluctuating course of HF, which makes it difficult to know if symptomatic change is related to CRT or not.

Due to the lack of an ideal response parameter, response should preferably be evaluated against more than one parameter. As an example, while patients with ischemic cardiomyopathy are less likely to experience reverse remodelling compared to patients with DCM (197), mortality benefit may still be present in both groups (198). Accordingly, larger clinical CRT trials often use composite endpoints (for example Packer's clinical composite score (199)) to define response to treatment. Composite endpoints are advantageous to single parameters as association to more than one measure of response increases relevance of the tested parameter. A composite endpoint in paper 3 would have strengthened the findings. LV reverse remodelling was predefined primary endpoint. To enhance clinical utility, we added long-term survival without heart transplantation as secondary endpoint. The pre-defined secondary endpoint was death at 12 months follow-up, but we extended follow-up time and included heart transplantation to increase number of events, and thus the strength of the study. Originally, we planned to include HF hospitalizations in the secondary endpoint, but information on cause of hospitalizations was unfortunately missing in a significant number of patients. Consistent results of septal LGE and septal flash as predictors of both reverse remodelling and long-term clinical outcome increases relevance of these parameters as markers of CRT response. In summary, there are advantages and disadvantages of all response parameters, and more than one parameter is favorable. Moreover, it emphasizes the need for randomized controlled trials.

In addition to the challenges regarding definition of CRT response, there are diverse reasons for non-response to the treatment. This thesis focuses on optimizing patient selection, aiming to implant CRT in patients who are likely to benefit and not in patients, whose risks outweigh expected gain. There are however, several reasons for poor response to CRT associated with how the therapy is delivered. Reasons for suboptimal CRT delivery include lack of accessible posterolateral vein for LV lead placement, transmural scar in the region of the LV lead and suboptimal device settings with inadequate percentage biventricular pacing. Unfortunately, information on LV lead placement and percentage biventricular pacing was not available in paper 3. Such analysis in the non-responders could potentially explain why some patients who were expected to respond to CRT according to the suggested algorithm, failed to do so. Paper 3 is also limited by the one-sided focus on intraventricular dyssynchrony and improvement of LV function. This is an oversimplification as CRT has several modes of action, including prevention of potentially fatal bradycardia, improvement of mitral regurgitation and correction of AV dyssynchrony. Although the effects on the LV is usually considered the main effect of CRT, there is no clear consensus on the relative importance of the various mechanisms and more data is needed (200).

By today's guidelines CRT response rate is particularly heterogeneous in patients with intermediate QRS-duration (130-150 ms) and non-LBBB morphology. Hence, it is in this patient group additional response parameters are most needed. Number one priority should be to avoid inflicting harm on patients, and because CRT comes with risks of complications and increased mortality in not eligible patients (89), it is essential not to implant CRT in patients who are not likely to benefit from the treatment. In this regard, a response parameter with a

high negative predictive value would be beneficial. On the other hand, such a strategy would inevitably result in withholding CRT to patients who would ultimately benefit from treatment. This balance poses an ethical dilemma, where both patient factors, risks of complications and economical aspects should be considered. In paper 3, we demonstrated that septal LGE and septal flash were equally accurate as predictors of CRT response in patients with intermediate QRS duration. Although promising results, patient number in this subgroup was low, and the results must be interpreted with caution. Randomized controlled trials are needed to validate our findings.

Methodological considerations

Patient inclusion

As previously mentioned, only approximately 35% of the patients that received a CRT in the largest contributing centres during the study period, were included in the CRID-CRT study. Furthermore, the proportion of included patients varied across the centres, which signals local differences. This may have caused a selection bias. In addition to the former mentioned reasons for study exclusion, logistical reasons precluded patient inclusion in some cases. Unfortunately, a systematic overview of reasons for non-inclusion is not available. This would have been beneficial, as it may have provided deeper into the interpretation and limitations of the present work.

Myocardial work

In all three papers, we calculated myocardial work based on strain and brachial systolic cuff pressure. There are several limitations of this methodology. First, the use of pressure instead of force/wall stress is a simplification that holds some uncertainty. Although optimal, force (or wall stress) is difficult to calculate in clinical practice, as it requires continuous recordings of radius of curvature and wall thickness, in addition to pressure. During dyssynchrony, wall thickness and radius of curvature differs between different LV segments at a given time-point, and such differences in regional wall stress is not taken into consideration when pressure is used to calculate regional work. However, previous work has demonstrated that substituting force with pressure provides a reasonable estimate of work in most circumstances (25, 201). Additionally, estimating wall stress based on Laplace's principle assumes a symmetric geometry, while the ventricles in CRT recipients generally have undergone substantial eccentric remodelling. Thinning of the walls and increased diameter both result in increased wall stress compared to normal hearts. As a result, calculations of force by Laplace's law may be less accurate in this patient group. Although work calculations based on force instead of pressure would change the numeric value of the work estimates, it would not change the overall picture with substantially increased work in the LV lateral wall compared to septum in LBBB.

A similar limitation is the substitution of segment length with strain. Strain is, unlike segment length, a measure of relative deformation. Consequently, a given segmental shortening (reported in mm) may give markedly different strain (reported in %) depending on baseline length of the segment and size of the heart (202). This aspect is important to keep in mind, and restricts comparison of myocardial work between hearts of different sizes. Hence, this represents a challenge to using a specific cut-off in LV work difference to predict CRT response. Moreover, the use of strain and work instead of segment length and force does not provide a measure of work per se, expressed in joules, but rather an index of myocardial work, expressed in a less familiar unit mmHg·%.

To calculate myocardial work by CMR, we extrapolated the LVP curve from the echocardiographic software (GE Echopac 202, Horten, Norway) as the pressure curve is not (yet) incorporated in the CMR software. Hence, inaccuracies in valvular events by both echocardiography and CMR may affect the work estimate. Through lower frame rate compared to echocardiography, this inaccuracy may be more prominent when CMR is used to

calculate myocardial work, but minor discrepancies in event timing are not decisive for work estimates (25). Brachial systolic cuff pressure was for obvious reasons not measured simultaneously as the CMR examinations. Instead, blood pressure was measured in conjugation with the echocardiographic examination. Although blood pressure may not be identical during these two situations, the measurements were performed in an equivalent resting condition on the same day in circulatory stable individuals. Furthermore, we studied relative magnitudes of myocardial work, which are not likely to change with slight variations in blood pressures.

In patients with atrial fibrillation, systolic brachial cuff pressure does not necessarily capture the beat-to-beat variations in LVP characteristic of this patient group. Strain traces may also be more difficult to obtain in the case of significant R-R variability. Hence, atrial fibrillation represents a challenge when calculating myocardial work. All individuals in paper 1 and the vast majority of patients in paper 3 were in sinus rhythm, minimizing this problem. In paper 2, we used the average systolic blood pressure of three measurements to calculate work, and reported work as the average of three beats. Still, numerical variations in absolute work would probably appear if measurements were repeated. The overall asymmetric work distribution in LBBB, on the other hand, is likely to remain unchanged.

In paper 1, we used work by STE and non-invasive LVP as reference modality to evaluate feasibility of work by FT-strain and non-invasive LVP. This choice could be debated. CMR tagging, which also is a well-established strain technique, would have been another alternative. Previous studies have demonstrated better agreement between FT-CMR and CMR tagging than between STE and CMR tagging in CRT candidates (203). On the other hand, CMR tagging is less clinically available and hampered with even lower temporal resolution than ordinary cine sequences used for FT. Furthermore, former validation studies have used longitudinal strain by STE for work calculations (25, 43), which led us to continue this approach for comparison to CMR-FT. The agreement between regional myocardial work and regional glucose metabolism by FDG-PET is well established, and used as reference method in previous similar studies (25), making it a natural basis for comparison.

The results of the feasibility paper (paper 1) demonstrate that lower frame rate of CMR compared to echocardiography is less critical for work calculations. Through higher frame rate, echocardiography might detect the rapid pathological septal pre-ejection shortening superiorly to CMR. This shortening, however, happens early in systole, when LVP is low, and hence represents little work. The slower movements later in systole, when LVP is much higher, are decisive for work calculations.

Lower frame rate of CMR also implies less accurate timing of valvular events compared to echocardiography. However, timing of systole (by closing and opening of the mitral valve) is also performed at time points where LVP is low. Consequently, minor inaccuracies will not change the overall picture of large heterogeneity in workload between regions in LBBB, although the absolute values of myocardial work are not accurate. We found similar heterogeneous work distribution by both work methods, corresponding to the asymmetric intraventricular distribution of glucose metabolism.

We used mitral valve opening to define end-systole to continue the approach used in the validation paper by Russell and co-workers (25). According to this definition, all segmental shortening in systole is “positive work”, while all lengthening counts as “negative work”. However, one could argue that segmental shortening in the isovolumic relaxation (IVR) phase is undesirable (“wasted”). GE Healthcare’s analysing software (Echopac) therefore provides additional concepts, where the signs, by this logic, are inverted during the IVR period. This

means that “constructive work” is defined as segmental shortening in systole until aortic valve closure and as lengthening during IVR, while “wasted work” is defined as lengthening before aortic valve closure and as shortening during IVR. While these more advanced definitions provide sound physiological logic, they are more complex and less intuitive. We therefore decided to present our data in the most easily available format. When we compare “positive work” to “constructive work” and “negative work” to “wasted work”, the differences are minor, and not expected to change the main message of the studies.

Strain by CMR-FT, as well as by STE, is more reproducible for global than for segmental values (204). As a result, also segmental work is afflicted with more uncertainty than global work values. This represents a limitation to paper 2, where segmental values of strain/work by STE were compared to segmental LGE. In paper 1 and 3, we evaluated regional myocardial work as average of two septal and two lateral segments, respectively, to minimize the effects of any segmental discrepancies. Furthermore, we focused on the two opposing LV regions at a mid-ventricular level only, for simplicity and reproducibility. Reproducibility analysis of regional work in paper 1 revealed rather large SD, but did not change the overall findings of heterogeneous LV work distribution in LBBB. Hence, the absolute numbers of the work estimates are not 100% accurate, but the method adequately captured the regional work differences in LBBB. An additional point is that segmental strain patterns (expressed in terms of the work index) seem to be more reproducible than strain values at specific time points (peak or end-systolic strain) (36). Currently, myocardial work is only a research tool and not recommended for clinical use.

Myocardial strain

Contrary to echocardiography, which measures deformation by tracking of myocardial “speckles”, CMR-FT algorithms focus on the endocardial and epicardial borders. The stronger weighing of endocardial deformation may explain some of the differences in results found in direct comparisons of CMR-FT and STE (204). Moreover, strain values, whether assessed by echocardiography or CMR, vary across patient age and gender (205, 206), as well as between different vendors (36-38). Lack of proper standardization remains an important limitation of the technique, and more research is warranted. In addition, global strain values are more reproducible than segmental values, independent of measured strain direction and image modality (204).

Of the STE-derived strain parameters, longitudinal strain is the most reproducible, while circumferential strain is the most robust parameter from CMR-FT (37, 204). We chose the most reproducible measure for each image technique, although not identical. Endocardial fibres are predominantly oriented in the longitudinal direction, while midwall layers are predominantly circumferential (207). Although they measure deformation in different directions, it seems reasonable to assume that in patients with HFrEF and LBBB, all myocardial fibre directions are affected. Furthermore, conservation of mass makes sure that deformation in the long axis is always accompanied by deformation in the short axis.

In paper 2, where we evaluated the agreement of strain by STE to scar (LGE), we chose peak systolic strain as the most suited strain measure of myocardial viability. Other alternatives could have been peak strain throughout heart cycle or end-systolic strain (strain at AVC). Peak strain throughout heart cycle, however, may also include shortening that occurs during diastole, and is therefore not necessarily an accurate measure of systolic function. Because early-diastolic LV pressure is lower than end-diastolic pressure, there will be net contraction

in early diastole due to passive forces only. In the LV lateral wall, peak systolic strain is often similar to end-systolic strain. However, this is not always the case, particularly in septum, where peak systolic strain often precedes AVC (in LBBB). Therefore, end-systolic strain may not reflect contractile force/viability in septum. One objection to the use of peak systolic strain is that the peak occurs against abnormally low afterload, and therefore does not necessarily reflect the segment's true contractile force. In total, however, we concluded that peak systolic strain probably best displays segmental systolic function. Accuracy of strain to identify scar did not improve if measured as peak strain throughout heart cycle or as end-systolic strain.

The majority of previous studies that explored the agreement between STE-strain and scar in CRT candidates used radial strain (66, 152). However, we found radial strain difficult to perform in the present patient population with dilated ventricles and thin walls. Therefore, we used longitudinal strain to evaluate LV function. In principle, LV radial strain should give similar results since deformation in the long axis is always accompanied by deformation in the short axis through conservation of mass. In total, the variable degree of myocardial dysfunction in CRT candidates, irrespective of scar, implies that strain will be limited as means to identify scar in this patient group, whether measured in the radial or longitudinal direction. In contrast, in other populations, where contractile function is otherwise preserved, a defined scar may be identified more reliably by reductions in myocardial deformation (strain/work) (208, 209).

Quantification of scar (LGE)

Assessment of myocardial scar (LGE) is relevant for all three papers. In paper 1, myocardial scar led to study exclusion, while quantification of LGE is essential for the results in paper 2 and 3. Although LGE-CMR is gold standard for assessing myocardial scar, no consensus exists on the optimal method for quantifying LGE. Several methods have been used with highly variable results (210). The simplest of these methods is visual assessment, where the reader determines the degree of hyperenhancement (i.e. signal intensity) per segment subjectively (211). This allows for a rapid assessment of scar size, but is inherently subjective and reader-dependent. Alternatively, scar size may be quantified by planimetry of hyperenhanced areas on the stack of short-axis images. Manual delineation is often used clinically, but its accuracy also depends on the experience of the reader and is less reproducible in certain patient groups (212).

To increase speed and improve objectivity and reproducibility, several semiautomatic methods have been proposed. Initial techniques were often based on a 2-6 SD threshold from remote viable myocardium. However, more recent findings suggest that remote myocardium is probably not an ideal comparison to define scar, because normal signal intensity regularly has a gradient throughout the MR image (213). An alternative method, the full-width at half-maximum (FWHM) method, uses a threshold value of 50% of the maximum intensity within the scar (212). On the other hand, FWHM assumes a bright surface core, and may not be accurate if the scar is homogeneously grey, if there are multiple scars or if the scar is patchy with multiple, separate islands of necrosis (214). Using a threshold by an Expectation Maximization (EM) (215) algorithm may be advantageous to FWHM. This algorithm calculates the most likely estimate of the mean and SD for the intensity distributions of normal myocardium and scar, and thereby the optimal intensity threshold to define scar tissue (133).

During the last years, a new method that combines the EM algorithm with a weighted approach has been introduced. This automatic algorithm called EWA (Expectation Maximization, weighted intensity, *a priori* information) (133), is based on intensity classification by Expectation Maximization and weighting each pixel according to its signal intensity to account for partial volume effects. The weighted approach has been shown to provide automatic quantification of scar with higher accuracy and lower variability than a dichotomous algorithm (216). In paper 2 and 3, where scar quantification is highly relevant, we used the EWA algorithm for scar quantification. The EWA algorithm has the advantage of being less user-dependent and has been validated against expert delineations in multicentre, multivendor patient data, which is beneficial in a multicentre trial like the one we conducted. However, like all automatic algorithms, the EWA algorithm requires manual control and correction as appropriate. In paper 2 and 3, we opted for a combined qualitative and quantitative method to secure representative LGE analysis. An experienced CMR reader performed the immediate qualitative analysis, focusing on the exclusion of bright artefacts, and positively classifying LGE as ischemic or non-ischemic. Quantitative analysis using the semi-automatic software was initially made independently of the qualitative analysis, and then controlled for the qualitative reading. Discrepancies and doubt were discussed, and conclusion was made between readers – based on the initial qualitative analysis and the automatic approach. Still, it is obvious that an inter-observer analysis of septal scar would have strengthened the findings of these papers. On the other hand, minor differences are not likely to alter the overall findings.

To complicate matters further, several methods to assess scar transmuralities exist, and the definition of a transmural scar is not consistent through literature. In paper 2, we defined transmural scar as LGE $\geq 50\%$ of segmental volume, as these segments are likely to have impaired function. However, another threshold for transmuralities could have been LGE $\geq 75\%$ of segmental volume, or simply maximal LGE extension at any point in the segment (217-219). Changing the definition of transmuralities could have affected the results of paper 2, and the lack of a uniform definition is a limitation of this paper. In paper 3, this is of less relevance, as we treated LGE % as a continuous variable or binary (LGE present or not present). In paper 1, we excluded patients with scar all together. In general, lack of consensus on defining transmural scar has potential important implications in the research setting, as scar size is often stated and used as surrogate endpoints in clinical trials. There is a need for further studies to obtain a validated and consensual study method.

Finally, there is the question whether to include the papillary muscles in scar analysis. We chose to regard the papillary muscles as part of the ventricular cavity, and not include them in scar analysis, in line with most other clinical studies not specifically investigating these anatomical structures. It is not likely that including the papillary muscles would have affected the results of the studies.

Septal flash

In some patients, there is pronounced abnormal motion of the interventricular septum (septal flash), easily detectable with the naked eye. In these, the visual interpretation is quick and simple. However, in others, there is more subtle septal movement, and the distinction from normal septal motion is less clear. The binary approach based on septal flash present or not present outlined in paper 3 did not include grading of the abnormal septal motion. Therefore, it does not take into account different degrees of pathological LV contraction pattern. This may be relevant as patients with obviously inappropriate septal movement may benefit more

from CRT than patients where pathological septal motion is barely visible (and perhaps graded as normal by a second reader). The visual interpretation of septal flash performed in paper 3, did not distinguish these patients, which is a limitation of the approach. Grading of septal flash would have allowed us to explore the continuous relationship between septal flash and LV reverse remodelling.

Despite lower temporal resolution, and thus inferior sensitivity to identify rapid septal motion, compared to echocardiography, we have demonstrated that septal flash assessed by CMR is equally clinically relevant to septal flash by echocardiography. The CMR acquisition triggers on peak R on ECG, and the first cine frame actually represents the first moment *after* peak R, defined by the magnitude of the time resolution of the sequence. One could speculate how CMR is able to identify the rapid septal movement that starts and mostly ends during isovolumic contraction time (septal flash). Such detection is dependent from visualization of the isovolumic contraction phase at the end of the R-R interval, to contrast the first frames of the sequence. In HF with LBBB, the isovolumic contraction time is relatively long, often over 150 ms at heart rate 80 beats per minute (220). The cine imaging used in our study typically had a resolution of 30 frames/heart cycle, which means that each frame lasts approximately 25 ms at this heart rate. Hence, there are 5-6 frames covering the isovolumic contraction phase, which allows visualizing the changes in septal positioning (septal flash) between early systole and the reference frame in late diastole. In accordance with this, the images used to illustrate septal flash in Figure 5 are from frame number 30 (at the end of the cine loop but still first image) and from frame number 3 (second image). Nevertheless, the lower frame rate of CMR compared to echocardiography may account for some of the discrepancies in identifying CRT responders between the image modalities. We specifically used commonly performed cine imaging to identify septal flash in order to make the technique as widely applicable as possible. Increasing scan time or reducing spatial resolution can further improve temporal resolution of CMR. Additionally, specific sampling and reconstruction techniques can be used to acquire high temporal resolution images within a reasonable breath hold (221). Previous findings of Revah et al. indicate that lower temporal resolution makes CMR less sensitive to identify septal flash compared to echocardiography (54). However, how the discrepancies relate to CRT response, and whether a combination of the methods could improve accuracy further, requires additional testing in future larger studies.

In paper 3, we found excellent reproducibility of septal flash by CMR. However, as previously mentioned, recognition of a dyssynchronous LV contraction pattern (by CMR as well as echocardiography), requires training, especially when it is less pronounced. Therefore, reproducibility of these parameters might be lower if performed by less experienced readers. This is important to keep in mind if the method is to be recommended in future guidelines. Importantly, before changing clinical recommendations, the utility of septal flash as a predictor of CRT response must be validated in larger, randomized trials.

Glucose metabolism

We used FDG-PET to assess regional and segmental glucose metabolism in paper 1 and 2, respectively. The examinations were performed at two centres, and the centres used different patient preparation protocols prior to FDG-PET. This resulted in divergent absolute values (expressed in activity Bq/cc) between the centres. To achieve comparable values, we reported segmental values as percentage of the segment with the highest mean glucose uptake per patient (relative values). Therefore, different preparation is unlikely to have affected the

results. Relative segmental values of FDG-uptake is an accepted method to report glucose metabolism (25, 27, 118).

In paper 1, we merged two septal and two lateral segments, and calculated average septal and lateral wall FDG-uptake (as with regional myocardial work), to minimize the effects of any segmental discrepancies. We chose the mid-ventricular segments to match the segments from which work was calculated. It is likely that repeated analyses would result in numerical variations in percentage FDG-uptake in many segments, but the overall picture would probably not change noticeably. Segmental inaccuracies is probably more challenging in paper 2, where values were reported on segmental levels. However, the precise agreement between reduced glucose metabolism and transmural scar in the LV lateral wall, suggests good conformity between segmentation by the various image modalities.

Ischemia leads to increased glucose metabolism, and thereby elevated FDG-uptake within the ischemic area. This phenomenon lasts for approximately 24 hours after an ischemic event. Because detection of scars with FDG-PET is based on relative FDG-uptake, increased FDG uptake due to reversible ischemia may have increased the number of LV lateral wall segments with FDG uptake <70% (paper 2) (222). Our patients had no clinical history of reversible ischemia, the investigation was carried out under resting conditions, and the patients were instructed to avoid exercise during the days before the FDG-PET/CT. Moreover, to increase the global myocardial FDG-uptake, the patients underwent either hyperinsulinemic euglycemic clamping or glucose loading to switch myocardial metabolism from fatty acids to glucose, decreasing the difference between a possible ischemic part and the remaining myocardium.

Unfortunately, PET, like CMR, is limited by costs and accessibility. In comparison, myocardial perfusion imaging by SPECT is cheaper and more accessible. It would have increased clinical applicability of paper 2 if we had also validated scar imaging by SPECT. Although we performed SPECT in some patients from Oslo, the number, unfortunately, was too low to conclude. SPECT may be comparable to FDG-PET in viability diagnostics (223), but it remains to be tested how accurate SPECT is for assessment of scar in patients with HFrEF and LBBB. Importantly, several studies confirm the utility of applying myocardial perfusion imaging by SPECT to predict response to CRT (123, 125, 156). Still, in direct comparison, asymmetric distribution of glucose metabolism appears to be more closely associated with electromechanical dyssynchrony and subsequent reverse remodelling than asymmetry in myocardial blood flow (perfusion) in non-ischemic CRT candidates (118, 224). Whether SPECT there is more suited to identify scar in dyssynchrony compared to FDG-PET requires further testing, but the pitfall of fixed perfusion defects misinterpreted as septal scar is distinct (154). Previous nuclear studies have also indicated that accuracy of PET to identify scar in LBBB may vary depending on which type of tracers is used (225). In summary, there are still unanswered questions in defining the role of nuclear imaging in CRT candidates, and more research is warranted.

Statistics

Statistical analyzes are essential to present results from medical research, but their interpretation requires knowledge of potential sources of errors. Two commonly used statistical methods will be discussed briefly in the following section; ROC and regression analysis.

The AUC derived from ROC analysis is commonly used as a measure to evaluate classifier performance, as in paper 2 and 3 in this thesis. A ROC curve displays the relationship between true positive rate and false positive rate (or sensitivity and 1-specificity) given by different thresholds. Ideally, the AUC value should be as close to 1.0 as possible, and the line of the curve as close to the upper left corner as possible (226). However, often there is a trade-off between high sensitivity and high specificity of a model's performance (true positive and false positive). Furthermore, one should be aware that even though the calculated AUC for two classifiers are numerically equal, it does not necessarily mean that their performance is similar. The AUC is dependent on the intrinsic properties of the classifier, which makes comparing classifier based on AUC an inappropriate measure for comparison in many cases. Additionally, when the AUC is calculated, both false and true positive rates are equally weighted, while in reality we often make a choice, which is more important; minimizing the false-positive rate or maximizing the true-positive rate. Consequently, different classifiers may be preferred in different settings, despite similar AUC (226). In total, AUC alone does not provide all the information needed to evaluate a model's performance, and supplemental information such as diagnostic accuracy may be useful, especially if sample size is small. A visual interpretation of the ROC curve may provide valuable information not reflected in the AUC value. To gauge the estimator's variance, it is crucial to evaluate the 95% CI of the AUC, as it gives a better understanding of the uncertainty that lies in the calculated value. The 95% CI in paper 2 are rather wide for some parameters due to low number of transmurally scarred segments in both regions. Consequently, the "true" AUC may be quite far from the calculated AUC and this should be kept in mind when interpreting the results.

Regression analysis is used to estimate the relationships between a dependent (outcome) variable and one or more independent variables (predictors). In paper 3, we used linear regression analysis to identify parameters associated with reverse remodeling after CRT. Only a limited number of independent variables should be included in multivariable regression analysis to avoid confounding. Furthermore, the predictive (independent) variables should not be closely correlated with each other (multicollinearity). Multicollinearity can be quantified by variance inflation factor (VIF), and VIF should be < 10 to assure independency between covariates (227). The VIF values in paper 3 are all < 3 , indicating that there is no troubling multicollinearity. The given R^2 is a goodness-of-fit measure for linear regression models. This statistics indicates the percentage of the variance in the dependent variable that the independent variables explain collectively. R^2 measures the strength of the relationship between the model and the dependent variable on a scale from 0-1, where zero equals no relationship and one signals the theoretical situation that the fitted values equal the data values. In general, the higher R^2 , the better the model fits. However, if R^2 is low, but the independent variables are statistically significant, still important conclusions about the relationships between the variables can be made. Accordingly, like in many studies in the field of medicine, the R^2 value from the regression model in paper 3 is less than 0.5. Still, the model quite accurately identified CRT responders and was superior to current guideline criteria. The dependent variable in linear regression is continuous (unlike the binary variable in logistic regression). This is statistically an advantage because it exploits the spectrum of the dependent variable. In paper 3, we used delta ESV change as dependent variable in linear regression analyses.

Specific limitations

Paper 1

We did not perform inter-vendor analysis, and the study size was relatively small. Hence, the eligibility of other available FT software to calculate myocardial work requires further investigation, and our findings should be further validated in a larger cohort. Further evaluation is also necessary to determine if work by FT-CMR and non-invasive LVP is suited in other patient groups.

Paper 2

There were a limited number of transmurally-scarred segments with available PET data, and not all segments were available for strain and work analysis due to insufficient echocardiographic image quality in some patients.

Paper 3

We used reverse remodelling as a surrogate for CRT response (primary endpoint). Pros and cons of this surrogate parameter are described earlier. To expand suitability, we also included long-term mortality and heart transplantation as a secondary endpoint. However, the relatively low numbers of adverse events represent a limitation, evident in the wide hazard ratio CI. Additionally, the stringent requirements for renal function, and exclusion of patients with pre-existing cardiac devices, may have resulted in a selection bias. Data on LV lead position and intrinsic LV electric delay were not available, and such data might have provided additional insights. The number of transmural LV lateral wall scars was too low to investigate to full extent. The study was observational and included a limited number of patients. To change clinical practice, there is need for a randomized trial with clinical endpoints.

Ethical considerations

Several patients and nine healthy controls participated in the present work. Importantly, study participants were not subjected to increased risk of complications in connection with CRT implantation as the procedure was performed according to clinical routine. The responsible electrophysiologist determined the indication for CRT independent of the study. Nevertheless, all studied subjects have endured time-consuming and occasionally uncomfortable imaging examinations beyond clinical guidelines. The long-lasting and demanding CMR and PET examinations, requiring breath holds and user collaboration, were particularly strenuous for some patients, afflicted by advanced heart disease. The majority of the patients have expressed an appreciation for the additional investigations and follow-up resulting from study participation. However, the comprehensive imaging has also led to incidental findings requiring follow-up and caused concerns in affected individuals. This issue is of particular importance in presumably healthy individuals (controls), and underscores the need for proper informed consent and approval from the Regional Ethical Committee.

Clinical implications and future perspectives

Currently, myocardial work is mainly a research tool, but the incorporation in commercial echocardiographic software (GE Echopac 202, Horten, Norway) has made work calculations by echocardiography widely available. Similar integration of work in CMR software would be beneficial to increase availability and promote further research and validation of the method in various patient groups.

As mentioned previously, substituting wall stress with pressure constitutes a limitation of the work method. Future studies should investigate if all relevant information (strain, valvular events, radius of curvature and wall thickness) is accessible from a single modality (CMR or 3D echocardiography), allowing for more accurate work estimates. This could increase the precision of the method and allow deeper insights in the pathophysiology of dyssynchronous hearts.

The role of myocardial work over strain is not yet determined, but the incorporation of afterload may be beneficial in some clinical scenarios. This thesis focuses on LV dyssynchrony and the implications in identifying CRT responders. Additionally, the work index could be used to identify the onset of LV lateral wall dysfunction, which has been suggested as a possible optimal time-point for CRT in patients with LBBB (137). Moreover, reduced myocardial work is associated with an increased risk of ventricular arrhythmias (140). Upcoming studies should explore if the work index could aid in the selection of which patients are likely to benefit from a defibrillator in addition to resynchronization.

The work index may also be advantageous over strain to identify subtle impairment in LV function in hypertensive patients or to identify chemotherapy-induced cardiotoxicity of clinical relevance, as previously mentioned. Recent research also indicate that RV work may be a more relevant measure of RV systolic function than conventional echocardiographic parameters (141).

Calculating myocardial work by CMR-FT and non-invasive LVP is particularly useful in patients with poor echocardiographic image quality, or when CMR is indicated for other reasons. Further research is required to determine if the method also is feasible in other patient groups and with different vendors.

Scar imaging by FDG-PET is particularly valuable in patients where CMR is not available or contraindicated. However, access to PET is also limited, and the costs exceeds that of CMR. Future studies should investigate the feasibility of SPECT (perfusion imaging) to identify LV lateral wall scar in LBBB. Additionally, there is a need to investigate if combined imaging of myocardial perfusion and metabolism could identify septal scar in CRT candidates.

There are gaps in knowledge regarding gender-specific differences in cardiovascular diseases. Women have smaller hearts, slightly higher EF, and different disease phenotypes compared to men (228). These differences may influence, among other things, the accuracy of current CRT selection criteria in women. Additionally, women are often underrepresented in randomized clinical trials (229). Future studies should investigate if adjusting for gender and body size could aid in the selecting of patients for CRT. CMR, which provides a comprehensive assessment of myocardial structure and function, may have a unique role in this setting.

CMR represents an additional cost compared to echocardiography, but given the importance of diagnosing septal LGE in CRT candidates, these patients should presumably be given higher priority for CMR than what is current practice. The results from paper 3 should be validated in a randomized prospective study with clinical endpoints. The ongoing randomized

AMEND-CRT trial will presumably shed more light on the role of electromechanical dyssynchrony in general in selecting patients for CRT.

Future research should also explore more thoroughly the correlation between septal flash assessed by echocardiography and by CMR, and how any discrepancies relate to CRT response. Correspondingly, correlations between septal flash, apical rocking and LV work difference in ventricles with varying degree of myocardial scar in different regions, as well as their relations to CRT response, require further investigation.

As of today, there is no evidence that the newer CMR technique T1 mapping has a role in patient selection for CRT (230). In paper 3, we chose to exclude T1 mapping because of low number of patients examined and different magnets used in different centres, and hence uncertain results. Whether T1 mapping could improve timing of CRT implantation (for example as a marker of septal structural changes before visible LGE) is not known and could be a potential topic for future studies.

To date, few studies have explored the effect of CRT in patients with LVEF > 35%, but current knowledge suggests that the treatment may also be beneficial in patients with less severe LV dysfunction (231). Theoretically, by restoring LV synchrony, as well as providing chronotropic support, CRT could potentially improve LV filling, and thereby alleviate symptoms and increase physical capacity in patients with HFpEF. Experimental studies suggest that the effect of CRT to reduce elevated LV filling pressures in LBBB may be heart rate dependent (232). Generally, changes in diastolic properties after CRT appear to be linked to changes in systolic function, but advanced diastolic dysfunction at baseline is associated with worse prognosis after CRT (233-235). An ongoing clinical study investigates the effects of CRT on chronotropic incompetence in patients with HFpEF (236). In total, the heterogeneity of the HFpEF population means that there is a need for extensive future research and individualized treatment strategies.

At present, CRT is considered contraindicated in patients with narrow QRS. However, a recent study has demonstrated superior long-term survival of AV node ablation combined with CRT over pharmacological therapy in patients with permanent atrial fibrillation and narrow QRS (237). More research is warranted.

Other areas for future research include technological improvements to maximize the potential CRT. An ongoing randomized trial aims to determine whether mapping-induced positioning of the LV lead according to the latest local electrical activation in the coronary sinus is beneficial compared to conventional LV lead placement (238). His-bundle pacing has emerged as a novel method to deliver CRT. Recent data indicate that effects on mechanical dyssynchrony and longitudinal contractile function are similar to conventional biventricular pacing (239).

Conclusions

General conclusions

The present thesis provides new insights into the effects of LV dyssynchrony on myocardial function and its relation to CRT response. Our findings strongly support that septal dysfunction in LV dyssynchrony constitutes a target for CRT, and that the likelihood of CRT response depends on structural septal remodelling (scar). We have demonstrated that CMR may assess both septal dysfunction (septal flash or LV work asymmetry) and septal scar, and that both parameters are predictive of CRT response. Therefore, our work encourage increased use of CMR in patients referred for CRT compared to current practice. We found that FDG-PET is a good alternative to CMR to identify transmural LV lateral wall scar, but neither FDG-PET nor echocardiography can identify septal scar in CRT candidates.

Specific conclusions

Paper 1

Myocardial work calculated from strain by FT-CMR in combination with non-invasive LVP is a relevant measure of regional myocardial function in LBBB, which correlates with glucose metabolism and with work by more established techniques.

Paper 2

FDG-PET accurately identifies transmural LV lateral wall scars in CRT candidates, compared to LGE-CMR. Echocardiographic strain is only moderately accurate, but preserved systolic strain in the LV lateral wall makes transmural scars in this region unlikely. Neither FDG-PET nor strain can identify septal scar in dyssynchronous ventricles.

Paper 3

Combined assessment of septal scar and septal flash by CMR identifies CRT responders with high accuracy. Patients without septal scar have excellent response rate. In patients with septal scar, where response rate is more variable, septal flash separates responders from non-responders with high precision. Further studies are needed to verify that the suggested algorithm can prospectively be used to improve patient selection for CRT.

References

1. Gorcsan J, 3rd, Abraham T, Agler DA, Bax JJ, Derumeaux G, Grimm RA, et al. Echocardiography for cardiac resynchronization therapy: recommendations for performance and reporting--a report from the American Society of Echocardiography Dyssynchrony Writing Group endorsed by the Heart Rhythm Society. *J Am Soc Echocardiogr*. 2008;21(3):191-213.
2. Bax JJ, Abraham T, Barold SS, Breithardt OA, Fung JW, Garrigue S, et al. Cardiac resynchronization therapy: Part 1--issues before device implantation. *J Am Coll Cardiol*. 2005;46(12):2153-67.
3. Bax JJ, Ansalone G, Breithardt OA, Derumeaux G, Leclercq C, Schalij MJ, et al. Echocardiographic evaluation of cardiac resynchronization therapy: ready for routine clinical use? *J Am Coll Cardiol*. 2004;44(1):1-9.
4. Kass DA. An epidemic of dyssynchrony: but what does it mean? *J Am Coll Cardiol*. 2008;51(1):12-7.
5. Smiseth OA, Russell K, Skulstad H. The role of echocardiography in quantification of left ventricular dyssynchrony: state of the art and future directions. *Eur Heart J Cardiovasc Imaging*. 2012;13(1):61-8.
6. Jaeschke RG, P; O'Byrne, P. *McMaster Textbook of Internal Medicine 2023*. Available from: <https://empendium.com/mcmtextbook/>.
7. Rawshani A. *ECGwaves.com 2021*. Available from: <https://ecgwaves.com>.
8. Glikson M, Nielsen JC, Kronborg MB, Michowitz Y, Auricchio A, Barbash IM, et al. 2021 ESC Guidelines on cardiac pacing and cardiac resynchronization therapy: Developed by the Task Force on cardiac pacing and cardiac resynchronization therapy of the European Society of Cardiology (ESC) With the special contribution of the European Heart Rhythm Association (EHRA). *European Heart Journal*. 2021.
9. Auricchio A, Fantoni C, Regoli F, Carbucicchio C, Goette A, Geller C, et al. Characterization of left ventricular activation in patients with heart failure and left bundle-branch block. *Circulation*. 2004;109(9):1133-9.
10. Vassallo JA, Cassidy DM, Marchlinski FE, Buxton AE, Waxman HL, Doherty JU, et al. Endocardial activation of left bundle branch block. *Circulation*. 1984;69(5):914-23.
11. Strauss DG, Selvester RH, Wagner GS. Defining left bundle branch block in the era of cardiac resynchronization therapy. *Am J Cardiol*. 2011;107(6):927-34.
12. Tse HF, Lau CP. Long-term effect of right ventricular pacing on myocardial perfusion and function. *J Am Coll Cardiol*. 1997;29(4):744-9.
13. Prinzen FW, Cheriex EC, Delhaas T, van Oosterhout MF, Arts T, Wellens HJ, et al. Asymmetric thickness of the left ventricular wall resulting from asynchronous electric activation: a study in dogs with ventricular pacing and in patients with left bundle branch block. *Am Heart J*. 1995;130(5):1045-53.
14. Imanishi R, Seto S, Ichimaru S, Nakashima E, Yano K, Akahoshi M. Prognostic significance of incident complete left bundle branch block observed over a 40-year period. *Am J Cardiol*. 2006;98(5):644-8.
15. Hardarson T, Arnason A, Eliasson GJ, Palsson K, Eyjolfsson K, Sigfusson N. Left bundle branch block: prevalence, incidence, follow-up and outcome. *Eur Heart J*. 1987;8(10):1075-9.
16. Eriksson P, Hansson PO, Eriksson H, Dellborg M. Bundle-branch block in a general male population: the study of men born 1913. *Circulation*. 1998;98(22):2494-500.
17. Clark AL, Goode K, Cleland JG. The prevalence and incidence of left bundle branch block in ambulant patients with chronic heart failure. *Eur J Heart Fail*. 2008;10(7):696-702.
18. Baldasseroni S, Opasich C, Gorini M, Lucci D, Marchionni N, Marini M, et al. Left bundle-branch block is associated with increased 1-year sudden and total mortality rate in

- 5517 outpatients with congestive heart failure: A report from the Italian Network on Congestive Heart Failure. *Am Heart J.* 2002;143(3):398-405.
19. Tabrizi F, Englund A, Rosenqvist M, Wallentin L, Stenestrand U. Influence of left bundle branch block on long-term mortality in a population with heart failure. *Eur Heart J.* 2007;28(20):2449-55.
 20. Lund LH, Benson L, Ståhlberg M, Braunschweig F, Edner M, Dahlström U, et al. Age, prognostic impact of QRS prolongation and left bundle branch block, and utilization of cardiac resynchronization therapy: findings from 14,713 patients in the Swedish Heart Failure Registry. *Eur J Heart Fail.* 2014;16(10):1073-81.
 21. Kumar V, Venkataraman R, Aljaroudi W, Osorio J, Heo J, Iskandrian AE, et al. Implications of left bundle branch block in patient treatment. *Am J Cardiol.* 2013;111(2):291-300.
 22. Schneider JF, Thomas HE, Kreger BE, McNamara PM, Kannel WB. Newly acquired left bundle-branch block: the Framingham study. *Ann Intern Med.* 1979;90(3):303-10.
 23. Sze E, Dunning A, Loring Z, Atwater BD, Chiswell K, Daubert JP, et al. Comparison of Incidence of Left Ventricular Systolic Dysfunction Among Patients With Left Bundle Branch Block Versus Those With Normal QRS Duration. *Am J Cardiol.* 2017;120(11):1990-7.
 24. Vernooij K, Verbeek XA, Peschar M, Crijns HJ, Arts T, Cornelussen RN, et al. Left bundle branch block induces ventricular remodelling and functional septal hypoperfusion. *Eur Heart J.* 2005;26(1):91-8.
 25. Russell K, Eriksen M, Aaberge L, Wilhelmsen N, Skulstad H, Remme EW, et al. A novel clinical method for quantification of regional left ventricular pressure-strain loop area: a non-invasive index of myocardial work. *Eur Heart J.* 2012;33(6):724-33.
 26. Prinzen FW, Hunter WC, Wyman BT, McVeigh ER. Mapping of regional myocardial strain and work during ventricular pacing: Experimental study using magnetic resonance imaging tagging. *J Am Coll Cardiol.* 1999;33(6):1735-42.
 27. Zanco P, Desideri A, Mobilia G, Cargnel S, Milan E, Celegon L, et al. Effects of left bundle branch block on myocardial FDG PET in patients without significant coronary artery stenoses. *J Nucl Med.* 2000;41(6):973-7.
 28. Ono S, Nohara R, Kambara H, Okuda K, Kawai C. Regional myocardial perfusion and glucose metabolism in experimental left bundle branch block. *Circulation.* 1992;85(3):1125-31.
 29. Mollema SA, Bleeker GB, van der Wall EE, Schalij MJ, Bax JJ. Usefulness of QRS duration to predict response to cardiac resynchronization therapy in patients with end-stage heart failure. *Am J Cardiol.* 2007;100(11):1665-70.
 30. Breithardt OA, Sinha AM, Schwammenthal E, Bidaoui N, Markus KU, Franke A, et al. Acute effects of cardiac resynchronization therapy on functional mitral regurgitation in advanced systolic heart failure. *J Am Coll Cardiol.* 2003;41(5):765-70.
 31. Ozdemir K, Altunkeser BB, Danis G, Ozdemir A, Uluca Y, Tokac M, et al. Effect of the isolated left bundle branch block on systolic and diastolic functions of left ventricle. *J Am Soc Echocardiogr.* 2001;14(11):1075-9.
 32. Larsen CK, Aalen J, Storsten P, Sirnes PA, Gjesdal O, Kongsgaard E, et al. Septal flash and rebound stretch are different entities. *European Heart Journal.* 2018;39(suppl_1):978. Abstract.
 33. Kuznetsova T, Herbots L, Richart T, D'Hooge J, Thijs L, Fagard RH, et al. Left ventricular strain and strain rate in a general population. *Eur Heart J.* 2008;29(16):2014-23.
 34. Voigt JU, Pedrizzetti G, Lysyansky P, Marwick TH, Houle H, Baumann R, et al. Definitions for a common standard for 2D speckle tracking echocardiography: consensus

- document of the EACVI/ASE/Industry Task Force to standardize deformation imaging. *Eur Heart J Cardiovasc Imaging*. 2015;16(1):1-11.
35. Marwick TH, Leano RL, Brown J, Sun JP, Hoffmann R, Lysyansky P, et al. Myocardial strain measurement with 2-dimensional speckle-tracking echocardiography: definition of normal range. *JACC Cardiovasc Imaging*. 2009;2(1):80-4.
 36. Mirea O, Pagourelas ED, Duchenne J, Bogaert J, Thomas JD, Badano LP, et al. Intervendor Differences in the Accuracy of Detecting Regional Functional Abnormalities: A Report From the EACVI-ASE Strain Standardization Task Force. *JACC Cardiovasc Imaging*. 2018;11(1):25-34.
 37. Scatteia A, Baritussio A, Bucciarelli-Ducci C. Strain imaging using cardiac magnetic resonance. *Heart Fail Rev*. 2017;22(4):465-76.
 38. Pedrizzetti G, Claus P, Kilner PJ, Nagel E. Principles of cardiovascular magnetic resonance feature tracking and echocardiographic speckle tracking for informed clinical use. *J Cardiovasc Magn R*. 2016;18(1):51.
 39. Urheim S, Edvardsen T, Torp H, Angelsen B, Smiseth OA. Myocardial strain by Doppler echocardiography. Validation of a new method to quantify regional myocardial function. *Circulation*. 2000;102(10):1158-64.
 40. Basford JR. The Law of Laplace and its relevance to contemporary medicine and rehabilitation. *Archives of Physical Medicine and Rehabilitation*. 2002;83(8):1165-70.
 41. Takaoka H, Takeuchi M, Odake M, Yokoyama M. Assessment of myocardial oxygen consumption (Vo₂) and systolic pressure-volume area (PVA) in human hearts. *Eur Heart J*. 1992;13 Suppl E:85-90.
 42. Hisano R, Cooper Gt. Correlation of force-length area with oxygen consumption in ferret papillary muscle. *Circ Res*. 1987;61(3):318-28.
 43. Urheim S, Rabben SI, Skulstad H, Lyseggen E, Ihlen H, Smiseth OA. Regional myocardial work by strain Doppler echocardiography and LV pressure: a new method for quantifying myocardial function. *Am J Physiol Heart Circ Physiol*. 2005;288(5):H2375-80.
 44. Aalen J IH, Duchenne J, Larsen CK, Storsten P, Sirnes PA, et al. Septal work is a more sensitive marker of myocardial dysfunction in dyssynchrony than strain. *European Heart Journal*. 2018;39(suppl 1):159. Abstract.
 45. Parsai C, Bijnens B, Sutherland GR, Baltabaeva A, Claus P, Marciniak M, et al. Toward understanding response to cardiac resynchronization therapy: left ventricular dyssynchrony is only one of multiple mechanisms. *Eur Heart J*. 2009;30(8):940-9.
 46. Dillon JC, Chang S, Feigenbaum H. Echocardiographic manifestations of left bundle branch block. *Circulation*. 1974;49(5):876-80.
 47. McDonald IG. Echocardiographic demonstration of abnormal motion of the interventricular septum in left bundle branch block. *Circulation*. 1973;48(2):272-80.
 48. Corteville B, De Pooter J, De Backer T, El Haddad M, Stroobandt R, Timmermans F. The electrocardiographic characteristics of septal flash in patients with left bundle branch block. *Europace*. 2017;19(1):103-9.
 49. Stankovic I, Prinz C, Ciarka A, Daraban AM, Kotrc M, Aaronson M, et al. Relationship of visually assessed apical rocking and septal flash to response and long-term survival following cardiac resynchronization therapy (PREDICT-CRT). *Eur Heart J Cardiovasc Imaging*. 2016;17(3):262-9.
 50. Leenders GE, Lumens J, Cramer MJ, De Boeck BWL, Doevendans PA, Delhaas T, et al. Septal Deformation Patterns Delineate Mechanical Dyssynchrony and Regional Differences in Contractility Analysis of Patient Data Using a Computer Model. *Circ-Heart Fail*. 2012;5(1):87-96.
 51. Voigt JU, Schneider TM, Korder S, Szulik M, Gurel E, Daniel WG, et al. Apical transverse motion as surrogate parameter to determine regional left ventricular function

- inhomogeneities: a new, integrative approach to left ventricular asynchrony assessment. *European Heart Journal*. 2009;30(8):959-68.
52. Beela AS, Ünlü S, Duchenne J, Ciarka A, Daraban AM, Kotrc M, et al. Assessment of mechanical dyssynchrony can improve the prognostic value of guideline-based patient selection for cardiac resynchronization therapy. *Eur Heart J Cardiovasc Imaging*. 2019;20(1):66-74.
 53. Gabrielli L, Marincheva G, Bijmens B, Doltra A, Tolosana JM, Borràs R, et al. Septal flash predicts cardiac resynchronization therapy response in patients with permanent atrial fibrillation. *Europace*. 2014;16(9):1342-9.
 54. Revah G, Wu V, Huntjens PR, Piekarski E, Chyou JY, Axel L. Cardiovascular magnetic resonance features of mechanical dyssynchrony in patients with left bundle branch block. *Int J Cardiovasc Imaging*. 2016;32(9):1427-38.
 55. Sohal M, Amraoui S, Chen Z, Sammut E, Jackson T, Wright M, et al. Combined identification of septal flash and absence of myocardial scar by cardiac magnetic resonance imaging improves prediction of response to cardiac resynchronization therapy. *Journal of Interventional Cardiac Electrophysiology*. 2014;40(2):179-90.
 56. Treibel TA, Kozor R, Schofield R, Benedetti G, Fontana M, Bhuvana AN, et al. Reverse Myocardial Remodeling Following Valve Replacement in Patients With Aortic Stenosis. *J Am Coll Cardiol*. 2018;71(8):860-71.
 57. Kim RJ, Fieno DS, Parrish TB, Harris K, Chen EL, Simonetti O, et al. Relationship of MRI delayed contrast enhancement to irreversible injury, infarct age, and contractile function. *Circulation*. 1999;100(19):1992-2002.
 58. Hundley WG, Bluemke DA, Finn JP, Flamm SD, Fogel MA, Friedrich MG, et al. ACCF/ACR/AHA/NASCI/SCMR 2010 expert consensus document on cardiovascular magnetic resonance: a report of the American College of Cardiology Foundation Task Force on Expert Consensus Documents. *J Am Coll Cardiol*. 2010;55(23):2614-62.
 59. McCrohon JA, Moon JC, Prasad SK, McKenna WJ, Lorenz CH, Coats AJ, et al. Differentiation of heart failure related to dilated cardiomyopathy and coronary artery disease using gadolinium-enhanced cardiovascular magnetic resonance. *Circulation*. 2003;108(1):54-9.
 60. Heling A, Zimmermann R, Kostin S, Maeno Y, Hein S, Devaux B, et al. Increased Expression of Cytoskeletal, Linkage, and Extracellular Proteins in Failing Human Myocardium. *Circ Res*. 2000;86(8):846-53.
 61. Gulati A, Jabbour A, Ismail TF, et al. Association of fibrosis with mortality and sudden cardiac death in patients with nonischemic dilated cardiomyopathy. *JAMA*. 2013;309(9):896-908.
 62. Leyva F, Taylor RJ, Foley PW, Umar F, Mulligan LJ, Patel K, et al. Left ventricular midwall fibrosis as a predictor of mortality and morbidity after cardiac resynchronization therapy in patients with nonischemic cardiomyopathy. *J Am Coll Cardiol*. 2012;60(17):1659-67.
 63. Klein C, Nekolla SG, Bengel FM, Momose M, Sammer A, Haas F, et al. Assessment of myocardial viability with contrast-enhanced magnetic resonance imaging: comparison with positron emission tomography. *Circulation*. 2002;105(2):162-7.
 64. Gjesdal O, Helle-Valle T, Hopp E, Lunde K, Vartdal T, Aakhus S, et al. Noninvasive Separation of Large, Medium, and Small Myocardial Infarcts in Survivors of Reperfused ST-Elevation Myocardial Infarction. *Circulation: Cardiovascular Imaging*. 2008;1(3):189-96.
 65. D'Andrea A, Caso P, Scarafile R, Riegler L, Salerno G, Castaldo F, et al. Effects of global longitudinal strain and total scar burden on response to cardiac resynchronization therapy in patients with ischaemic dilated cardiomyopathy. *Eur J Heart Fail*. 2009;11(1):58-67.

66. Delgado V, van Bommel RJ, Bertini M, Borleffs CJ, Marsan NA, Arnold CT, et al. Relative merits of left ventricular dyssynchrony, left ventricular lead position, and myocardial scar to predict long-term survival of ischemic heart failure patients undergoing cardiac resynchronization therapy. *Circulation*. 2011;123(1):70-8.
67. Kydd AC, Khan F, Gopalan D, Ring L, Rana BS, Virdee MS, et al. Utility of speckle tracking echocardiography to characterize dysfunctional myocardium in patients with ischemic cardiomyopathy referred for cardiac resynchronization therapy. *Echocardiography*. 2014;31(6):736-43.
68. McDonagh TA, Metra M, Adamo M, Gardner RS, Baumbach A, Böhm M, et al. 2021 ESC Guidelines for the diagnosis and treatment of acute and chronic heart failure: Developed by the Task Force for the diagnosis and treatment of acute and chronic heart failure of the European Society of Cardiology (ESC) With the special contribution of the Heart Failure Association (HFA) of the ESC. *European Heart Journal*. 2021.
69. Francis GS, Goldsmith SR, Levine TB, Olivari MT, Cohn JN. The neurohumoral axis in congestive heart failure. *Ann Intern Med*. 1984;101(3):370-7.
70. Benedict CR, Weiner DH, Johnstone DE, Bourassa MG, Ghali JK, Nicklas J, et al. Comparative neurohormonal responses in patients with preserved and impaired left ventricular ejection fraction: results of the Studies of Left Ventricular Dysfunction (SOLVD) Registry. The SOLVD Investigators. *J Am Coll Cardiol*. 1993;22(4 Suppl A):146a-53a.
71. Bleumink GS, Knetsch AM, Sturkenboom MC, Straus SM, Hofman A, Deckers JW, et al. Quantifying the heart failure epidemic: prevalence, incidence rate, lifetime risk and prognosis of heart failure The Rotterdam Study. *Eur Heart J*. 2004;25(18):1614-9.
72. Mosterd A, Hoes AW. Clinical epidemiology of heart failure. *Heart*. 2007;93(9):1137-46.
73. Redfield MM, Jacobsen SJ, Burnett JC, Jr., Mahoney DW, Bailey KR, Rodeheffer RJ. Burden of systolic and diastolic ventricular dysfunction in the community: appreciating the scope of the heart failure epidemic. *Jama*. 2003;289(2):194-202.
74. Ceia F, Fonseca C, Mota T, Morais H, Matias F, de Sousa A, et al. Prevalence of chronic heart failure in Southwestern Europe: the EPICA study. *Eur J Heart Fail*. 2002;4(4):531-9.
75. Cleland JG, McDonagh T, Rigby AS, Yassin A, Whittaker T, Dargie HJ. The national heart failure audit for England and Wales 2008-2009. *Heart*. 2011;97(11):876-86.
76. Harjola VP, Follath F, Nieminen MS, Brutsaert D, Dickstein K, Drexler H, et al. Characteristics, outcomes, and predictors of mortality at 3 months and 1 year in patients hospitalized for acute heart failure. *Eur J Heart Fail*. 2010;12(3):239-48.
77. Yancy CW, Jessup M, Bozkurt B, Butler J, Casey DE, Colvin MM, et al. 2017 ACC/AHA/HFSA Focused Update of the 2013 ACCF/AHA Guideline for the Management of Heart Failure: A Report of the American College of Cardiology/American Heart Association Task Force on Clinical Practice Guidelines and the Heart Failure Society of America. *Circulation*. 2017;136(6):e137-e61.
78. Butler J, Fonarow GC, Zile MR, Lam CS, Roessig L, Schelbert EB, et al. Developing therapies for heart failure with preserved ejection fraction: current state and future directions. *JACC Heart Fail*. 2014;2(2):97-112.
79. Granger CB, McMurray JJ, Yusuf S, Held P, Michelson EL, Olofsson B, et al. Effects of candesartan in patients with chronic heart failure and reduced left-ventricular systolic function intolerant to angiotensin-converting-enzyme inhibitors: the CHARM-Alternative trial. *Lancet*. 2003;362(9386):772-6.
80. Anker SD, Butler J, Filippatos G, Ferreira JP, Bocchi E, Böhm M, et al. Empagliflozin in Heart Failure with a Preserved Ejection Fraction. *New England Journal of Medicine*. 2021;385(16):1451-61.

81. Heidenreich PA, Bozkurt B, Aguilar D, Allen LA, Byun JJ, Colvin MM, et al. 2022 AHA/ACC/HFSA Guideline for the Management of Heart Failure: A Report of the American College of Cardiology/American Heart Association Joint Committee on Clinical Practice Guidelines. *J Am Coll Cardiol*. 2022;79(17):e263-e421.
82. Kosiborod MN, Abildstrøm SZ, Borlaug BA, Butler J, Rasmussen S, Davies M, et al. Semaglutide in Patients with Heart Failure with Preserved Ejection Fraction and Obesity. *New England Journal of Medicine*. 2023.
83. Cleland JG, Daubert JC, Erdmann E, Freemantle N, Gras D, Kappenberger L, et al. The effect of cardiac resynchronization on morbidity and mortality in heart failure. *N Engl J Med*. 2005;352(15):1539-49.
84. Abraham WT, Fisher WG, Smith AL, Delurgio DB, Leon AR, Loh E, et al. Cardiac Resynchronization in Chronic Heart Failure. *New England Journal of Medicine*. 2002;346(24):1845-53.
85. Al-Majed NS, McAlister FA, Bakal JA, Ezekowitz JA. Meta-analysis: cardiac resynchronization therapy for patients with less symptomatic heart failure. *Ann Intern Med*. 2011;154(6):401-12.
86. Koplan BA, Kaplan AJ, Weiner S, Jones PW, Seth M, Christman SA. Heart failure decompensation and all-cause mortality in relation to percent biventricular pacing in patients with heart failure: is a goal of 100% biventricular pacing necessary? *J Am Coll Cardiol*. 2009;53(4):355-60.
87. Hayes DL, Boehmer JP, Day JD, Gilliam FR, 3rd, Heidenreich PA, Seth M, et al. Cardiac resynchronization therapy and the relationship of percent biventricular pacing to symptoms and survival. *Heart Rhythm*. 2011;8(9):1469-75.
88. Curtis AB, Worley SJ, Adamson PB, Chung ES, Niazi I, Sherfese L, et al. Biventricular pacing for atrioventricular block and systolic dysfunction. *N Engl J Med*. 2013;368(17):1585-93.
89. Ruschitzka F, Abraham WT, Singh JP, Bax JJ, Borer JS, Brugada J, et al. Cardiac-resynchronization therapy in heart failure with a narrow QRS complex. *N Engl J Med*. 2013;369(15):1395-405.
90. Køber L, Thune JJ, Nielsen JC, Haarlo J, Videbæk L, Korup E, et al. Defibrillator Implantation in Patients with Nonischemic Systolic Heart Failure. *N Engl J Med*. 2016;375(13):1221-30.
91. Auricchio A, Prinzen FW. Non-responders to cardiac resynchronization therapy: the magnitude of the problem and the issues. *Circ J*. 2011;75(3):521-7.
92. Khidir MJ, Delgado V, Ajmone Marsan N, Schaliij MJ, Bax JJ. QRS duration versus morphology and survival after cardiac resynchronization therapy. *ESC Heart Fail*. 2017;4(1):23-30.
93. Poole JE, Singh JP, Birgersdotter-Green U. QRS Duration or QRS Morphology: What Really Matters in Cardiac Resynchronization Therapy? *J Am Coll Cardiol*. 2016;67(9):1104-17.
94. Cleland JG, Abraham WT, Linde C, Gold MR, Young JB, Claude Daubert J, et al. An individual patient meta-analysis of five randomized trials assessing the effects of cardiac resynchronization therapy on morbidity and mortality in patients with symptomatic heart failure. *Eur Heart J*. 2013;34(46):3547-56.
95. Linde C, Abraham WT, Gold MR, Daubert JC, Tang ASL, Young JB, et al. Predictors of short-term clinical response to cardiac resynchronization therapy. *Eur J Heart Fail*. 2017;19(8):1056-63.
96. Delgado-Montero A, Tayal B, Goda A, Ryo K, Marek JJ, Sugahara M, et al. Additive Prognostic Value of Echocardiographic Global Longitudinal and Global Circumferential

- Strain to Electrocardiographic Criteria in Patients With Heart Failure Undergoing Cardiac Resynchronization Therapy. *Circ Cardiovasc Imaging*. 2016;9(6).
97. Gorcsan J, 3rd, Anderson CP, Tayal B, Sugahara M, Walmsley J, Starling RC, et al. Systolic Stretch Characterizes the Electromechanical Substrate Responsive to Cardiac Resynchronization Therapy. *JACC Cardiovasc Imaging*. 2018.
98. Risum N, Strauss D, Sogaard P, Loring Z, Hansen TF, Bruun NE, et al. Left bundle-branch block: The relationship between electrocardiogram electrical activation and echocardiography mechanical contraction. *Am Heart J*. 2013;166(2):340-8.
99. Yu CM, Fung WH, Lin H, Zhang Q, Sanderson JE, Lau CP. Predictors of left ventricular reverse remodeling after cardiac resynchronization therapy for heart failure secondary to idiopathic dilated or ischemic cardiomyopathy. *Am J Cardiol*. 2003;91(6):684-8.
100. Pitzalis MV, Iacoviello M, Romito R, Massari F, Rizzon B, Luzzi G, et al. Cardiac resynchronization therapy tailored by echocardiographic evaluation of ventricular asynchrony. *J Am Coll Cardiol*. 2002;40(9):1615-22.
101. Bax JJ, Bleeker GB, Marwick TH, Molhoek SG, Boersma E, Steendijk P, et al. Left ventricular dyssynchrony predicts response and prognosis after cardiac resynchronization therapy. *J Am Coll Cardiol*. 2004;44(9):1834-40.
102. Chalil S, Stegemann B, Muhyaldeen S, Khadjooi K, Smith RE, Jordan PJ, et al. Intraventricular dyssynchrony predicts mortality and morbidity after cardiac resynchronization therapy: a study using cardiovascular magnetic resonance tissue synchronization imaging. *J Am Coll Cardiol*. 2007;50(3):243-52.
103. Bilchick KC, Dimaano V, Wu KC, Helm RH, Weiss RG, Lima JA, et al. Cardiac magnetic resonance assessment of dyssynchrony and myocardial scar predicts function class improvement following cardiac resynchronization therapy. *JACC Cardiovasc Imaging*. 2008;1(5):561-8.
104. Marsan NA, Westenberg JJ, Ypenburg C, van Bommel RJ, Roes S, Delgado V, et al. Magnetic resonance imaging and response to cardiac resynchronization therapy: relative merits of left ventricular dyssynchrony and scar tissue. *Eur Heart J*. 2009;30(19):2360-7.
105. Henneman MM, Chen J, Dibbets-Schneider P, Stokkel MP, Bleeker GB, Ypenburg C, et al. Can LV dyssynchrony as assessed with phase analysis on gated myocardial perfusion SPECT predict response to CRT? *J Nucl Med*. 2007;48(7):1104-11.
106. Boogers MM, Van Kriekinge SD, Henneman MM, Ypenburg C, Van Bommel RJ, Boersma E, et al. Quantitative gated SPECT-derived phase analysis on gated myocardial perfusion SPECT detects left ventricular dyssynchrony and predicts response to cardiac resynchronization therapy. *J Nucl Med*. 2009;50(5):718-25.
107. Chung ES, Leon AR, Tavazzi L, Sun JP, Nihoyannopoulos P, Merlino J, et al. Results of the Predictors of Response to CRT (PROSPECT) trial. *Circulation*. 2008;117(20):2608-16.
108. Tayal B, Sogaard P, Risum N. Why Dyssynchrony Matters in Heart Failure? *Card Electrophysiol Clin*. 2019;11(1):39-47.
109. Lumens J, Leenders GE, Cramer MJ, De Boeck BW, Doevendans PA, Prinzen FW, et al. Mechanistic evaluation of echocardiographic dyssynchrony indices: patient data combined with multiscale computer simulations. *Circ Cardiovasc Imaging*. 2012;5(4):491-9.
110. Miyazaki C, Redfield MM, Powell BD, Lin GM, Herges RM, Hodge DO, et al. Dyssynchrony indices to predict response to cardiac resynchronization therapy: a comprehensive prospective single-center study. *Circ Heart Fail*. 2010;3(5):565-73.
111. Risum N, Tayal B, Hansen TF, Bruun NE, Jensen MT, Lauridsen TK, et al. Identification of Typical Left Bundle Branch Block Contraction by Strain Echocardiography Is Additive to Electrocardiography in Prediction of Long-Term Outcome After Cardiac Resynchronization Therapy. *J Am Coll Cardiol*. 2015;66(6):631-41.

112. De Boeck BW, Teske AJ, Meine M, Leenders GE, Cramer MJ, Prinzen FW, et al. Septal rebound stretch reflects the functional substrate to cardiac resynchronization therapy and predicts volumetric and neurohormonal response. *Eur J Heart Fail.* 2009;11(9):863-71.
113. Menet A, Bernard A, Tribouilloy C, Leclercq C, Gevaert C, Guyomar Y, et al. Clinical significance of septal deformation patterns in heart failure patients receiving cardiac resynchronization therapy. *Eur Heart J Cardiovasc Imaging.* 2016;0:1-10.
114. Vecera J, Penicka M, Eriksen M, Russell K, Bartunek J, Vanderheyden M, et al. Wasted septal work in left ventricular dyssynchrony: a novel principle to predict response to cardiac resynchronization therapy. *Eur Heart J Cardiovasc Imaging.* 2016;17(6):624-32.
115. Zweerink A, de Roest GJ, Wu L, Nijveldt R, de Cock CC, van Rossum AC, et al. Prediction of Acute Response to Cardiac Resynchronization Therapy by Means of the Misbalance in Regional Left Ventricular Myocardial Work. *J Card Fail.* 2016;22(2):133-42.
116. Birnie D, de Kemp RA, Tang AS, Ruddy TD, Gollob MH, Guo A, et al. Reduced septal glucose metabolism predicts response to cardiac resynchronization therapy. *J Nucl Cardiol.* 2012;19(1):73-83.
117. Vernooy K, Cornelussen RNM, Verbeek XAAM, Vanagt WYR, van Hunnik A, Kuiper M, et al. Cardiac resynchronization therapy cures dyssynchronopathy in canine left bundle-branch block hearts. *European Heart Journal.* 2007;28(17):2148-55.
118. Nowak B, Sinha AM, Schaefer WM, Koch KC, Kaiser HJ, Hanrath P, et al. Cardiac resynchronization therapy homogenizes myocardial glucose metabolism and perfusion in dilated cardiomyopathy and left bundle branch block. *J Am Coll Cardiol.* 2003;41(9):1523-8.
119. Bleeker GB, Kaandorp TA, Lamb HJ, Boersma E, Steendijk P, de Roos A, et al. Effect of posterolateral scar tissue on clinical and echocardiographic improvement after cardiac resynchronization therapy. *Circulation.* 2006;113(7):969-76.
120. Chalil S, Foley PW, Muyhaldeen SA, Patel KCR, Yousef ZR, Smith REA, et al. Late gadolinium enhancement-cardiovascular magnetic resonance as a predictor of response to cardiac resynchronization therapy in patients with ischaemic cardiomyopathy. *Europace.* 2007;9(11):1031-7.
121. Chalil S, Stegemann B, Muhyaldeen SA, Khadjooi K, Foley PW, Smith RE, et al. Effect of posterolateral left ventricular scar on mortality and morbidity following cardiac resynchronization therapy. *Pacing Clin Electrophysiol.* 2007;30(10):1201-9.
122. Birnie D, DeKemp RA, Ruddy TD, Tang AS, Guo A, Williams K, et al. Effect of lateral wall scar on reverse remodeling with cardiac resynchronization therapy. *Heart Rhythm.* 2009;6(12):1721-6.
123. Ypenburg C, Schalijs MJ, Bleeker GB, Steendijk P, Boersma E, Dibbets-Schneider P, et al. Impact of viability and scar tissue on response to cardiac resynchronization therapy in ischaemic heart failure patients. *Eur Heart J.* 2007;28(1):33-41.
124. Adelstein EC, Saba S. Scar burden by myocardial perfusion imaging predicts echocardiographic response to cardiac resynchronization therapy in ischemic cardiomyopathy. *Am Heart J.* 2007;153(1):105-12.
125. Adelstein EC, Tanaka H, Soman P, Miske G, Haberman SC, Saba SF, et al. Impact of scar burden by single-photon emission computed tomography myocardial perfusion imaging on patient outcomes following cardiac resynchronization therapy. *Eur Heart J.* 2011;32(1):93-103.
126. White JA, Yee R, Yuan X, Krahn A, Skanes A, Parker M, et al. Delayed enhancement magnetic resonance imaging predicts response to cardiac resynchronization therapy in patients with intraventricular dyssynchrony. *J Am Coll Cardiol.* 2006;48(10):1953-60.
127. Duckett SG, Ginks M, Shetty A, Kirubakaran S, Bostock J, Kapetanakis S, et al. Adverse response to cardiac resynchronisation therapy in patients with septal scar on cardiac

- MRI preventing a septal right ventricular lead position. *J Interv Card Electrophysiol*. 2012;33(2):151-60.
128. Khan FZ, Virdee MS, Palmer CR, Pugh PJ, O'Halloran D, Elvik M, et al. Targeted left ventricular lead placement to guide cardiac resynchronization therapy: the TARGET study: a randomized, controlled trial. *J Am Coll Cardiol*. 2012;59(17):1509-18.
129. Birnie D, Lemke B, Aonuma K, Krum H, Lee KL, Gasparini M, et al. Clinical outcomes with synchronized left ventricular pacing: analysis of the adaptive CRT trial. *Heart Rhythm*. 2013;10(9):1368-74.
130. Brignole M, Auricchio A, Baron-Esquivias G, Bordachar P, Boriani G, Breithardt OA, et al. 2013 ESC Guidelines on cardiac pacing and cardiac resynchronization therapy The Task Force on cardiac pacing and resynchronization therapy of the European Society of Cardiology (ESC). Developed in collaboration with the European Heart Rhythm Association (EHRA). *European Heart Journal*. 2013;34(29):2281-329.
131. Heiberg E, Sjögren J, Ugander M, Carlsson M, Engblom H, Arheden H. Design and validation of Segment--freely available software for cardiovascular image analysis. *BMC Med Imaging*. 2010;10:1.
132. Cerqueira MD, Weissman NJ, Dilsizian V, Jacobs AK, Kaul S, Laskey WK, et al. Standardized myocardial segmentation and nomenclature for tomographic imaging of the heart. A statement for healthcare professionals from the Cardiac Imaging Committee of the Council on Clinical Cardiology of the American Heart Association. *Circulation*. 2002;105(4):539-42.
133. Engblom H, Tufvesson J, Jablonowski R, Carlsson M, Aletras AH, Hoffmann P, et al. A new automatic algorithm for quantification of myocardial infarction imaged by late gadolinium enhancement cardiovascular magnetic resonance: experimental validation and comparison to expert delineations in multi-center, multi-vendor patient data. *J Cardiovasc Magn Reson*. 2016;18(1):27.
134. Knuuti MJ, Nuutila P, Ruotsalainen U, Saraste M, Harkonen R, Ahonen A, et al. Euglycemic hyperinsulinemic clamp and oral glucose load in stimulating myocardial glucose utilization during positron emission tomography. *J Nucl Med*. 1992;33(7):1255-62.
135. Thavendiranathan P, Grant AD, Negishi T, Plana JC, Popović ZB, Marwick TH. Reproducibility of echocardiographic techniques for sequential assessment of left ventricular ejection fraction and volumes: application to patients undergoing cancer chemotherapy. *J Am Coll Cardiol*. 2013;61(1):77-84.
136. Hanley JA, McNeil BJ. A method of comparing the areas under receiver operating characteristic curves derived from the same cases. *Radiology*. 1983;148(3):839-43.
137. Sletten OJ, Aalen JM, Izc H, Duchenne J, Remme EW, Larsen CK, et al. Lateral Wall Dysfunction Signals Onset of Progressive Heart Failure in Left Bundle Branch Block. *JACC Cardiovasc Imaging*. 2021;14(11):2059-69.
138. Aalen JM, Donal E, Larsen CK, Duchenne J, Lederlin M, Cvijic M, et al. Imaging predictors of response to cardiac resynchronization therapy: left ventricular work asymmetry by echocardiography and septal viability by cardiac magnetic resonance. *Eur Heart J*. 2020;41(39):3813-23.
139. Duchenne J, Aalen JM, Cvijic M, Larsen CK, Galli E, Bézy S, et al. Acute redistribution of regional left ventricular work by cardiac resynchronization therapy determines long-term remodelling. *Eur Heart J Cardiovasc Imaging*. 2020;21(6):619-28.
140. Saffi H, Winsløw U, Sakthivel T, Højgaard EV, Linde J, Philbert B, et al. Global Constructive Work is associated with ventricular arrhythmias after cardiac resynchronization therapy. *Eur Heart J Cardiovasc Imaging*. 2023.

141. Butcher SC, Fortuni F, Montero-Cabezas JM, Abou R, El Mahdiui M, van der Bijl P, et al. Right ventricular myocardial work: proof-of-concept for non-invasive assessment of right ventricular function. *Eur Heart J Cardiovasc Imaging*. 2021;22(2):142-52.
142. Storsten P, Aalen JM, Boe E, Remme EW, Gjesdal O, Larsen CK, et al. Mechanical Effects on Right Ventricular Function From Left Bundle Branch Block and Cardiac Resynchronization Therapy. *JACC Cardiovasc Imaging*. 2020;13(7):1475-84.
143. Kjaergaard J, Ghio S, St. John Sutton M, Hassager C. Tricuspid Annular Plane Systolic Excursion and Response to Cardiac Resynchronization Therapy: Results From the REVERSE Trial. *Journal of Cardiac Failure*. 2011;17(2):100-7.
144. Galli E, Le Rolle V, Smiseth OA, Duchenne J, Aalen JM, Larsen CK, et al. Importance of Systematic Right Ventricular Assessment in Cardiac Resynchronization Therapy Candidates: A Machine Learning Approach. *J Am Soc Echocardiogr*. 2021;34(5):494-502.
145. Boe E, Russell K, Eek C, Eriksen M, Remme EW, Smiseth OA, et al. Non-invasive myocardial work index identifies acute coronary occlusion in patients with non-ST-segment elevation-acute coronary syndrome. *Eur Heart J Cardiovasc Imaging*. 2015;16(11):1247-55.
146. Thavendiranathan P, Poulin F, Lim KD, Plana JC, Woo A, Marwick TH. Use of myocardial strain imaging by echocardiography for the early detection of cardiotoxicity in patients during and after cancer chemotherapy: a systematic review. *J Am Coll Cardiol*. 2014;63(25 Pt A):2751-68.
147. Aalen J, Storsten P, Remme EW, Sirnes PA, Gjesdal O, Larsen CK, et al. Afterload Hypersensitivity in Patients With Left Bundle Branch Block. *JACC Cardiovasc Imaging*. 2018.
148. Knuuti J, Schelbert HR, Bax JJ. The need for standardisation of cardiac FDG PET imaging in the evaluation of myocardial viability in patients with chronic ischaemic left ventricular dysfunction. *Eur J Nucl Med Mol Imaging*. 2002;29(9):1257-66.
149. Lehner S, Uebleis C, Schüßler F, Haug A, Kääb S, Bartenstein P, et al. The amount of viable and dyssynchronous myocardium is associated with response to cardiac resynchronization therapy: initial clinical results using multiparametric ECG-gated [18F]FDG PET. *Eur J Nucl Med Mol Imaging*. 2013;40(12):1876-83.
150. Degtiarova G, Claus P, Duchenne J, Bogaert J, Nuyts J, Vöros G, et al. Left ventricular regional glucose metabolism in combination with septal scar extent identifies CRT responders. *Eur J Nucl Med Mol Imaging*. 2021;48(8):2437-46.
151. Khan FZ, Virdee MS, Read PA, Pugh PJ, O'Halloran D, Fahey M, et al. Effect of low-amplitude two-dimensional radial strain at left ventricular pacing sites on response to cardiac resynchronization therapy. *J Am Soc Echocardiogr*. 2010;23(11):1168-76.
152. Sade LE, Saba S, Marek JJ, Onishi T, Schwartzman D, Adelstein EC, et al. The association of left ventricular lead position related to regional scar by speckle-tracking echocardiography with clinical outcomes in patients receiving cardiac resynchronization therapy. *J Am Soc Echocardiogr*. 2014;27(6):648-56.
153. Aalen JM, Remme EW, Larsen CK, Andersen OS, Krogh M, Duchenne J, et al. Mechanism of Abnormal Septal Motion in Left Bundle Branch Block: Role of Left Ventricular Wall Interactions and Myocardial Scar. *JACC Cardiovasc Imaging*. 2019;12(12):2402-13.
154. Mahrholdt H, Zhydkov A, Hager S, Meinhardt G, Vogelsberg H, Wagner A, et al. Left ventricular wall motion abnormalities as well as reduced wall thickness can cause false positive results of routine SPECT perfusion imaging for detection of myocardial infarction. *European Heart Journal*. 2005;26(20):2127-35.

155. Dilsizian V, Bacharach SL, Beanlands RS, Bergmann SR, Delbeke D, Gropler RJ, et al. PET myocardial perfusion and metabolism clinical imaging. *Journal of Nuclear Cardiology*. 2009;16(4):651-.
156. Morishima I, Okumura K, Tsuboi H, Morita Y, Takagi K, Yoshida R, et al. Impact of basal inferolateral scar burden determined by automatic analysis of 99mTc-MIBI myocardial perfusion SPECT on the long-term prognosis of cardiac resynchronization therapy. *Europace*. 2017;19(4):573-80.
157. Duchenne J, Larsen CK, Cvijic M, Galli E, Aalen JM, Klop B, et al. Visual Presence of Mechanical Dyssynchrony Combined With Septal Scarring Identifies Responders to Cardiac Resynchronization Therapy. *JACC: Cardiovascular Imaging*. 2022.
158. Lumens J, Ploux S, Strik M, Gorcsan J, 3rd, Cochet H, Derval N, et al. Comparative electromechanical and hemodynamic effects of left ventricular and biventricular pacing in dyssynchronous heart failure: electrical resynchronization versus left-right ventricular interaction. *J Am Coll Cardiol*. 2013;62(25):2395-403.
159. Leclercq C. Systolic Improvement and Mechanical Resynchronization Does Not Require Electrical Synchrony in the Dilated Failing Heart With Left Bundle-Branch Block. *Circulation*. 2002;106(14):1760-3.
160. Zweerink A, Friedman DJ, Klem I, van de Ven PM, Vink C, Biesbroek PS, et al. Segment Length in Cine Strain Analysis Predicts Cardiac Resynchronization Therapy Outcome Beyond Current Guidelines. *Circ Cardiovasc Imaging*. 2021;14(7):e012350.
161. Hunold P, Schlosser T, Vogt FM, Eggebrecht H, Schmermund A, Bruder O, et al. Myocardial late enhancement in contrast-enhanced cardiac MRI: distinction between infarction scar and non-infarction-related disease. *AJR Am J Roentgenol*. 2005;184(5):1420-6.
162. Bello D, Fieno DS, Kim RJ, Pereles FS, Passman R, Song G, et al. Infarct morphology identifies patients with substrate for sustained ventricular tachycardia. *J Am Coll Cardiol*. 2005;45(7):1104-8.
163. Bogun FM, Desjardins B, Good E, Gupta S, Crawford T, Oral H, et al. Delayed-enhanced magnetic resonance imaging in nonischemic cardiomyopathy: utility for identifying the ventricular arrhythmia substrate. *J Am Coll Cardiol*. 2009;53(13):1138-45.
164. Grigoratos C, Liga R, Bennati E, Barison A, Todiere G, Aquaro GD, et al. Magnetic Resonance Imaging Correlates of Left Bundle Branch Disease in Patients With Nonischemic Cardiomyopathy. *Am J Cardiol*. 2017.
165. Masci PG, Schuurman R, Andrea B, Ripoli A, Coceani M, Chiappino S, et al. Myocardial fibrosis as a key determinant of left ventricular remodeling in idiopathic dilated cardiomyopathy: a contrast-enhanced cardiovascular magnetic study. *Circ Cardiovasc Imaging*. 2013;6(5):790-9.
166. Gulati A, Jabbour A, Ismail TF, Guha K, Khwaja J, Raza S, et al. Association of fibrosis with mortality and sudden cardiac death in patients with nonischemic dilated cardiomyopathy. *Jama*. 2013;309(9):896-908.
167. Steelant B, Stankovic I, Roijackers I, Aarones M, Bogaert J, Desmet W, et al. The Impact of Infarct Location and Extent on LV Motion Patterns: Implications for Dyssynchrony Assessment. *JACC Cardiovasc Imaging*. 2016;9(6):655-64.
168. Calle S, Delens C, Kamoen V, De Pooter J, Timmermans F. Septal flash: At the heart of cardiac dyssynchrony. *Trends Cardiovasc Med*. 2020;30(2):115-22.
169. Little WC, Reeves RC, Arciniegas J, Katholi RE, Rogers EW. Mechanism of abnormal interventricular septal motion during delayed left ventricular activation. *Circulation*. 1982;65(7):1486-91.
170. Kingma I, Tyberg JV, Smith ER. Effects of diastolic transseptal pressure gradient on ventricular septal position and motion. *Circulation*. 1983;68(6):1304-14.

171. Gjesdal O, Remme EW, Opdahl A, Skulstad H, Russell K, Kongsgaard E, et al. Mechanisms of abnormal systolic motion of the interventricular septum during left bundle-branch block. *Circ Cardiovasc Imaging*. 2011;4(3):264-73.
172. Walmsley J, Huntjens PR, Prinzen FW, Delhaas T, Lumens J. Septal flash and septal rebound stretch have different underlying mechanisms. *Am J Physiol-Heart C*. 2016;310(3):H394-H403.
173. Remme EW, Niederer S, Gjesdal O, Russell K, Hyde ER, Smith N, et al. Factors determining the magnitude of the pre-ejection leftward septal motion in left bundle branch block. *Europace*. 2015.
174. Burri H, Domenichini G, Sunthorn H, Fleury E, Stettler C, Foulkes I, et al. Right ventricular systolic function and cardiac resynchronization therapy. *Europace*. 2010;12(3):389-94.
175. Alpendurada F, Guha K, Sharma R, Ismail TF, Clifford A, Banya W, et al. Right ventricular dysfunction is a predictor of non-response and clinical outcome following cardiac resynchronization therapy. *J Cardiovasc Magn R*. 2011;13(1):68.
176. Gimbel JR, Bello D, Schmitt M, Merkely B, Schwitter J, Hayes DL, et al. Randomized trial of pacemaker and lead system for safe scanning at 1.5 Tesla. *Heart Rhythm*. 2013;10(5):685-91.
177. Williamson BD, Gohn DC, Ramza BM, Singh B, Zhong Y, Li S, et al. Real-World Evaluation of Magnetic Resonance Imaging in Patients With a Magnetic Resonance Imaging Conditional Pacemaker System: Results of 4-Year Prospective Follow-Up in 2,629 Patients. *JACC Clin Electrophysiol*. 2017;3(11):1231-9.
178. Russo RJ, Costa HS, Silva PD, Anderson JL, Arshad A, Biederman RW, et al. Assessing the Risks Associated with MRI in Patients with a Pacemaker or Defibrillator. *N Engl J Med*. 2017;376(8):755-64.
179. Bhuva AN, Moralee R, Bruncker T, Lascelles K, Cash L, Patel KP, et al. Evidence to support magnetic resonance conditional labelling of all pacemaker and defibrillator leads in patients with cardiac implantable electronic devices. *Eur Heart J*. 2022;43(26):2469-78.
180. Munawar DA, Chan JEZ, Emami M, Kadhim K, Khokhar K, O'Shea C, et al. Magnetic resonance imaging in non-conditional pacemakers and implantable cardioverter-defibrillators: a systematic review and meta-analysis. *Europace*. 2020;22(2):288-98.
181. Hopp ES, P.T.; Landa, M.; Lyseggen, E.; Tomterstad, A.H.; Pedersen, H.K. MR-undersøkelse av pasienter med pacemaker eller implantert hjertestarter. *Tidsskrift for den norske legeforening*. 2017;Utgave 21, 14. november 2017
182. Kodzwa R. *ACR Manual on Contrast Media: 2018 Updates*. *Radiol Technol*. 2019;91(1):97-100.
183. Woolen SA, Shankar PR, Gagnier JJ, MacEachern MP, Singer L, Davenport MS. Risk of Nephrogenic Systemic Fibrosis in Patients With Stage 4 or 5 Chronic Kidney Disease Receiving a Group II Gadolinium-Based Contrast Agent: A Systematic Review and Meta-analysis. *JAMA Internal Medicine*. 2020;180(2):223-30.
184. Radiology ESOU. *ESUR Guidelines on Contrast Agents 10.0*. https://www.esur.org/fileadmin/content/2019/ESUR_Guidelines_100_Final_Versionpdf. 2019:A.3.2 Nephrogenic systemic fibrosis.
185. Kaasalainen T, Kivistö S, Holmström M, Peltonen J, Pakarinen S, Hänninen H, et al. Cardiac MRI in patients with cardiac pacemakers: practical methods for reducing susceptibility artifacts and optimizing image quality. *Acta Radiol*. 2016;57(2):178-87.
186. Daubert C, Behar N, Martins RP, Mabo P, Leclercq C. Avoiding non-responders to cardiac resynchronization therapy: a practical guide. *Eur Heart J*. 2017;38(19):1463-72.
187. Daubert JC, Saxon L, Adamson PB, Auricchio A, Berger RD, Beshai JF, et al. 2012 EHRA/HRS expert consensus statement on cardiac resynchronization therapy in heart failure:

- implant and follow-up recommendations and management. *Heart Rhythm*. 2012;9(9):1524-76.
188. Linde C, Abraham WT, Gold MR, St John Sutton M, Ghio S, Daubert C. Randomized trial of cardiac resynchronization in mildly symptomatic heart failure patients and in asymptomatic patients with left ventricular dysfunction and previous heart failure symptoms. *J Am Coll Cardiol*. 2008;52(23):1834-43.
189. Moss AJ, Hall WJ, Cannom DS, Klein H, Brown MW, Daubert JP, et al. Cardiac-resynchronization therapy for the prevention of heart-failure events. *N Engl J Med*. 2009;361(14):1329-38.
190. Yu CM, Bleeker GB, Fung JW, Schalij MJ, Zhang Q, van der Wall EE, et al. Left ventricular reverse remodeling but not clinical improvement predicts long-term survival after cardiac resynchronization therapy. *Circulation*. 2005;112(11):1580-6.
191. Gold MR, Daubert C, Abraham WT, Ghio S, St John Sutton M, Hudnall JH, et al. The effect of reverse remodeling on long-term survival in mildly symptomatic patients with heart failure receiving cardiac resynchronization therapy: results of the REVERSE study. *Heart Rhythm*. 2015;12(3):524-30.
192. Stankovic I, Belmans A, Prinz C, Ciarka A, Maria Daraban A, Kotrc M, et al. The association of volumetric response and long-term survival after cardiac resynchronization therapy. *Eur Heart J Cardiovasc Imaging*. 2017;18(10):1109-17.
193. Ypenburg C, van Bommel RJ, Borleffs CJ, Bleeker GB, Boersma E, Schalij MJ, et al. Long-term prognosis after cardiac resynchronization therapy is related to the extent of left ventricular reverse remodeling at midterm follow-up. *J Am Coll Cardiol*. 2009;53(6):483-90.
194. Cikes M, Solomon SD. Beyond ejection fraction: an integrative approach for assessment of cardiac structure and function in heart failure. *Eur Heart J*. 2016;37(21):1642-50.
195. Ghio S, Freemantle N, Scelsi L, Serio A, Magrini G, Pasotti M, et al. Long-term left ventricular reverse remodeling with cardiac resynchronization therapy: results from the CARE-HF trial. *Eur J Heart Fail*. 2009;11(5):480-8.
196. Bleeker GB, Mollema SA, Holman ER, Veire NVD, Ypenburg C, Boersma E, et al. Left Ventricular Resynchronization Is Mandatory for Response to Cardiac Resynchronization Therapy. *Circulation*. 2007;116(13):1440-8.
197. Woo GW, Petersen-Stejskal S, Johnson JW, Conti JB, Aranda JA, Jr., Curtis AB. Ventricular reverse remodeling and 6-month outcomes in patients receiving cardiac resynchronization therapy: analysis of the MIRACLE study. *J Interv Card Electrophysiol*. 2005;12(2):107-13.
198. Goldenberg I, Kutyifa V, Klein HU, Cannom DS, Brown MW, Dan A, et al. Survival with cardiac-resynchronization therapy in mild heart failure. *N Engl J Med*. 2014;370(18):1694-701.
199. Packer M. Proposal for a new clinical end point to evaluate the efficacy of drugs and devices in the treatment of chronic heart failure. *J Card Fail*. 2001;7(2):176-82.
200. Cleland J, Tageldien A, Buga L, Wong KYK, Gorcsan J. Should we be trying to define responders to cardiac resynchronization therapy? *JACC Cardiovascular imaging*. 2010;3 5:541-9.
201. Skulstad H, Edvardsen T, Urheim S, Rabben SI, Stugaard M, Lyseggen E, et al. Postsystolic shortening in ischemic myocardium: active contraction or passive recoil? *Circulation*. 2002;106(6):718-24.
202. Rösner A, Bijnens B, Hansen M, How OJ, Aarsaether E, Müller S, et al. Left ventricular size determines tissue Doppler-derived longitudinal strain and strain rate. *Eur J Echocardiogr*. 2009;10(2):271-7.

203. van Everdingen WM, Zweerink A, Nijveldt R, Salden OAE, Meine M, Maass AH, et al. Comparison of strain imaging techniques in CRT candidates: CMR tagging, CMR feature tracking and speckle tracking echocardiography. *Int J Cardiovasc Imaging*. 2018;34(3):443-56.
204. Claus P, Omar AM, Pedrizzetti G, Sengupta PP, Nagel E. Tissue Tracking Technology for Assessing Cardiac Mechanics: Principles, Normal Values, and Clinical Applications. *JACC Cardiovasc Imaging*. 2015;8(12):1444-60.
205. Hung CL, Gonçalves A, Shah AM, Cheng S, Kitzman D, Solomon SD. Age- and Sex-Related Influences on Left Ventricular Mechanics in Elderly Individuals Free of Prevalent Heart Failure: The ARIC Study (Atherosclerosis Risk in Communities). *Circ Cardiovasc Imaging*. 2017;10(1).
206. Augustine D, Lewandowski AJ, Lazdam M, Rai A, Francis J, Myerson S, et al. Global and regional left ventricular myocardial deformation measures by magnetic resonance feature tracking in healthy volunteers: comparison with tagging and relevance of gender. *J Cardiovasc Magn Reson*. 2013;15:8.
207. Greenbaum RA, Ho SY, Gibson DG, Becker AE, Anderson RH. Left-Ventricular Fiber Architecture in Man. *Brit Heart J*. 1981;45(3):248-63.
208. Gjesdal O, Hopp E, Vartdal T, Lunde K, Helle-Valle T, Aakhus S, et al. Global longitudinal strain measured by two-dimensional speckle tracking echocardiography is closely related to myocardial infarct size in chronic ischaemic heart disease. *Clin Sci (Lond)*. 2007;113(6):287-96.
209. Gonçalves AV, Rosa SA, Branco L, Galrinho A, Fiarresga A, Lopes LR, et al. Myocardial work is associated with significant left ventricular myocardial fibrosis in patients with hypertrophic cardiomyopathy. *Int J Cardiovasc Imaging*. 2021;37(7):2237-44.
210. McAlindon E, Pufulete M, Lawton C, Angelini GD, Bucciarelli-Ducci C. Quantification of infarct size and myocardium at risk: evaluation of different techniques and its implications. *Eur Heart J Cardiovasc Imaging*. 2015;16(7):738-46.
211. Sievers B, Elliott MD, Hurwitz LM, Albert TS, Klem I, Rehwald WG, et al. Rapid detection of myocardial infarction by subsecond, free-breathing delayed contrast-enhancement cardiovascular magnetic resonance. *Circulation*. 2007;115(2):236-44.
212. Flett AS, Hasleton J, Cook C, Hausenloy D, Quarta G, Ariti C, et al. Evaluation of techniques for the quantification of myocardial scar of differing etiology using cardiac magnetic resonance. *JACC Cardiovasc Imaging*. 2011;4(2):150-6.
213. Bondarenko O, Beek AM, Hofman MB, Köhl HP, Twisk JW, van Dockum WG, et al. Standardizing the definition of hyperenhancement in the quantitative assessment of infarct size and myocardial viability using delayed contrast-enhanced CMR. *J Cardiovasc Magn Reson*. 2005;7(2):481-5.
214. Kim HW, Farzaneh-Far A, Kim RJ. Cardiovascular magnetic resonance in patients with myocardial infarction: current and emerging applications. *J Am Coll Cardiol*. 2009;55(1):1-16.
215. Dempster AP, Laird NM, Rubin DB. Maximum Likelihood from Incomplete Data via the EM Algorithm. *Journal of the Royal Statistical Society Series B (Methodological)*. 1977;39(1):1-38.
216. Heiberg E, Ugander M, Engblom H, Götberg M, Olivecrona GK, Erlinge D, et al. Automated quantification of myocardial infarction from MR images by accounting for partial volume effects: animal, phantom, and human study. *Radiology*. 2008;246(2):581-8.
217. Alexandre J, Saloux E, Dugue AE, Lebon A, Lemaitre A, Roule V, et al. Scar extent evaluated by late gadolinium enhancement CMR: a powerful predictor of long term appropriate ICD therapy in patients with coronary artery disease. *J Cardiovasc Magn Reson*. 2013;15:12.




218. Kim RJ, Wu E, Rafael A, Chen EL, Parker MA, Simonetti O, et al. The use of contrast-enhanced magnetic resonance imaging to identify reversible myocardial dysfunction. *N Engl J Med*. 2000;343(20):1445-53.
219. Tarantini G, Razzolini R, Cacciavillani L, Bilato C, Sarais C, Corbetti F, et al. Influence of transmural, infarct size, and severe microvascular obstruction on left ventricular remodeling and function after primary coronary angioplasty. *Am J Cardiol*. 2006;98(8):1033-40.
220. Özdemir K, Altunkeser BB, Korkut B, Tokaç M, Gök H. Effect of Left Bundle Branch Block on Systolic and Diastolic Function of Left Ventricle in Heart Failure. *Angiology*. 2004;55(1):63-71.
221. Tsao J, Boesiger P, Pruessmann KP. k-t BLAST and k-t SENSE: dynamic MRI with high frame rate exploiting spatiotemporal correlations. *Magn Reson Med*. 2003;50(5):1031-42.
222. Dilsizian V. 18F-FDG Uptake as a Surrogate Marker for Antecedent Ischemia. *J Nucl Med*. 2008;49(12):1909-11.
223. Garcia MJ, Kwong RY, Scherrer-Crosbie M, Taub CC, Blankstein R, Lima J, et al. State of the Art: Imaging for Myocardial Viability: A Scientific Statement From the American Heart Association. *Circ Cardiovasc Imaging*. 2020;13(7):e000053.
224. Degtiarova G, Claus P, Duchenne J, Cvijic M, Schramm G, Nuyts J, et al. Low septal to lateral wall 18F-FDG ratio is highly associated with mechanical dyssynchrony in non-ischemic CRT candidates. *EJNMMI Research*. 2019;9(1):105.
225. Degtiarova G, Claus P, Duchenne J, Schramm G, Nuyts J, Bogaert J, et al. Can nuclear imaging accurately detect scar in ischemic cardiac resynchronization therapy candidates? *Nucl Med Commun*. 2022;43(5):502-9.
226. Fawcett T. An introduction to ROC analysis. *Pattern Recognition Letters*. 2006;27(8):861-74.
227. Kutner MH, Nachtsheim, C.J. and Neter, J. *Applied Linear Regression Models*. 4th Edition ed: McGraw-Hill/Irwin, New York; 2004.
228. Bucciarelli-Ducci C, Ostendorf E, Baldassarre LA, Ferreira VM, Frank L, Kallianos K, et al. Cardiovascular disease in women: insights from magnetic resonance imaging. *J Cardiovasc Magn Reson*. 2020;22(1):71.
229. Melloni C, Berger JS, Wang TY, Gunes F, Stebbins A, Pieper KS, et al. Representation of women in randomized clinical trials of cardiovascular disease prevention. *Circ Cardiovasc Qual Outcomes*. 2010;3(2):135-42.
230. Chen Z, Sohal M, Sammut E, Child N, Jackson T, Claridge S, et al. Focal But Not Diffuse Myocardial Fibrosis Burden Quantification Using Cardiac Magnetic Resonance Imaging Predicts Left Ventricular Reverse Modeling Following Cardiac Resynchronization Therapy. *Journal of Cardiovascular Electrophysiology*. 2016;27(2):203-9.
231. Chung ES, Katra RP, Ghio S, Bax J, Gerritse B, Hilpisch K, et al. Cardiac resynchronization therapy may benefit patients with left ventricular ejection fraction >35%: a PROSPECT trial substudy. *Eur J Heart Fail*. 2010;12(6):581-7.
232. Andersen Ø S, Krogh MR, Boe E, Storsten P, Aalen JM, Larsen CK, et al. Left bundle branch block increases left ventricular diastolic pressure during tachycardia due to incomplete relaxation. *J Appl Physiol (1985)*. 2020;128(4):729-38.
233. Egnaczyk GF, Chung ES. The relationship between cardiac resynchronization therapy and diastolic function. *Curr Heart Fail Rep*. 2014;11(1):64-9.
234. Gradaus R, Stuckenberg V, Löher A, Köbe J, Reinke F, Gunia S, et al. Diastolic filling pattern and left ventricular diameter predict response and prognosis after cardiac resynchronisation therapy. *Heart*. 2008;94(8):1026-31.

235. Galli E, Smiseth Oa Md P, Aalen JM, Larsen CK, Sade E, Hubert A, et al. Prognostic utility of the assessment of diastolic function in patients undergoing cardiac resynchronization therapy. *Int J Cardiol.* 2021;331:144-51.
236. Cardiac Resynchronisation Therapy Versus Rate-responsive Pacing in Heart Failure With Preserved Ejection Fraction (PREFECTUS). July 24, 2020. ClinicalTrials.gov identifier: NCT03338374 [Internet]. Available from: <https://clinicaltrials.gov/ct2/show/NCT03338374>.
237. Brignole M, Pentimalli F, Palmisano P, Landolina M, Quartieri F, Occhetta E, et al. AV junction ablation and cardiac resynchronization for patients with permanent atrial fibrillation and narrow QRS: the APAF-CRT mortality trial. *European Heart Journal.* 2021.
238. Kronborg MB, Frausing M, Svendsen JH, Johansen JB, Riahi S, Haarbo J, et al. Does targeted positioning of the left ventricular pacing lead towards the latest local electrical activation in cardiac resynchronization therapy reduce the incidence of death or hospitalization for heart failure? *Am Heart J.* 2023;263:112-22.
239. Højgaard EV, Philbert BT, Linde JJ, Winløw UC, Svendsen JH, Vinther M, et al. Efficacy on resynchronization and longitudinal contractile function comparing His-bundle pacing with conventional biventricular pacing: a substudy to the His-alternative study. *European Heart Journal - Cardiovascular Imaging.* 2023.

Paper 1



Regional myocardial work by cardiac magnetic resonance and non-invasive left ventricular pressure: a feasibility study in left bundle branch block

Camilla Kjellstad Larsen ^{1,2,3,4}, John M. Aalen^{1,2,3,4}, Caroline Stokke^{5,6,7}, Jan Gunnar Fjeld^{6,7}, Erik Kongsgaard^{2,3}, Jürgen Duchenne^{8,9}, Ganna Degtiarova ^{10,11}, Olivier Gheysens^{10,11}, Jens-Uwe Voigt^{8,9}, Otto A. Smiseth^{1,2,3,4}, and Einar Hopp ^{2,6*}

¹Institute for Surgical Research, Oslo University Hospital, Oslo, Norway; ²Center for Cardiological Innovation, Oslo University Hospital, Oslo, Norway; ³Department of Cardiology, Oslo University Hospital, Oslo, Norway; ⁴Institute of Clinical Medicine, University of Oslo, Oslo, Norway; ⁵Department of Diagnostic Physics, Oslo University Hospital, Oslo, Norway; ⁶Division of Radiology and Nuclear Medicine, Oslo University Hospital, Rikshospitalet, N-0027 Oslo, Norway; ⁷Oslo Metropolitan University, Oslo, Norway; ⁸Department of Cardiovascular Diseases, University Hospitals Leuven, Leuven, Belgium; ⁹Department of Cardiovascular Sciences, KU Leuven – University of Leuven, Leuven, Belgium; ¹⁰Department of Nuclear Medicine, University Hospitals Leuven, Leuven, Belgium; and ¹¹Department of Imaging and Pathology, KU Leuven – University of Leuven, Leuven, Belgium

Received 11 April 2019; editorial decision 18 August 2019; accepted 16 September 2019; online publish-ahead-of-print 10 October 2019

Aims

Regional myocardial work may be assessed by pressure–strain analysis using a non-invasive estimate of left ventricular pressure (LVP). Strain by speckle tracking echocardiography (STE) is not always accessible due to poor image quality. This study investigated the estimation of regional myocardial work from strain by feature tracking (FT) cardiac magnetic resonance (CMR) and non-invasive LVP.

Methods and results

Thirty-seven heart failure patients with reduced ejection fraction, left bundle branch block (LBBB), and no myocardial scar were compared to nine controls without LBBB. Circumferential strain was measured by FT-CMR in a mid-ventricular short-axis cine view, and longitudinal strain by STE. Segmental work was calculated by pressure–strain analysis. Twenty-five patients underwent ¹⁸F-fluorodeoxyglucose (FDG) positron emission tomography. Segmental values were reported as percentages of the segment with maximum myocardial FDG uptake. In LBBB patients, net CMR-derived work was 51 ± 537 (mean \pm standard deviation) in septum vs. 1978 ± 1084 mmHg-% in the left ventricular (LV) lateral wall ($P < 0.001$). In controls, however, there was homogeneous work distribution with similar values in septum and the LV lateral wall (non-significant). Reproducibility was good. Segmental CMR-derived work correlated with segmental STE-derived work and with segmental FDG uptake (average $r = 0.71$ and 0.80 , respectively).

Conclusion

FT-CMR in combination with non-invasive LVP demonstrated markedly reduced work in septum compared to the LV lateral wall in patients with LBBB. Work distribution correlated with STE-derived work and energy demand as reflected in FDG uptake. These results suggest that FT-CMR in combination with non-invasive LVP is a relevant clinical tool to measure regional myocardial work.

Keywords

dyssynchrony • myocardial work • strain • feature tracking • cardiac magnetic resonance • ¹⁸F-fluorodeoxyglucose • positron emission tomography • heart failure

* Corresponding author. Tel: +47 (23) 0700 00; Fax: +47 (23) 0726 10. E-mail: ehopp@ous-hf.no

© The Author(s) 2019. Published by Oxford University Press on behalf of the European Society of Cardiology.

This is an Open Access article distributed under the terms of the Creative Commons Attribution Non-Commercial License (<http://creativecommons.org/licenses/by-nc/4.0/>), which permits non-commercial re-use, distribution, and reproduction in any medium, provided the original work is properly cited. For commercial re-use, please contact journals.permissions@oup.com

Introduction

Indices of myocardial fibre shortening, such as ejection fraction (EF) and strain assess left ventricular (LV) systolic function. However, these parameters do not account for the variable mechanical load caused by LV pressure (LVP) variations.¹ Myocardial work incorporates load and wall tension and reflects both regional oxygen consumption^{2,3} and glucose metabolism.^{4,5} Work calculations, therefore, provide a more comprehensive assessment of myocardial function than deformation parameters alone.^{5,6}

Global LV work corresponds to the area of the LV pressure–volume loop, and regional myocardial work is accordingly reflected in the area of the local myocardial force–segmental length loop.⁷ Calculation of myocardial force, however, is challenging. Substitution of force with LVP and segment length with strain constitutes a suitable index of myocardial work.^{5,8–10} The introduction of a non-invasive estimate of LVP⁵ has made myocardial work calculations more readily applicable.

Myocardial work by pressure–strain analysis has until now most often been based on strain by speckle tracking echocardiography (STE) or cardiac magnetic resonance (CMR) tagging.^{5,6,11–13} However, in up to 20% of echocardiographic examinations, image quality is inadequate for strain analysis,¹⁴ and the CMR tagging technique has limited clinical utility due to specialized scanning sequences and complex post-processing analyses. CMR feature tracking (FT) only requires standard cine sequences, and analyses are significantly less time consuming. Therefore, FT-CMR makes CMR strain analysis more accessible.

CMR is considered gold standard for detection of scar,¹⁵ and proper detection of myocardial scar prior to cardiac resynchronization therapy (CRT) is preferable, as both the location and amount of scar appear to affect the outcome.^{16,17} Extensive functional assessment performed in the same examination, would, therefore, make FT-CMR a highly relevant clinical tool, especially in patients with poor echocardiographic images.

In order to explore regional myocardial work, we studied a patient group with heart failure and left bundle branch block (LBBB), thereby a non-uniform distribution of myocardial work. We compared them to controls with normal electrical conduction. In LBBB, the LV lateral wall is pre-stretched due to early septal contraction, which leads to increased workload on the LV lateral wall.^{5,6,18} The early-activated septum, however, shows reduced myocardial work in LBBB. Therefore, there is reduced myocardial glucose metabolism in septum compared to the LV lateral wall.^{19,20} We used glucose metabolism as a marker of myocardial energy demand and as a useful correlate for regional myocardial work.

The main objective was to investigate the feasibility of calculating regional myocardial work from strain by FT-CMR and non-invasive LVP by means of CMR data alone. We aimed to cover the broad range of workload measurement and to assess variability.

Methods

Study population

Thirty-seven heart failure patients (age 66 ± 10 years) referred for CRT were recruited through the cardiology departments at Oslo University

Hospital, Rikshospitalet, Norway and University Hospitals Leuven, Belgium, from the clinical study *Contractile Reserve in Dysynchrony: A Novel Principle to Identify Candidates for Cardiac Resynchronization Therapy (CRID-CRT)*. For comparison, we included nine controls (age 58 ± 10 years) with no known cardiac disease.

Exclusion criteria included evidence of myocardial infarction by late gadolinium enhancement (LGE) CMR, atrial fibrillation, severe aortic stenosis, insufficient renal function for contrast administration, and contraindications for CMR.

The Regional Ethics Committee approved the study, and all subjects gave written informed consent.

Cardiac magnetic resonance

Subjects were examined with a 1.5 T magnet (in Oslo: Aera, Siemens, Erlangen, Germany, in Leuven: Ingenia, Philips Healthcare, Best, the Netherlands). Cine sequences had frame rate 30/heart cycle. LGE images covering the ventricles were performed in the steady-state after intravenous injection of 0.15 mmol/kg gadoterate meglumine (Doteram™, Guerbet, Villepinte, France). An experienced observer performed a qualitative interpretation of the LGE images to exclude individuals with myocardial infarctions.

Strain from cine images was analysed semi-automatically with FT software (2D CPA MR; TomTec Imaging Systems, Unterschleissheim, Germany) (Figure 1), in mid-ventricular short-axis view. ‘Septum’ was defined as the anteroseptal and septal segments and the ‘LV lateral wall’ as the lateral and posterolateral segments.

Echocardiography

2D grey-scale images from three apical views with average frame rate $60 \pm 8/s$ were acquired with a Vivid E9 or E95 ultrasound scanner (GE Vingmed, Horten, Norway). LV volumes and EF were calculated by the biplane Simpson’s method. Longitudinal strain analyses were performed using STE (Echopac, GE Vingmed Ultrasound, Horten, Norway), blinded to other results. ‘Septum’ and the ‘LV lateral wall’ were defined similarly to CMR analysis.

Estimation of regional work

Segmental myocardial work was calculated by LV pressure–strain analysis with a non-invasive estimate of LVP.⁵ The estimated LVP curve was derived from a semi-automated analysis tool (Echopac, version 202, GE Vingmed Ultrasound, Horten, Norway), and adjusted to the duration of the cardiac phases by visual assessment of valvular events by CMR and echocardiography, respectively. The amplitude of the estimated LVP curve was scaled by the patient’s systolic brachial cuff pressure (a substitute for peak LVP). Strain was assessed by CMR and STE. The work index (mmHg-%) was calculated by multiplying the rate of segmental shortening (strain rate) with instantaneous LVP. This resulted in a measure of instantaneous power, which was integrated over time to give work as a function of time in systole. Systole was defined as the time interval from mitral valve closure to mitral valve opening.²¹ Septal and LV lateral wall work were calculated as the average of the two associated segments.

Normally, LV segments shorten in systole when LVP increases and by definition do positive work. Contrary, elongation in systole when LVP increases by definition implies negative work. In the present study, net work for a myocardial segment was calculated as the sum of positive and negative work.

FDG-PET/CT

¹⁸F-fluorodeoxyglucose (FDG) positron emission tomography (PET) was performed in accepting patients. Scanners used were Biograph 64 or 16

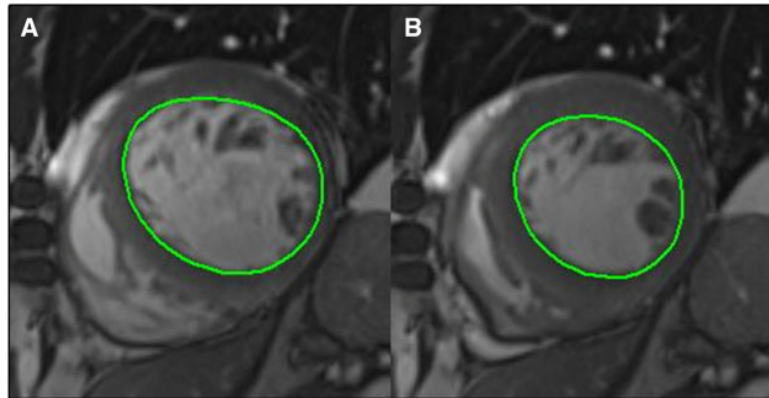


Figure 1 Contours for strain analysis. Manually drawn endocardial border of the left ventricle in a mid-ventricular short-axis view in end-diastole (A) and automatically propagated by the software to end-systole (B).

Table 1 Clinical variables (mean \pm standard deviation)

Variables	All LBBB patients (n = 37)	LBBB patients who underwent FDG-PET (n = 25)	Healthy controls (n = 9)	All LBBB patients vs. LBBB patients with FDG-PET	All LBBB patients vs. controls
Age (years)	66 \pm 10	65 \pm 10	58 \pm 10	0.47	0.03
Male sex (%)	51	48	56	0.80	0.83
Heart rate (bpm)	70 \pm 9	69 \pm 9	67 \pm 16	0.76	0.54
QRS duration (ms)	165 \pm 15	166 \pm 17	90 \pm 9	0.84	<0.001
Systolic blood pressure (mmHg)	133 \pm 23	129 \pm 19	136 \pm 20	0.48	0.62
End-diastolic volume (mL)	203 \pm 87	211 \pm 99	127 \pm 36	0.76	0.005
Ejection fraction (%)	32 \pm 6	30 \pm 7	54 \pm 4	0.41	<0.001

Clinical variables in all LBBB patients, the subgroup of LBBB patients who underwent FDG-PET and healthy controls. The two first groups were similar for all relevant variables, whereas controls differed in terms of age, QRS duration, volumes, and ejection fraction. FDG-PET, fluorodeoxyglucose positron emission tomography; LBBB, left bundle branch block.

HiRez PET/CT (Siemens, Erlangen, Germany) and Discovery MI PET/CT (GE Healthcare, Chicago, IL, USA).

The euglycaemic hyperinsulinaemic clamp technique²² was used. After stabilization of the glucose levels, 370 MBq FDG was administered and a 40-min acquisition was performed 45 min after injection. Images were reconstructed using ordered-subsets expectation-maximization algorithms (four iterations and eight subsets), matrix size 256 \times 256, and a 5.0-mm Gaussian filter. Attenuation correction was performed. The myocardial image was resampled into 16 radial slices,²³ and polar maps using the 17 segment model²⁴ constructed. Segmental values were reported as percentage of the segment with the highest mean FDG uptake. The given percentage for respectively septum and LV lateral wall is the calculated average of the two predefined mid-ventricular segments.

Inter- and intraobserver variability

Work calculations were repeated in 15 randomly selected patients from both centres by the prime observer and a second investigator. The prime observer performed repeated measurements several months after original measurements. The second investigator was blinded to the results of the prime observer.

Statistical analysis

Continuous variables are presented as mean \pm standard deviation (SD), and categorical variables as percentages. Comparisons within and between groups were performed with two-sampled *t*-tests or Mann-Whitney as appropriate. All tests were two-tailed, and a *P*-value <0.05 was considered significant. Continuous variables were compared using scatter plots and Pearson's correlation coefficient. Intra- and interobserver variability was assessed by intraclass correlation coefficient (ICC) and Bland-Altman plots with calculation of the 95% limits of agreement. SPSS version 25.0 (IBM Corporation, Armonk, NY, USA) was used for the analyses.

Results

Study population

Clinical variables are listed in Table 1. All patients had typical electrocardiogram (ECG) features of LBBB according to Strauss,²⁵ while controls had normal ECGs. QRS-duration was 165 \pm 15 and 90 \pm 9

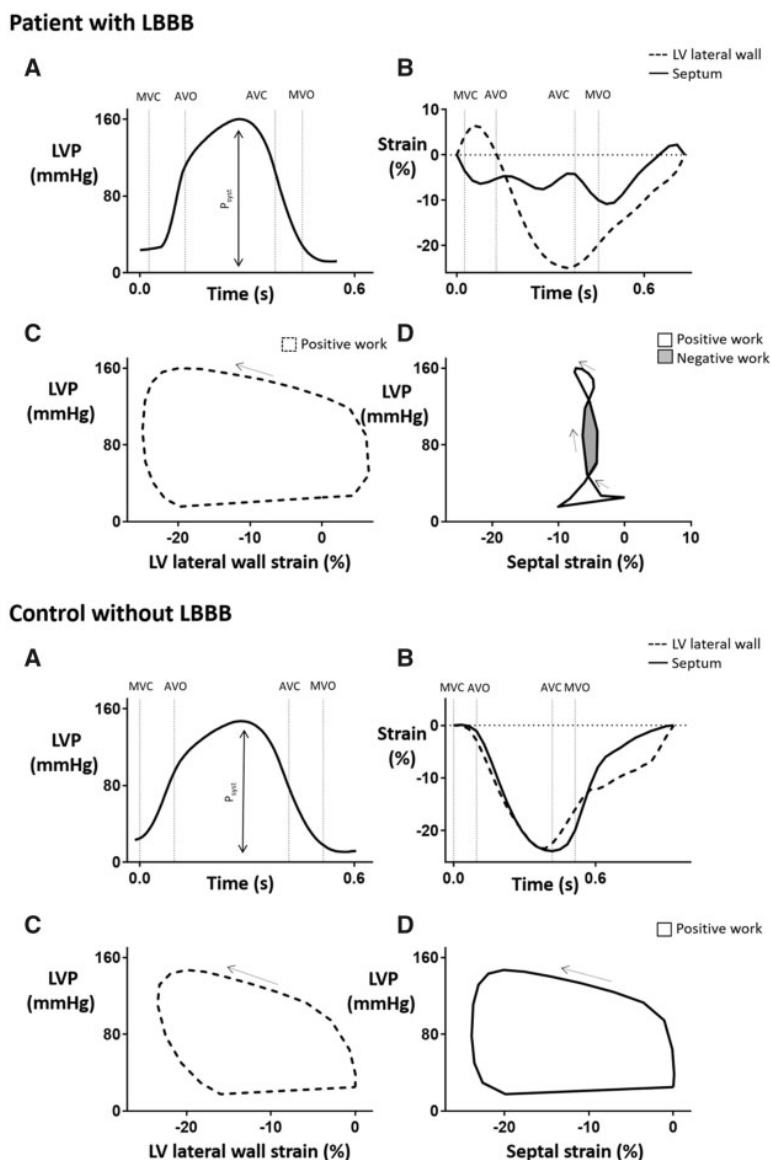


Figure 2 Calculations of pressure–strain loops from non-invasive LVP and circumferential strain by FT-CMR. Data from one representative LBBB patient (upper panel) and one representative control without conduction delay (lower panel). (A) Estimated LVP curves. (B) In the LBBB patient, strain by FT-CMR shows a typical LBBB-deformation pattern. The septal segment (solid line) is, after a short initial contraction, stretched through most systole. The lateral wall (dashed line) is slightly stretched during early systole, followed by contraction. In the control, there are more synchronous strain traces from the two segments. (C and D) Pressure–strain loops from the LV lateral wall and septum. In the LBBB patient, the LV pressure–strain loop from the lateral wall segment rotates counterclockwise, indicating positive work throughout the entire heart cycle. In septum, the LV pressure–strain loop rotates clockwise during part of systole, reducing net work. The pressure–strain loops from the LV lateral wall and septum in the representative control without LBBB both perform positive work. AVC, aortic valve closure; AVO, aortic valve opening; FT-CMR, feature tracking cardiovascular magnetic resonance; LV, left ventricular; LVP, left ventricular pressure; MVC, mitral valve closure; MVO, mitral valve opening; P_{sys} , systolic arterial cuff pressure.

ms in the two groups, respectively ($P < 0.001$). All were in sinus rhythm.

Most of the patients ($n = 29$) had dilated cardiomyopathy, three patients had coronary artery disease diagnosed by coronary angiogram, two had heart failure due to valvular pathology

and three heart failure of unknown aetiology. One patient did not receive CRT due to significant EF improvement after referral.

The subgroup of patients who agreed to perform FDG-PET scans ($n = 25$) was similar to the entire study population in all relevant

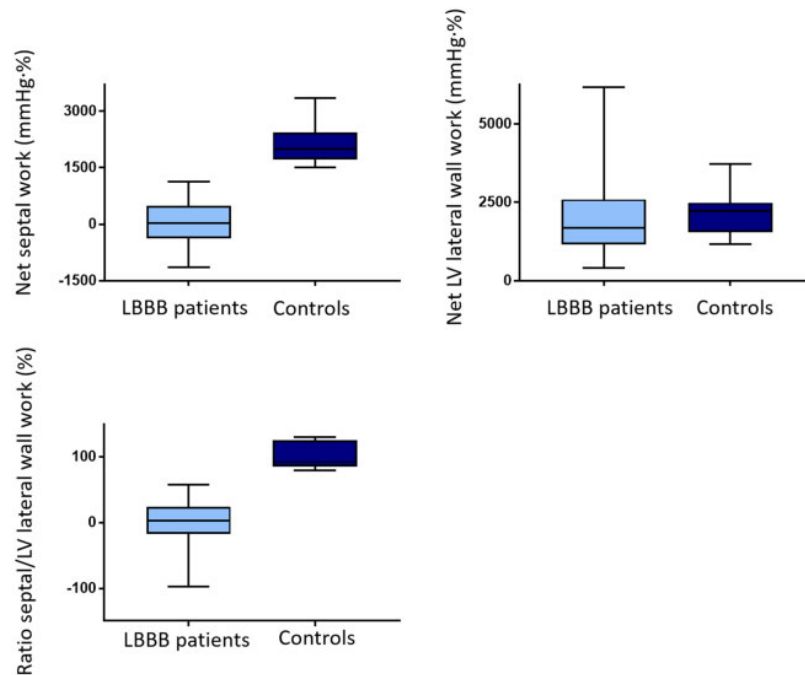


Figure 3 Boxplots of net septal and LV lateral wall work and ratio between septal and LV lateral wall work in LBBB patients and controls. Both net septal work and septal/lateral work ratio are markedly reduced in LBBB patients, compared to controls. LV lateral wall work is similar in the two groups. Minimum to maximum values are shown.

variables (Table 1) and considered to be a random selection of the study population.

Regional myocardial work by FT-CMR

No segment was excluded from strain analysis by FT-CMR. In LBBB patients, circumferential strain by FT-CMR revealed typical LBBB-deformation pattern and associated pressure-strain loops (Figure 2, upper panel). As demonstrated in a representative patient in Figure 2, the septal pressure-strain loop typically rotated both counterclockwise and clockwise during ejection. This pattern indicates both positive and negative work, reducing net work. In the LV lateral wall, however, there was only counterclockwise rotation, indicating predominantly positive work. Average net work in septum was 51 ± 537 , compared to 1978 ± 1084 mmHg-% in the LV lateral wall ($P < 0.001$). The septal/LV lateral wall work ratio was 0.00 ± 0.31 (range -0.33 to 0.57).

In contrast, there was homogenous deformation pattern in the controls without LBBB, without regional net work differences (Figure 2, lower panel). Average net septal work was 2131 ± 563 vs. 2182 ± 747 mmHg-% in the LV lateral wall ($P = 0.73$). The septal/LV lateral wall work ratio was 1.02 ± 0.20 (range 0.80–1.30).

Both net septal work and septal/LV lateral wall work ratio were significantly lower in LBBB patients compared to controls ($P < 0.001$ for both), illustrated in Figure 3. LV lateral wall work was similar in the two groups ($P = 0.37$). Correlations were poor between QRS-width and work in septum, LV lateral wall and the ratio of the two ($r = 0.04$, 0.26, and 0.05, respectively).

Regional myocardial work by STE

Regional myocardial work by STE was performed in the LBBB patients with adequate image quality (96% of the septal and 74% of the LV lateral wall segments). Net septal work was 110 ± 454 , compared to 1735 ± 714 mmHg-% in the LV lateral wall ($P < 0.001$). For comparison, Figure 4 shows the deformation curves and pressure-strain loops based on STE from the same representative individuals as in Figure 2.

Regional glucose metabolism

Glucose metabolism in the LBBB patients ($n = 25$), showed significant regional differences. Average septal FDG uptake was $51.1 \pm 17.6\%$, of the segment with highest uptake, whereas average uptake in the LV lateral wall was $94.5 \pm 4.2\%$ ($P < 0.001$). A representative patient in Figure 5 (upper panel) illustrates the regional differences in glucose metabolism typical of LBBB, with low FDG uptake in septum and high uptake in the LV lateral wall. The lower panel of the figure displays a direct comparison of segmental glucose metabolism and myocardial work estimate.

Consistency

Calculations of work by FT-CMR and non-invasive LVP in 15 patients by two independent observers showed a mean difference of 11 mmHg-%, with an average work of 870 mmHg-%. Repeated work calculations by the same observer revealed a mean difference of 41 mmHg-%, with an average work of 897 mmHg-% (Figure 6). The ICC between the two observers

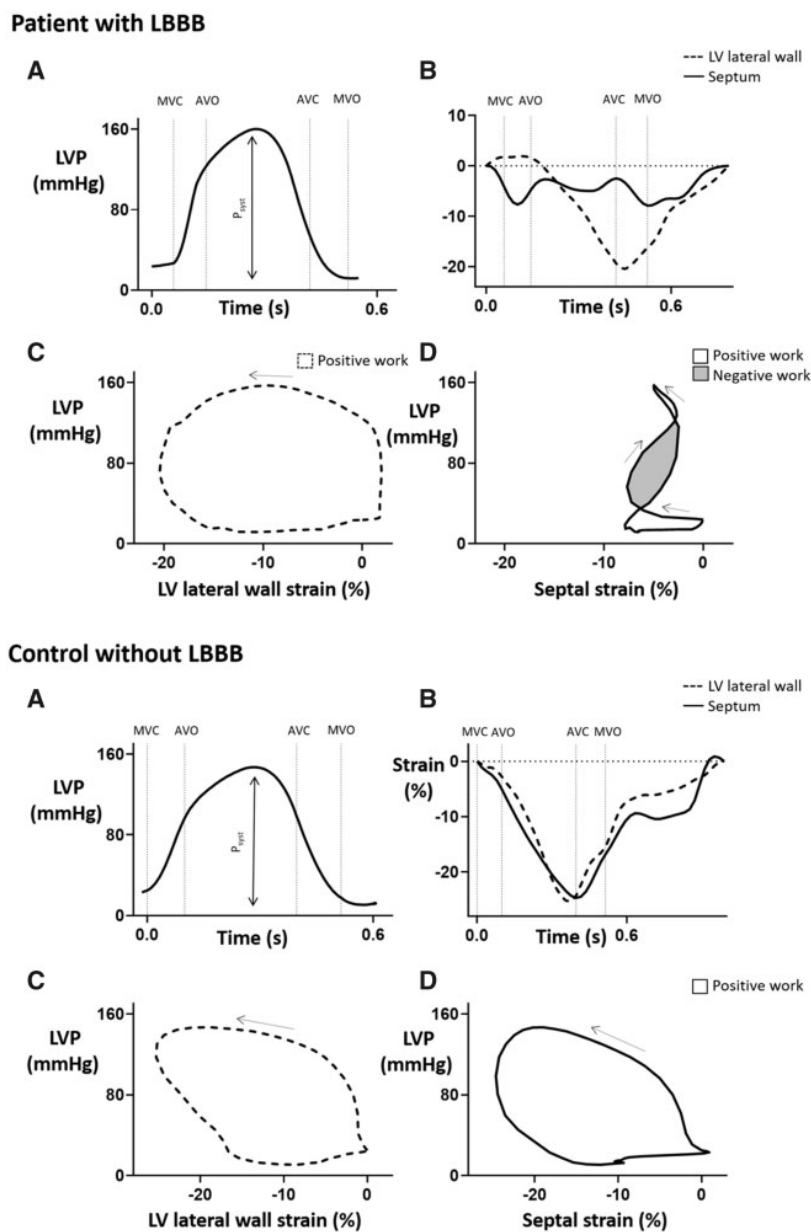


Figure 4 Calculations of pressure–strain loops from non-invasive LVP and strain by STE. Data from one representative LBBB patient (upper panel) and one representative control without conduction delay (lower panel). (A) Estimated LVP curves. (B) In the LBBB patient, strain by FT-CMR shows a typical LBBB-deformation pattern. The septal segment (solid line) is, after a short initial contraction, stretched through most systole. The lateral wall (dashed line) is slightly stretched during early systole, followed by contraction. In the control, there are more synchronous strain traces from the two segments. (C and D) Pressure–strain loops from the LV lateral wall and septum. In the LBBB patient, the LV pressure–strain loop from the lateral wall segment rotates counterclockwise, indicating positive work throughout the entire heart cycle. In septum, the LV pressure–strain loop rotates clockwise during part of systole, reducing net work. The pressure–strain loops from the LV lateral wall and septum in the representative control without LBBB both perform positive work. AVC, aortic valve closure; AVO, aortic valve opening; FT-CMR, feature tracking cardiovascular magnetic resonance; LV, left ventricular; LVP, left ventricular pressure; MVC, mitral valve closure; MVO, mitral valve opening; P_{syst} , systolic arterial cuff pressure; STE, speckle tracking echocardiography.

was 0.96 (95% confidence interval 0.91–0.98). Intraobserver ICC was 0.98 (95% confidence interval 0.96–0.99), indicating good reproducibility.

The two work estimates by STE and FT-CMR showed a similar pattern of regional work distribution. In patients with adequate tracking of all six mid-ventricular segments by STE ($n = 25$), correlation

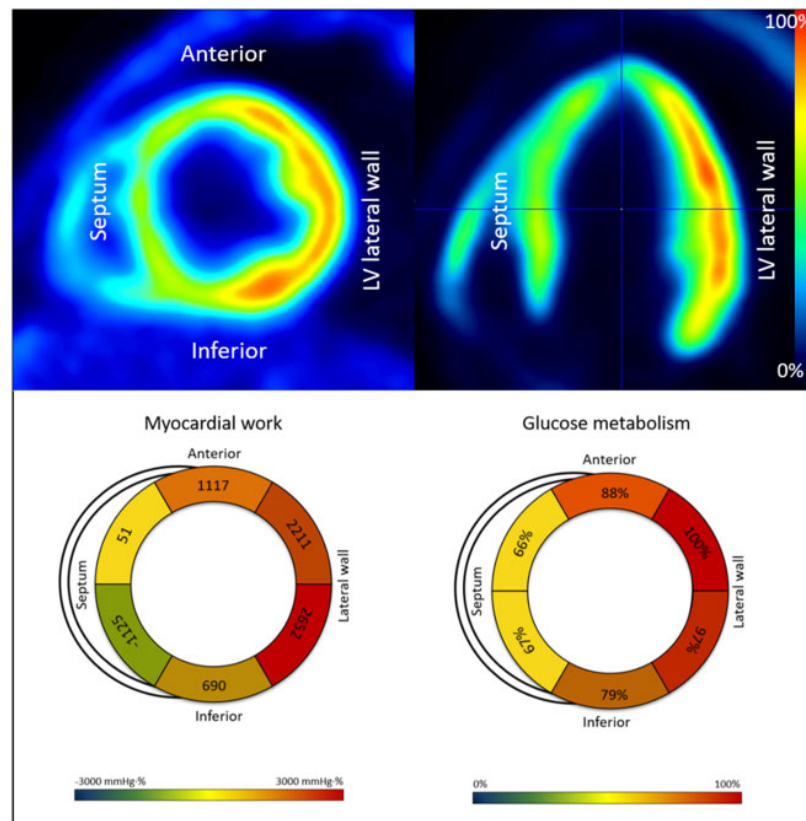


Figure 5 Regional distribution of glucose metabolism in LBBB by FDG-PET. Data from one representative patient. Upper panel: regional distribution of glucose metabolism by FDG-PET in a short-axis (left) and four-chamber (right) view. Lower panel: mid-ventricular view in the same patient illustrates the distribution of myocardial work calculated by FT-CMR and non-invasive LVP (left) compared to the distribution of glucose metabolism by FDG-PET (right). The segment with the highest amount of glucose metabolism was a reference (100%), and segmental values were reported as percentage of this value. Segments with reduced metabolism correspond to segments with reduced work. FDG-PET, fluorodeoxyglucose positron emission tomography; FT-CMR, feature tracking cardiovascular magnetic resonance; LBBB, left bundle branch block; LVP, left ventricular pressure.

between segmental values within the same patient was on average $r = 0.71$, with individual values ranging from 0.37 to 0.99. *Figure 7A* illustrates the correlation in one representative patient, and *Figure 7B* shows a scatterplot from all patients.

Correlation between segmental values of regional work distribution by CMR and glucose metabolism within the same patient was strong with average $r = 0.80$, individual values ranging from 0.54 to 0.96. *Figure 7C* illustrates the correlation in one representative patient (similar patient as *Figure 7A*), and *Figure 7D* shows a scatterplot from all patients ($n = 25$). Segmental values of STE-derived work and glucose metabolism showed a similar correlation, with average $r = 0.82$ and individual values ranging from 0.30 to 0.98.

Discussion

In this proof of concept study, we demonstrate markedly different workloads on septum and the LV lateral wall in patients with LBBB, calculated by circumferential strain by FT-CMR in combination with non-invasive LVP. The method adequately distinguishes LBBB

patients from controls without LBBB. Reproducibility is good, and our findings correlate with STE-derived work. Furthermore, we show that calculated myocardial work distribution reflects regional glucose metabolism by FDG-PET. In ventricles with normal electrical conduction, myocardial strains and metabolism show relatively uniform distribution between different LV segments,^{20,26} corresponding to our findings in healthy controls. The LBBB patients in the present study, however, showed markedly reduced strains and metabolism in septum relative to the LV lateral wall, consistent with earlier observations in LBBB.^{5,6,18–20} This indicates that myocardial work calculated from strain by FT-CMR in combination with non-invasive LVP is a relevant measure of myocardial function in LBBB.

Strain measurements and work calculations

FT-CMR is, like STE, more reproducible for global than segmental values.²⁷ We chose to merge the two septal and the two LV lateral wall segments to even out potential segmental inaccuracies. Focus was on two opposing regions of the ventricle at a mid-ventricular

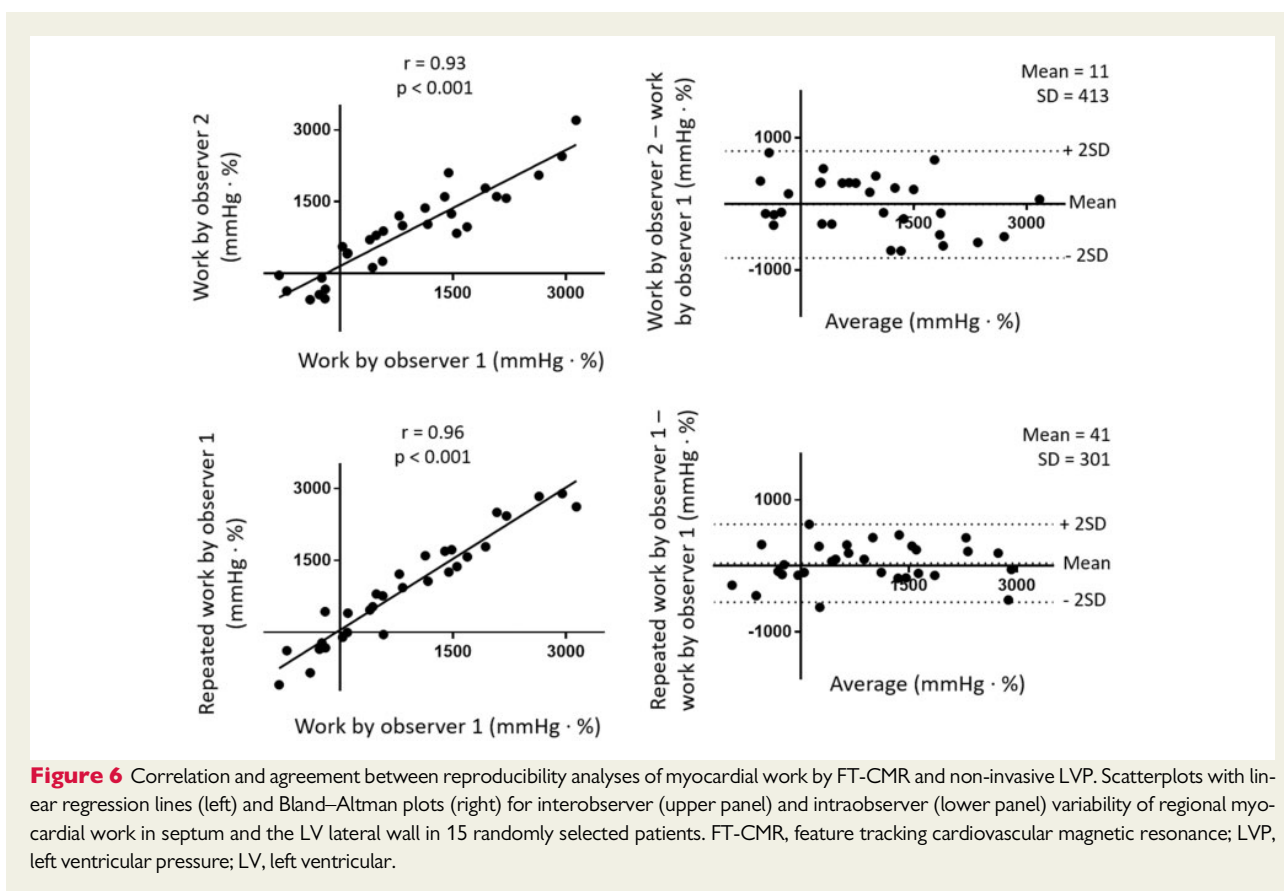


Figure 6 Correlation and agreement between reproducibility analyses of myocardial work by FT-CMR and non-invasive LVP. Scatterplots with linear regression lines (left) and Bland–Altman plots (right) for interobserver (upper panel) and intraobserver (lower panel) variability of regional myocardial work in septum and the LV lateral wall in 15 randomly selected patients. FT-CMR, feature tracking cardiovascular magnetic resonance; LVP, left ventricular pressure; LV, left ventricular.

level only, for simplicity and reproducibility. Although not necessarily true for other patient groups, it seems reasonable that mid-ventricular values are representative for the complete myocardial wall. The inhomogeneous contraction pattern illustrated by a representative patient in the left panel of Figure 2 is consistent with LBBB,¹⁸ and the pressure–strain loops are in accordance with loops from an experimental reference study.⁵ The similarity between the results based on FT-CMR (Figure 2) and STE (Figure 4) strengthens the findings.

The most robust deformation parameter of both FT-CMR and STE were tested²⁷ although they track different fibre directions: circumferential strain for FT-CMR and longitudinal strain for STE. In former validation studies, longitudinal strain by STE has been used for work calculations,^{5,8} leading us to continue this methodology for comparison to FT-CMR. Similar work distribution heterogeneity was found by both methods, corresponding to the heterogeneous distribution of glucose metabolism. In the present patient group, it seems reasonable that all myocardial fibre directions are affected, thereby revealing work distribution typical of LBBB, irrespective of circumferential or longitudinal measurement. Although the degree of segmental correlation varied, average segmental correlation between the two work estimates was good. Misalignment in segmental data analysis by both CMR and echocardiography might partly explain the observed differences in some patients.

We chose echocardiography as the reference modality for work calculations, as this technique has been thoroughly validated in

former studies.^{5,8} Through the higher frame rate of echocardiography, STE might detect short duration deformation superiorly. Even though previous work has demonstrated better agreement between FT-CMR and CMR tagging in CRT candidates,²⁸ CMR tagging was not chosen as a comparison to FT-CMR, as a less clinically available technique hampered with even lower temporal resolution. Our results indicate that reduced CMR frame rate is less important for work calculations. As an example, too low frame rate might not detect the abnormal early systolic left–right motion of the interventricular septum (septal flash) in LBBB. Septal flash, however, represents low work, because of low amplitude at low LVP. The slower movements at increased LVP are decisive for work calculations.

Lower frame rate also implies less accurate valvular event timing by CMR. Accurate timing of mitral valve closing and opening (to define systole) is however less important, as measurement is performed at low LVP, and therefore, with less impact on work calculations. These simplifications mean that the absolute values of regional work are not accurate, but the overall picture illustrates the abnormal work distribution adequately.

The absolute values of work varied rather substantially between different individuals, both in the LBBB group and among the controls, reflecting large biological variation. Repeated analysis revealed large SD. For this proof of concept study, however, we aimed to demonstrate the abnormal work distribution in LBBB patients. Both net septal work and ratio between septal and LV lateral wall work

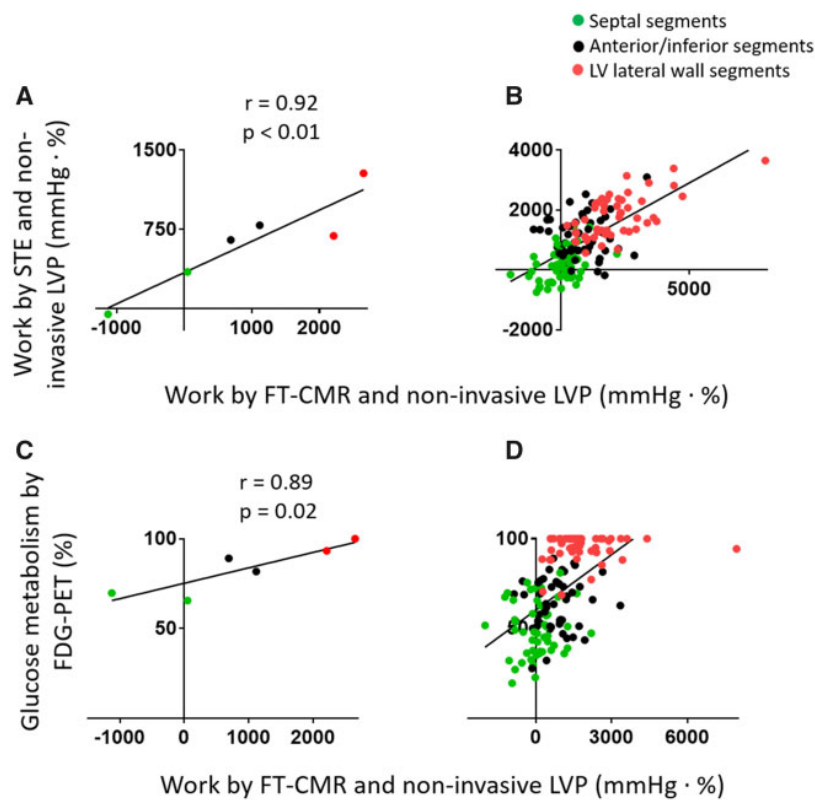


Figure 7 (A and B) Correlation between estimated regional myocardial work by circumferential strain by FT-CMR and non-invasive LVP and estimated regional myocardial work by longitudinal strain by STE and non-invasive LVP. The scatterplot to the left (A) illustrates the correlation in six mid-ventricular segments from one representative patient. In the scatterplot to the right (B) six segments from all patients with adequate tracking by STE ($n = 25$) are shown. (C and D) Correlation between estimated regional myocardial work by circumferential strain by FT-CMR and non-invasive LVP, and regional glucose metabolism by FDG-PET. The scatterplot to the left (C) illustrates the correlation in six mid-ventricular segments from one representative patient (same as in A). In the scatterplot to the right six segments from all patients with FDG-PET ($n = 25$) are shown. The septal segments (green points) have a low amount of myocardial work by both estimates and correspondingly low glucose metabolism. The LV lateral wall segments (red points) display a high workload by both work estimates and a high glucose metabolism. Work values for anterior and inferior segments (black points) are in-between the extremes. Correlation coefficients are reported for the representative patient in A and C, but not in the combined scatterplots in B and D due to interdependency between measurements. FT-CMR, feature tracking cardiovascular magnetic resonance; LVP, left ventricular pressure; STE, speckle tracking echocardiography; FDG-PET, fluorodeoxyglucose positron emission tomography; LV, left ventricular.

adequately identified the LBBB patients from the controls (Figure 3). Repeated analyses did not change this picture. This implies that the method is able to demonstrate the regional differences in LBBB, despite large SD in reproducibility analysis. No LBBB patient showed equal contribution of septum compared to the LV lateral wall. However, this may not be the case in patients with large LV lateral wall scars, in whom septal contribution to total myocardial workload would probably be higher.

Myocardial work and glucose metabolism

Regional myocardial work correlated with regional glucose metabolism in the LBBB patients (Figures 5 and 7 lower panels). In the present study, we were interested in the relative metabolism and chose to report the segmental values as percentages of the segment with the

highest FDG uptake. In most of the patients, the highest FDG uptake was in one of the LV lateral wall segments, and this explains the ‘flattening’ of the curve in Figure 7D. The figure suggests agreement between the two image modalities.

Clinical implications

CRT causes reverse LV remodelling and improves survival in heart failure patients with LBBB.²⁹ However, a substantial number of patients do not benefit from this treatment.³⁰ Work distribution during LV dyssynchrony may be relevant to identify responders to CRT.^{5,11–13,21} Detection of myocardial scar by CMR prior to CRT implantation is also of clinical value, as both the amount and location of scar tissue appear to predict CRT response.^{16,17} When also regional functional assessment from standard cine sequences has sufficient accuracy, CMR could have a unique position in the preoperative imaging assessment of CRT candidates.

Limitations

Atrial fibrillation patients were not included given the difficulty in obtaining strain traces and myocardial work in the case of significant R-R variability. Similarly, patients with myocardial scar were excluded. Scars have reduced myocardial work and glucose metabolism. This will be explored in an ongoing clinical study in patients who receive CRT. Although image quality was adequate for strain analysis by FT-CMR in all patients in the present study, this may not be the case in less selected patient groups, for example, in patients with arrhythmia or intracardiac devices.

Myocardial work was calculated with LVP as a substitute for force. This modification has, however, previously been shown to have minor effect on the results.⁵

Brachial systolic blood pressure was not measured simultaneously to the CMR recordings, but in an equivalent resting condition on the same day in circulatory stable individuals. Although blood pressure may not be identical during these two situations, the most important data in this study are relative magnitudes of myocardial work and metabolism.

Inter-vendor analysis was not performed in this feasibility study, and the eligibility of other available FT software should be further evaluated.

The sample size in the present study is small and we recommend further validation in a larger cohort. Further evaluation is also necessary to determine if the method is suited in other patient groups.

Conclusions

Myocardial work calculated from strain by FT-CMR in combination with non-invasive LVP is a relevant measure of myocardial function in LBBB. The calculated work distribution correlates with both regional glucose metabolism and with STE-derived work estimate. The methodology allows for a rapid, yet comprehensive, assessment of LV function, which could be particularly useful in patients with poor echocardiographic image quality. Work distribution during LV dyssynchrony may be relevant to identify responders to CRT. The combined assessment of work distribution and myocardial scar during one CMR examination could give CMR a unique position in the pre-operative imaging assessment of CRT candidates.

Acknowledgements

The authors would like to thank radiographer Bac Nguyen for his help with the CMR protocol and nurse Kari Melberg for her help with the completion of the study.

Funding

C.K.L. and J.M.A. were recipients of clinical research fellowship from the South-Eastern Norway Regional Health Authority and the Norwegian Health Association, respectively. Investment in TomTec software was supported by funds of the University of Oslo and Haakon and Sigrun Ødegaard's Research Foundation through the Norwegian Society of Radiology.

Conflict of interest: O.A.S. is a co-inventor but has no longer ownership of the patent 'Method for myocardial segment work analysis'. All other authors have no conflict of interest to declare.

References


1. Urheim S, Edvardsen T, Torp H, Angelsen B, Smiseth OA. Myocardial strain by Doppler echocardiography. Validation of a new method to quantify regional myocardial function. *Circulation* 2000;**102**:1158–64.
2. Suga H. Total mechanical energy of a ventricle model and cardiac oxygen consumption. *Am J Physiol* 1979;**236**:H498–505.
3. Takaoka H, Takeuchi M, Otake M, Yokoyama M. Assessment of myocardial oxygen consumption (Vo₂) and systolic pressure–volume area (PVA) in human hearts. *Eur Heart J* 1992;**13** Suppl E:85–90.
4. Bergman BC, Tsvetkova T, Lowes B, Wolfel EE. Myocardial glucose and lactate metabolism during rest and atrial pacing in humans. *J Physiol* 2009;**587**:2087–99.
5. Russell K, Eriksen M, Aaberge L, Wilhelmsen N, Skulstad H, Remme EW. A novel clinical method for quantification of regional left ventricular pressure–strain loop area: a non-invasive index of myocardial work. *Eur Heart J* 2012;**33**:724–33.
6. Prinzen FW, Hunter WC, Wyman BT, McVeigh ER. Mapping of regional myocardial strain and work during ventricular pacing: experimental study using magnetic resonance imaging tagging. *J Am Coll Cardiol* 1999;**33**:1735–42.
7. Hisano R, Cooper G. Correlation of force-length area with oxygen consumption in ferret papillary muscle. *Circ Res* 1987;**61**:318–28.
8. Urheim S, Rabben SI, Skulstad H, Lyseggen E, Ihlen H, Smiseth OA. Regional myocardial work by strain Doppler echocardiography and LV pressure: a new method for quantifying myocardial function. *Am J Physiol Heart Circ Physiol* 2005;**288**:H2375–80.
9. Delhaas T, Arts T, Prinzen FW, Reneman RS. Regional fibre stress-fibre strain area as an estimate of regional blood flow and oxygen demand in the canine heart. *J Physiol* 1994;**477**:481–96.
10. Forrester JS, Tyberg JV, Wyatt HL, Goldner S, Parmely WW, Swan HJ. Pressure–length loop: a new method for simultaneous measurement of segmental and total cardiac function. *J Appl Physiol* 1974;**37**:771–5.
11. Vecera J, Penicka M, Eriksen M, Russell K, Bartunek J, Vanderheyden M et al. Wasted septal work in left ventricular dyssynchrony: a novel principle to predict response to cardiac resynchronization therapy. *Eur Heart J Cardiovasc Imaging* 2016;**17**:624–32.
12. Galli E, Leclercq C, Hubert A, Bernard A, Smiseth OA, Mabo P et al. Role of myocardial constructive work in the identification of responders to CRT. *Eur Heart J Cardiovasc Imaging* 2018;**19**:1010–8.
13. Zweerink A, de Roest GJ, Wu L, Nijveldt R, de Cock CC, van Rossum AC et al. Prediction of acute response to cardiac resynchronization therapy by means of the imbalance in regional left ventricular myocardial work. *J Card Fail* 2016;**22**:133–42.
14. Marwick TH, Leano RL, Brown J, Sun JP, Hoffmann R, Lysyansky P et al. Myocardial strain measurement with 2-dimensional speckle-tracking echocardiography: definition of normal range. *JACC Cardiovasc Imaging* 2009;**2**:80–4.
15. Klein C, Nekolla SG, Bengel FM, Momose M, Sammer A, Haas F et al. Assessment of myocardial viability with contrast-enhanced magnetic resonance imaging: comparison with positron emission tomography. *Circulation* 2002;**105**:162–7.
16. Bleeker GB, Kaandorp TA, Lamb HJ, Boersma E, Steendijk P, de Roos A et al. Effect of posterolateral scar tissue on clinical and echocardiographic improvement after cardiac resynchronization therapy. *Circulation* 2006;**113**:969–76.
17. Ypenburg C, Roes SD, Bleeker GB, Kaandorp TAM, de Roos A, Schalij MJ et al. Effect of total scar burden on contrast-enhanced magnetic resonance imaging on response to cardiac resynchronization therapy. *Am J Cardiol* 2007;**99**:657–60.
18. Vernooij K, Verbeek XA, Peschar M, Crijns HJ, Arts T, Cornelussen RN et al. Left bundle branch block induces ventricular remodelling and functional septal hypoperfusion. *Eur Heart J* 2005;**26**:91–8.
19. Ono S, Nohara R, Kambara H, Okuda K, Kawai C. Regional myocardial perfusion and glucose metabolism in experimental left bundle branch block. *Circulation* 1992;**85**:1125–31.
20. Zanco P, Desideri A, Mobilia G, Cargnel S, Milan E, Celegon L et al. Effects of left bundle branch block on myocardial FDG PET in patients without significant coronary artery stenoses. *J Nucl Med* 2000;**41**:973–7.
21. Russell K, Eriksen M, Aaberge L, Wilhelmsen N, Skulstad H, Gjesdal O et al. Assessment of wasted myocardial work: a novel method to quantify energy loss due to uncoordinated left ventricular contractions. *Am J Physiol Heart Circ Physiol* 2013;**305**:H996–1003.
22. Knuuti MJ, Nuutila P, Ruotsalainen U, Saraste M, Harkonen R, Ahonen A et al. Euglycemic hyperinsulinemic clamp and oral glucose load in stimulating myocardial glucose utilization during positron emission tomography. *J Nucl Med* 1992;**33**:1255–62.
23. Nuyts J, Suetens P, Oosterlinck A, De Roo M, Mortelmans L. Delineation of ECT images using global constraints and dynamic-programming. *IEEE Trans Med Imaging* 1991;**10**:489–98.

24. Cerqueira MD, Weissman NJ, Dilsizian V, Jacobs AK, Kaul S, Laskey WK *et al.* Standardized myocardial segmentation and nomenclature for tomographic imaging of the heart. A statement for healthcare professionals from the Cardiac Imaging Committee of the Council on Clinical Cardiology of the American Heart Association. *Circulation* 2002;**105**: 539–42.
25. Strauss DG, Selvester RH, Wagner GS. Defining left bundle branch block in the era of cardiac resynchronization therapy. *Am J Cardiol* 2011;**107**: 927–34.
26. Gotte MJ, Germans T, Russel IK, Zwanenburg JJ, Marcus JT, van Rossum AC *et al.* Myocardial strain and torsion quantified by cardiovascular magnetic resonance tissue tagging: studies in normal and impaired left ventricular function. *J Am Coll Cardiol* 2006;**48**:2002–11.
27. Claus P, Omar AM, Pedrizzetti G, Sengupta PP, Nagel E. Tissue tracking technology for assessing cardiac mechanics: principles, normal values, and clinical applications. *JACC Cardiovasc Imaging* 2015;**8**:1444–60.
28. van Everdingen WM, Zweerink A, Nijveldt R, Salden OAE, Meine M, Maass AH *et al.* Comparison of strain imaging techniques in CRT candidates: CMR tagging, CMR feature tracking and speckle tracking echocardiography. *Int J Cardiovasc Imaging* 2018;**34**:443–56.
29. Cleland JG, Daubert JC, Erdmann E, Freemantle N, Gras D, Kappenberger L *et al.* The effect of cardiac resynchronization on morbidity and mortality in heart failure. *N Engl J Med* 2005;**352**:1539–49.
30. Chung ES, Leon AR, Tavazzi L, Sun JP, Nihoyannopoulos P, Merlino J *et al.* Results of the predictors of response to CRT (PROSPECT) trial. *Circulation* 2008; **117**:2608–16.

IMAGE FOCUS

doi:10.1093/ehjci/jez214
Online publish-ahead-of-print 22 August 2019

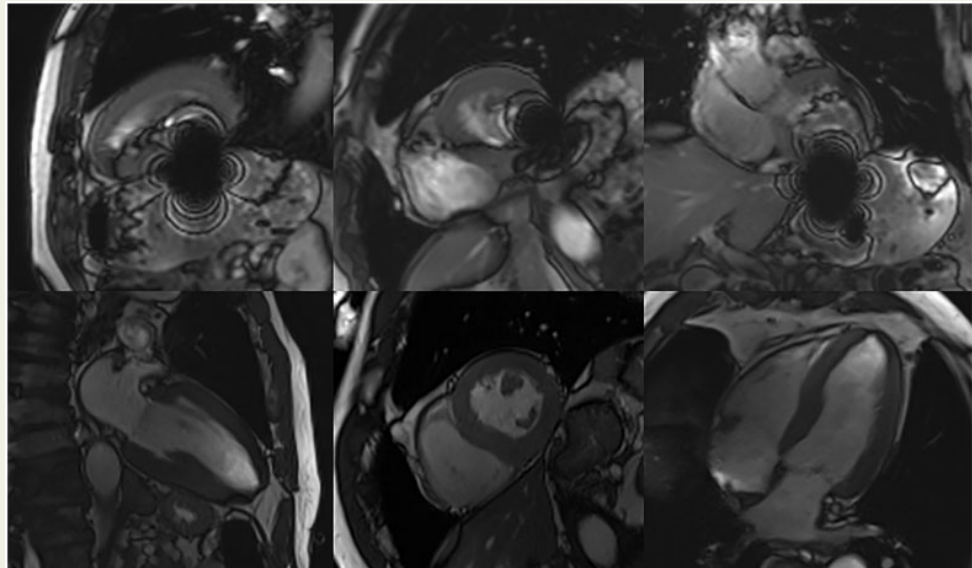
Moving ferromagnetic objects distorting cardiac magnetic resonance imaging

Torvald Espeland ^{1*}, Erik Andreas Rye Berg¹, Marius Eriksen², and Knut Haakon Stensaeth²

¹Faculty of Medicine and Health Sciences, Department of Circulation and Medical Imaging, Norwegian University of Science and Technology (NTNU), PO Box 8905, 7491 Trondheim, Trondheim, Norway; and ²Department of Radiology and Nuclear Medicine, St. Olavs Hospital HF, PO Box 3250 Torgarden, NO-7006 Trondheim, Norway

* Corresponding author. Tel: +47 99 70 31 56. E-mail: torvald.espeland@ntnu.no

A 78-year-old male patient, with a history of hypertension and aortic valve stenosis, underwent cardiac magnetic resonance (CMR) imaging. The CMR scan was aborted due to two significant artefacts. One of the artefacts, presumably located in the ventricle, made interpretation of the heart impossible (Panels A–C). We suspected that the artefacts were caused by ferromagnetic objects. The patient experienced no discomfort during the scan.



The patient had neither experienced injury nor undergone surgery suggesting any internal metal objects. Recent X-ray and computer tomography (CT) exams of the same region did not reveal any signs of metal objects. Surprised by the finding, the patient recalled removing a piece of aluminium foil from his salad 1 h prior to the CMR scan and added that he might have ingested some pieces.

The patient was offered an additional CMR scan 2 days later, as the risk of harm was considered very low. At this point, a similar artefact was seen more distally, possibly in the transverse colon. Interpretation of the heart was now possible (Panels D–F). Independent of these findings, an abdominal CT-scan performed 3 days later did not reveal any signs of metal objects.

We suspect that these artefacts were caused by ingestion of small aluminium pieces 1 h prior to the initial CMR scan, distorting cardiac imaging. To our knowledge, there are no reports on similar cases.

Upper row shows localizer images with artefacts from the initial aborted CMR exam (Panels A–C). Lower row displays two-chamber, short axis, and four-chamber views from the second exam (Panels D–F).

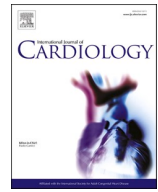
© The Author(s) 2019. Published by Oxford University Press on behalf of the European Society of Cardiology.

This is an Open Access article distributed under the terms of the Creative Commons Attribution Non-Commercial License (<http://creativecommons.org/licenses/by-nc/4.0/>), which permits non-commercial re-use, distribution, and reproduction in any medium, provided the original work is properly cited. For commercial re-use, please contact journals.permissions@oup.com

Paper 2

Contents lists available at [ScienceDirect](https://www.sciencedirect.com)

International Journal of Cardiology

journal homepage: www.elsevier.com/locate/ijcard

Scar imaging in the dyssynchronous left ventricle: Accuracy of myocardial metabolism by positron emission tomography and function by echocardiographic strain

Camilla Kjellstad Larsen^{a,b}, Elena Galli^c, Jürgen Duchenne^d, John M. Aalen^{a,b},
 Caroline Stokke^{e,f}, Jan Gunnar Fjeld^{e,g}, Ganna Degtiarova^h, Piet Claus^h, Olivier Gheysensⁱ,
 Jorg Saberniak^j, Per Anton Sirnes^k, Erik Lyseggen^b, Jan Bogaert^l, Erik Kongsgaard^b,
 Martin Penicka^m, Jens-Uwe Voigt^d, Erwan Donal^c, Einar Hopp^e, Otto A. Smiseth^{a,b,*}

^a Institute for Surgical Research, Oslo University Hospital and University of Oslo, Oslo, Norway

^b Department of Cardiology, Oslo University Hospital, Oslo, Norway

^c Department of Cardiology, University Hospital of Rennes and University of Rennes, Rennes, France

^d Department of Cardiovascular Diseases, University Hospitals Leuven and Department of Cardiovascular Sciences, KU Leuven – University of Leuven, Leuven, Belgium

^e Division of Radiology and Nuclear Medicine, Oslo University Hospital, Oslo, Norway

^f Department of Physics, University of Oslo, Oslo, Norway

^g Oslo Metropolitan University, Oslo, Norway

^h Department of Nuclear Medicine, University Hospitals Leuven and Department of Imaging and Pathology, KU Leuven – University of Leuven, Leuven, Belgium

ⁱ Department of Nuclear Medicine, Cliniques Universitaires Saint-Luc and Institute of Clinical and Experimental Research (IREC), Université Catholique de Louvain, Brussels, Belgium

^j Department of Cardiology, Akershus University Hospital, Lorenskog, Norway

^k Ostlandske Hertesenter, Moss, Norway

^l Department of Radiology, University Hospitals Leuven, Leuven, Belgium

^m Cardiovascular Center, OLV Clinic, Aalst, Belgium

ARTICLE INFO

Keywords:

Dyssynchrony
 Heart failure
 Myocardial scar
 Late gadolinium enhancement cardiac
 magnetic resonance
 Glucose metabolism
 Positron emission tomography
 Strain
 Speckle tracking echocardiography

ABSTRACT

Purpose: Response to cardiac resynchronization therapy (CRT) is reduced in patients with high left ventricular (LV) scar burden, in particular when scar is located in the LV lateral wall or septum. Late gadolinium enhancement (LGE) cardiac magnetic resonance (CMR) can identify scar, but is not feasible in all patients. This study investigates if myocardial metabolism by ¹⁸F-fluorodeoxyglucose positron emission tomography (FDG-PET) and contractile function by echocardiographic strain are alternatives to LGE-CMR.

Methods: In a prospective multicenter study, 132 CRT candidates (91% with left bundle branch block) were studied by speckle tracking strain echocardiography, and 53 of these by FDG-PET. Regional myocardial FDG metabolism and peak systolic strain were compared to LGE-CMR as reference method.

Results: Reduced FDG metabolism (<70% relative) precisely identified transmural scars (≥50% of myocardial volume) in the LV lateral wall, with area under the curve (AUC) 0.96 (95% confidence interval (CI) 0.90–1.00). Reduced contractile function by strain identified transmural scars in the LV lateral wall with only moderate accuracy (AUC = 0.77, CI 0.71–0.84). However, absolute peak systolic strain >10% could rule out transmural scar with high sensitivity (80%) and high negative predictive value (96%). Neither FDG-PET nor strain identified septal scars (for both, AUC < 0.80).

Conclusions: In CRT candidates, FDG-PET is an excellent alternative to LGE-CMR to identify scar in the LV lateral wall. Furthermore, preserved strain in the LV lateral wall has good accuracy to rule out transmural scar. None of the modalities can identify septal scar.

Abbreviations: CRT, Cardiac Resynchronization Therapy; LV, Left Ventricular; EF, Ejection Fraction; LGE, Late Gadolinium Enhancement; CMR, Cardiac Magnetic Resonance; FDG, ¹⁸F-fluorodeoxyglucose; PET, Positron Emission Tomography; LBBB, Left Bundle Branch Block; AVC, Aortic Valve Closure; SD, Standard Deviation; ROC, Receiver Characteristics Curve; AUC, Area Under the Curve; CI, Confidence Interval.

* Corresponding author at: Institute for Surgical Research, Oslo University Hospital, Rikshospitalet, N-0027 Oslo, Norway.

E-mail address: otto.smiseth@gmail.com (O.A. Smiseth).

<https://doi.org/10.1016/j.ijcard.2022.11.042>

Received 2 September 2022; Received in revised form 20 October 2022; Accepted 22 November 2022

Available online 29 November 2022

0167-5273/© 2022 The Author(s). Published by Elsevier B.V. This is an open access article under the CC BY license (<http://creativecommons.org/licenses/by/4.0/>).

Clinical trial registration: The present study is part of the clinical study “Contractile Reserve in Dyssynchrony: A Novel Principle to Identify Candidates for Cardiac Resynchronization Therapy (CRID–CRT)”, which was registered at clinicaltrials.gov (identifier NCT02525185).

1. Introduction

Cardiac resynchronization therapy (CRT) is an established treatment for patients with symptomatic heart failure, reduced left ventricular (LV) ejection fraction (EF) and broad QRS, preferably with left bundle branch block (LBBB) morphology. Nevertheless, CRT fails to improve symptoms in one-third of the patients, and reduced therapeutic response is related to LV scar burden (1,2). As shown by Bleeker et al., who evaluated myocardial scar by late gadolinium enhancement cardiac magnetic resonance (LGE-CMR), patients with transmural scar in the LV posterolateral wall have markedly reduced clinical response and attenuated LV reverse remodeling after CRT (3). Furthermore, as shown recently by our group in a prospective, multicenter study, septal scar is associated with poor response to CRT (4). Therefore, identification of scar in the LV lateral wall and septum may aid in selecting patients who are likely to respond to CRT.

Cardiac magnetic resonance (CMR) with late gadolinium enhancement (LGE) is the clinical gold standard for myocardial scar (5), but is not feasible in all patients, and is limited by accessibility. Therefore, there is need for alternative methods to image myocardial scar. In the present study, we investigate if myocardial glucose metabolism by positron emission tomography (PET) with ^{18}F -fluorodeoxyglucose (FDG) can identify LV myocardial scars in patients with LBBB or other causes of LV intraventricular conduction delay, who are referred for CRT. Additionally, we investigate if myocardial contractile function measured by echocardiographic strain imaging can be used to identify scar.

The principle behind FDG-PET to identify scar, is that myocardial uptake of the radioactive glucose analogue reflects metabolic activity, i. e. viability of the myocardium. Myocardial shortening by strain imaging is directly related to viability since non-viable myocardium does not contract and when only part of the wall is viable, there is reduced contraction as reflected in reduced systolic strain. In CRT candidates, however, scar imaging by FDG-PET and strain may be challenging, as LBBB markedly alters myocardial function and metabolism (6–8). No previous study has validated scar imaging by FDG-PET against LGE-CMR in CRT candidates. Scar imaging by strain imaging has been compared to LGE-CMR in ischemic cardiomyopathy (9–11), but not in non-ischemic cardiomyopathy, which represent a large fraction of patients who receive CRT.

The objectives of the present study were to determine if assessment of myocardial metabolism by FDG-PET and LV systolic function by strain echocardiography can identify LV scar in patients referred for CRT. As reference method for scar, we used LGE-CMR.

2. Methods

2.1. Study population

From a prospective, multicenter CRT study, we consecutively included all patients with QRS width > 120 ms and available LGE-CMR scan ($n = 132$). The background for not performing LGE-CMR has been described previously (4). Criteria for LBBB was according to guidelines of the European Society of Cardiology (1). Reversible ischemia was excluded by clinical history taking, supplemented with coronary angiography if considered necessary by the treating physician. Inclusion criterion was indication for CRT according to 2013 European Society of Cardiology guidelines. LGE-CMR served as reference standard for scar. All 132 patients underwent echocardiography and 53 of these were studied by FDG-PET.

The study was conducted following the “Good Clinical Practice” guidelines of the Declaration of Helsinki and was approved by the Regional Ethical Committees of every participating center. All patients gave their written informed consent for study participation. The present study is part of the clinical study “Contractile Reserve in Dyssynchrony: A Novel Principle to Identify Candidates for Cardiac Resynchronization Therapy (CRID–CRT)”, which was registered at clinicaltrials.gov (identifier NCT02525185).

2.2. Cardiac magnetic resonance (CMR)

The CMR imaging was performed as previously described (4). An experienced radiologist in a designated core lab, blinded to other results, determined if LGE was present and if so, whether distribution was consistent with ischemic etiology or not. All LGE, independent of etiology, was quantified with a specific analysis tool (12). Transmural segmental scar was pre-specified as LGE $\geq 50\%$ of segmental volume, and non-transmural segmental scar as $<50\%$ of segmental volume, irrespective of wall thickness. Heart failure etiology was considered ischemic if history of previous myocardial infarction and/or significant coronary artery disease by angiography, and if LGE pattern with scar extending from the subendocardium, consistent with previous infarction.

2.3. Nuclear imaging

Glucose metabolism was assessed by FDG-PET. Scanners were Biograph 64 or 16 HiRez PET/computer tomography (CT) (Siemens, Erlangen, Germany) and Discovery MI PET/CT (GE Healthcare, Chicago, Illinois, US). The investigation was performed during resting conditions and the patients were instructed to avoid exercise the days before. Patient preparation consisted of a hyperinsulinemic euglycemic clamping method (13) or an oral glucose loading protocol. After stabilization of the glucose levels, 370 MBq FDG was administered and a 40-min acquisition was performed 45 min after injection.

PET-images were reconstructed using ordered-subsets expectation maximization algorithms (4 iterations and 8 subsets), matrix size 256×256 , and a 5.0 mm Gaussian filter. Attenuation correction was performed. A trained reader in a designated core lab, blinded to other results, performed the PET analyses. Segmental values were reported as percentage of the segment with highest mean tracer uptake.

2.4. Echocardiographic analysis

A Vivid E9 or E95 ultrasound scanner (GE Vingmed Ultrasound, Horten, Norway) was used for two-dimensional (2D) grey-scale echocardiographic acquisitions from the apical views. Average frame rate was 65 ± 10 /s. Ventricular volumes and LV ejection fraction were calculated by the biplane Simpson’s method. Blood pressure was measured non-invasively at examination start.

Longitudinal strain was measured by speckle tracking echocardiography (Echopac, GE Vingmed Ultrasound, Horten, Norway). Peak systolic strain was defined as maximum negative value prior to aortic valve closure (AVC). Post-systolic shortening was measured as shortening after AVC. Radial strain measurements were attempted, but was often unsuccessful due to thin LV wall in many patients. Therefore, radial strain is not part of this study. A trained reader in a designated core lab, blinded to other results, performed the strain analyses.

An index of segmental myocardial work was calculated by LV pressure-strain analysis using a semi-automated analysis tool (Echopac,

version 202, GE Vingmed Ultrasound, Horten, Norway) and a non-invasive estimate of LV pressure (14).

All investigated parameters (CMR, nuclear and echocardiographic) were reported on a segmental level using the 17 segment model (15), where all segments except the apex (segment 17) were analyzed. Analyses were performed on a segmental level. In total, 2112 segments (132 patients \times 16 segments per patient) were available for analysis. In one patient, we excluded six segments from LGE analysis because of regional artefacts from pacemaker leads. Of the remaining 2106 segments, 108 were excluded from strain and work analysis due to inadequate echocardiographic image quality. All 848 segments (53 patients \times 16 segments per patient) available for PET analyses were studied. The ratio between septal metabolism and myocardial work was calculated for each segment.

Echocardiography was performed within a time range of 24 h and PET within 5 days from the CMR examination.

2.5. Statistical analyses

Continuous variables are expressed as mean \pm standard deviation (SD) if normally distributed, otherwise as median (10, 90% percentile). Comparisons between groups were made by Student's *t*-test or Mann-Whitney *U* test, as appropriate. Statistical significance was set at a two-tailed probability level of $p < 0.05$. Each parameter's ability to detect scar was evaluated by receiver operating characteristic (ROC) curves with calculation of area under the curve (AUC). SPSS version 25.0 (IBM Corporation, Armonk, NY) was used for analyses.

3. Results

3.1. Study population

Patient characteristics, number of interpretable segments and number of scarred segments in each LV region are presented in Table 1. Mean QRS-width was 164 ± 17 ms, and 91% had LBBB, with 95% in sinus rhythm and 5% in atrial fibrillation. Mean LV EF was $30 \pm 8\%$ and average NYHA functional class 2.3 ± 0.6 .

Myocardial scar by FDG-PET.

Table 1
Patient characteristics.

Variable	Average \pm SD
Age (years)	66 \pm 10
Male sex (%)	67
Heart failure etiology (no)	
Ischemic	55 (42%)
Non-ischemic	77 (58%)
Rhythm	
Sinus rhythm (%)	95
Atrial fibrillation (%)	5
QRS duration (milliseconds)	164 \pm 17
QRS configuration (%)	
LBBB	91
Non-LBBB	9
Systolic blood pressure (mmHg)	126 \pm 21
Diastolic blood pressure (mmHg)	70 \pm 12
LV End diastolic volume (milliliter)	201 \pm 76
LV Ejection fraction (%)	30 \pm 8
Segments available for scar analysis (no)	Segments with non-transmural/transmural scar (no)
Lateral wall (660)	96/44
Septum (657)	170/40
Anterior wall (393)	88/24
Inferior wall (396)	106/34

LBBB = left bundle branch block; LV = left ventricular.

Fig. 1 shows FDG-PET images from 3 representative patients: one with no scar, one with scar in the lateral wall and one with septal scar. In the patient with no scar, the figure shows markedly asymmetric distribution of myocardial glucose metabolism, with hypo-metabolism in the septum relative to the LV lateral wall. The figure also illustrates that lateral wall scar was associated with marked reduction in glucose metabolism in the lateral wall. Numbers are given in Table 2.

FDG-PET identified transmural scars (LGE $\geq 50\%$) in the LV lateral wall with high accuracy (AUC = 0.96, 95% CI 0.90–1.00) (Table 3 and 4, Figs. 1 and 2). By ROC curve analysis, optimal cut off to identify transmural scar in the LV lateral wall was glucose uptake $<70\%$ relative to the segment with highest uptake. Using this cut off, sensitivity and specificity for identifying transmural scar was 94% and 91%, respectively. Replacing the statistically optimal threshold value with a cut off value of 50% FDG uptake, yielded a very high specificity (99%), but at the expense of a much lower sensitivity (56%).

In septal segments with no scar, glucose metabolism was reduced to 52% (95% CI: 25–86%) relative to the segment with highest uptake, generally located in the LV lateral wall. In septal segments with transmural scar, metabolism was further reduced to 42% (95% CI: 21–74%), $p = 0.012$. As indicated by the confidence intervals, there was substantial overlap between metabolism in normal septal segments and those with myocardial scar (Table 2). Therefore, FDG-PET could not identify septal scar. This is illustrated in Fig. 2, which shows weak association between glucose metabolism by FDG-PET and scar by LGE-CMR.

With regard to non-transmural scars, neither septal nor LV lateral wall scars were identified by FDG-PET (Table 3).

3.2. Myocardial scar by strain imaging

Peak systolic strain differed markedly between the LV lateral wall and septum (Table 2). In ventricles with no scar, peak lateral wall strain was -12.6% (95% CI: -1.3 to -24.7), whereas peak septal strain was -8.9% (95% CI: -0.4 to -20.1) ($p < 0.001$). As expected, in both LV lateral wall and septal segments, transmural scars were associated with reductions in absolute values of peak systolic strain (Table 2).

Fig. 3 shows individual values of peak systolic strain in LV lateral wall segments with different degrees of scar. The accuracy to identify lateral wall transmural scar by peak systolic strain was moderate, with AUC of 0.77 (95% CI: 0.71–0.84). However, absolute peak systolic strain $>10\%$ identified lateral wall segments without transmural scar with high sensitivity (80%) and high negative predictive value (96%). Values of absolute strain $<10\%$, however, were inconclusive with regard to transmural scar (Fig. 3, Table 4). We also tested if post-systolic strain could identify myocardial scar, but this parameter provided no added value compared to measuring peak systolic strain (Table 2).

For the septum, however, there were relatively weak associations between peak systolic strain and transmural scar, with AUC 0.69 (95% CI: 0.60–0.78), indicating low accuracy of peak systolic strain to identify transmural septal scars. With regard to non-transmural scars, they were not identified by strain imaging in the septum or LV lateral wall.

We also investigated if myocardial work index, as an additional parameter of myocardial function, could identify segments with myocardial scar. LV lateral wall segments with transmural scar had lower ($p < 0.001$) values for positive work (1020 mmHg.% (95% CI: 85–2348) than lateral segments with no scar (1729 mmHg.% (95% CI: 425–3577)). Similarly, in the septum, absence of scar was associated with increased ($p < 0.001$) positive myocardial work of 881 mmHg.% (95% CI: 178–2176), as compared to 583 mmHg.% (95% CI: 127–1532) in septal segments with transmural scar. When comparing ability to identify scar, however, septal and lateral wall work indices were not superior to peak systolic strain and therefore provided no added value.

The asymmetry in FDG metabolism correlated with asymmetry in workload ($r = 0.44$, $p = 0.001$, Fig. 4).

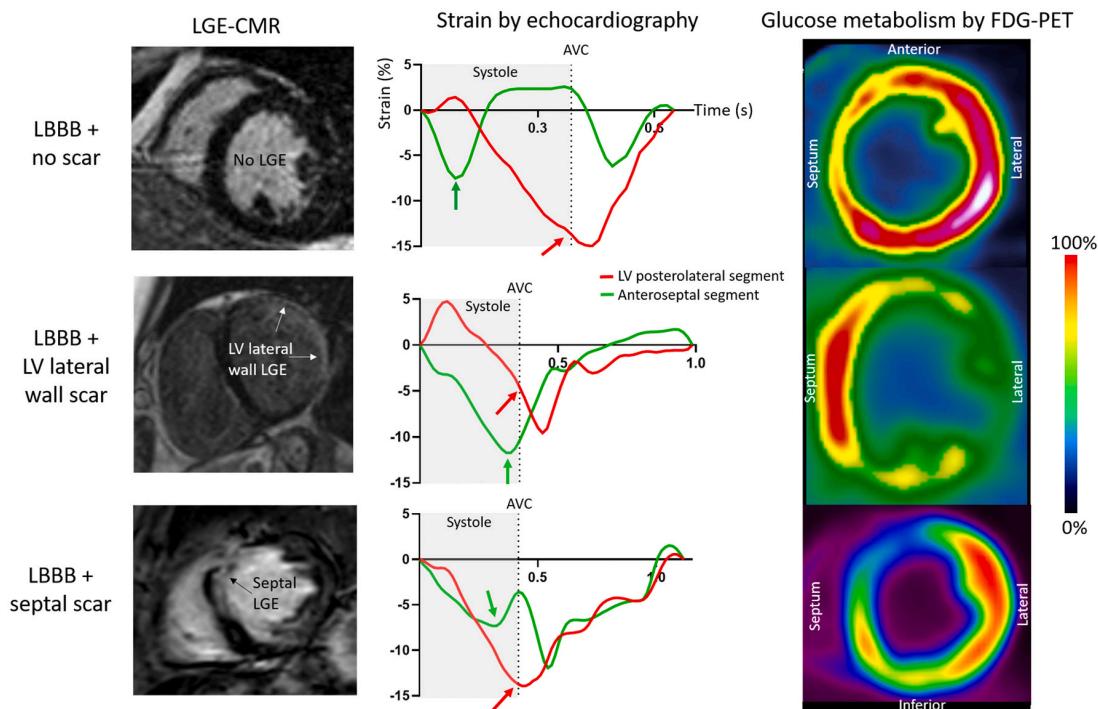


Fig. 1. Recordings from representative patients: The images are from patients where LGE-CMR shows no myocardial scar (upper panels), transmural scar in the LV lateral wall (middle panels) and transmural scar in the septum (lower panels). Green and red arrows indicate peak systolic strain for septum and the LV lateral wall, respectively. The anteroseptal and posterolateral segments are used.

The three patients illustrate typical spatial non-uniformities in distributions of LV myocardial metabolism and strain in patients with different locations of LV scar. The patient with no scar has markedly reduced septal strain and metabolism relative to the LV lateral wall. In the patient with lateral wall scar there is reduction in both metabolism and strain in the lateral wall relative to septum. In the patient with septal scar, there are reductions in both septal metabolism and strain. Please note that the patient with no septal scar has approximately similar reduction in peak systolic strain as the patient with septal scar, and both patients have reductions in septal metabolism relative to the lateral wall.

LV = left ventricular, LBBB = left bundle branch block, LGE-CMR = late gadolinium enhancement cardiac magnetic resonance, FDG-PET = ¹⁸F-fluorodeoxyglucose Positron Emission Tomography, AVC = aortic valve closure. (For interpretation of the references to colour in this figure legend, the reader is referred to the web version of this article.)

Table 2
Strain and glucose metabolism in segments with varying degree of scar.

Variable	Lateral wall			Septum		
	No scar	Non-transmural scar	Transmural scar	No scar	Non-transmural scar	Transmural scar
Peak negative systolic strain (%)	-12.6 (-1.3 to -24.7)	-9.0* (0.0 to -22.8)	-6.2*† (-0.0 to -15.8)	-8.9 (-0.4 to -20.1)	-8.4 (-0.7 to -19.7)	-5.6*† (-0.1 to -14.6)
Post systolic strain (%)	-2.0 (0.0 to -8.1)	-2.5* (0.0 to -8.0)	-4.0*† (0.0 to -14.0)	-4.0 (0.0 to -11.5)	-2.9* (0.0 to -8.6)	-3.1 (0.0 to -13.3)
Glucose metabolism (%)	86.5 (63.9 to 100.0)	81.7* (46.2 to 100.0)	48.4*† (26.0 to 85.8)	51.5 (25.0 to 85.7)	54.2 (19.3 to 98.3)	41.8*† (21.1 to 73.7)

Values are given in average (95% confidence interval). * = $p < 0.05$ compared to segments without scar. † = $p < 0.05$ compared to segments with non-transmural scar.

Table 3
The ability of strain and metabolism to identify scarred segments by receiver operating characteristic curve analysis.

	Area under the curve (95% confidence interval)	
	Non-transmural scar	Transmural scar
Lateral wall		
Peak negative systolic strain	0.67 (0.61–0.73) [94]	0.77 (0.71–0.84) [44]
Glucose metabolism	0.58 (0.49–0.67) [54]	0.96 (0.90–1.00) [16]
Septum		
Peak negative systolic strain	0.53 (0.48–0.58) [165]	0.69 (0.60–0.78) [39]
Glucose metabolism	0.53 (0.48–0.61) [77]	0.68 (0.57–0.79) [21]

Only the parameters that best identified scars in each region are included in the table. Number of scarred segments for each analysis in square brackets.

4. Discussion

From this prospective multicenter study, we present the novel finding that FDG-PET identifies LV lateral wall scar with high accuracy in patients with LBBB. These results imply that FDG-PET represents an alternative to LGE-CMR for scar imaging in CRT candidates. The other novel finding is that preserved peak systolic strain (>10%) in the LV lateral wall excludes transmural scar with high accuracy. A more marked reduction in systolic strain was nonspecific regarding scar detection.

In our study population, there were marked reductions in septal metabolism and function caused by the abnormal electrical activation. Patients with septal scarring had additional reductions in function and

Table 4

The ability of peak systolic strain and glucose metabolism to identify segmental transmural scars (LGE ≥ 50%) in the lateral wall and septum, and their derived optimal cut offs.

	Cut off	Sensitivity (%)	Specificity (%)	PPV (%)	NPV (%)	Accuracy (%)
Peak negative systolic strain	%					
- Lateral wall	-10.2	80	61	18	96	78
- Septum	-7.1	69	58	11	96	69
Glucose uptake	%					
- Lateral wall	69.6	94	91	41	100	91
- Septum	44.1	76	64	16	97	65

LGE = late gadolinium enhancement; PPV = positive predictive value; NPV = negative predictive value.

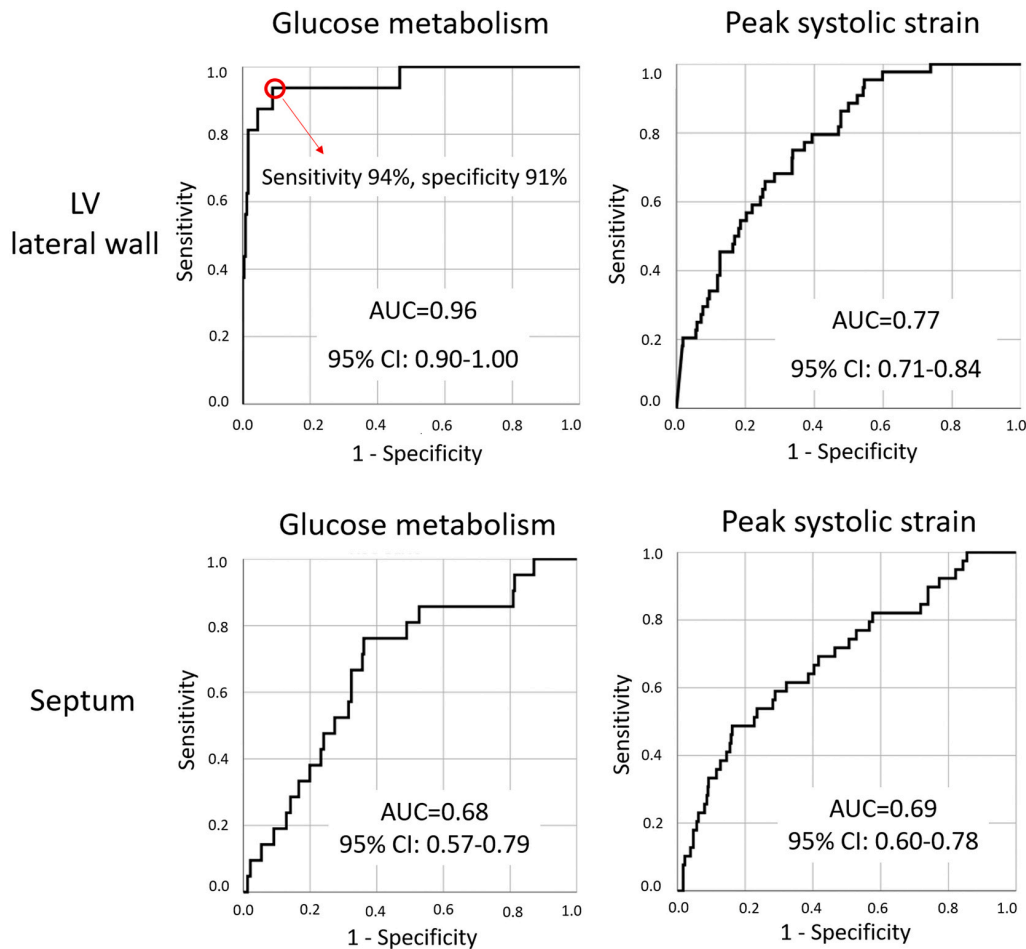


Fig. 2. ROC curves of the ability of peak systolic strain and glucose metabolism to identify transmural scars (LGE ≥50%) in the LV lateral wall and septum. Glucose metabolism by FDG-PET predicted transmural scars in the LV lateral wall with high accuracy, with glucose uptake of 70% as optimal cut off. Myocardial strain and work by echocardiography were less precise. Neither FDG-PET (glucose metabolism) nor echocardiographic parameters identified transmural septal scars. ROC = receiving operating characteristic; LGE = late gadolinium enhancement; LV = left ventricular; FDG-PET = ¹⁸F-fluorodeoxyglucose Positron Emission Tomography; AUC = area under the curve; CI = confidence interval.

metabolism, and neither FDG-PET nor strain imaging could differentiate between changes in metabolism and function due to scarring and electrical dyssynchrony. This was evident as marked overlap between values for glucose metabolism and strain in patients with and without transmural septal scars. Therefore, none of the imaging modalities FDG-PET and systolic strain could identify scar tissue in the septum.

4.1. Nuclear imaging

In the present study, optimal cut-off for FDG uptake to identify

transmural scar in the LV lateral wall was 70% calculated relative to the segment with highest uptake. Previous studies in patients with coronary disease have found somewhat lower cut-offs (16). This apparent inconsistency may be related to the abnormal distribution of myocardial metabolism in LBBB, with relative hypo-metabolism in the septum compared to the LV lateral wall. Our results shows that a lower cut off (50% FDG uptake) identifies transmural lateral wall scar with lower sensitivity. Hence, clinically relevant scars is likely to go unrecognized using this lower cut off in the present patient population. Of note, our results only suggest using the threshold of 70% FDG uptake to identify

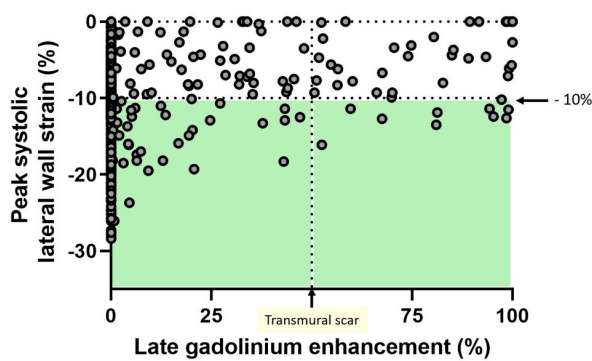


Fig. 3. Relationship between peak systolic strain and percentage LGE (scar) in lateral wall segments.

Peak absolute strain $<10\%$ was nonspecific with regard to scar extension by late gadolinium enhancement. As indicated by the green-enhanced area, absolute peak systolic strain $>10\%$ correctly classified segments with regard to transmural scar in a majority ($n = 356$) of segments and incorrectly in only a few ($n = 10$). (For interpretation of the references to colour in this figure legend, the reader is referred to the web version of this article.)

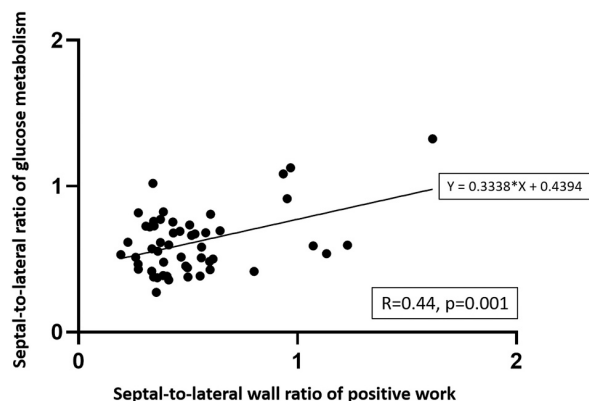


Fig. 4. Correlation between asymmetry in work and metabolism between septum and the lateral wall.

The asymmetry in metabolism between septum and LV lateral wall correlated significantly with the asymmetry in workload. One outlier was excluded.

transmural lateral wall scars, not to identify less extensive scarring or scarring in other myocardial region.

We have previously shown that high glucose metabolism in the LV lateral wall (relative to septum) predicts CRT response (17).

Inability to detect septal scars by FDG-PET is most likely related to altered mechanical function in the septum, which impacts metabolism. As proposed by Prinzen et al (6), reduced septal work in the dyssynchronous ventricle reduces metabolic demand, which explains the reduced glucose metabolism in septum relative to the lateral wall (7). These experimental data are supported by our observations of a significant association between asymmetry in work and asymmetry in metabolism between septum and the LV lateral wall. As suggested by our study in dyssynchronous ventricles, FDG-PET cannot differentiate between reductions in glucose metabolism caused by septal scar and reduced metabolic demand due to reduction in septal work load.

4.2. Echocardiographic strain imaging

The demonstration that *preserved* strain in the LV lateral wall could rule out transmural scar is consistent with observations in previous studies of radial strain that were limited to ischemic cardiomyopathy (11). In the present study, however, *reduced* lateral wall strain ($\leq 10\%$)

was nonspecific with regard to the presence of lateral wall scar. This is in apparent conflict with previous studies limited to ischemic cardiomyopathy, which have shown a strong association between radial (10,18) and longitudinal (9) strain in the LV lateral wall and transmural scar. However, not all studies used LGE-CMR as reference standard for scar and suggested cut offs for strain varies between studies. In patients with non-ischemic cardiomyopathy, there is typically reduction in LV shortening in all or most segments regardless of tissue viability. This probably explains why low values of lateral wall strain had no diagnostic value as marker of myocardial scar in our patient group. Taken together, the observations in the present study show that preserved myocardial strain in the LV lateral wall can be used to rule out transmural scar, which may be useful when considering LV electrode placement in the LV lateral wall in CRT candidates.

4.3. Alternative methods to image scar in dyssynchronous ventricles

Studies in patients with coronary disease show that PET perfusion imaging, and single photon emission computed tomography (SPECT) are comparable to FDG-PET in viability diagnostics (16). However, it remains to be tested how accurate these imaging modalities are for assessment of LV scar in patients with heart failure and LBBB. A previous study in patients with LBBB indicates that resting SPECT images may show fixed perfusion defects that may be misinterpreted as septal scar (19). Importantly, several studies confirm the utility of applying myocardial perfusion imaging by SPECT to predict response to CRT (20–22). Furthermore, SPECT is less expensive and more available than PET, which, like CMR, is limited by accessibility.

In the present study, we used longitudinal strain to evaluate LV function. In principle, LV radial strain should give similar results since deformation in the long axis is always accompanied by deformation in the short axis (conservation of mass). In the present study, however, we found longitudinal strain easier to perform, probably due to markedly dilated ventricles with wall thinning.

Traditional echocardiographic parameters such as LV wall thickness and wall motion score may also be used to evaluate myocardial scar, but these methods are challenging to use in the dyssynchronous heart.

4.4. Clinical implications

Selecting patients for CRT based on scar characterization in the LV lateral wall and septum may improve responder rates to the therapy. Our findings that FDG-PET is a good alternative to LGE-CMR to identify transmural LV lateral wall scar in these patients, is clinically relevant, for example in patients where LGE-CMR is contraindicated. Furthermore, well-preserved LV lateral wall strain indicates that transmural scar in this region is unlikely. Reduced LV lateral wall strain, on the other hand, is not conclusive of scar and should be interpreted with caution. Recent studies have demonstrated that septal scar by CMR combined with information on either LV workload by echocardiography (4) or glucose metabolism by FDG-PET (17), accurately identifies CRT responders. Both approaches rely on LGE-CMR to identify septal scar, in line with findings from the present study that neither echocardiography nor PET can reliably assess scars in septum.

4.5. Limitations

The PET imaging part of the study was of moderate size, and a larger study population may have provided additional information, in particular for assessment of non-transmural scars. Increased FDG uptake due to reversible ischemia may affect the number of LV lateral wall segments with FDG uptake $<70\%$. However, included patients had no history of reversible ischemia, were instructed to avoid exercise the days before, and the investigations were performed under resting conditions. Furthermore, patient preparation was performed to ensure globally high glucose uptake within the myocardium, minimizing the potential effect

of this confounder. In total, with regard to transmural scars in the LV lateral wall, the data were convincing and clearly showed the utility of FDG-PET as an alternative to LGE-CMR. It does not seem likely that a larger study would have given different results for FDG-PET imaging of septal scars since differentiation between reduced metabolism due to reduced septal work caused by dyssynchrony, would not be easy to separate from reduced metabolism due to reduced mass of viable myocardium.

The present study did not include nuclear perfusion imaging which could potentially provide additional information regarding septal scar. In principle, however, a similar limitation as for FDG-PET may apply to perfusion imaging since myocardial microvascular flow is autoregulated and determined by metabolism.

5. Conclusions

We present the novel finding that FDG-PET is an excellent modality to identify scar in the LV lateral wall in CRT candidates, and is therefore an alternative to LGE-CMR. Myocardial strain imaging by speckle tracking echocardiography also provides important diagnostic information as preserved strain in the LV lateral wall has good accuracy to rule out transmural scar. None of the modalities could identify septal scar because reductions in metabolism and strain due to abnormal electrical activation, overlapped with reductions due to scar. Therefore, currently LGE-CMR is the only clinical method to identify septal scars in CRT candidates.

Sources of funding

CKL was a recipient of clinical research fellowship from the South-Eastern Norway Regional Health Authority. JD and JMA were supported by research grants of the University of Leuven (OT12/084) and the Norwegian Health Association, respectively. JD and JUV hold research mandates of the Research Foundation Flanders (FWO) (12ZZN22N and FKMI832917N). The funding bodies had no role in the design of the study, the collection, analysis and interpretation of data, or in writing the manuscript.

Disclosures

OAS is co-inventor of the “Method for myocardial segment work analysis”, which was used to calculate myocardial work. The other authors have no disclosures.

CRedit authorship contribution statement

Camilla Kjellstad Larsen: Methodology, Formal analysis, Investigation, Writing – original draft, Visualization. **Elena Galli:** Formal analysis, Investigation, Writing – review & editing. **Jürgen Duchenne:** Formal analysis, Investigation, Writing – review & editing. **John M. Aalen:** Formal analysis, Investigation, Writing – review & editing. **Caroline Stokke:** Resources, Writing – review & editing, Visualization. **Jan Gunnar Fjeld:** Resources, Writing – review & editing, Visualization. **Ganna Degtiarova:** Formal analysis, Writing – review & editing. **Piet Claus:** Resources, Writing – review & editing. **Olivier Gheysens:** Resources, Writing – review & editing. **Jorg Saberniak:** Formal analysis, Writing – review & editing. **Per Anton Sirnes:** Formal analysis, Writing – review & editing. **Erik Lyseggen:** Resources, Writing – review & editing. **Jan Bogaert:** Resources, Writing – review & editing. **Erik Kongsgaard:** Resources, Writing – review & editing. **Martin Penicka:** Methodology, Resources, Writing – review & editing, Funding acquisition. **Jens-Uwe Voigt:** Methodology, Resources, Writing – review & editing, Funding acquisition. **Erwan Donal:** Methodology, Resources, Writing – review & editing, Funding acquisition. **Einar Hopp:** Methodology, Validation, Resources, Writing – review & editing, Visualization, Supervision, Funding acquisition. **Otto A. Smiseth:**

Conceptualization, Methodology, Validation, Resources, Writing – review & editing, Visualization, Supervision, Project administration, Funding acquisition.

Acknowledgements

The authors thank study nurse Kari Melberg, MRI radiographer Bac Nguyen and PET radiographer Alexander Gul Sherwani for their important contributions to the study.

References

- [1] M. Glikson, J.C. Nielsen, M.B. Kronborg, Y. Michowitz, A. Auricchio, I.M. Barbash, et al., 2021 ESC guidelines on cardiac pacing and cardiac resynchronization therapy: developed by the task force on cardiac pacing and cardiac resynchronization therapy of the European Society of Cardiology (ESC) with the special contribution of the European Heart Rhythm Association (EHRA), *Eur. Heart J.* 42 (35) (2021) 3427–3520.
- [2] J.G. Cleland, J.C. Daubert, E. Erdmann, N. Freemantle, D. Gras, L. Kappenberger, et al., The effect of cardiac resynchronization on morbidity and mortality in heart failure, *N. Engl. J. Med.* 352 (15) (2005) 1539–1549.
- [3] G.B. Bleeker, T.A. Kaandorp, H.J. Lamb, E. Boersma, P. Steendijk, A. de Roos, et al., Effect of posterolateral scar tissue on clinical and echocardiographic improvement after cardiac resynchronization therapy, *Circulation.* 113 (7) (2006) 969–976.
- [4] J.M. Aalen, E. Donal, C.K. Larsen, J. Duchenne, M. Lederlin, M. Cvijic, et al., Imaging predictors of response to cardiac resynchronization therapy: left ventricular work asymmetry by echocardiography and septal viability by cardiac magnetic resonance, *Eur. Heart J.* 41 (39) (2020) 3813–3823.
- [5] R.J. Kim, D.S. Fieno, T.B. Parrish, K. Harris, E.L. Chen, O. Simonetti, et al., Relationship of MRI delayed contrast enhancement to irreversible injury, infarct age, and contractile function, *Circulation.* 100 (19) (1999) 1992–2002.
- [6] F.W. Prinzen, W.C. Hunter, B.T. Wyman, E.R. McVeigh, Mapping of regional myocardial strain and work during ventricular pacing: experimental study using magnetic resonance imaging tagging, *J. Am. Coll. Cardiol.* 33 (6) (1999) 1735–1742.
- [7] S. Ono, R. Nohara, H. Kambara, K. Okuda, C. Kawai, Regional myocardial perfusion and glucose metabolism in experimental left bundle branch block, *Circulation.* 85 (3) (1992) 1125–1131.
- [8] J. Duchenne, A. Turco, S. Ünlü, E.D. Pagourelis, K. Vunckx, G. Degtiarova, et al., Left ventricular remodeling results in homogenization of myocardial work distribution, *Circ. Arrhythm. Electrophysiol.* 12 (5) (2019), e007224.
- [9] A. D'Andrea, P. Caso, R. Scarafale, L. Riegler, G. Salerno, F. Castaldo, et al., Effects of global longitudinal strain and total scar burden on response to cardiac resynchronization therapy in patients with ischaemic dilated cardiomyopathy, *Eur. J. Heart Fail.* 11 (1) (2009) 58–67.
- [10] V. Delgado, R.J. van Bommel, M. Bertini, C.J. Borleffs, N.A. Marsan, C.T. Arnold, et al., Relative merits of left ventricular dyssynchrony, left ventricular lead position, and myocardial scar to predict long-term survival of ischemic heart failure patients undergoing cardiac resynchronization therapy, *Circulation.* 123 (1) (2011) 70–78.
- [11] A.C. Kydd, F. Khan, D. Gopalan, L. Ring, B.S. Rana, M.S. Virdee, et al., Utility of speckle tracking echocardiography to characterize dysfunctional myocardium in patients with ischemic cardiomyopathy referred for cardiac resynchronization therapy, *Echocardiography.* 31 (6) (2014) 736–743.
- [12] H. Engblom, J. Tufvesson, R. Jablonowski, M. Carlsson, A.H. Aletras, P. Hoffmann, et al., A new automatic algorithm for quantification of myocardial infarction imaged by late gadolinium enhancement cardiovascular magnetic resonance: experimental validation and comparison to expert delineations in multi-center, multi-vendor patient data, *J. Cardiovasc. Magn. Reson.* 18 (1) (2016) 27.
- [13] M.J. Knuuti, P. Nuutila, U. Ruotsalainen, M. Saraste, R. Harkonen, A. Ahonen, et al., Euglycemic hyperinsulinemic clamp and oral glucose load in stimulating myocardial glucose utilization during positron emission tomography, *J. Nucl. Med.* 33 (7) (1992) 1255–1262.
- [14] K. Russell, M. Eriksen, L. Aaberge, N. Wilhelmssen, H. Skulstad, E.W. Remme, et al., A novel clinical method for quantification of regional left ventricular pressure-strain loop area: a non-invasive index of myocardial work, *Eur. Heart J.* 33 (6) (2012) 724–733.
- [15] M.D. Cerqueira, N.J. Weissman, V. Dilsizian, A.K. Jacobs, S. Kaul, W.K. Laskey, et al., Standardized myocardial segmentation and nomenclature for tomographic imaging of the heart. A statement for healthcare professionals from the cardiac imaging Committee of the Council on clinical cardiology of the American Heart Association, *Circulation.* 105 (4) (2002) 539–542.
- [16] M.J. Garcia, R.Y. Kwong, M. Scherrer-Crosbie, C.C. Taub, R. Blankstein, J. Lima, et al., State of the art: imaging for myocardial viability: a scientific statement from the American Heart Association, *Circ Cardiovasc Imaging.* 13 (7) (2020), e000053.
- [17] G. Degtiarova, P. Claus, J. Duchenne, J. Bogaert, J. Nuyts, G. Vörös, et al., Left ventricular regional glucose metabolism in combination with septal scar extent identifies CRT responders, *Eur. J. Nucl. Med. Mol. Imaging* 48 (8) (2011) 2437–2446.
- [18] L.E. Sade, S. Saba, J.J. Marek, T. Onishi, D. Schwartzman, E.C. Adelstein, et al., The association of left ventricular lead position related to regional scar by speckle-tracking echocardiography with clinical outcomes in patients receiving cardiac resynchronization therapy, *J. Am. Soc. Echocardiogr.* 27 (6) (2014) 648–656.

- [19] H. Mahrholdt, A. Zhydkov, S. Hager, G. Meinhardt, H. Vogelsberg, A. Wagner, et al., Left ventricular wall motion abnormalities as well as reduced wall thickness can cause false positive results of routine SPECT perfusion imaging for detection of myocardial infarction, *Eur. Heart J.* 26 (20) (2005) 2127–2135.
- [20] E.C. Adelstein, H. Tanaka, P. Soman, G. Miske, S.C. Haberman, S.F. Saba, et al., Impact of scar burden by single-photon emission computed tomography myocardial perfusion imaging on patient outcomes following cardiac resynchronization therapy, *Eur. Heart J.* 32 (1) (2011) 93–103.
- [21] C. Ypenburg, M.J. Schalij, G.B. Bleeker, P. Steendijk, E. Boersma, P. Dibbets-Schneider, et al., Impact of viability and scar tissue on response to cardiac resynchronization therapy in ischaemic heart failure patients, *Eur. Heart J.* 28 (1) (2007) 33–41.
- [22] I. Morishima, K. Okumura, H. Tsuboi, Y. Morita, K. Takagi, R. Yoshida, et al., Impact of basal inferolateral scar burden determined by automatic analysis of ^{99m}Tc-MIBI myocardial perfusion SPECT on the long-term prognosis of cardiac resynchronization therapy, *Europace.* 19 (4) (2017) 573–580.

Paper 3

Cardiac magnetic resonance identifies responders to cardiac resynchronization therapy by assessment of septal scar and left ventricular dyssynchrony

Authors: Camilla Kjellstad Larsen, MD¹, Otto A. Smiseth, MD, PhD¹, Jürgen Duchenne, PhD², Elena Galli, MD, PhD³ John M. Aalen, MD, PhD¹, Mathieu Lederlin, MD, PhD⁴, Jan Bogaert, MD, PhD⁵, Erik Kongsgaard, MD, PhD⁶, Cecilia Linde, MD, PhD⁷, Martin Penicka, MD, PhD⁸, Erwan Donal, MD, PhD³, Jens-Uwe Voigt, MD, PhD², Einar Hopp, MD, PhD⁹

¹Institute for Surgical Research and Department of Cardiology, Oslo University Hospital, and Institute of Clinical Medicine, University of Oslo, Oslo, Norway

²Department of Cardiovascular Diseases, University Hospitals Leuven and Department of Cardiovascular Sciences, KU Leuven – University of Leuven, Leuven, Belgium

³Department of Cardiology, University Hospital of Rennes, Rennes, France

⁴Department of Radiology, University Hospital of Rennes, Rennes, France

⁵Department of Radiology, University Hospitals Leuven, Leuven, Belgium

⁶Department of Cardiology, Oslo University Hospital, Oslo, Norway

⁷Department of Cardiology, Karolinska University Hospital, Stockholm, Sweden

⁸Cardiovascular Center, OLV Clinic, Belgium

⁹Division of Radiology and Nuclear Medicine, Oslo University Hospital, Oslo, Norway

All authors take responsibility for all aspects of the reliability and freedom from bias of the data presented and their discussed interpretation.

Address for correspondence:

Einar Hopp, MD, PhD
Division of Radiology and Nuclear Medicine,
Oslo University Hospital, Rikshospitalet
N-0027 Oslo, Norway
Phone: + 47 23 07 00 00
Fax: + 47 23 07 26 10
E-mail: ehopp@ous-hf.no

Sources of funding: CKL was a recipient of clinical research fellowship from the South-Eastern Norway Regional Health Authority. JD and JMA were supported by research grants of the University of Leuven (OT12/084) and the Norwegian Health Association, respectively. JD and JUV hold research mandates of the Research Foundation Flanders (FWO) (12ZZN22N and FKM1832917N). The funding bodies had no role in the design of the study, the collection, analysis and interpretation of data, or in writing the manuscript.

Conflict of interest: OAS is co-inventor of the “Method for myocardial segment work analysis” and has received one speaker honorarium from GE Healthcare. The other authors have no disclosures.

Key words: Cardiac magnetic resonance; Cardiac resynchronization therapy; Scar; Dyssynchrony; Septal flash; Myocardial work

Abstract

Background

Response to cardiac resynchronization therapy (CRT) depends on septal viability and correction of abnormal septal motion. This study investigates if cardiac magnetic resonance (CMR) as single modality can identify CRT responders by combined imaging of pathological septal motion (septal flash) and septal scar.

Methods

In a prospective, multicenter, observational study of 136 CRT recipients, septal scar was assessed by late gadolinium enhancement (LGE) (n=127) and septal flash visually from cine CMR sequences. Primary endpoint was CRT response, defined as $\geq 15\%$ reduction in LV end-systolic volume by echocardiography after 6 months. Secondary endpoint was heart transplantation or death of any cause assessed after 39 ± 13 months.

Results

Septal scar and septal flash were independent predictors of CRT response in multivariable analysis (both $p < 0.001$), while QRS-duration and -morphology were not. The combined approach of septal scar and septal flash predicted CRT response with area under the curve 0.86 (95% confidence interval (CI): 0.78-0.94) and was a strong predictor of long-term survival without heart transplantation (hazard ratio 0.27, 95% CI: 0.10-0.79). Accuracy of the approach was similar in the subgroup with intermediate (130-150ms) QRS duration. The combined approach was superior to septal scar and septal flash alone ($p < 0.01$).

Conclusions

Combined assessment of septal scar and septal flash by CMR as single image modality identifies CRT responders with high accuracy and predicts long-term survival.

Trial registration

The study was registered at clinicaltrials.gov (identifier NCT02525185). Registered 17 August 2015.

Introduction

Cardiac resynchronization therapy (CRT) improves left ventricular (LV) function, and reduces mortality and morbidity in selected patients with dyssynchronous heart failure (1, 2). Current guidelines advocate CRT in patients with symptomatic heart failure, LV ejection fraction (EF) $\leq 35\%$ and QRS duration $\geq 130\text{ms}$, preferably with left bundle branch block (LBBB) morphology (3). However, QRS duration, which reflects electrical dyssynchrony, is only a moderate predictor of CRT response, and adherence to the guidelines criteria results in a non-responder rate of about 30 % (4). Therefore, better predictive tools are needed.

Patients with LBBB typically have reduced function of the interventricular septum, which directly impairs global LV function, and results in compensatory increased work of the LV lateral wall (5, 6). Such LV electromechanical dyssynchrony appears to be a substrate for CRT, and restoring septal function by CRT improves global LV performance (5). Studies have confirmed that echocardiographic dyssynchrony indices, such as septal flash and myocardial work distribution, are associated with beneficial response to CRT (7-10). Contrary, myocardial scar, particularly if located in the LV posterolateral wall or septum, reduces response rate (11-13). Septal viability is essential considering recovery of septal function a main mechanism of CRT response (5). In line with these findings, we have recently shown that asymmetric LV work distribution by echocardiography, combined with septal scar by cardiac magnetic resonance (CMR) identifies CRT responders better than the criteria recommended in current guidelines (14). In patients with suboptimal echocardiographic images, however, alternative approaches for LV dyssynchrony imaging are needed. Unlike echocardiography, CMR image quality is independent of acoustic window. Furthermore, CMR is needed to assess septal scar (15). We hypothesized that imaging of LV dyssynchrony and myocardial work as well as septal scar by CMR may be used to identify patients who are likely to respond positively to CRT.

Thus, in a prospective, multicenter, observational study, we investigate if CMR as single modality for imaging both LV dyssynchrony, myocardial work and myocardial scar identifies CRT responders beyond the selection criteria recommended in current guidelines.

Methods

Study population

The present study is part of a prospective, multicenter, observational study previously reported (14). Of the total 236 patients originally enrolled, all patients who successfully completed a CMR scan and had available follow-up data were consecutively included in the present study (n=136). Main reason for not performing CMR was previously implanted CMR incompatible cardiac device (n=53). For the remaining patients (n=30) reasons included patient refusal, intracranial metal implants and logistical causes/no available CMR slot. Additionally, 3 patients were excluded due to inadequate CMR image quality. Reasons for no available follow-up data included CRT not implanted (n = 11), lost to follow-up (n = 1), lead extraction because of endocarditis (n = 1) and no follow-up echocardiography (n = 1).

Study inclusion criteria were indication for CRT according to European Society of Cardiology (ESC) guidelines (3). The study was conducted following the ethical guidelines of the Declaration of Helsinki and was approved by the Regional Ethical Committees of every participating centre. Informed consent was obtained from each patient. The study was

registered at clinicaltrials.gov (identifier NCT02525185). The present study is an exploratory observational outcome study.

Cardiac magnetic resonance (CMR)

Patients were scanned with a 1.5 or 3.0 Tesla unit (Aera, Skyra or Verio, Siemens, Erlangen, Germany, or Ingenia, Philips Healthcare, Best, the Netherlands, or Signa HDXT, GE, Boston, US). Acquisition was performed with ECG gating and during breath-holds. Standard long- and short axis cine sequences covering the entire left ventricle were acquired using a steady-state free precession sequence with 31 ± 3 frames per heart cycle. LV volumes were measured and EF was calculated from short axis slices with the freely available software Segment v2.0 R5270 (Medviso AB, Lund, Sweden) (16). All CMR analyses were performed at the same center.

Myocardial scar

We performed late gadolinium enhancement (LGE) to define myocardial scar in individuals with preserved renal function ($eGFR \geq 45$ ml/min/1.73 m²). Images in long- and short axis projections were obtained during steady state after intravenous injection of either 0.15 (n=79) or 0.20 (n=44) mmol/kg gadoterate meglumine (Doteram™, Guerbet, Villepinte, France), 0.15 mmol/kg gadobutrol (Gadovist™, Bayer AB, Stockholm, Sweden) (n=3) or 0.15 mmol/kg gadobenate dimeglumine (MultiHance®, Bracco, Milan, Italy) (n=2). A trained CMR radiologist assessed LGE visually, and defined etiology as ischemic or not. From a stack of short axis slices LGE volume was quantified semi automatically with Segment software v2.0 R5270 and reported with percentage LGE per associated tissue volume in a 17-segment model. We utilized the automatic algorithm EWA (expectation maximization, weighted intensity, a priori information) (17). Quantitative analysis by the semi-automatic software was made independently of the visual analysis, and any discrepancies between the two were addressed and conclusions made between readers.

Reduced renal function precluded contrast agent administration in eight of 136 patients. Patients available for LGE analysis included the 125 patients previously reported (14), and three patients with incomplete echocardiographic strain data. In one patient, image artefacts from an implantable cardioverter defibrillator led us to exclude LGE analysis in the anterior wall and septum. Hence, total number of patients available for analyses involving septal LGE was 127.

Indices of LV dyssynchrony

Septal flash

Septal flash (7) was defined as an early and fast left-right motion (thickening/thinning) of the interventricular septum that starts and mostly ends during the isovolumic contraction phase prior to aortic valve opening (Figure 1 and Video 1). It was determined to be present if visualized in 4-chamber long axis or any of the short axis cine images as a yes or no phenomenon. To test reproducibility of septal flash, we performed intercenter variability testing in 25 randomly selected patients. Septal flash was assessed in all 136 patients.

Myocardial work

Septal and lateral myocardial work was calculated by LV pressure-strain analysis as previously described (18), using circumferential strain from feature tracking software (2D CPA MR; TomTec Imaging Systems, Unterschleissheim, Germany) and non-invasive LV pressure (19). Systolic shortening is positive work, while lengthening is negative work. Net work is the sum of positive and negative work. Lateral-to-septal work difference was calculated as the absolute difference in net work performed by the LV lateral wall and septum, and used as a marker of dyssynchronous LV workload. Blood pressure was measured by the brachial cuff method on the same day as the CMR examination in an equivalent resting condition. Myocardial work was assessed in 130 of 136 patients. In the remaining six patients, image quality was insufficient for strain analysis.

Echocardiography

All patients underwent echocardiographic examination (Vivid E9 or E95, GE Vingmed Ultrasound, Horten, Norway) at baseline and 6 (6±1) months follow-up. LV volumes were calculated by the biplane Simpson's method using two-dimensional images from the apical views. Septal flash was assessed with similar criteria as by CMR as previously reported (14).

Device implantation

A biventricular system was implanted according to standardized directions. Coronary venography was used to delineate venous anatomy, and the LV lead was placed in a lateral or posterolateral vein if possible. The device was programmed in a conventional biventricular pacing modus, and tested to ensure technically well-functioning prior to hospital discharge.

Endpoints

Primary endpoint was reverse remodeling defined as $\geq 15\%$ reduction in LV end-systolic volume (ESV) by echocardiography at 6 (6±1) months follow-up compared to baseline. Three different centers measured all volumes independently. In case of disagreement on response between readers, we used averaged volumes from the two agreeing readers.

Secondary endpoint was heart transplantation or death of any cause 39±13 months after device implantation.

Statistical analyses

Continuous variables are expressed as mean±SD if normally distributed, otherwise as median (interquartile range). Student's t-test, Mann-Whitney U test or chi-square test were used, as appropriate, to compare groups. To identify significant predictors for reverse remodeling (primary endpoint), we used linear regression analysis with left ventricular end systolic volume change as dependent continuous variable. Variance inflation factor (VIF) was used as a measure of multicollinearity, and VIF <5 was considered acceptable for inclusion in multivariable regression analysis.

Receiver operating characteristic (ROC) curves with area under the curve (AUC) and 95% confidence interval (CI) were used to determine discriminative ability. To assess discriminative ability of two parameters combined, we used logistic regression to calculate a linear combination of the parameters, which was then used for ROC curves. The Hanley and McNeil method (20) was used to compare ROC curves.

To assess long-term survival (secondary endpoint), we used hazard ratio with 95% CI from Cox regression and log-rank test from Kaplan-Meier curves. Censoring was administrative due to individuals entering the study on different time points and, hence, different observation times. Intercenter variability of septal flash was assessed by intraclass correlation coefficient (ICC). Statistical significance was set at a two-tailed probability level of $p < 0.05$. SPSS version 25.0 (IBM Corporation, Armonk, NY) and MedCalc version 20.010 (MedCalc Software Ltd, Ostend, Belgium) were used for analyses.

Results

Study population

Baseline characteristics of all patients are presented in Table 1. In the total population, 103 patients (76%) responded to CRT in terms of reverse remodeling. In the subgroup with intermediate QRS-duration (130-150ms) ($n=29$), response rate was 62%. One patient received a heart transplant and two died during 6 months follow-up, all three were considered non-responders. Responders had broader QRS complexes and were more likely to have LBBB morphology compared to non-responders (Table 1). Eighteen patients (13%) died or underwent heart transplantation during follow-up.

Septal scar (LGE)

Median total scar burden was 0.3% (interquartile range: 0.0-10.0) in all patients, and 10.0% (interquartile range 3.2-20.0) in patients with LGE. Sixty-four patients had some degree of LGE: 47 in the anterior wall, 59 in septum, 56 in the inferior wall and 39 in the lateral wall. LGE classification and distribution is illustrated in Table 2. Several patients had LGE in more than one location, like RV insertion fibrosis, which almost always affected both septum and the inferior wall. Supplemental Figure S1 illustrates non-ischemic LGE examples and one artefact example.

In multivariable regression analysis with LV end systolic volume change as dependent continuous variable, we tested percentage LGE in the different four walls in addition to QRS-duration and QRS-morphology. Septal LGE was identified as the only significant predictor of reverse remodeling. Percentage septal LGE correlated inversely to reverse remodeling ($r_s = -0.56$, $p < 0.001$), and predicted CRT response with AUC 0.79 (95% CI: 0.70-0.89). In comparison, AUC for QRS-duration was 0.62 (95% CI: 0.51-0.74) and for QRS-morphology 0.58 (95% CI: 0.46-0.70).

As illustrated in Figure 2, response rate declined with increasing amount of septal LGE. However, the mere presence of septal LGE significantly reduced the likelihood of CRT response. With no septal LGE ($n=68$), response rate was excellent (93%). In comparison, response rate was only 58% in patients with any septal LGE ($n=59$) ($p < 0.001$, compared to no

septal LGE). Response rates were similar whether septal LGE was ischemic or non-ischemic (54% vs. 67%, respectively, $p=0.352$). LGE in other regions, not affecting septum, did not reduce response rate in the same way as LGE involving septum (80% vs 53% response).

Septal LGE was a strong predictor of long-term mortality and heart transplantation with hazard ratio 5.0 (95% CI: 1.8-14.4) compared to no septal LGE ($p=0.0026$), and was the only significant predictor in multivariable analysis including age, indexed end-diastolic volume and NYHA-class.

Septal flash

Septal flash was more frequent in responders (Table 1). Response rate was 88% if septal flash was present, as compared to 34% if septal flash was absent ($p<0.001$). AUC for CRT response prediction was 0.77 (95% CI: 0.66-0.87). Septal flash was associated with improved long-term survival without heart transplantation with hazard ratio 0.24 (95% CI: 0.08-0.75).

Reproducibility testing revealed agreement in 24 of the 25 randomly selected patients. Intercenter ICC was 0.96 (95% CI 0.90-0.98), indicating excellent reproducibility.

Combining septal LGE and septal flash

In multivariable regression analysis including percentage septal LGE, septal flash, QRS-duration and QRS-morphology, septal LGE and septal flash were the only significant independent predictors of reverse remodeling (Table 3). Furthermore, percentage septal LGE and septal flash showed incremental value to a multivariable model for CRT response including QRS-duration, QRS-morphology, heart failure etiology and indexed LV ESV (both $p<0.01$). The combined approach of percentage septal LGE and septal flash predicted CRT response with AUC=0.86 (95% CI: 0.78-0.94). Predictive power was similar in the subgroup with intermediate QRS-duration (AUC=0.99 (95% CI 0.97-1.00)) (Figure 3).

Absent septal LGE indicated excellent response rate. Thus incremental value of septal flash was most pronounced in patients with septal LGE, where response was more diverse. In this group, septal flash significantly improved predictive power compared to septal LGE alone ($p=0.0045$ for ROC curve comparison). Patients with septal LGE and septal flash had a high likelihood of response (78%), while patients with septal LGE and *no* septal flash were unlikely to respond (23%). The graphical abstract outlines an algorithm based on the two parameters, which correctly classified 86% of all patients as responders or non-responders. Importantly, accuracy of the algorithm was similar in the subgroup of patients with intermediate QRS-duration (93% of patients correctly classified). Furthermore, patients that were classified as likely responders by the algorithm had significantly better long-term survival without heart transplantation compared to patients that were classified as likely non-responders (hazard ratio 0.27 (95% CI: 0.10-0.79) (Figure 4).

Lateral-to-septal work difference

The difference in myocardial workload between the LV lateral wall and septum correlated to reverse remodeling ($r_s=-0.25$, $p=0.005$). Increased work difference was associated with more

reverse remodeling. Combining septal LGE and lateral-to-septal work difference predicted CRT response with AUC=0.84 (95% CI: 0.75-0.92). However, work difference was less suited than septal flash to distinguish responders from non-responders among patients with septal LGE, where it was not better than percentage septal LGE alone ($p>0.1$ for comparison of ROC curves).

Septal flash by echocardiography

Septal flash by CMR agreed with septal flash by echocardiography in 121 of 133 patients (91%): Six had septal flash by CMR and not by echocardiography and six had septal flash by echocardiography and not by CMR. Combining septal flash by echocardiography with septal LGE by CMR yielded AUC=0.82 (95% CI 0.73-0.92) for CRT response prediction, which was similar to the equivalent combination by CMR as single modality ($p=0.22$).

Discussion

The novel finding of the present prospective, multicenter study is that combined assessment of septal scar (LGE) and septal flash by CMR as single image modality identifies CRT responders with high accuracy and predicts long-term survival. We suggest a simple algorithm based on these two parameters, which predicts CRT response beyond current guideline criteria. With no septal LGE, response rate to CRT is excellent irrespective of other parameters. If septal LGE is present, and there is septal flash, patients are likely to respond. If, on the other hand, septal LGE is present and there is no septal flash, response to CRT is highly unlikely. Importantly, accuracy of the algorithm is similar in patients with intermediate QRS-duration. In this group, the method may be particularly useful, because benefit of CRT is less consistent.

The suggested approach, unlike many previously reported methods (3), does not require multimodality imaging. It is available in patients where poor image quality precludes echocardiographic evaluation, and quick and easy to perform. Therefore, it is a clinically attractive improvement to patient selection for CRT.

Septal markers define CRT response

LGE is a marker of adverse structural remodeling in response to myocardial injury and increased wall stress, and the extent of LGE varies in patients despite similar degrees of myocardial dysfunction (21). We found septal LGE, ischemic or non-ischemic, to be a strong predictor of non-response to CRT and adverse long-term outcome. A former study of 23 CRT recipients found that septal LGE $\leq 40\%$ provided a 100% sensitivity and specificity for CRT response (13). In the present larger study, however, the mere presence of septal LGE, rather than the absolute amount, is the factor to affect response to CRT. In contrast, LGE in other regions, not affecting septum, did not seem to affect response rate. While transmural posterolateral wall scar is an established risk factor for poor CRT response, the significance of lateral wall LGE per se seemed minor compared to septal LGE in the present study. A plausible explanation for this could be that most LV lateral wall scars in the present study were not transmural, and therefore probably did not affect regional function notably.

Nevertheless, limited number of lateral wall scars, necessitate further validation in future larger trials.

Despite inferior temporal resolution compared to echocardiography, the present study demonstrates that CMR identification of septal flash is equally clinically important. Therefore, CMR and echocardiography may be complementary image modalities in identifying LV dyssynchrony in some patients. Intercenter reproducibility of septal flash by CMR in our material was excellent. However, reproducibility might be lower if performed by less experienced readers.

Septal flash signals a potential substrate for CRT response (7). In line with our findings, a former smaller study by Sohal et.al also identified septal flash assessed by CMR as an independent predictor of reverse remodeling after CRT (22). Sohal assessed septal flash by analyzing time-volume curves, while we performed a rapid visual assessment. Along the same line, Zweerink and co-workers demonstrated that systolic septal stretching, evaluated on CMR cine sequences, is a prognostic measure for good clinical outcome after CRT (23). The approach used in the present study has obvious clinical advantages, but did not allow quantification of the degree of septal flash and its relation to CRT response. In total, the results of the present study add to the growing evidence that septum plays an essential role in transferring the harmful effects of LBBB on myocardial function, and that reversing septal dysfunction constitutes a key for CRT response. The results in the clinically challenging subgroup with intermediate QRS-duration are promising, but further research is warranted due to the low patient number in this subgroup.

LV lateral-to septal work difference

We have previously shown, applying speckle-tracking echocardiography to measure myocardial strain, that a high LV lateral-to-septal work difference indicates CRT response (14). The present study demonstrates that the lateral-to-septal work difference assessed by CMR also is a predictor for response to the treatment. Somewhat lower AUC may reflect that LV segmental strain by speckle tracking echocardiography is superior to current versions of feature tracking CMR. In patients with low quality echocardiographic images, however, myocardial work index by CMR may have a role.

Nevertheless, in the present material we identified septal flash as a more suited signal of unexploited contractile reserve in septum potentially recovered by CRT than the LV work difference. One possible explanation is that there may be a high difference in workload between the lateral wall and septum both in cases of pure LV electromechanical dyssynchrony (with excellent response rate to CRT) and in cases with large septal scar and a viable LV lateral wall – and no electrical substrate for CRT response. In contrast to echocardiography, CMR may characterize both septal scar and LV dyssynchrony as single image modality. Future larger studies should compare clinical relevance of LV dyssynchrony assessed by CMR and echocardiography, respectively.

Clinical implications

The persistently high number of non-responders to CRT calls for better tools to identify responders. The present study suggests a novel and clinically attractive algorithm based on septal LGE and septal flash by CMR as stand-alone image modality, which identified CRT

responders with high accuracy and predicted long-term survival. CMR represents an additional cost compared to echocardiography, but given the importance of diagnosing septal LGE in CRT candidates, we advocate increased priority for these patients to CMR. Less stringent requirements for renal function and increased use of CMR compatible devices will probably result in more patients being eligible for CMR in near future. Due to lower number of responders, the proposed approach appears especially valuable for patients with intermediate QRS-duration.

Limitations

In the present study, we did not include patients with low eGFR nor patients with CMR incompatible implants to avoid any harm inflicted upon study participants. This may have caused a selection bias. Data on LV lead position and intrinsic LV electric delay were not available, and such data might have provided additional insights. The number of transmural LV lateral wall scars was too low to investigate to full extent. The present study was observational, included a limited number of patients and the primary endpoint was the surrogate marker ESV reduction. Survival analysis should be interpreted with caution due to low numbers of events. To change clinical practice, there is need for a randomized trial with clinical endpoints.

Conclusions

The combined assessment of septal LGE and septal flash by CMR accurately identifies CRT responders. Accuracy is similar in the clinically relevant subgroup with intermediate QRS-duration. Patients with no septal LGE have excellent response rates. In patients with septal LGE, septal flash separates responders from non-responders with high precision. Further studies are needed to verify that the novel algorithm might be used to improve patient selection for CRT.

Acknowledgements

The authors would like to thank study nurse Kari Melberg, MRI radiographer Bac Nguyen, physicist Oliver Marcel Geier and professor of medical statistics Odd Aalen for their important contributions to the study.

References

1. Cleland JG, Daubert JC, Erdmann E, Freemantle N, Gras D, Kappenberger L, et al. The effect of cardiac resynchronization on morbidity and mortality in heart failure. *N Engl J Med.* 2005;352(15):1539-49.
2. Abraham WT, Fisher WG, Smith AL, Delurgio DB, Leon AR, Loh E, et al. Cardiac Resynchronization in Chronic Heart Failure. *New England Journal of Medicine.* 2002;346(24):1845-53.
3. Glikson M, Nielsen JC, Kronborg MB, Michowitz Y, Auricchio A, Barbash IM, et al. 2021 ESC Guidelines on cardiac pacing and cardiac resynchronization therapy: Developed by the Task Force on cardiac pacing and cardiac resynchronization therapy of the European Society of Cardiology (ESC) With the special contribution of the European Heart Rhythm Association (EHRA). *European Heart Journal.* 2021.
4. Mollema SA, Bleeker GB, van der Wall EE, Schalij MJ, Bax JJ. Usefulness of QRS duration to predict response to cardiac resynchronization therapy in patients with end-stage heart failure. *Am J Cardiol.* 2007;100(11):1665-70.
5. Vernooy K, Cornelussen RNM, Verbeek XAAM, Vanagt WYR, van Hunnik A, Kuiper M, et al. Cardiac resynchronization therapy cures dyssynchronopathy in canine left bundle-branch block hearts. *European Heart Journal.* 2007;28(17):2148-55.
6. Vernooy K, Verbeek XA, Peschar M, Crijns HJ, Arts T, Cornelussen RN, et al. Left bundle branch block induces ventricular remodelling and functional septal hypoperfusion. *Eur Heart J.* 2005;26(1):91-8.
7. Parsai C, Bijmens B, Sutherland GR, Baltabaeva A, Claus P, Marciniak M, et al. Toward understanding response to cardiac resynchronization therapy: left ventricular dyssynchrony is only one of multiple mechanisms. *Eur Heart J.* 2009;30(8):940-9.
8. Stankovic I, Prinz C, Ciarka A, Daraban AM, Kotrc M, Aaronson M, et al. Relationship of visually assessed apical rocking and septal flash to response and long-term survival following cardiac resynchronization therapy (PREDICT-CRT). *Eur Heart J Cardiovasc Imaging.* 2016;17(3):262-9.
9. Maass AH, Vernooy K, Wijers SC, van 't Sant J, Cramer MJ, Meine M, et al. Refining success of cardiac resynchronization therapy using a simple score predicting the amount of reverse ventricular remodelling: results from the Markers and Response to CRT (MARC) study. *Europace.* 2018;20(2):e1-e10.
10. Vecera J, Penicka M, Eriksen M, Russell K, Bartunek J, Vanderheyden M, et al. Wasted septal work in left ventricular dyssynchrony: a novel principle to predict response to cardiac resynchronization therapy. *Eur Heart J Cardiovasc Imaging.* 2016;17(6):624-32.
11. Bleeker GB, Kaandorp TA, Lamb HJ, Boersma E, Steendijk P, de Roos A, et al. Effect of posterolateral scar tissue on clinical and echocardiographic improvement after cardiac resynchronization therapy. *Circulation.* 2006;113(7):969-76.
12. Chalil S, Stegemann B, Muhyaldeen SA, Khadjooi K, Foley PW, Smith RE, et al. Effect of posterolateral left ventricular scar on mortality and morbidity following cardiac resynchronization therapy. *Pacing Clin Electrophysiol.* 2007;30(10):1201-9.
13. White JA, Yee R, Yuan X, Krahn A, Skanes A, Parker M, et al. Delayed enhancement magnetic resonance imaging predicts response to cardiac resynchronization therapy in patients with intraventricular dyssynchrony. *J Am Coll Cardiol.* 2006;48(10):1953-60.
14. Aalen JM, Donal E, Larsen CK, Duchenne J, Lederlin M, Cvijic M, et al. Imaging predictors of response to cardiac resynchronization therapy: left ventricular work asymmetry by echocardiography and septal viability by cardiac magnetic resonance. *Eur Heart J.* 2020;41(39):3813-23.

15. Larsen CK, Galli E, Duchenne J, Aalen JM, Stokke C, Fjeld JG, et al. Scar imaging in the dyssynchronous left ventricle: Accuracy of myocardial metabolism by positron emission tomography and function by echocardiographic strain. *Int J Cardiol.* 2023;372:122-9.
16. Heiberg E, Sjøgren J, Ugander M, Carlsson M, Engblom H, Arheden H. Design and validation of Segment--freely available software for cardiovascular image analysis. *BMC Med Imaging.* 2010;10:1.
17. Engblom H, Tufvesson J, Jablonowski R, Carlsson M, Aletras AH, Hoffmann P, et al. A new automatic algorithm for quantification of myocardial infarction imaged by late gadolinium enhancement cardiovascular magnetic resonance: experimental validation and comparison to expert delineations in multi-center, multi-vendor patient data. *J Cardiovasc Magn Reson.* 2016;18(1):27.
18. Larsen CK, Aalen JM, Stokke C, Fjeld JG, Kongsgaard E, Duchenne J, et al. Regional myocardial work by cardiac magnetic resonance and non-invasive left ventricular pressure: a feasibility study in left bundle branch block. *Eur Heart J Cardiovasc Imaging.* 2020;21(2):143-53.
19. Russell K, Eriksen M, Aaberge L, Wilhelmsen N, Skulstad H, Remme EW, et al. A novel clinical method for quantification of regional left ventricular pressure-strain loop area: a non-invasive index of myocardial work. *Eur Heart J.* 2012;33(6):724-33.
20. Hanley JA, McNeil BJ. A method of comparing the areas under receiver operating characteristic curves derived from the same cases. *Radiology.* 1983;148(3):839-43.
21. Hunold P, Schlosser T, Vogt FM, Eggebrecht H, Schmermund A, Bruder O, et al. Myocardial late enhancement in contrast-enhanced cardiac MRI: distinction between infarction scar and non-infarction-related disease. *AJR Am J Roentgenol.* 2005;184(5):1420-6.
22. Sohal M, Amraoui S, Chen Z, Sammut E, Jackson T, Wright M, et al. Combined identification of septal flash and absence of myocardial scar by cardiac magnetic resonance imaging improves prediction of response to cardiac resynchronization therapy. *Journal of Interventional Cardiac Electrophysiology.* 2014;40(2):179-90.
23. Zweerink A, Friedman DJ, Klem I, van de Ven PM, Vink C, Biesbroek PS, et al. Segment Length in Cine Strain Analysis Predicts Cardiac Resynchronization Therapy Outcome Beyond Current Guidelines. *Circ Cardiovasc Imaging.* 2021;14(7):e012350.

Table 1. Baseline clinical and CMR characteristics

	All patients (n=136)	Responders (n=103)	Non-responders (n=33)	P-value
Age (years)	66±10	67±9	64±11	0.071
Male sex (%)	68	63	82	0.046
NYHA functional class	2.3±0.6	2.3±0.6	2.4±0.6	0.125
Medications (%)				
<i>ACE-inhibitor/ARB</i>	96	97	94	0.403
<i>Beta blocker</i>	91	89	97	0.178
<i>Aldosterone antagonist</i>	41	41	44	0.797
Sinus rhythm (%)	95	96	91	0.239
Heart failure etiology (%)				
<i>Ischemic</i>	31	22	56	<0.001
<i>Non-ischemic</i>	69	78	42	<0.001
QRS duration (milliseconds)	164±17	166±16	158±18	0.021
Left bundle branch block (%)	91	95	79	0.004
LV EDV indexed (ml/m²)	145±46	139±46	164±41	0.008
LV ESV indexed (ml/m²)	76±32	73±31	88±32	0.580
LV ejection fraction (%)	27±8	28±8	23±6	0.003
Anterior LGE (%)	0 (0-6.5)	0 (0-0.1)	12.2 (0.8-36.2)	<0.001
Septal LGE (%)	0 (0-12.2)	0 (0-3.2)	16.3 (1.7-39.6)	<0.001
Inferior LGE (%)	0 (0-9.8)	0 (0-3.9)	10.5 (0.4-30.1)	<0.001
Lateral LGE (%)	0 (0-5.5)	0 (0-0)	5.6 (0-23.1)	<0.001
Septal flash (%)	76	89	36	<0.001
Lateral-to-septal work difference (mmHg·%)	1551±1080	1710±1085	1061±917	0.003

Continuous variables are given as mean±standard deviation or median (interquartile range), as appropriate. P-value reports comparison of responders vs. non-responders.

CMR=cardiac magnetic resonance; LBBB = left bundle branch block; NYHA = New York Heart Association; LV = left ventricular; LGE=late gadolinium enhancement

Table 2. Classification and distribution of LGE

	Number of patients	Number with septal involvement (% of total)
LGE present	64	59 (92%)
• Ischemic	37	33 (89%)
• Non-ischemic	20	19 (95%)
• Combined	7	6 (86%)
Location of infarcts (ischemic LGE)		
• Anterior wall	25	25 (100%)
• Lateral wall	14	10 (71%)
• Inferior wall	12	11 (92%)
Classification of non-ischemic LGE		
• RV insertion point fibrosis	12	11 (92%)
• Septal midwall fibrosis	7	7 (100%)
• Other	12	11 (92%)

LGE=late gadolinium enhancement

Table 3. Multivariable linear regression analysis with left ventricular end systolic volume change as dependent continuous variable

Regression variable	Multivariable analysis			
	B	95% CI	VIF	P-value
QRS duration (ms)	-0.036	-0.249 to 0.177	1.158	0.738
Left bundle branch block (yes/no)	-9.18	-21.31 to 2.94	1.110	0.136
Septal LGE (%)	0.521	0.311 to 0.731	1.153	<0.001
Septal flash (yes/no)	-18.39	-27.16 to -9.61	1.325	<0.001
Constant term	-8.513			

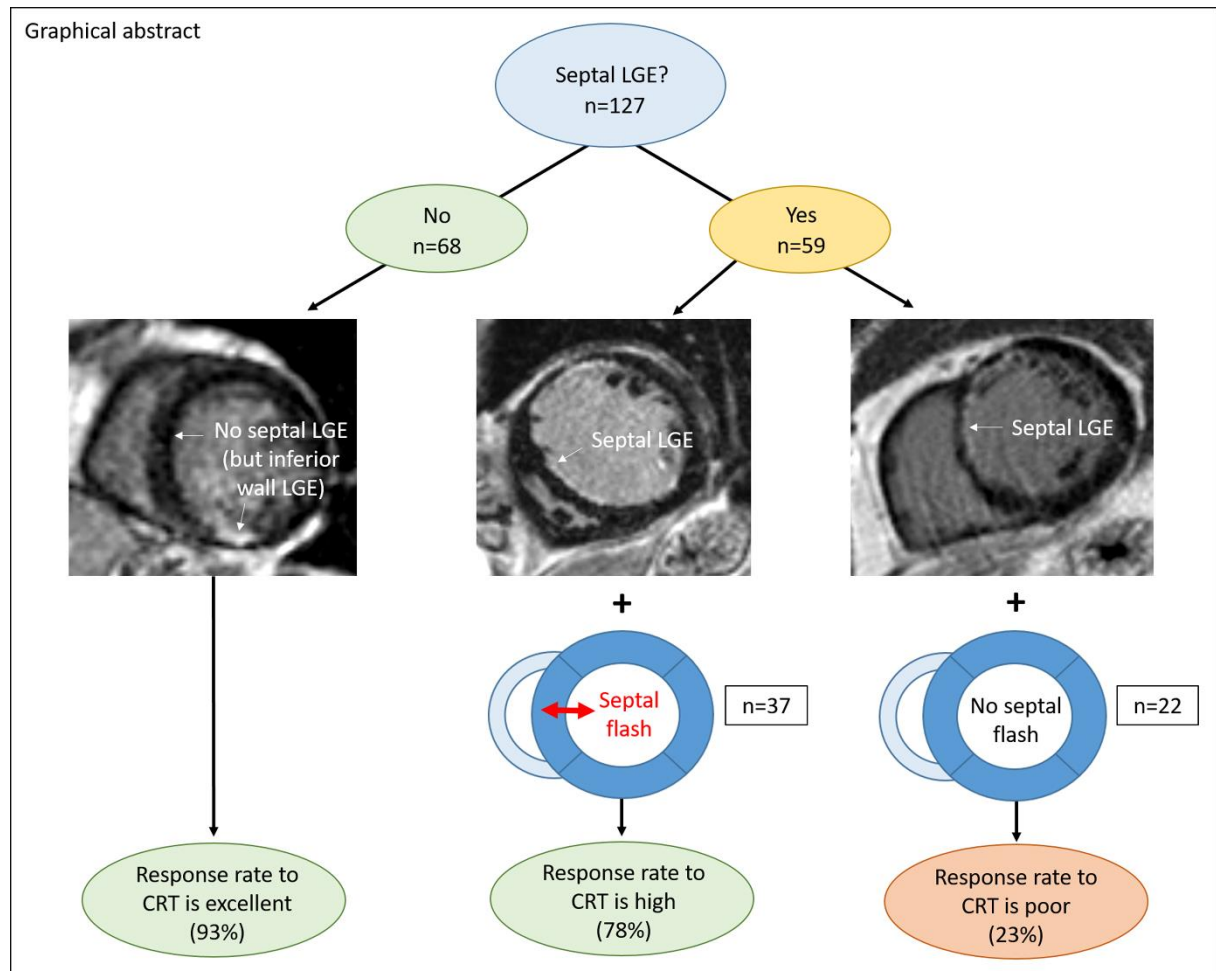
N=125. R²=0.40. Septal LGE is given as a continuous variable (%).

CI=confidence interval; VIF=variance inflation factor; LGE=late gadolinium enhancement

Figures

Graphical abstract. A novel algorithm to identify CRT responders.

Without septal scar, response rate to CRT is excellent (93%), irrespective of other parameters. If septal scar is present, and the patient displays septal flash, response rate is also high (78%). However, if septal scar is present and there is no septal flash, response rate to CRT is low (23%), and these patients are classified as likely non-responders by the algorithm. The algorithm correctly separated CRT responders from non-responders with 86% accuracy, and was equally accurate in patients with intermediate QRS-duration (130-150ms).



CRT=cardiac resynchronization therapy

Figure 1. Schematic illustration of septal flash by cine 4-chamber images.

The two images per patient are sequential phases of the 4-chamber cine-CMR images. The yellow longitudinal line is in the similar position and of the same length in both images from each patient. The short, transverse blue line marks the endocardial contour of septum.

Patient A displays an early contractile motion of the interventricular septum (septal flash) with no apparent motion of the lateral wall during iso-volumic contraction phase (second image). Patient B demonstrates no pre-ejection septal movement (no septal flash).

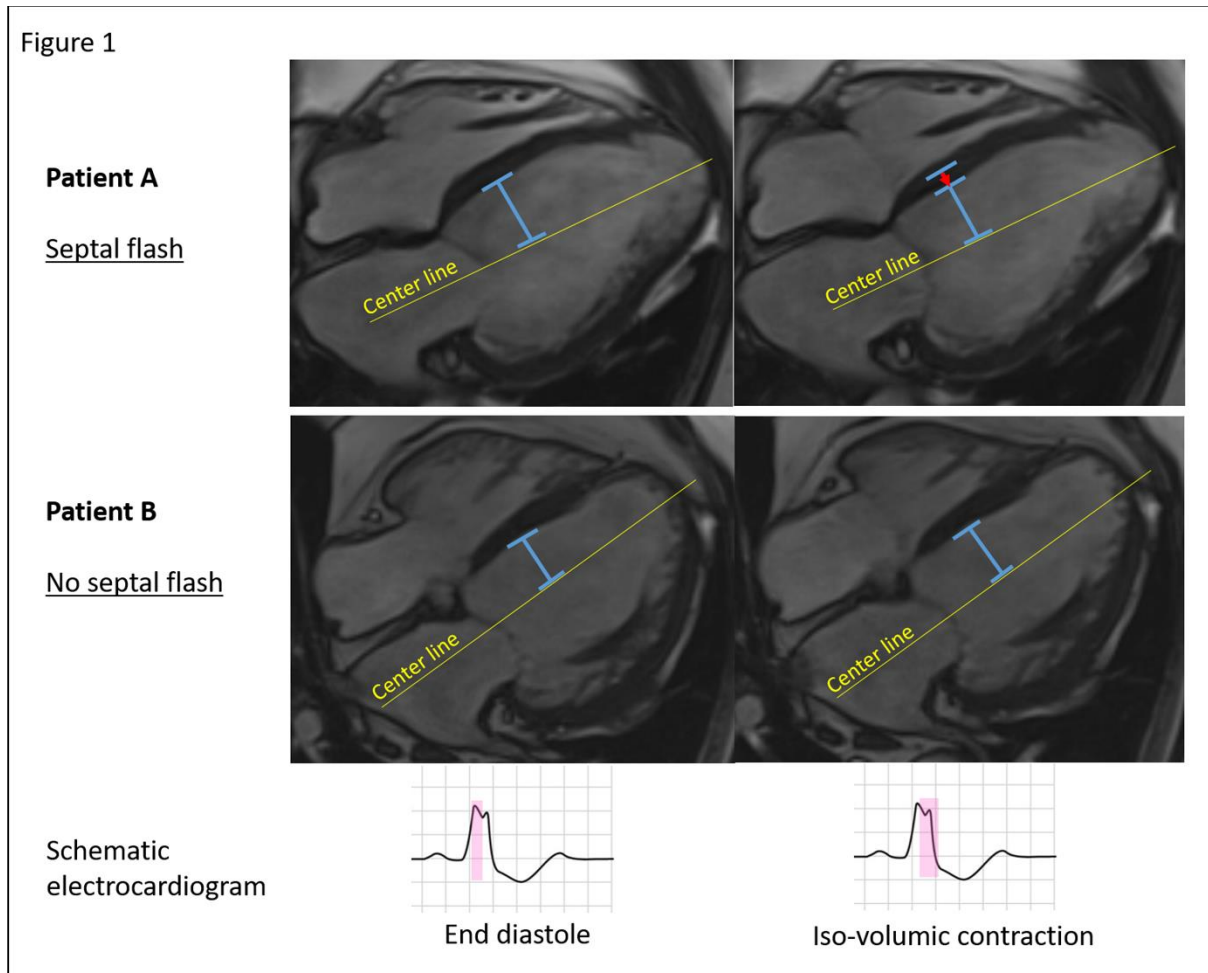
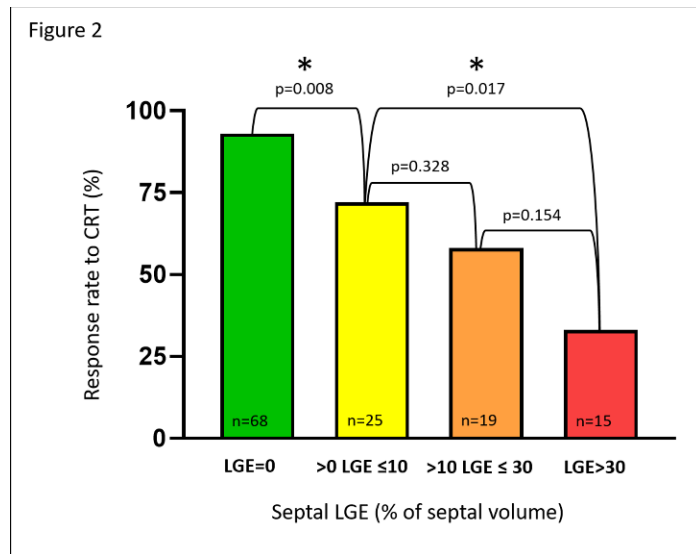


Figure 2. Response rates to CRT stratified to increasing amounts of septal LGE.

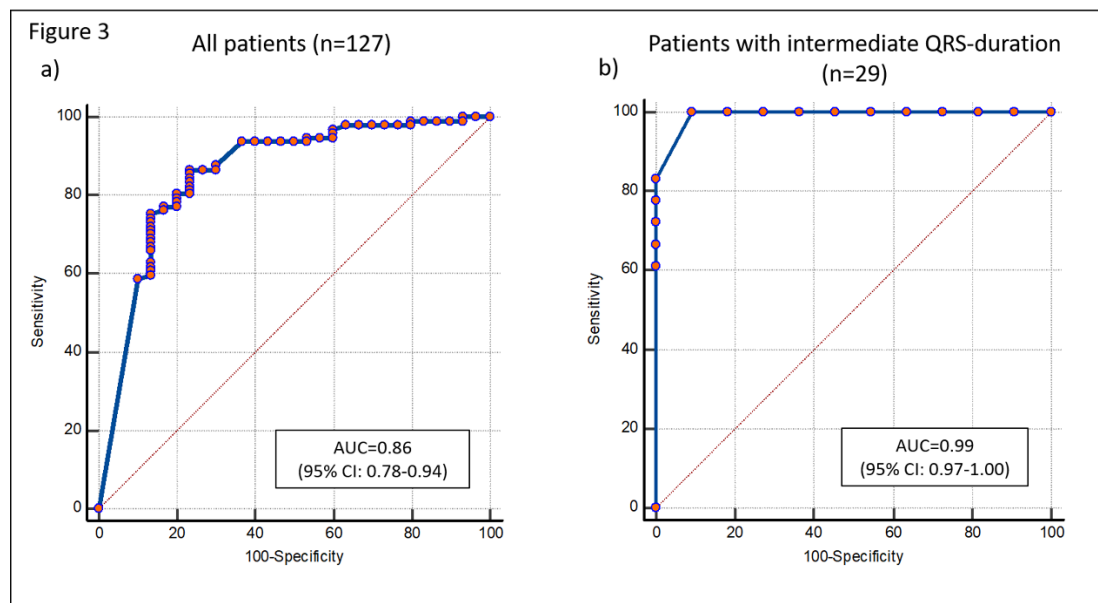
Increasing amount of septal LGE resulted in decreasing response rates to CRT. Even minor septal LGE significantly reduced the likelihood of response compared to no septal LGE.



LGE=late gadolinium enhancement; CRT=cardiac resynchronization therapy

Figure 3. Receiver operator characteristic curve for predicting CRT response by the combined approach of percentage septal LGE and septal flash.

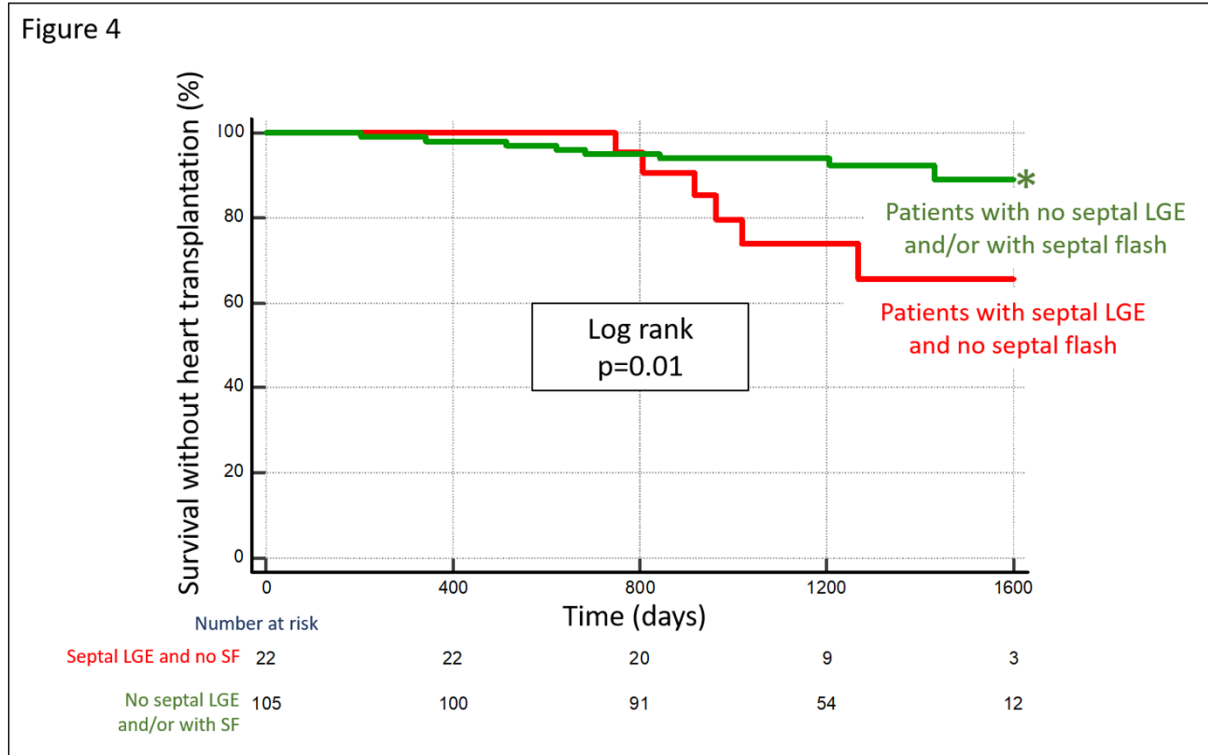
- In all available patients (n=127).
- In the subgroup of patients with intermediate QRS-duration (n=29).



CRT=cardiac resynchronization therapy; LGE=late gadolinium enhancement; AUC=area under the curve; CI=confidence interval

Figure 4. Patients without septal LGE and/or with septal flash have significantly better long-term survival as compared to patients with septal LGE and no septal flash.

Kaplan-Meier curve stratified according to whether patients had 1) no septal LGE and/or with septal flash (green) or 2) septal LGE and no septal flash (red).

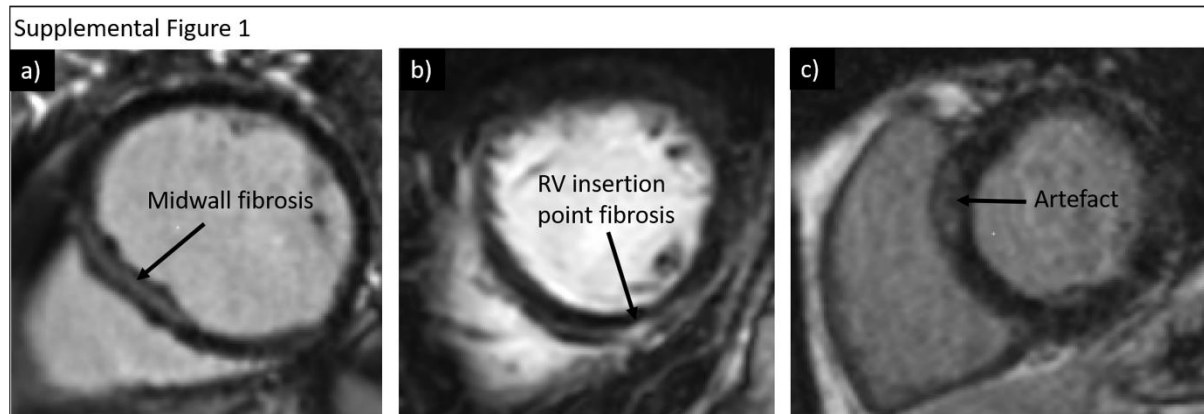


LGE=late gadolinium enhancement; SF=septal flash

Supplemental material

Figure S1. Examples of non-ischemic LGE.

A): Example of midwall fibrosis (LGE) located in septum. B): Illustration of fibrosis (LGE) in the RV insertion point. C): Apparent hyperenhancement in the most basal short-axis slice, classified as partial volume effect, and not LGE.



LGE=late gadolinium enhancement; RV=right ventricular

Video 1. Septal flash.

The video displays the rapid, early movement of the interventricular septum (septal flash) in 4-chamber view in a representative patient.

